



MARSOL

Demonstrating Managed Aquifer Recharge as a Solution to Water Scarcity and Drought

White book on MAR modelling: Selected results from MARSOL PROJECT

Deliverable D12.7

| | |
|----------------------------|--|
| Deliverable No. | D12.7 |
| Version | 1.0 |
| Version Date | 31.01.2017 |
| Author(s) | J.P. LOBO FERREIRA, TERESA LEITÃO, TIAGO MARTINS and ANA MARIA CARMEN ILIE (LNEC), JOSÉ PAULO MONTEIRO, LUÍS COSTA and RUI HUGMAN (UALG), TIAGO CARVALHO, RUI AGOSTINHO and RAQUEL SOUSA (TARH), LAURA FOGLIA, ANJA TOEGL AND CHRISTOS POULIARIS (TU DARMSTADT), RUDY ROSSETTO (SSSA), IACOPO BORSI (TEA), XAVIER SANCHEZ-VILA AND PAULA RODRIGUEZ-ESCALES (UPC), ENRIQUE F. ESCALANTE (TRAGSA), MANUEL M. OLIVEIRA (LNEC), ANDREAS KALLIORAS (NTUA), YORAM KATZ (MEKOROT) |
| Dissemination Level | PU |
| Status | Final |



The MARSOL project has received funding from the European Union's Seventh Framework Programme for Research, Technological Development and Demonstration under grant agreement no 619120.

Contents

| | |
|---|----|
| CHAPTER 1 – MARSOL WP12 MODELLING ACTIVITIES AND DEMO-SITES INTRODUCTION | 21 |
| 1 MARSOL WP12 MODELLING ACTIVITIES | 21 |
| 1.1 OBJECTIVES AND DETAILS OF TASKS..... | 21 |
| 1.1.1 On Task 12.1: Methods evaluation (month 1-6): | 22 |
| 1.1.2 On Task 12.2: Water budget and conceptual modelling (month 1-12) | 22 |
| 1.1.3 On Task 12.3: Climate change impact (month 6-12)..... | 22 |
| 1.1.4 On Task 12.4: Hydrogeological modelling (month 6-30)..... | 23 |
| 1.1.5 On Task 12.5: Physical models at LNEC (month 24-33)..... | 23 |
| 1.1.6 On Task 12.6: Guide lines for best practices (month 27-36) | 23 |
| 1.1.7 On Task 12.7: Visualization..... | 23 |
| 1.2 SIGNIFICANT RESULTS | 24 |
| 2 MARSOL WP 12 DEMO-SITES INTRODUCTION..... | 25 |
| 2.1 DEMO SITE 1: LAVRION TECHNOLOGICAL & CULTURAL PARK, LAVRION, GREECE | 25 |
| 2.2 DEMO SITE 2: ALGARVE AND ALENTEJO, SOUTH PORTUGAL | 26 |
| 2.3 DEMO SITE 3: LOS ARENALES AQUIFER, CASTILLE AND LEON, SPAIN | 28 |
| 2.4 DEMO SITE 5: RIVER BRENTA CATCHMENT, VICENZA, ITALY | 29 |
| 2.5 DEMO SITE 7: MENASHE INFILTRATION BASIN, HADERA, ISRAEL..... | 30 |
| 2.6 DEMO SITE 8: SOUTH MALTA COASTAL AQUIFER, MALTA | 31 |
| 2.7 VISUALISATION AND INTERACTION WITH MARSOL WPs | 32 |
| 3 MARSOL WP 12 MODELLING PUBLICATIONS..... | 34 |
| CHAPTER 2 – STATE OF THE ART AND LITERATURE REVIEW IN MANAGED AQUIFER RECHARGE MODELLING | 37 |
| 4 INTRODUCTION TO THE STATE OF THE ART AND LITERATURE REVIEW IN MANAGED AQUIFER RECHARGE MODELLING | 37 |
| 5 FLOW AND TRANSPORT MODELLING MAR..... | 38 |
| 5.1 FLOW AND TRANSPORT NUMERICAL MODELS OVERVIEW..... | 38 |
| 5.1.1 CODE_BRIGHT | 38 |
| 5.1.2 COMSOL Multiphysics | 38 |

| | | |
|---|---|----|
| 5.1.3 | FEFLOW | 39 |
| 5.1.4 | FEMWATER..... | 39 |
| 5.1.5 | HYDRUS | 39 |
| 5.1.6 | MOCdense | 40 |
| 5.1.7 | MODFLOW and related programs..... | 40 |
| 5.1.7.1 | MODPATH..... | 40 |
| 5.1.7.2 | MT3D | 41 |
| 5.1.7.3 | SEAWAT | 41 |
| 5.1.7.4 | MODRET | 42 |
| 5.1.8 | TOUGH..... | 43 |
| 5.2 | CASE STUDIES AND APPLICATIONS IN FLOW AND TRANSPORT MODELLING | 43 |
| 6 | HYDROGEOCHEMICAL MODELLING MAR..... | 67 |
| 6.1 | HYDROGEOCHEMICAL MODELS OVERVIEW | 67 |
| 6.1.1 | INFOMI | 67 |
| 6.1.2 | EASY-LEACHER..... | 68 |
| 6.1.3 | HP1 | 68 |
| 6.1.4 | HYDROGEOCHEM | 69 |
| 6.1.5 | PHREEQC | 69 |
| 6.2 | CASE STUDIES AND APPLICATIONS IN HYDROGEOCHEMICAL MODELLING..... | 70 |
| 7 | CONCLUSIONS OF THE STATE OF THE ART AND LITERATURE REVIEW IN MANAGED AQUIFER RECHARGE MODELLING | 73 |
| CHAPTER 3 – WATER BUDGET AND CLIMATE CHANGE IMPACT: ASSESSMENT OF DEMO SITE 2 ALGARVE AND ALENTEJO, PORTUGAL AND DEMO SITE 7 MENASHE, ISRAEL | | 81 |
| 8 | WATER BUDGET AND CLIMATE CHANGE IMPACT: ASSESSMENT OF DEMO SITE 2 ALGARVE AND ALENTEJO, PORTUGAL AND DEMO SITE 7 MENASHE, ISRAEL | 81 |
| 8.1 | DEMO SITE 2 DEMO SITE 2: ALGARVE AND ALENTEJO, SOUTH PORTUGAL..... | 81 |
| 8.1.1 | Conceptual model | 82 |
| 8.1.2 | Large diameter infiltrating wells in Campina de Faro aquifer system | 82 |
| 8.1.3 | Rio Seco infiltration basins | 84 |
| 8.1.4 | Querença-Silves aquifer system | 86 |
| 8.1.5 | Querença-Silves infiltration basins..... | 88 |

| | | |
|--|--|-----|
| 8.1.6 | Water budget | 89 |
| 8.1.6.1 | Natural water budget | 89 |
| 8.1.6.2 | Campina de Faro..... | 90 |
| 8.1.6.3 | Rio Seco hydrographic basin upstream the infiltration basins..... | 91 |
| 8.1.7 | Querença-Silves | 96 |
| 8.1.8 | Water available for MAR and sources of water | 97 |
| 8.1.8.1 | Greenhouse rain harvesting | 97 |
| 8.1.9 | Climate change | 100 |
| 8.1.9.1 | Emission scenarios and Predicted climate change..... | 100 |
| 8.1.9.2 | Climate change impacts | 102 |
| 8.2 | DEMO SITE 7: MENASHE INFILTRATION BASIN, HADERA, ISRAEL | 105 |
| 8.2.1 | Introduction..... | 105 |
| 8.2.2 | Conceptual model | 105 |
| 8.2.3 | Water budget | 108 |
| 8.2.4 | Watershed Model Water Budget and Climate Change..... | 108 |
| 8.2.4.1 | Watershed Scale Model | 108 |
| 8.2.4.2 | Natural Water Budget | 109 |
| 8.2.4.3 | Climate Change..... | 109 |
| 8.3 | CONCLUSIONS | 110 |
| CHAPTER 4 – MAR THROUGH FORESTED INFILTRATION: THE EXEMPLE OF MARSOL RIVER | | |
| | BRENTA CATCHMENT DEMO SITE 5, IN VICENZA, ITALY | 113 |
| 9 | EXECUTIVE SUMMARY OF MAR THROUGH FORESTED INFILTRATION: THE EXEMPLE OF | |
| | MARSOL RIVER BRENTA CATCHMENT DEMO SITE 5, IN VICENZA, ITALY..... | 113 |
| 10 | DEMO SITE 5 STUDY AREA..... | 114 |
| 11 | DEMO SITE 5 MONITORING AND SITE CHARACTERIZATION | 117 |
| 11.1 | SITE CHARACTERIZATION | 117 |
| 11.1.1 | Loria Infiltration Basin | 118 |
| 11.1.2 | Schiavon Forested Infiltration Site | 119 |
| 11.2 | UNSATURATED ZONE MONITORING | 120 |

| | | |
|---|--|-----|
| 11.3 | MODELLING ACTIVITY OF DEMO SITE..... | 122 |
| 11.3.1 | Hydrodynamic model..... | 122 |
| 11.4 | WATER QUALITY MODEL | 133 |
| 12 | CONCLUSION OF MAR THROUGH FORESTED INFILTRATION IN THE RIVER BRENTA CATCHMENT, VICENZA, ITALY | 135 |
| CHAPTER 5 – THE EFFICIENCY OF MAR IN AN IRRIGATION AREA WITH A LARGE DEVELOPMENT OF AGROINDUSTRY: THE EXEMPLE OF MARSOL DEMO SITE 3 LOS ARENALES AQUIFER, CASTILLE AND LEON, SPAIN..... | | |
| 13 | MODELLING OF DEMO SITE 3 LOS ARENALES AQUIFER, CASTILLE AND LEON, SPAIN..... | 137 |
| 13.1 | INTRODUCTION | 137 |
| 13.2 | MODELLING BACKGROUND IN LOS ARENALES AQUIFER..... | 139 |
| 13.2.1 | Santiuste Basin | 139 |
| 13.2.1.1 | Boundary conditions | 140 |
| 13.2.1.2 | River-aquifer relations and extractions..... | 140 |
| 13.2.2 | Carracillo District | 141 |
| 13.2.2.1 | Aquifer characterization. Boundary and environmental conditions..... | 142 |
| 13.2.2.2 | River-aquifer relations..... | 142 |
| 13.2.2.3 | Extractions..... | 143 |
| 13.2.2.4 | Natural recharge simulation..... | 143 |
| 13.2.2.5 | Calibration: | 144 |
| 13.2.3 | Alcazarén Area..... | 145 |
| 13.3 | MODELLING ACTIVITIES..... | 146 |
| 13.3.1 | Santiuste Basin | 146 |
| 13.3.1.1 | New MAR channel path..... | 146 |
| 13.3.1.2 | New monitoring Network design | 147 |
| 13.3.1.3 | Water budget in the different zones to manage MAR facilities | 148 |
| 13.3.2 | Carracillo District | 148 |
| 13.3.2.1 | Modelling the new “triplet” scheme (stagnation pond-biofilter-artificial wetland) | 149 |

| | | |
|--|---|-----|
| 13.3.3 | Alcazarén Area..... | 150 |
| 13.4 | CONCLUSIONS | 151 |
| CHAPTER 6 – PHYSICAL MODEL EXPERIMENTS AT LNEC AND THEIR NUMERICAL MODELLING | | |
| | RESULTS..... | 153 |
| 14 | INTRODUCTION TO MARSOL PHYSICAL MODELLING..... | 153 |
| 15 | PHYSICAL SANDBOX MODEL..... | 154 |
| 15.1 | POTENTIALITIES AND AIM | 154 |
| 15.2 | SANDBOX CONSTRUCTION AND DESCRIPTION | 154 |
| 15.3 | EXPERIMENTAL SETUP..... | 155 |
| 15.3.1 | Sandbox set-up..... | 155 |
| 15.3.2 | Materials..... | 157 |
| 15.3.3 | Methodology | 158 |
| 15.3.3.1 | Tracer selection | 158 |
| 15.3.3.2 | Experiment 1 | 158 |
| 15.3.3.3 | Experiment 2 | 160 |
| 15.4 | MONITORING..... | 160 |
| 15.5 | RESULTS AND CONCLUSIONS..... | 162 |
| 15.5.1 | Experiment 1 | 162 |
| 15.5.2 | Experiment 2 | 171 |
| 15.5.3 | Conclusions..... | 174 |
| 16 | NUMERICAL MODELLING | 175 |
| 16.1 | INPUT DATA | 175 |
| 16.2 | RESULTS..... | 178 |
| 16.2.1 | Section A..... | 178 |
| 16.2.2 | Section B..... | 179 |
| 16.2.3 | Section C..... | 181 |
| 16.3 | GENERAL RESULTS DISCUSSION..... | 182 |
| CHAPTER 7 – NUMERICAL MODELLING OF COLUMN EXPERIMENTS | | |
| 17 | INTRODUCTION TO NUMERICAL MODELLING OF COLUMN EXPERIMENTS | 183 |

| | | |
|--------|--|-----|
| 18 | INPUT DATA..... | 185 |
| 19 | RESULTS..... | 187 |
| 20 | DISCUSSION AND CONCLUSIONS TO NUMERICAL MODELLING OF COLUMN EXPERIMENTS | 191 |
| | CHAPTER 8 – NATURAL ATTENUATION PROCESS MODELLING..... | 193 |
| 21 | INTRODUCTION TO NATURAL ATTENUATION PROCESS MODELLING..... | 193 |
| 21.1 | BRIEF DESCRIPTION OF SITE AND MODEL CODE | 194 |
| 21.2 | MODEL CONSTRUCTION | 194 |
| 21.3 | RESULTS AND DISCUSSION | 195 |
| 21.4 | CONCLUSIONS | 199 |
| | CHAPTER 9 – MAR DISSEMINATION AND WRAP-UP..... | 201 |
| 22 | MAR DISSEMINATION AND WRAP-UP..... | 201 |
| 22.1 | MAR DISSEMINATION..... | 201 |
| 22.1.1 | EIP Water AG128 MARtoMARKET | 201 |
| 22.1.2 | IAH Working Group (WG) Mar To Market Strategies And Actions To Bring Managed Aquifer Recharge Technique To The Industry..... | 204 |
| 22.2 | MANAGED AQUIFER RECHARGE SITES KNOWLEDGE BASIS..... | 206 |
| 22.3 | MODELLING IN WATER RESOURCE MANAGEMENT APPLICATION OVERVIEW AND REVIEW | 206 |
| 22.4 | MARSOL DELIVERABLE 12.4 FINAL REPORT ON NUMERICAL MODEL WRAP-UP | 207 |
| | ANNEX 1 – SELECTION OF FURTHER MODELLING RESEARCH ACTIVITIES EXTRACTED FROM INTERIM REPORTS | 211 |
| 23 | INTERIM REPORT DECEMBER 2013 – AUGUST 2014..... | 211 |
| 23.1 | DEMO SITE 4 ACTIVITIES: LLOBREGAT RIVER INFILTRATION BASINS, SANT VICENÇ DELS HORTS (BARCELONA)..... | 211 |
| 24 | INTERIM REPORT SEPTEMBER 2014 - MAY 2015 | 215 |
| 24.1 | GEOPHYSICAL SURVEY, WITH THE RESISTIVITY METHOD, FOR PT QUERENÇA-SILVES DEMO SITE CONCEPTUAL MODEL | 215 |
| 24.2 | MODELLING CONTRIBUTIONS OF THE LOCAL AND REGIONAL GROUNDWATER FLOW OF MANAGED AQUIFER RECHARGE ACTIVITIES AT QUERENÇA-SILVES AQUIFER SYSTEM (WP4) | 217 |

| | | |
|--------|---|-----|
| 24.3 | HYDROLOGICAL/HYDROGEOLOGICAL MODELS FOR THE LAVRIO TEST SITE (WP 3) AND THE MENASHE TEST SITE (WP 9) | 218 |
| 24.3.1 | TUDa Modelling effort..... | 218 |
| 24.3.2 | Status of model development at Lavrion (Greece) | 220 |
| 24.3.3 | Data collection: Menashe test site | 220 |
| 24.3.4 | Modelling the potential impact of chaotic advection to enhance degradation of organic matter and emergent compounds. | 221 |
| 24.3.5 | Saturated flow model of the Coastal aquifer – Menashe region | 224 |
| 24.4 | MODELLING CONTRIBUTIONS IN DEMO SITE 6 SERCHIO RIVER WELL FIELD..... | 228 |
| 24.5 | MARSOL WP 12 MODELLING WORKSHOP, PISA, ITALY, APRIL, 2015 | 230 |
| 25 | INTERIM REPORT JUNE 2015 - FEBRUARY 2016..... | 231 |
| 25.1 | MODELLING CONTRIBUTIONS OF THE LOCAL AND REGIONAL GROUNDWATER FLOW OF MANAGED AQUIFER RECHARGE ACTIVITIES AT WP 4 ALGARVE CAMPINA DE FARO AND QUERENÇA-SILVES AQUIFER SYSTEMS | 231 |
| 25.1.1 | Introduction..... | 231 |
| 25.1.2 | Campina de Faro (PT1) | 231 |
| 25.1.3 | Cerro do Bardo (PT2)..... | 233 |
| 25.2 | UALG NUMERICAL MODELLING OF THE MEAN SEA LEVEL AQUIFER (MSLA) OF MALTA | 235 |
| 25.3 | MODELLING CONTRIBUTIONS IN DEMO SITE 6 - SERCHIO RIVER WELL FIELD..... | 236 |
| 25.3.1 | Modelling tools finalized | 236 |
| 25.3.2 | Update on modelling tools already described in previous reports..... | 237 |
| 25.4 | TUDa MODELLING ACTIVITIES AT DEMO SITE 1 (LAVRIO, GREECE) | 238 |
| 25.5 | TUDa MODELLING CONTRIBUTIONS IN DEMO SITE 7: MENASHE INFILTRATION BASIN, HADERA, ISRAEL..... | 243 |
| 25.5.1 | Progress of Work on Model | 243 |
| 25.5.2 | Model Setup | 244 |
| 25.5.3 | Model Evaluation | 245 |
| | ANNEX 2 – EIP WATER AG 128 MARTOMARKET REPORT | 247 |

Figures

| | |
|---|----|
| Figure 1 – Geographical locations and points of interest the Lavrion basin..... | 25 |
| Figure 2 – PT MARSOL DEMO sites location (the aquifers boundaries are marked in grey) | 27 |
| Figure 3 – Map of Arenales aquifer area and the zones with an advance deployment of MAR facilities | 29 |
| Figure 4- Location of the two test areas in the Demonstration Site 5, River Brenta Catchment, Vicenza, Italy | 30 |
| Figure 5 - Menashe infiltration site and catchment area – Location map and setting | 31 |
| Figure 6 - Geographical location and main hydrogeological features of the Maltese islands.... | 32 |
| Figure 7 – Finite element grid of area of artificial recharge. Shaded Area represents basin (Adapted from Sunada et al. 1983) | 44 |
| Figure 8 – List of Selected models (Adapted from PSI/Jammal & Associates Division, 1993) | 44 |
| Figure 9 - Comparison of Predicted Recovery Times for a Hypothetical Pond (Adapted from PSI/Jammal & Associates Division, 1993)..... | 45 |
| Figure 10 – Horizontal network and locations of pumping and recharge areas (Adapted from Stefanescu & Dessargues, 1998) | 46 |
| Figure 11 – Recharge Water Simulation Model in Hydrus 2-D (Adapted from Chatdarong, 2000) | 47 |
| Figure 12 - Model grid and boundary conditions for layers 1–4 of the Rialto–Colton Basin ground-water flow model, San Bernardino County, California (Adapted from Woolfenden & Koczot, 2001)..... | 49 |
| Figure 13 – Measured and Computed Water pressures within different calibration adjustments (Adapted from Haimerl, 2002) | 50 |
| Figure 14 - The groundwater model grid of the study area, the type and the locations of characteristic cells, the boundaries of the main lateral groundwater inflows and outflows and the monitoring wells (Adapted from Pliakas et al. 2005) | 51 |
| Figure 15 - Campina de Faro aquifer system regional model (model grid, active cells in white, inactive cells in green, GHB in light-green cells, CHB in red cells and observation wells in green) (Adapted from Lobo Ferreira, 2006) | 52 |
| Figure 16 - Campina de Faro aquifer system local model (model grid, active cells in white, inactive cells in green, GHB in light-green cells, in the northern limit, CHB in red cells, in the southern limit, and observation wells in green) (Adapted from Lobo Ferreira, 2006)..... | 52 |

| | |
|---|----|
| Figure 17 – Local Northern Gaza Strip model grid (adapted from Lobo Ferreira et al, 2006) | 54 |
| Figure 18 – 2D Finite Element vertical grid used in ASR well injection modelling..... | 55 |
| Figure 19 – Active aquifer model area (GRAY) (adapted from EPTISA, 2009) | 56 |
| Figure 20 – Model grid and boundary conditions of a finite-difference model used to simulate groundwater mounding beneath hypothetical stormwater infiltration basins on a 10-acre development (adapted from Carlton, 2010)..... | 58 |
| Figure 21 – Existing wells and suggested ponds locations (ADAPTED from Kareem, 2012)..... | 59 |
| Figure 22 – View and characteristics of the 3D grid design | 60 |
| Figure 23 – Three dimensional model of the Isfara Aquifer (Adapted from Karimov et al. 2013) | 60 |
| Figure 24 – Horizontal discretization of the model (Adapted from Sirhan & Koch, 2013) | 61 |
| Figure 25 – Wells and River Boundary conditions (Adapted from Vicente, 2013) | 62 |
| Figure 26 – Variable-spacing finite-difference grid of model area (May et al, 2013)..... | 63 |
| Figure 27 – Average groundwater contour map with active pumping wells and no surface recharge (Adapted from Hashemi et al, 2013)..... | 63 |
| Figure 28 - Simulated hydraulic heads (left two plots) and water contents (right two plots) for the small-diameter well using layered Ks profile A (top two plots) and B (bottom two plots) at 40 days. White stars in the bottom two plots indicate the depth of 6 m where the lowest-K layer in the vadose zone is present. Other than Ks, other model settings are the same as the previous homogeneous base case simulation. Note that results are only shown for a small portion of the simulation domain (30 out of 130 m) to facilitate visualization of the near-well region (ADAPTED FROM Handel et al 2014) | 64 |
| Figure 29 - Simulated hydraulic heads (left two plots) and water contents (right two plots) for the infiltration basin using layered Ks profile A (top two plots) and B (bottom two plots) at 40 days. White stars in the bottom two plots indicate the depth of 6 m where the lowest-K layer in the vadose zone is present. The plots represent a vertical cross-section through the center of the infiltration basin (adapted from Handel et al 2014)..... | 65 |
| Figure 30 - Water saturation along a N-S and a W-E vertical section through the infiltration pond at the infiltration begin and after 16, 30 and 50 days of infiltration (Adapted from Martelli et al, 2015)..... | 66 |
| Figure 31 - Model of Gotvand-Aghili Plain groundwater along with networking and boundary condition (Adapted from Chitsazan & Movehedian, 2015) | 67 |
| Figure 32 – Campina de Faro N-S hydrogeological section (Stigter, 2005)..... | 82 |

| | |
|---|----|
| Figure 33 – Campina de Faro hydrogeological model, presented in JK15 well log (Silva <i>et al.</i> , 1986) | 83 |
| Figure 34 – Hydrograph basin above Rio Seco MAR facilities and groundwater bodies | 84 |
| Figure 35 – Querença-Silves aquifer system's geology. Underlined features are the ones identified within the aquifer limits. Almeida <i>et al.</i> (2000) | 87 |
| Figure 36 - Geometry of the carbonated rocks of early Jurassic which constitute the most important support of the aquifer system Querença-Silves (dark blue colour, to the left of the Alibre thrust). Adapted from Manuppella <i>et al.</i> , (1993) | 87 |
| Figure 37 – Site location along Ribeiro Meirinho stream and central-western area of Querença-Silves aquifer and its piezometry (upper right: modelled; lower right: measured) (Leitão <i>et al.</i> , 2014) | 88 |
| Figure 38 – Hydrograph basin above selected MAR facilities in PT2 and related groundwater bodies | 89 |
| Figure 39 – Distribution of recharge in the Campina de Faro aquifer system (Lobo Ferreira <i>et al.</i> , 2006) | 90 |
| Figure 40 – Yearly variation of the modelled parameters (including aquifer recharge) in the artificial recharge area in an alluvium soil (Soil = “Atac”) and in a regossoil (Soil = “Rgc”) (Lobo Ferreira <i>et al.</i> , 2006) | 91 |
| Figure 41 - River flow cumulative curve and infiltration capacity of the IB (depending on the area of the IB), considering the infiltration capacity = 1.2 m/d | 91 |
| Figure 42 - Monthly rainfall and reference evapotranspiration (ETo) fluctuation for the period 10/2001-09/2014 in São Brás de Alportel meteorological station | 92 |
| Figure 43 - Yearly rainfall and reference evapotranspiration (ETo) fluctuation for the period 10/2001-09/2014 in São Brás de Alportel meteorological station | 93 |
| Figure 44 - Monthly surface runoff, natural recharge and actual evapotranspiration fluctuation for the period 10/2001-09/2014 in Rio Seco hydrographic basin upstream the infiltration basins | 93 |
| Figure 45 - Yearly surface runoff, natural recharge and actual evapotranspiration fluctuation for the period 10/2001-09/2014 in Rio Seco hydrographic basin upstream the infiltration basins | 94 |
| Figure 46 – Average surface runoff distribution in Rio Seco hydrographic basin upstream the infiltration basins | 94 |
| Figure 47 – Average groundwater recharge distribution in Rio Seco hydrographic basin upstream the infiltration basins | 95 |

| | |
|---|-----|
| Figure 48 – Average actual evapotranspiration distribution in Rio Seco hydrographic basin upstream the infiltration basins..... | 95 |
| Figure 49 - Average Querença-Silves aquifer recharge (period 1941-1991)..... | 96 |
| Figure 50 - Intensive greenhouse agricultural activity in the Campina de Faro aquifer system and traditional system of drains for collection of rainwater | 98 |
| Figure 51 – Traditional large diameter wells potentially suited for injection of harvested water | 98 |
| Figure 52 - Top: 32 year average annual rainfall spatial distribution on Campina de Faro aquifer system (CFAS) (based on Nicolau, 2002) and greenhouse's locations (based on APA-ARH Algarve, unpublished). Bottom left: 32 year average monthly and annual rainfall distribution values for the CFAS (based on Nicolau, 2002) | 99 |
| Figure 53 – Climate change impact in the water cycle in PT2 – Querença-Silves aquifer system (source: Oliveira <i>et al.</i> , 2012) | 103 |
| Figure 54 – Climate change impact in the water cycle in PT3 – Melide hydrographic basin (source: Oliveira <i>et al.</i> , 2012) | 104 |
| Figure 55 - Menashe infiltration site and catchment area – Location map and setting | 105 |
| Figure 56 - Geological setting of the Menashe site and its catchment area..... | 106 |
| Figure 57 - Menashe site model structure | 107 |
| Figure 58. (a) Watershed-scale model and MARSOL demosite location on geological map; surface watershed outline (white), stream discharge diversion channel (red), approximate chalk aquitard outline (blue) and sandstone aquifer outline (yellow); (b) geological cross-section A – A', conceptual groundwater level and flow directions | 108 |
| Figure 59. Annual precipitation sum in mm of the Regavim station (1965/66 - 2012/13) of the Israel Meteorological Service and monthly stream discharge at the infiltration basin inlet in Mio. m ³ (1966/67 – 2012/13) from MEKOROT Company..... | 109 |
| Figure 60- Location of the two test areas in the Demonstration Site 5, River Brenta Catchment, Vicenza, Italy | 114 |
| Figure 61- Map of the demonstration sites identified..... | 115 |
| Figure 62 – Scheme of the monitoring system in Schiavon (figure on left) and Loria Demo site (right figure) | 116 |
| Figure 63 - Direct Push investigation locations (numbered 1-10) and selected Direct Push electrical conductivity logging results | 119 |

| | |
|--|-----|
| Figure 64 - Results of the site characterization. Results of the electromagnetic survey, EM32 with 6m penetration depth (left) and location of Direct Push investigation points; Electrical Resistivity Tomography (Top); selected results of vertical Direct Push electrical conductivity logging (bottom)..... | 120 |
| Figure 65 - Installation of developed TDR sensors in (a) Schiavon and (b) Loria, MAR sites | 121 |
| Figure 66 - Sample TDR reading at Schiavon site | 122 |
| Figure 67 - Study area (Venetian Central Basin, Italy), model domain, boundary conditions.. | 123 |
| Figure 68 - Spatial distribution of hydraulic conductivity in x-direction inside the 3D model. | 124 |
| Figure 69 - Soil use/cover map and pedological map for the recharge area | 125 |
| Figure 70- Comparison between the simulated isophreatic contour lines and the observed ones (green line on the background)..... | 126 |
| Figure 71 – Comparison between the simulated and observed groundwater heads for the monitoring station in Crosara di Nove | 127 |
| Figure 72 – Comparison between the dispersive/drainage trunks of the rivers, well known in literature, and those ones obtained by the simulations carried out | 128 |
| Figure 73 – Comparison between the simulated and calculated outflows for some resurgence areas..... | 129 |
| Figure 74 – F.I.A.s considered in the second <i>post operam</i> scenario..... | 130 |
| Figure 75– F.I.A. recharge flows assumed in the second <i>post operam</i> scenario | 130 |
| Figure 76– Water table levels recorded in the Schiavon station from January 1992 to July 2011 | 131 |
| Figure 77– Average water table rise induced by the F.I.A. systems in the two simulated post operam scenarios | 131 |
| Figure 78– Simulated temporal trend of the water table rise induced by the F.I.A. systems in the fictitious monitoring station for the two post operam scenarios. | 132 |
| Figure 79 – Average Nitrates concentration in Veneto Region and in study area – ARPAV 2015 | 133 |
| Figure 80– Average Nitrates concentration in study area resulting from modelling activity – year 2007..... | 134 |
| Figure 81 – GroundWater bodies in the high venetian plain (in red the potential area for MAR) | 134 |

| | |
|--|-----|
| Figure 82 – Map of Arenales aquifer area and the zones with an advance deployment of MAR facilities. | 139 |
| Figures 83 – Scheme for Santiuste basin charting the boundary conditions taken into account for modeling (a), the storage capacity (b) and the hydraulic conductivity distribution (c) | 140 |
| Figures 84 – Scheme for the river-aquifer relations, distinguishing five different sections (a) and the representation of the wells used for irrigation (b) | 141 |
| Figure 85 – 4th alternative scheme. Direct pumping from boreholes plus infiltration ponds and a double irrigation network | 142 |
| Figure 86 – Changes in river-aquifer relations due to seasonal period and MAR activities | 143 |
| Figure 87 – Inventory of water points and extractions simulation in Carracillo Council | 143 |
| Figure 88 – Modflow screen shot used to dissociate natural and artificial recharge components | 144 |
| Figure 89 a) & b). Changes in water storage with different calibration premises causing divergent results | 145 |
| Figure 90 – Alcazarén area and the existing MAR facilities on it on orthophoto | 146 |
| Figure 91 – Santiuste basin. Initial MAR canal path and relevant features | 147 |
| Figure 92 – Santiuste basin scheme and groundwater monitoring network..... | 147 |
| Figure 93 – Example for zonal water budgets for Santiuste basin..... | 148 |
| Figures 94 – Triplet scheme deployed in Carracillo council composed by an infiltration pond, a canal and an artificial wetland. Natural vegetation is preserved and used to improve the water quality prior MAR water is spread in the flat area behind the artificial wetland | 149 |
| Figures 95 (a) (b) Initial results based on modelling in the Dehesa Boyal area (right), where the triplet scheme is being tested, to assess its convenience (a). A profile showing the expected groundwater evolution (b) | 149 |
| Figure 96 – Alcazarén aquifer scheme and main fault detected during geophysical prospecting phase | 150 |
| Figures 97. 3D Modelling for each structural subdivision in the conceptualization stage | 150 |
| Figure 98 – LNEC physical (sandbox) model construction | 154 |
| Figure 99 – LNEC physical (sandbox) model sections, A, B and C | 155 |
| Figure 100 – Detail of three soil layers being tested simultaneously (left) and the external piezometer (right) | 156 |

| | |
|--|-----|
| Figure 101 – Schematic diagram of the physical (sandbox) model dimensions and soil mixtures used in MARSol SAT experiments | 156 |
| Figure 102 – Vadose zone monitoring devices used in the physical (sandbox) model..... | 157 |
| Figure 103 – In situ monitoring devices, both for the saturated and vadose zones..... | 157 |
| Figure 104 – Bottles used to store the tracer for the physical (sandbox) model Experiment 1 | 159 |
| Figure 105 – Tracer grains on the top of the soil from the physical (sandbox) model, Experiment 2 | 160 |
| Figure 106 – Piezometric water level and electrical conductivity values in the three piezometers, Experiment 1 | 163 |
| Figure 107 – Breakthrough curves obtained for the water samples from the Section A piezometer | 166 |
| Figure 108 – Nitrogen concentrations in the vadose zone capsules (30 cm and 60 cm) from Section A..... | 167 |
| Figure 109 – Breakthrough curves obtained for the water samples from the Section B piezometer | 168 |
| Figure 110 – Nitrogen concentrations in the vadose zone capsules (30 cm and 60 cm) from Section B..... | 169 |
| Figure 111 – Breakthrough curves obtained for the water samples from the Section C piezometer | 170 |
| Figure 112 – Nitrogen concentrations in the vadose zone capsules (30 cm and 60 cm) from Section C..... | 170 |
| Figure 113 – Detail of the soil surface with the tracer used for Experiment 2 | 171 |
| Figure 114 – Piezometric water level and electrical conductivity values in the three piezometers, Experiment 2 | 172 |
| Figure 115 – Concentrations of N cycle in the water from the vadose (30 and 60 cm) and saturated (GW) zones | 174 |
| Figure 116 – Finite element grid for each modelled vertical section. Red cells represent natural soil while purple cells show the position of the soil mixture in Section B and organic matter layers in Section C | 176 |
| Figure 117 – Position of the observation points along each vertical section | 178 |
| Figure 118 – Nitrates distribution throughout the experiment per observation point in section A | 179 |

| | |
|--|-----|
| Figure 119 – Nitrites distribution throughout the experiment per observation point in section A | 179 |
| Figure 120 - Ammonia distribution throughout the experiment per observation point in section A | 179 |
| Figure 121 – Nitrates distribution throughout the experiment per observation point in section B..... | 180 |
| Figure 122 – Nitrites distribution throughout the experiment per observation point in section B | 180 |
| Figure 123 – Ammonia distribution throughout the experiment per observation point in section B | 181 |
| Figure 124 – Nitrates distribution throughout the experiment per observation point in section C..... | 181 |
| Figure 125 – Nitrites distribution throughout the experiment per observation point in section C | 182 |
| Figure 126 – Ammonia distribution throughout the experiment per observation point in section C | 182 |
| Figure 127 – Soil-column apparatus and diagram of operation | 184 |
| Figure 128 – Nitrogen cycle components concentration in Column 3 inflow/outflow | 185 |
| Figure 129 – Nitrogen cycle components concentration in Column 4 inflow/outflow | 186 |
| Figure 130 – Hydrus-1D results for nitrogen simulation (concentration through depth) | 188 |
| Figure 131– Hydrus-1D results for nitrogen simulation for node 1and 2 (S1 – ammonia, S2 – nitrites, S3 – nitrates)..... | 189 |
| Figure 132– Hydrus-1D results for nitrogen simulation for nodes 3, 4 and 5 (S1 – ammonia, S2 – nitrites, S3 – nitrates)..... | 190 |
| Figure 133 - Bromide BTCs at two observations points of the model. | 196 |
| Figure 134 - Modelling results (lines) versus observations (●) for MW-2 and MW-3. Solid lines correspond to 434 m a.s.l., dashed lines correspond to 435 m a.s.l. Red lines correspond to sulfate-reducer biomass, and green lines represent the results of the conservative model without reactions | 197 |
| Figure 135 - Simulation of nitrate isotope data in MW-2. Solid lines correspond to 434 m a.s.l., dashed lines correspond to 435 m a.s.l. and green lines represent the results of the conservative model without reactions | 197 |
| Figure 136 - Denitrification modelling cross section..... | 198 |

| | |
|--|-----|
| Figure 137 - Bacteria growth at the micrometer scale under fixed conditions of light and T at the topsoil (top), and corresponding isotropic variogram (bottom). | 212 |
| Figure 138 - 2D view of a heterogeneous 3D aquifer with a plume modelled by particle tracking..... | 212 |
| Figure 139 - Breakthrough curves of the different species in a network reaction | 213 |
| Figure 140 Set-up of the infiltration experiment. A 1 m tank was packed with soil, water infiltrated from the top. Several sensors were placed within the system to record a suite of physical, chemical and biological parameters. | 213 |
| Figure 141 - Several snapshots of the tracer test performed with fluoresceine (top). Recorded breakthrough at the outlet (bottom)..... | 214 |
| Figure 142 - Geophysical survey in Querença-Silves aquifer at Cerro do Bardo | 216 |
| Figure 143 - Modelling Contributions of the Local and Regional Groundwater Flow of Managed Aquifer Recharge Activities at Querença-Silves Aquifer System | 218 |
| Figure 144 - Integration scheme of partial models..... | 219 |
| Figure 145- Shape of an injection blobs with equal volume and very different contact area.. | 222 |
| Figure 146 - Location of injection and extraction wells (left). Distribution of extraction and injection flow rates as a function of time (right) for the different wells involved..... | 222 |
| Figure 147 - Variation of anaerobic surface as a function of time under continuous pumping and chaotic advection approaches. Homogeneous and heterogeneous permeability fields are investigated | 223 |
| Figure 148 - Conceptual model structure. The modelled area (a), the major marine clay lenses (b) and the combined deterministic and stochastic material array representing the aquifer . | 225 |
| Figure 149 - Modelled water levels before (a) and after (b) infiltration..... | 226 |
| Figure 150 - Cumulative water balance for the surface and subsurface water bodies during and after MAR of 2.6×10^6 m ³ (evaporation is estimated as only $\sim 0.3\%$ of the total discharge) ... | 227 |
| Figure 151 - Observed Vs. calculated groundwater level at the pilot site (PA well, pond #3).. | 227 |
| Figure 152– Campina de Faro river bed MAR facilities | 232 |
| Figure 153 – Location of Piezometers CB1 and CB2 in the recharge field | 233 |
| Figure 154- Hydrogeological conceptual model | 234 |
| Figure 155– Results of the falling head infiltration test in Cerro do Bardo (December, 2014) | 234 |

| | |
|--|-----|
| Figure 156 - Conceptual cross-section representing the lithological setting which supports the main aquifers on the Island of Malta | 235 |
| Figure 157 - Preliminary groundwater flow model presented by Monteiro et al., (2016). Finite element mesh, spatial distribution of transmissivity and scatter plot between observed and calculated hydraulic head for the year of 1944 | 236 |
| Figure 158 - Screenshots of solute transport module within FREEWAT modelling platform... | 237 |
| Figure 159 - QGIS Plugins web page, showing DataExplorer (last access March 7th, 2016) | 238 |
| Figure 160 - Composite scaled sensitivity for the surface water model | 240 |
| Figure 161 - Dimensionless scaled sensitivity for the surface water model parameters | 241 |
| Figure 162 - Dimensionless scaled sensitivity for the groundwater model | 242 |
| Figure 163 - Composite scaled sensitivity graph for the groundwater flow model..... | 242 |
| Figure 164 - a) PRMS domain, Menashe streams (light blue lines), diversion channel (red lines), watershed location (black line), HRUs (colored polygons), and the MODFLOW grids (grey lines); b) MODFLOW model domain, layer depth in meter (vertical exaggeration of 10), colors representing hydraulic conductivity (red - high, green - low, blue - very low) | 244 |
| Figure 165 - Model fit for the sensitivity and calibration period of the hydrological year 2003/04, comparing simulated and field observed a) groundwater heads, b) distribution of residuals and c) sum of discharge of the four gauging stations..... | 246 |

Tables

| | |
|---|-----|
| Table 1 – Groundwater bodies intersected by the hydrographic basin above Rio Seco MAR facilities | 85 |
| Table 2 - Estimated average monthly and annual potential rainfall harvested from greenhouses | 100 |
| Table 3 – Projected precipitation and temperature variations in different climate change scenarios | 101 |
| Table 4 – Average yearly values of natural groundwater recharge and surface runoff obtained by the actual 1979-2009 time series and estimated values under the different climate change scenarios | 104 |
| Table 5 – Physical sandbox compartment's dimensions..... | 158 |
| Table 6 – Fertilizer tracer concentration calculation for Experiment 1 | 159 |
| Table 7 – Hydrocarbon (HC) and NaCl tracer concentration calculation for Experiment 1 | 160 |
| Table 8 – Sampling protocol for the Experiment 1 | 161 |
| Table 9 – Sampling protocol for the Experiment 2 | 161 |
| Table 10 – Main characteristics of Experiment 1 | 162 |
| Table 11 – Results from the chemical analysis of water samples collected during Experiment 1 | 163 |
| Table 12 – Results from the chemical analysis of soil samples collected after Experiment 1 finished..... | 167 |
| Table 13 – Main characteristics of Experiment 2 | 172 |
| Table 14 – Results from the chemical analysis of water samples collected during Experiment 2 | 173 |
| Table 15 – Input data for artificial aquifer FEFLOW models | 175 |
| Table 16 - Synthesis of the operating details of the soil-column experiments conducted in the natural soil..... | 184 |
| Table 17 – Input data for HYDRUS-1D C3 and C4 models | 186 |
| Table 18. Reactive processes involved in biogeochemical modelling..... | 195 |
| Table 19. Reactions considered in the system, with the corresponding reactive terms | 223 |

White book on MAR modelling

Deliverable D12.7

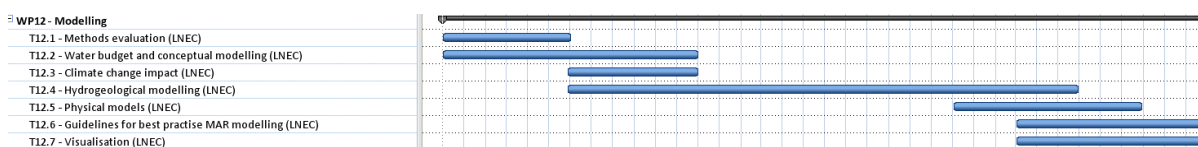
CHAPTER 1 – MARSOL WP12 MODELLING ACTIVITIES AND DEMO-SITES INTRODUCTION

J.P. LOBO FERREIRA, TERESA LEITÃO, TIAGO MARTINS, MANUEL M. OLIVEIRA AND ANA MARIA CARMEN ILIE (LNEC), JOSÉ PAULO MONTEIRO, LUÍS COSTA AND RUI HUGMAN (UALG), TIAGO CARVALHO, RUI AGOSTINHO AND RAQUEL SOUSA (TARH), LAURA FOGLIA, ANJA TOEGL AND CHRISTOS POULIARIS (TU DARMSTADT), RUDY ROSSETTO (SSSA), IACOPO BORSI (TEA), XAVIER SANCHEZ-VILA AND PAULA RODRIGUEZ-ESCALES (UPC), ENRIQUE FERNÁNDEZ ESCALANTE, RODRIGO CALERO GIL, FRANCISCO DE BORJA GONZÁLEZ HERRARTE, MARÍA VILLANUEVA LAGO (TRAGSA), JON SAN SEBASTIÁN SAUTO (TRAGSATEC), ANDREAS KALLIORAS (NTUA), YORAM KATZ (MEKOROT)

1 MARSOL WP12 MODELLING ACTIVITIES

1.1 OBJECTIVES AND DETAILS OF TASKS

The contribution of Workpackage 12 to MARSOL Final report addresses the work developed in all Tasks, i.e. not only T12.1 (month 1-6), T12.2 (month 1-12), T12.3 (month 6-12), T12.4 (month 6-30), already addressed in the Mid-term report (dated July 14th, 2015) but also in the new addressed tasks T12.5 – Physical models (month 24-33), T1.6 - Guide lines for best practices (month 27-36) and T12.7 – Visualisation (month 27-36):



Concerning Task 12.1, the general literature review on modelling approaches for MAR sites task, included several previous MAR projects developed by MARSOL partners. Some of the more relevant MAR modelling applications collected in this review are summarised in D12.7 White book on MAR modelling, besides having being preliminary presented in the Interim

Report for the Project Period December 2013 – August 2014, where the scale of application, the model used and the application objective have been described.

Concerning Tasks 12.2 and 12.3, Deliverable 12.1 on water budget and climate change impact assessment of selected MARSOL demo site areas (Portugal, Greece, Israel and Spain) was developed during the 2nd reporting period September 2014 – May 2015. During the second report period Deliverable 12.2 has also addressed. This included the development of specifications towards its achievement and also completed the requirements analysis (first round) based on the demo sites visits and the Field Trip Books provided for three MARSOL demo sites (Menashe - Israel, Arenales - Spain, and Sant'Alessio - Italy), plus the Portuguese demo sites, in order to identify the elements that could be incorporated in D12.2 GIS database of the MARSOL demo sites.

Concerning Task 12.4, aiming data gathering for hydrogeological modelling, infiltration tests with tracer experiments were performed in PT demo sites by partner TARH, UAlg and LNEC. Follow-up groundwater quantity and quality monitoring and specifically designed two geophysical experiments by partner LNEC have been conducted at PT Querença-Silves Demo site during December 2014 and April 2016, aiming data gathering for the conceptual model and the follow-up of the tracer into the aquifer during the 90 hours MAR tracer experiment. For PT Campina de Faro Demo site, and for south Malta new finite element groundwater flow models (with FEFLOW model purchased with MARSOL budget) was developed by partner UAlg.

1.1.1 On Task 12.1: Methods evaluation (month 1-6):

A literature review on potential and currently applied modelling approaches for MAR sites and the evaluation of weaknesses and strengths has been developed. A 40 page report was concluded December 2016, to be included as Chapter 1 of D12.7 (due month 36), with the title STATE OF THE ART AND LITERATURE REVIEW IN MANAGED AQUIFER RECHARGE MODELLING, authored by LNEC (Martins, T. and Lobo-Ferreira, JP., 2016).

1.1.2 On Task 12.2: Water budget and conceptual modelling (month 1-12)

Deliverable 12.1 “Water budget and climate change impact” assessed for selected MARSOL case-study areas (Portugal, Greece, Israel and Spain) information on their water budget and on modelling expertise, in connection with the work developed for specific case-studies and thematic deliverables, e.g. for Portugal in Deliverable 4.2 on “South Portugal MARSOL demonstration sites characterisation” and Deliverable 8.1 on “DSS with integrated modelling capabilities”, with modelling examples from Italy, e.g. “first application of the FREEWAT preliminary scripts on the S. Alessio site”.

1.1.3 On Task 12.3: Climate change impact (month 6-12)

The starting point for this task was the DEMO Site 2 – PT2 Querença-Silves Aquifer. Groundwater recharge assessments models, e.g. BALSEQ_MOD developed by partner LNEC, and groundwater vulnerability assessment methods, e.g. DRASTIC mentioned in the DoW, have been applied to PT demo site. Concerning the climate change impact in the study area DEMO Site 2 – PT2 Querença-Silves Aquifer, the research team of the University of the Algarve

(UAlg) presented a description regarding groundwater flow simulation of future scenarios using the ENSEMBLES projections (A1b scenarios) for recharge. These predictions were compared with others made for instance during the Portuguese FCT sponsored ProWaterMan project for the same area, by UAlg and LNEC partners. These PT results are useful to assess the role of MAR in MARSOL aquifer systems, taking into account the future trends of climate change patterns expected for the other MARSOL demo sites.

1.1.4 On Task 12.4: Hydrogeological modelling (month 6-30)

The reporting of Deliverables 12.3 on “Progress report on numerical models of the MARSOL DEMO sites” was concluded in September 2015, for selected MARSOL case-study areas (Portugal, Italy, Spain, Israel and Greece). A contribution from TUDa on to the hydrological/hydrogeological models for the Lavrio test site (WP 3) and the Menashe test site (WP 9) was included. These contributions are related to regional and local scales. Complementary contributions on laboratorial scales, from LNEC and IWW, on WP 14s “Contaminants modelling at column scale”, and from UPC on “Modelling the potential impact of chaotic advection to enhance degradation of organic matter and emergent compounds” have been included. Partner IWW worked on hydrochemical modelling within WP 14. Partner TUDa implemented a coupled surface water/groundwater model for both the Lavrio (Greece) and Menashe (Israel) demo sites and the saturated flow model of the Coastal aquifer – Menashe region, Israel, was developed by partner Mekorot.

1.1.5 On Task 12.5: Physical models at LNEC (month 24-33)

Regarding Task 12.5, the construction of MARSOL physical sandbox model (nicknamed at LNEC as the “artificial aquifer” model) was achieved and research MAR tracer experiments have been developed and concluded by partner LNEC. The aim was to get knowledge on quantity and quality tracer experiment percolation through three different natural and man-made soil types, to be used in two prototype basins for SAT-MAR “artificial recharge” towards gathering data for later SAT-MAR modelling in PT3_7 Melides, included in Deliverable D12.7 White book on MAR modelling.

1.1.6 On Task 12.6: Guide lines for best practices (month 27-36)

The results achieved in the development of this task will be presented in MARSOL D12.7 White book on MAR modelling (due month 36), that includes (1) the STATE OF THE ART AND LITERATURE REVIEW IN MANAGED AQUIFER RECHARGE MODELLING, by LNEC (Martins, T. and Lobo-Ferreira, JP., 2016), (2) MAR THROUGH FORESTED INFILTRATION IN THE RIVER BRENTA CATCHMENT, VICENZA, ITALY, by SGI and AAWA (Elisa Filippi (SGI), Vincenzo Marsala (SGI), Michele Ferri (AAWA), Alberto Cisotto (AAWA), Giovanni Tomei (AAWA) (3) the SANDBOX MODEL EXPERIMENTS RESULTS AND NUMERICAL MODELLING, by LNEC (Leitão, T.E., Martins, T., Henriques, M.J., Ilie, A.M.C. and Lobo-Ferreira, J. P., 2016), and (4) TRAGSA MARSOL MODELING ACTIVITIES by TRAGSA (Enrique F. Escalante et al.).

1.1.7 On Task 12.7: Visualization

Deliverable 12.4 on the Final Report on numerical model, for all MARSOL demo sites in Greece, Portugal, Spain, Italy, Israel and Malta, was ready for publishing July 2016. Complementing the work developed in Workpackage WP12 on Modelling, as presented in the above mentioned

Deliverable 12.4, several pdfs and videos have been developed to facilitate the visualisation of the hydrogeological assessment, the experiments carried on MARSOL demo sites, as well as their modelling results.

The achievements related to modelling addressed in other Workpackages have also been considered, e.g. the latest results, in video format, obtained in WP4 Deliverable 4.4 on the Hydrogeological modelling at the South Portugal MARSOL demonstration sites, the overview presented in Deliverable 9.4 on “A combined un-saturated and aquifer flow model for the Menashe site” co-authored by Yoram Katz (Mekorot), Yonatan Ganot (ARO), Daniel Kurtzman (ARO) and the Demo Site 8, South Malta Coastal Aquifer results achieved by the University of the Algarve (UALG) depicting the development of a numerical groundwater 3D model for the MSLA sector of the aquifer south to the Victoria Fault. Also a video with modelling information for Italy Deliverable 8.1 on “DSS with integrated modelling capabilities” has been included.

The videos, Demo site by Demo site, have been uploaded in MARSOL cloud, and are available in

https://cloud.marsol.eu/apps/files/?dir=%2F12%20Modelling%2FWP12%20D12_6%20Videos .

The EIP water "MAR Solutions - Managed Aquifer Recharge Strategies and Actions (AG128)", coordinated by MARSOL partner LNEC, was used as a forum for transferring the knowledge and work developed in MARSOL worldwide. Background Activity 5 MODELLING docs, MARSOL WP 12 Modelling Workshop Lisbon July 2104 and MARSOL Algarve Water Quality Workshop June 2015 modelling pdfs are available in http://www.eip-water.eu/MAR_Solutions and in <http://www.eip-water.eu/algarve-water-quality-workshop-great-success> .

1.2 SIGNIFICANT RESULTS

The outputs of WP 12 have been included in Deliverables D12.1 Water budget and climate change (due month 12), D12.2 GIS database of the MARSOL demo sites (due month 18), D12.3 Progress report on numerical models of the MARSOL DEMO sites: Interim progress report on numerical models of the MARSOL artificial recharge DEMO sites (due month 21), D12.4 Numerical models of artificial recharge at the MARSOL DEMO sites: Numerical hydrogeological models of artificial recharge for all MARSOL DEMO sites (due month 30), D12.5 - Physical modelling of selected MARSOL DEMO sites: Report on the physical modelling of selected case study sites (sandbox models, due month 33), D12.6 Video visualisation of MAR at the MARSOL DEMO sites (due month 36), and D12.7 White book on MAR modelling (due month 36). Three requested by the coordinator TUDa, detailed interim reports have been submitted on time, *i.e.* the Interim Report for the Project Period December 2013 – August 2014, the Interim Report for the Project Period September 2014 - May 2015 and the Interim Report for the Project Period June 2015 - February 2016.

Four Workshops have been organized during the project to facilitate the work reported on WP 12. Besides Lisbon WP 12 Modelling Workshop, held July 2014, we highlight the “Progress Report” Modelling Workshop during the 1st Year MARSOL Meeting held in Tel-Aviv (Israel),

December 2014, and the DoW programmed MARSOL workshop on „Modelling“, held in Pisa during the 21-23 April 2015. Around 100 people attended a complementary one-day international „Modelling“ workshop, organized by partner SSSA. The ppts of the presentations are available in <http://www.eip-water.eu/working-groups/mar-solutions-managed-aquifer-recharge-strategies-and-actions-ag128>.

MARSOL WP 12 Modelling Workshop Lisbon July 2104 and MARSOL Algarve Water Quality Workshop June 2015 modelling pdfs are available in EIP water AG 128 Mar to Market site http://www.eip-water.eu/MAR_Solutions and in EIP water innovation news <http://www.eip-water.eu/algarve-water-quality-workshop-great-success>.

Several publications have been prepared and presented to international conferences, *e.g.* the one on “Modelling Contributions of the Local and Regional Groundwater Flow of Managed Aquifer Recharge Activities at Querença-Silves Aquifer System (UALG, TARH, LNEC)”, available from

https://www.researchgate.net/publication/275716406_Modelling_Contributions_of_the_Local_and_Regional_Groundwater_Flow_of_Managed_Aquifer_Recharge_Activities_at_Querença-Silves_Aquifer_System.

2 MARSOL WP 12 DEMO-SITES INTRODUCTION

2.1 DEMO SITE 1: LAVRION TECHNOLOGICAL & CULTURAL PARK, LAVRION, GREECE

The Lavrion Technological & Cultural Park, Lavrion, Greece area (**Figure 1**) is characterized by a complicated geological structure with many controversies.

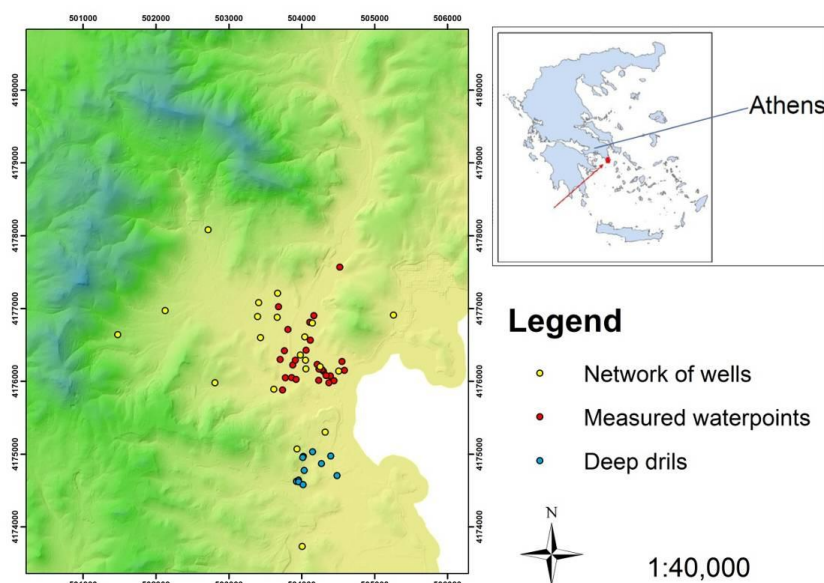


Figure 1 – Geographical locations and points of interest the Lavrion basin

The climate is a typical Mediterranean climate with dry and hot summer periods.

In the alluvial plain there is a dense network of shallow wells extending in an area of about 5 km². These wells have been sampled for heavy metals and major ions and where the water level depth was also measured in May and August 2014. This network is completed by a cluster of deeper drills placed in the Lavrion Technological and Cultural Park.

2.2 DEMO SITE 2: ALGARVE AND ALENTEJO, SOUTH PORTUGAL

Deliverable 4.5 integrates an update of all the relevant work done for WP4 “DEMO Site 2: Algarve and Alentejo, South Portugal”, previously reported. This Deliverable 4.5, together with Deliverable 4.4 concerning hydrogeological modelling at the South Portugal MARSOL demonstration sites, summarize all work performed in the Portuguese DEMO sites.

The main objectives of WP4 are to demonstrate how MAR can contribute as an alternative source of water, in the context of an integrated and inter-annual water resources management, as well as in solving groundwater quality problems caused by previous agricultural practices and wastewater discharges.

Three DEMO sites (Figure 2) have been chosen for WP4:

PT1: Rio Seco and Campina de Faro aquifer system (Algarve)

PT2: Querença-Silves limestone karstic aquifer system (Algarve)

PT3: Melides aquifer, river and lagoon (Alentejo)

In PT1 – Rio Seco and Campina de Faro aquifer system (Algarve) – the main goal is to improve the groundwater quality heavily contaminated with nitrates (vulnerable zone), mainly due to agriculture bad practices.

In PT2 – Querença-Silves limestone karstic aquifer system (Algarve) – there are two main sub-areas and two goals: (1) develop a soil-aquifer-treatment (SAT) system to improve the water quality of treated effluents from a waste water treatment plant (WWTP) (PT2_4), which discharges into Ribeiro Meirinho river (PT2_5) that recharges the karstic aquifer, and (2) increase groundwater storage at Cerro do Bardo karstic area using wet years surface water surplus to increase the water availability in dry years and facilitate downstream water supply.

In PT3 – Melides aquifer, river and lagoon (Alentejo) – the main goal is to use SAT-MAR to remove rice field pollutants prior to their discharge in Melides lagoon.

The work developed for the different DEMO sites was developed in the following tasks:

Task 4.1: Recharge water availability

Task 4.2: Developing the (MAR) infrastructures

Task 4.3: Investigation and monitoring

Task 4.4: Modelling

The results are being presented in five main deliverables:

D4.1: Water sources and availability at the South Portugal MARSOL demonstration sites

D4.2: South Portugal MARSOL demonstration sites characterisation

D4.3: Monitoring results from the South Portugal MARSOL demonstration sites

D4.4: Hydrogeological modelling at the South Portugal MARSOL demonstration sites

D4.5: MAR to improve the groundwater status in South Portugal (Algarve and Alentejo)

This report presents the results from D4.3: Monitoring results from the South Portugal MARSOL demonstration sites.

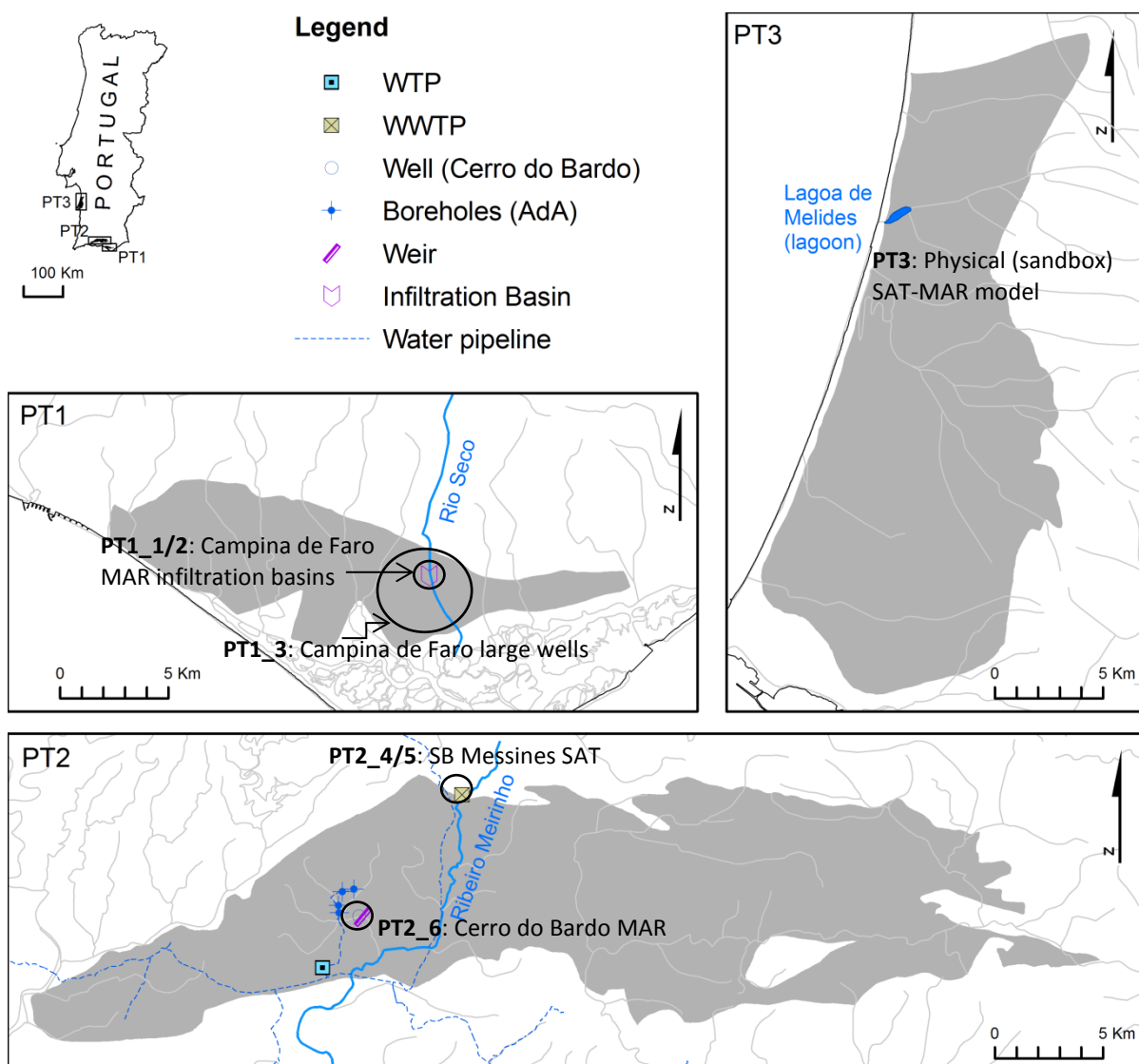


Figure 2 – PT MARSOL DEMO sites location (the aquifers boundaries are marked in grey)

2.3 DEMO SITE 3: LOS ARENALES AQUIFER, CASTILLE AND LEON, SPAIN

The WP activities involve the three areas integrated into the Demo Site 4 “Arenales aquifer, Castilla y León, Spain). These zones with important MAR facilities deployed are Santiuste basin, Carracillo district and Alcazarén Area, represented in the Figure 3.

Within the framework of MARSOL project, the modeling activity for this demo site has a complex background what deserves to be introduced and explained. The partner in charge, Tragsa, has conducted two models in Visual Modflow for Santiuste and Carracillo areas, by direct request of the Spanish Ministry of Agriculture... These models are active and new simulations might be performed. The biggest constraint is the property of the datasets and the results, which are in the hands of the client. Consequently, neither the models nor the files can be shared between partners.

The third area, Alcazarén, is a new one and activities have begun in 2012, after some years of litigations in the court due to the fact that there was a transfer between two different provinces and both claimed the property of water. The model is in a very initial stage, with the conceptualization and definition of boundary conditions phases already done. Now the main activity is related to the capture of datasets, in order to advance in the development of the modeling endeavor.

Apart from the description of the areas, the geo-referenced files with all the operative facilities for three sites were provided in deliverable 12-2. They are in a compatible format to be included in any GIS program and available for potential users.

This chapter exposes, firstly, the works done by Tragsa Group regarding modeling for external clients and the advance in the knowledge of the aquifer thanks to the use of this tool.

Later, regarding the activity related to MARSOL, the models have been used to achieve some specific results and to provide guidance for very concrete actions and presentation of alternatives: in specific areas, such as zonal balances (Zbud) for defined sections in the aquifer of Santiuste (at both sides of the hydrogeological barrier); the behavior around MARSOL “piezostar” in Carracillo (see deliverable 5-1 for a detailed description of the environmental conditions and the groundwater behavior).

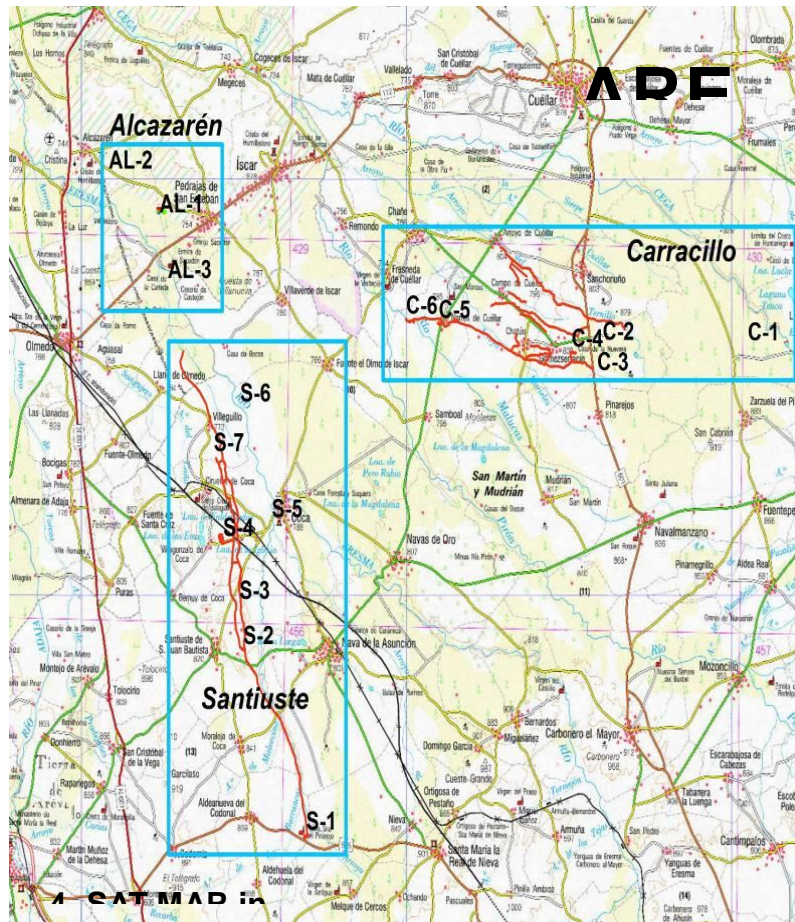


Figure 3 – Map of Arenales aquifer area and the zones with an advance deployment of MAR facilities

2.4 DEMO SITE 5: RIVER BRENTA CATCHMENT, VICENZA, ITALY

The two Marsol pilot sites selected in Italy, namely **Demo Site 5 “River Brenta Catchment, Vicenza, Italy”**, are located in the upper plain of the Veneto Region (**Figure 4**). The first one site is a F.I.A. (Forested Infiltration Area) used during the LIFE+ funded TRUST project, while the other site is suitable for serving two different functions: floods retention area and managed artificial recharge.

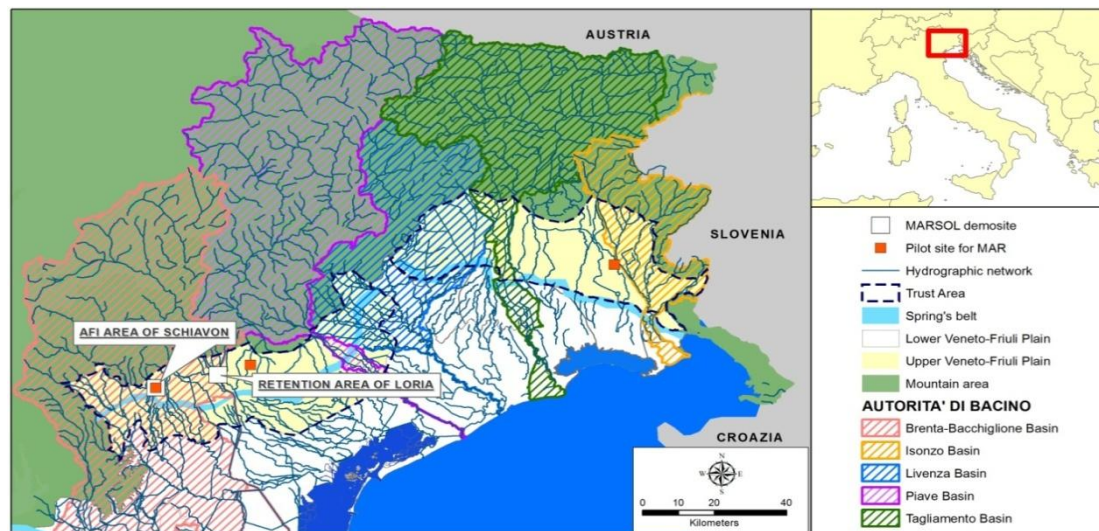


Figure 4- Location of the two test areas in the Demonstration Site 5, River Brenta Catchment, Vicenza, Italy

DEMO site activities included the implementation of monitoring and mathematical modelling in order to monitor and model infiltration rates and quality processes. The monitoring has provided insight about the enhancements that the F.I.A. and flood retention basin offer for MAR both in quantity (improving infiltration rates) and quality terms (due to the effects of the biological systems linked to the plant roots). Mathematical modelling focused on assessing the impact of the MAR in the restoration of the resurgence system. The benefits of cultivation in the MAR area to prevent clogging have been assessed as well as the potential of MAR to improve water quality aspects.

2.5 DEMO SITE 7: MENASHE INFILTRATION BASIN, HADERA, ISRAEL

The Menashe facility is being used over 40 years for groundwater enrichment of the coastal aquifer using collected surface water. During the winter, as the major streams draining the southern Mt. Carmel slopes and the Menashe hills start to flow, part of the water is diverted by a system of dams and canals into a main conveyance canal. Driven further 16 Km west by gravitation the water is introduced into infiltration ponds for coastal aquifer enrichment, and later pumped by production wells (Figure 5). In addition to runoff infiltration, desalinated water originating from the nearby Hadera desalination plant is periodically introduced into the aquifer according to maintenance requirements. The physical and chemical processes involved in this type of aquifer enrichment are the essence of the demo site activity and research.

The mid-scale model deals with saturated flow within the coastal aquifer, underlying the Menashe infiltration facility area. It will correspond to both the larger watershed scale and the smaller, infiltration pond scale future models.

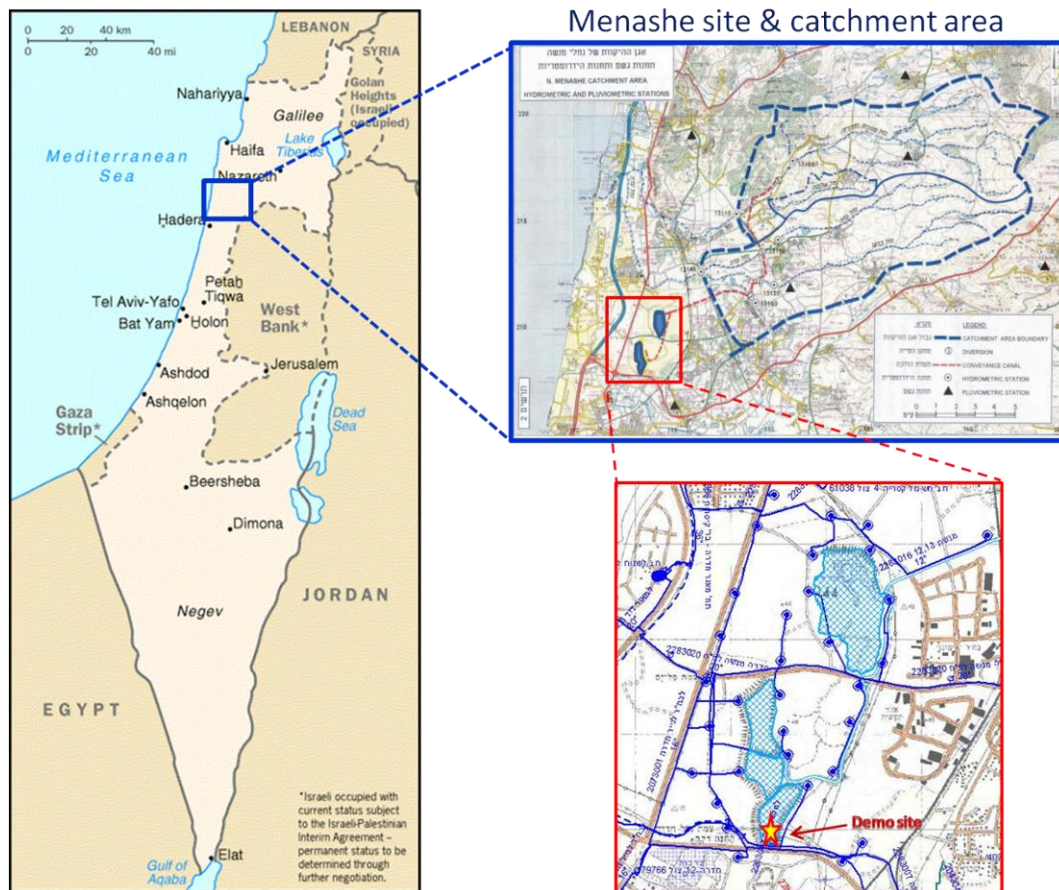


Figure 5 - Menashe infiltration site and catchment area – Location map and setting

2.6 DEMO SITE 8: SOUTH MALTA COASTAL AQUIFER, MALTA

On the island of Malta groundwater resources are extremely limited due to high population density and low recharge, and the aquifers are affected by seawater intrusion and by high NO₃ concentration. Groundwater for public water supply is mostly obtained by means of excavated deep shaft wells that penetrate down to the karstified limestone where a thin freshwater lens floats on saline water. To reduce the localized effect of drawdowns and associated upcoming, these wells are connected by a radial network of drainage galleries with variable height spillways to control groundwater drainage. Since the 1960's potable water supply has been supplemented by desalinated water, which currently accounts for approximately 50% of municipal supply. Despite this supplement, increasing water demand for irrigation has maintained pressure on groundwater high and current estimates suggest that groundwater use is close to or exceeds average annual recharge.

Most of the treated wastewater in the island of Malta is driven for agriculture irrigation, yet some part is rejected to the sea (circa 2 hm³/year), once it is not necessary. Adding to this, the increase in groundwater exploration has reflected in a degradation of groundwater quality and

quantity. Quality degradation is due to the thin freshwater lenses that overlap seawater, leading to a fragile system that can easily suffer seawater intrusion with the increase in groundwater exploitation of the Malta Mean Sea Level aquifer system (MSLA).

A proposed solution to contribute to achieving a good status of fresh groundwater applied during the MARSOL project consists in inverting the quantitative and qualitative degradation of the MSLA aquifer originated from the seawater intrusion, by means of infiltrating the surplus of treated wastewater. The goal of the MAR scheme in this case study consists in increasing groundwater level at MSLA at the Southeast section of the island, thus, creating a barrier to the lateral and vertical seawater intrusion. To achieve this goal, it is being proposed the infiltration of the surplus of treated wastewater in deep boreholes.

The case study area is located in the island of Malta and consists of the area of the Malta Mean Sea Level Aquifer (MSLA) to south of the Victoria Fault (**Figure 6**). The MSLA has a total area of 217 km² and the case study modeled area has a total area of 185.79 km².

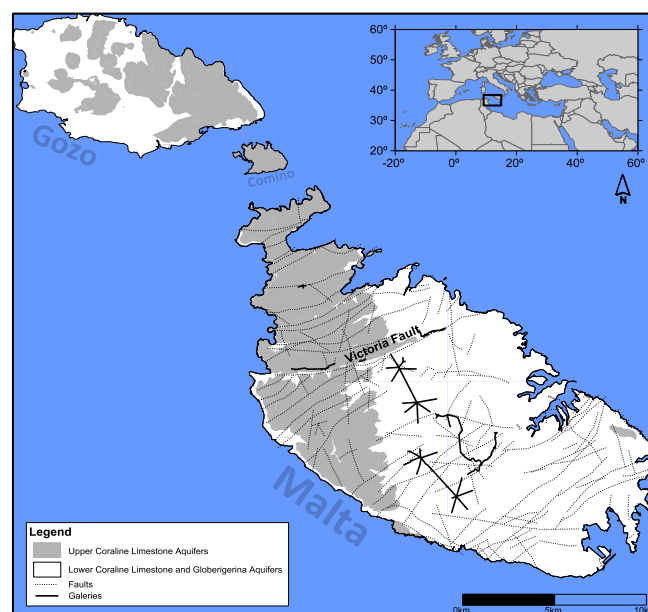


Figure 6 - Geographical location and main hydrogeological features of the Maltese islands


2.7 VISUALISATION AND INTERACTION WITH MARSOL WPs

The Deliverable 12.4 on the Final Report on numerical model, for all MARSOL demo sites in Greece, Portugal, Spain, Italy, Israel and Malta, was ready for publishing July 2016.

Complementing the work developed in Workpackage WP12 on Modelling, as presented in the above mentioned Deliverable 12.4, several pdfs and videos have been developed to facilitate the visualisation of the hydrogeological assessment, the experiments carried on MARSOL demo sites, as well as their modelling results.

The achievements related to modelling addressed in other Workpackages have also been considered, e.g. the latest results, in video format, obtained in WP4 Deliverable 4.4 on the Hydrogeological modelling at the South Portugal MARSOL demonstration sites, the overview presented in Deliverable 9.4 on “A combined un-saturated and aquifer flow model for the Menashe site” co-authored by Yoram Katz (Mekorot), Yonatan Ganot (ARO), Daniel Kurtzman (ARO) and the Demo Site 8, South Malta Coastal Aquifer results achieved by the University of the Algarve (UALG) depicting the development of a numerical groundwater 3D model for the MSLA sector of the aquifer south to the Victoria Fault. The following chapters address videos, Demo site by Demo site, that have been uploaded in MARSOL cloud, available in

https://cloud.marsol.eu/apps/files/?dir=%2F12%20Modelling%2FWP12%20D12_6%20Videos



| | Nome | Groupmanager | Tamanho |
|--|--------------------------------------|--------------|---------|
| | 03 Lavrion | Groupmanager | 55.6 MB |
| | 04 Algarve | Groupmanager | 2.3 GB |
| | 05 Arenales | Groupmanager | 97.1 MB |
| | 06 Llobregat | Groupmanager | 17 MB |
| | 07 Brenta | Groupmanager | 27.7 MB |
| | 08 Serchio | Groupmanager | 3.5 MB |
| | 09 Menashe | Groupmanager | 95.7 MB |
| | 10 Malta | Groupmanager | 51.6 MB |
| | WP-12_Modelling_LNEC_LF_Leipzig.pptx | Groupmanager | 49.3 MB |

Complementary pdfs introducing the Demo Sites areas (including Serchio and Llobregat demo sites) are also available in the above mentioned site.

MARSOL project partners also researched developed and applied in different Work Packages, for several MARSOL Demo Sites, modelling activities. A selection of those modelling activities, extracted from MARSOL Interim Reports is presented in ANNEX 1:

- Demo site 4 activities: Llobregat river infiltration basins, Sant Vicenç dels Horts (Barcelona)
- Geophysical survey, with the resistivity method, for PT Querença-Silves demo site conceptual model
- Modelling contributions of the local and regional groundwater flow of managed aquifer recharge activities at Querença-Silves aquifer system (WP4)
- Hydrological/hydrogeological models for the Lavrio test site (WP 3) and the Menashe test site (WP 9)
- Modelling contributions in demo site 6 Serchio river well field
- Marsol WP 12 modelling workshop, Pisa, Italy, April, 2015

- Modelling contributions of the local and regional groundwater flow of managed aquifer recharge activities at WP 4 Algarve Campina de Faro and Querença-Silves aquifer systems
- UAlg numerical modelling of the mean sea level aquifer (MSLA) of Malta
- Modelling contributions in demo site 6 - Serchio river well field
- TUDa modelling activities at demo site 1 (Lavrio, Greece)
- TUDa modelling contributions in demo site 7: Menashe infiltration basin, Hadera, Israel

3 MARSOL WP 12 MODELLING PUBLICATIONS

PAPERS

- LEITÃO, T. E., MOTA, R., NOVO, M.E. e LOBO FERREIRA, J.P. (2014) - Combined Use of Electrical Resistivity Tomography and Hydrochemical Data to Assess Anthropogenic Impacts on Water Quality of a Karstic Region: a Case Study from Querença-Silves, South Portugal. *Environmental Processes. An International Journal*, ISSN 2198-7491, Volume 1, Number 1. (2014) 1:43–57, DOI 10.1007/s40710-014-0002-1.
- COSTA, L.; MONTEIRO, J.P.; HUGMAN, R.; LOBO-FERREIRA, J.P.; CARVALHO, T. (2015) Estimating harvested rainwater at greenhouses in south Portugal aquifer Campina de Faro for potential infiltration in Managed Aquifer Recharge. Manuscript submitted for publication on the special edition 'Environmental and socio-economic methodologies and solutions towards integrated water resources management' of the Science of The Total Environment on 31 December 2015
- MONTEIRO, J. P.; HUGMA, R.; COSTA, L.; OLIVEIRA, M. M.; SCHEMBRI, M.; SAPIANO, M. (2016). Contributo de Modelação no Aquífero Costeiro da Ilha de Malta para a Gestão Integrada de Recursos Hídricos (English title: Contribute of Modelling in the Coastal Aquifer of the Malta Island for the Integrated Management of Water Resources). 13º Congresso da Água, 11-13 Março, Lisboa.
- NEVES, M.; COSTA, L.; MONTEIRO, J.P. (2016) "Climatic and geologic controls on the piezometry of the Querença-Silves karst aquifer (Algarve)". *Hydrogeology Journal*. Springer
- HUGMAN, R.; MONTEIRO, J.P.; VIEGAS, J.; GÓIS, A.; COSTA, L.; STIGTER, T. (2015) Re-assessing the coastal groundwater management policy in the Algarve (Portugal) based on estimates of the potential for seawater intrusion. 42nd IAH Congress. Rome, Italy.
- MARTINS, T. (2016) Contaminants retention in soils as a complementary water treatment method: application in soil-aquifer treatment processes. Master Thesis. Faculty of Sciences. University of Lisbon, 2016.

MARSOL WP 12 REPORTS AND DELIVERABLES

- LOBO FERREIRA, J.P., OLIVEIRA, M.M., MARTINS, T., MONTEIRO, J.P., COSTA, L., FOGLIA, L., POULIARIS, C., KALLIORAS, A., SANCHEZ-VILA, X. (2014) – WP12 Modelling.

- Interim Report for the Project Period December 2013 – August 2014. MARSOL Demonstration Sites Characterisation. Projeto UE MARSOL - Demonstrating Managed Aquifer Recharge as a Solution to Water Scarcity and Drought, julho 2014, 33 pp.
- LOBO FERREIRA, J.P., OLIVEIRA, M.M., MONTEIRO, J.P., COSTA, L., FOGLIA, L., POULIARIS, C., KALLIORAS, A., KATZ, Y., ESCALANTE, E. (2015) – “Deliverable 12.1 Water budget and climate change impact”. MARSOL Demonstrating Managed Aquifer Recharge as a Solution to Water Scarcity and Drought, janeiro 2015, 69 pp.
 - OLIVEIRA, M.M., LOBO FERREIRA, J.P., MONTEIRO, J.P., COSTA, L., HUGMAN, R., CARVALHO, T., LEITÃO, T., POULIARIS, C., FOGLIA, L., ESCALANTE, E., SAUTO, J.S.S., HERRARTE, F.B.G., FILIPPI, E., ROSSETTO, R., BARBAGLI, A., SCHEMBRI, M. (2015) – Deliverable 12.2 GIS database of the MARSOL DEMO Sites - Projeto UE MARSOL Demonstrating Managed Aquifer Recharge as a Solution to Water Scarcity and Drought, junho 2015, 17 pp + 1 ficheiro com a base de dados geográfica.
 - LOBO FERREIRA, J.P., OLIVEIRA, M.M., MOTA, R., LEITÃO, T.E., MONTEIRO, J.P., COSTA L.R.D., FOGLIA, L., POULIARIS, C., KÜBECK, C., KATZ, Y., GUTTMAN, Y., ROSSETTO, R., ESCALANTE, E., CARVALHO, T., SANCHEZ-VILA, X., RODRIGUEZ-ESCALES, P. (2015) – WP12 Modelling. Second Interim report. Projeto UE MARSOL Demonstration Sites Characterisation. Projeto UE MARSOL - Demonstrating Managed Aquifer Recharge as a Solution to Water Scarcity and Drought, julho 2015, 18 pp.
 - LOBO FERREIRA, J.P., OLIVEIRA, M.M., MARTINS, T., LEITÃO, T.E., ILLIE, A.M., MONTEIRO, J.P., COSTA L.R.D., ESCALANTE, E., SCARINCI, A., FERRI, M., ROSSETTO, R., BORSI, I., KATZ, Y., FOGLIA, L., POULIARIS, C., KALLIORAS, A. (2015) – Deliverable 12.3 Progress Report on Numerical Model. Projeto UE MARSOL - Demonstrating Managed Aquifer Recharge as a Solution to Water Scarcity and Drought, setembro 2015, 95 pp.
 - LOBO FERREIRA, J.P., LEITÃO, T.E., MARTINS, T., ILLIE, A.M., MOTA, R., MONTEIRO, J.P., COSTA L.R.D., HUGMAN, R., CARVALHO, T., AGOSTINHO, R., SOUSA, R., FOGLIA, L., TOEGL, A., POULIARIS, C., ROSSETTO, R., BORSI, I., SANCHEZ-VILA, X., RODRIGUEZ-ESCALES, P., ESCALANTE, E. (2016) – WP12 Modelling. Third Interim Report. MARSOL Demonstration Sites Characterisation. Projeto UE MARSOL - Demonstrating Managed Aquifer Recharge as a Solution to Water Scarcity and Drought, março 2016, 38 pp.
 - LOBO FERREIRA, J.P., LEITÃO, T.E., MARTINS, T., OLIVEIRA, M.M., MONTEIRO, J.P., COSTA L.R.D., HUGMAN, R., CARVALHO, T., AGOSTINHO, R., SOUSA, R., FOGLIA, L., TOEGL, A., POULIARIS, C., ROSSETTO, R., BORSI, I., SANCHEZ-VILA, X., RODRIGUEZ-ESCALES, P., ESCALANTE, E., KATZ, Y., YONATAN GANOT, Y., KURTZMAN, D. (2016) – Deliverable 12.4 Final Report on numerical model. Projeto UE MARSOL - Demonstrating Managed Aquifer Recharge as a Solution to Water Scarcity and Drought, julho 2016, 152 pp.
 - LEITÃO, T.E., MARTINS, T., HENRIQUES, M.J., LOBO FERREIRA, J.P., ROGEIRO, J. e CARMEN, A.M. (2016) - Deliverable 12.5 Physical (Sandbox) Modelling of Melides Demo Site. Projeto UE MARSOL - Demonstrating Managed Aquifer Recharge as a Solution to Water Scarcity and Drought, outubro 2016, 50 pp.

MARSOL PAPERS PRESENTED TO CONGRESS

- LOBO FERREIRA, J.P., ESCALANTE, E., SCHÜTH, C. e LEITÃO, T.E. (2014) - Demonstrating Managed Aquifer Recharge (MAR) as a Solution for Water Scarcity and Drought in Portugal and Spain. "12.º Congresso da Água /16.ºENASB/XVISILUBESA", organizado pela APRH, APESB e ABES, Lisboa, 5-8 de março de 2014, 15 pp.
- LEITÃO, T.E., LOBO FERREIRA, J.P., CARVALHO, T.M., MONTEIRO, J.P., OLIVEIRA, M.M., AGOSTINHO, R., COSTA, L.R.D., HENRIQUES, M.J., MARTINS, T., MARTINS DE CARVALHO, J. (2015) - Demonstrating Managed Aquifer Recharge as a Solution to Water Scarcity and Drought: Description of Marsol Project Demo Sites in Portugal. 10.º Seminário de Águas Subterrâneas, Évora, 9-10 de abril de 2015, pp. 29-32.
- COSTA, L.R.D., MONTEIRO, J.P., OLIVEIRA, M.M., LOBO FERREIRA, J.P., LEITÃO, T.E., Carvalho, T.M., MARTINS DE CARVALHO, J., AGOSTINHO, R. (2015) - Interpretation of an Injection Test in a Large Diameter Well in South Portugal and Contribution to the Understanding of the Local Hydrogeology. 10.º Seminário de Águas Subterrâneas, Évora, 9-10 de abril de 2015, pp. 61-64.
- OLIVEIRA, M.M., LOBO FERREIRA, J.P., LEITÃO, T.E., COSTA, L.R.D., MONTEIRO, J.P., CARVALHO, T.M., AGOSTINHO, R. (2015) - New Test of the GABARDINE Infiltration Basin for MAR in Rio Seco (Campina da Faro aquifer system, Algarve). 10.º Seminário de Águas Subterrâneas, Évora, 9-10 de abril de 2015, pp. 73-76.
- LOBO-FERREIRA J.P. (2015) - MARSOL demonstration case-study areas: modeling studies to fulfill the aim of "comparable" modeling. Joint International Workshop EU FP7 MARSOL and EU HORIZON 2020 FREEWAT projects and EU EIP MAR Solutions - Managed Aquifer Recharge Strategies and Actions (AG128), Pisa - April 21st 2015
- COSTA, L.; MONTEIRO, J.P.; LEITÃO, T.; LOBO-FERREIRA, J.P.; OLIVEIRA, M.M.; MARTINS DE CARVALHO, J.; CARVALHO, T.; AGOSTINHO, R. (2015) Estimating harvested rainwater at greenhouses in south Portugal aquifer Campina de Faro for potential infiltration in Managed Aquifer Recharge. Geophysical Research Abstracts, Vol. 17, EGU2015-10415-3, 2015. EGU General Assembly 2015, 12 to 17 April, Wien. Available at <http://meetingorganizer.copernicus.org/EGU2015/EGU2015-10415-3.pdf>
- COSTA, L.; MONTEIRO, J.P.; OLIVEIRA, M.M.; MOTA, R.; LOBO-FERREIRA, J.P.; MARTINS DE CARVALHO, J.; CARVALHO, T.; AGOSTINHO, R. (2015) Modelling Contributions of the Local and Regional Groundwater Flow of Managed Aquifer Recharge Activities at Querença-Silves Aquifer System. Geophysical Research Abstracts, Vol. 17, EGU2015-11930, 2015. EGU General Assembly 2015, 12 to 17 April, Wien. Available at <http://meetingorganizer.copernicus.org/EGU2015/EGU2015-11930.pdf>
- LEITÃO, T.E., LOBO FERREIRA, J.P., CARVALHO, T.M., MONTEIRO, J.P., OLIVEIRA, M.M., AGOSTINHO, R., COSTA L.R.D., MARTINS, T., HENRIQUES, M.J. (2016) - Gestão de Recarga Induzida de Aquíferos. Exemplos do Projeto MARSol no Algarve. 13.º Congresso da Água, 7-9 de março de 2016, 15 pp.

White book on MAR modelling

Deliverable D12.7

CHAPTER 2 – STATE OF THE ART AND LITERATURE REVIEW IN MANAGED AQUIFER RECHARGE MODELLING

TIAGO MARTINS AND JP LOBO FERREIRA (LNEC)

4 INTRODUCTION TO THE STATE OF THE ART AND LITERATURE REVIEW IN MANAGED AQUIFER RECHARGE MODELLING

In the context of Managed Aquifer Recharge (MAR) numerical modelling has been an important process in several applications, since the prediction of rise of groundwater mounds, to determine where ground water must eventually be pumped, understand quality changes in infiltration water and aquifer water, predict the success of treatment induced by MAR methodologies or to calculate the necessary injected volumes to counter a saltwater intrusion problem. A proper estimation of AR, by means of arithmetic methods, depends firstly on the conceptual approach of the groundwater problem and secondly on the selection of the appropriate AR method (Pliakas et al. 2005), and its widely known that the Success of artificial recharge as a management technique depends highly on how well the system is understood (Sunada et al. 1983). Koukidou et al. (2010) referred numerical modeling as an invaluable tool that enables accurate and reliable assessment of alternative strategic management plans, with the results of well calibrated and verified models as a solid basis for justification of capital investment required for infrastructure that is necessary to support water resources management scenarios.

It is then essential, as a state of the art overview, to compile several applications in different demo-areas and scales, where modelling was essential to refine artificial recharge strategies, to help to understand the main impacts of a MAR project or to what to expect in field experiments.

The following sections address the state of the art of modelling methodologies and tools in Managed Aquifer Recharge, in both flow and transport model applications and in hydrogeochemical modelling.

Also a brief overview of commonly used flow and transport models as well as their capabilities is presented in section 5.1. A hydrogeochemical model overview, some of them also coupled with transport models, is presented in section 6.1.

5 FLOW AND TRANSPORT MODELLING MAR

The following sections present the flow and transport numerical software/code overview as well as a brief selection of MAR modelling case studies.

5.1 FLOW AND TRANSPORT NUMERICAL MODELS OVERVIEW

In this section the most used software and numerical models characteristics are summarized. The selection of these models resulted mainly from the literature review – the most used and referenced tools/software were chosen.

5.1.1 CODE_BRIGHT

The CODE_BRIGHT program (originally developed by Olivella et al. 1995) is a tool designed to handle coupled problems in geological media (Restrepo, et al. 2016) was developed on the basis of a new general theory for saline media. Then the program has been generalized for modelling thermo-hydro-mechanical (THM) processes in a coupled way in geological media. Basically, the code couples mechanical, hydraulic and thermal problems in geological media. The theoretical approach consists in a set of governing equations, a set of constitutive laws and a special computational approach. The code is composed by several subroutines and uses GiD (Coll et al. 2016) system for preprocessing and post-processing. GiD is developed by the International Center for Numerical Methods in Engineering (CIMNE). GiD is an interactive graphical user interface that is used for the definition, preparation and visualization of all the data related to numerical simulations. This data includes the definition of the geometry, materials, conditions, solution information and other parameters. The program can also generate the finite element mesh and write the information for a numerical simulation program in its adequate format for CODE_BRIGHT. It is also possible to run the numerical simulation directly from the system and to visualize the resulting information without transfer of files.

5.1.2 COMSOL Multiphysics

Accordingly to Li et al. (2009) COMSOL (formerly known as FEMLAB) is a finite element analysis and solver software package for various physics and engineering applications, especially coupled phenomena, or multiphysics. It includes a complete environment for modelling any physical phenomenon that can be described using ordinary or partial differential equations (PDEs). Coupled with Earth Science Module, the software code can handle time-dependent and stationary problems for one-dimensional (1D), 2D, and 3D systems with axisymmetric for 1D and 2D problems of fluid flow, heat transfer, and solute transport. It has been used in

several applications such as saturated and unsaturated porous media flow, well head analyses, water table analyses and saline intrusion into groundwater, flow, advection, and diffusion of groundwater, geological storage of oil–gas and sequestration of CO₂, groundwater monitoring and remediation, gas and petroleum extraction analysis, pollutant plume analyses in subsurface, surface, and atmospheric flows, shallow water flows and sediment transport.

Except for the definition of PDEs, the process of modelling and analysis is similar to other commercial software packages with graphical interface for ground water simulations (e.g., Visual MODFLOW). In addition COMSOL supports post processing options, such as particle tracing, exportable to third-party software.

5.1.3 FEFLOW

Trefry & Muffels (2007) described FEFLOW as a Finite-Element subsurface FLOW and transport modeling system with an extensive list of functionalities, including variably saturated flow, variable fluid density mass and heat transport, and multi-species reactive transport. It is a proprietary code and not freely available; it supports an array of features of interest in subsurface flow and transport. Theoretical and numerical methods and FEFLOW capabilities are well described in Diersch (2014). This software is applicable in groundwater, porous media and heat transport studies - from local to regional scale.

5.1.4 FEMWATER

FEMWATER (Finite Element Model of Water Flow Through Saturated-Unsaturated Media) model developed initially by Athens Laboratory of the U.S. Environmental Protection Agency (AERL) and the U.S. Army Engineer Waterways Experiment Station (WES) from 3DFEMWATER (Yeh, 1987). The program structure was reformulated to allow its integration into the Department of Defense Groundwater Modeling System (GMS). FEMWATER capabilities are described by Lin et al. (1997).

5.1.5 HYDRUS

Accordingly to Yu & Zeng (2010), HYDRUS is a software program for solving Richards equation for water flow and the advection-dispersion equation for heat and solute transport in variably saturated subsurface media. Variably saturated zones are fundamental to understanding many aspects of hydrology, including infiltration, soil moisture storage, evaporation, plant water uptake, groundwater recharge, runoff, and erosion. More and more studies are now focusing on the integrated water cycle, and the consideration of water, heat, and solute exchanges between groundwater and surface water must include both saturated and unsaturated zones. It uses the finite-element (FE) method to simulate one-, two- or three-dimensional movement of water, heat, and multiple solutes in unsaturated, partially saturated, or fully saturated porous media. There are two main variants of HYDRUS: (1) HYDRUS-1D and (2) HYDRUS-2D/3D. HYDRUS-1D is free and its source code is open, being initially developed by Simunek et al. (1998) for academic purposes. HYDRUS-2D/3D is a commercial product developed by PC-Progress Company⁽¹⁾.

5.1.6 MOCDENSE

MOCDENSE is a two-constituent solute transport model for ground water having variable density developed by Sanford & Konikow (1985). The model couples the ground-water flow equation with the solute-transport equation. The digital computer program uses an iterative strongly-implicit procedure to solve a finite-difference approximation to the ground-water flow equation. The model uses the method of characteristics to solve the solute-transport equation. This incorporates a particle-tracking procedure to represent advective transport and a two-step explicit finite-difference procedure to solve equations that describe the effects of hydrodynamic dispersion and fluid sources. This explicit procedure has several stability criteria associated with it, but the consequent time-step limitations are automatically determined by the program. It is applicable to two-dimensional, cross-sectional problems involving ground water with constant or variable density. The model computes changes in concentration over time caused by the processes of advective transport, hydrodynamic dispersion, mixing or dilution from fluid sources. The concentrations of two independent solutes can be modeled simultaneously. Temperature is assumed to be constant, but fluid density and viscosity are assumed to be a linear function of the first specified solute. If a second solute is specified, it is assumed to be of a trace amount such that it does not affect the fluid density or viscosity. The aquifer may be heterogeneous and anisotropic. The model has been used mostly in studies of either saltwater intrusion or dense contaminant plumes.

5.1.7 MODFLOW and related programs

MODFLOW is a 3D finite-difference groundwater model that was first published in 1984 (McDonald & Harbaugh, 1984). It has a modular structure that allows it to be easily modified to adapt the code for a particular application. Many new capabilities have been added to the original model. MODFLOW-2005 (Harbaugh, 2005) is the most current release of MODFLOW [\(2\)](#). In this version groundwater flow is simulated using a block-centered finite-difference approach. Layers can be simulated as confined or unconfined. Flow associated with external stresses, such as wells, areal recharge, evapotranspiration, drains, and rivers, also can be simulated. The report includes detailed explanations of physical and mathematical concepts on which the model is based, an explanation of how those concepts are incorporated in the modular structure of the computer program, instructions for using the model, and details of the computer code. The modular structure consists of a main program and a series of highly independent subroutines. The subroutines are grouped into packages. Each package deals with a specific feature of the hydrologic system that is to be simulated, such as flow from rivers or flow into drains, or with a specific method of solving the set of simultaneous equations resulting from the finite-difference method. Several solution methods are incorporated, including the Preconditioned Conjugate-Gradient method. The division of the program into packages permits the user to examine specific hydrologic features of the model independently.

MODFLOW based software is the most commonly used in general groundwater and MAR studies, and has several particle tracking and solute transport variants.

5.1.7.1 MODPATH

MODPATH, originally published by Pollock (1989) is a particle-tracking post-processing program designed to work with MODFLOW, where the flow data produced in the budget is

used by MODPATH to construct the groundwater velocity distribution that forms the basis for particle-tracking calculations. MODPATH Version 7 (Pollock, 2016) is the most recent version of the program. The program uses a semi-analytical particle-tracking scheme that allows an analytical expression of a particle's flow path to be obtained within each finite-difference grid cell. A particle's path is computed by tracking the particle from one cell to the next until it reaches a boundary, an internal sink/source, or satisfies another termination criterion. Data input to MODPATH consists of a combination of MODFLOW input data files, MODFLOW head and flow output files, and other input files specific to MODPATH. Output from MODPATH consists of several output files, including a number of particle coordinate output files intended to serve as input data for other programs that process, analyze, and display the results in various ways.

5.1.7.2 MT3D

MT3D-USGS (Bedekar et al. 2016) is a USGS updated release of the groundwater solute transport code MT3DMS (Zheng et al. 2001). MT3D-USGS includes new transport modeling capabilities to accommodate flow terms calculated by MODFLOW packages aiming to provide greater flexibility in the simulation of solute transport and reactive solute transport. Unsaturated-zone transport and transport within streams and lakes, including solute exchange with connected groundwater, are among the program capabilities, such as (1) the separate specification of the partitioning coefficient (K_d) within mobile and immobile domains; (2) the capability to assign prescribed concentrations to the top-most active layer; (3) the change in mass storage owing to the change in water volume now appears as its own budget item in the global mass balance summary; (4) the ability to ignore cross-dispersion terms; (5) the definition of Hydrocarbon Spill-Source Package (HSS) mass loading zones using regular and irregular polygons, in addition to the currently supported circular zones; and (6) the ability to specify an absolute minimum thickness rather than the default percent minimum thickness in dry-cell circumstances.

MT3DMS can be used to simulate changes in concentrations of miscible contaminants in groundwater considering advection, dispersion, diffusion and some basic chemical reactions, with various types of boundary conditions and external sources or sinks. The chemical reactions included in the model are equilibrium-controlled or rate-limited linear or non-linear sorption, and first-order irreversible or reversible kinetic reactions. It should be noted that the basic chemical reaction package included in MT3DMS is intended for single-species systems. MT3DMS can accommodate very general spatial discretization schemes and transport boundary conditions, including: 1) confined, unconfined or variably confined/unconfined aquifer layers; 2) inclined model layers and variable cell thickness within the same layer; 3) specified concentration or mass flux boundaries; and 4) the solute transport effects of external hydraulic sources and sinks such as wells, drains, rivers, areal recharge and evapotranspiration.

5.1.7.3 SEAWAT

The SEAWAT program (Langevin et al. 2008) is a coupled version of MODFLOW and MT3DMS designed to simulate three-dimensional, variable-density, saturated groundwater flow. Accordingly to Guo & Langevin (2002) was developed to simulate three-dimensional, variable-density, transient ground-water flow in porous media. The source code for SEAWAT was

developed by combining MODFLOW and MT3DMS into a single program that solves the coupled flow and solute-transport equations. The SEAWAT code follows a modular structure, and thus, new capabilities can be added with only minor modifications to the main program. SEAWAT reads and writes standard MODFLOW and MT3DMS data sets, although some extra input may be required for some SEAWAT simulations. This means that many of the existing pre- and post-processors can be used to create input data sets and analyze simulation results. Users familiar with MODFLOW and MT3DMS should have little difficulty applying SEAWAT to problems of variable-density ground-water flow.

MODFLOW was modified to solve the variable-density flow equation by reformulating the matrix equations in terms of fluid mass rather than fluid volume and by including the appropriate density terms. Fluid density is assumed to be solely a function of the concentration of dissolved constituents; the effects of temperature on fluid density are not considered. Temporally and spatially varying salt concentrations are simulated in SEAWAT using routines from the MT3DMS program. SEAWAT uses either an explicit or implicit procedure to couple the ground-water flow equation with the solute-transport equation. With the explicit procedure, the flow equation is solved first for each timestep, and the resulting advective velocity field is then used in the solution to the solute-transport equation. This procedure for alternately solving the flow and transport equations is repeated until the stress periods and simulation are complete. With the implicit procedure for coupling, the flow and transport equations are solved multiple times for the same timestep until the maximum difference in fluid density between consecutive iterations is less than a user-specified tolerance.

5.1.7.4 MODRET

MODRET⁽³⁾ (Computer MODEL to Design RETENTION Ponds) was originally developed in 1990 as a complement to a research and development project for Southwest Florida Water Management District (Jammal & Associates Division, 1993). The scope of this project was to develop a practical design manual for site investigation criteria, laboratory and field testing requirements and guidelines to calculate infiltration losses from stormwater retention ponds in unconfined shallow aquifers. Since 1990, there have been several revisions to the original model. The model allows generation of runoff hydrographs with various methods, calculation of infiltration losses from a retention pond, discharge (overflow) through various types of weirs and orifices, and generation of graphical. MODRET includes preprocessor and postprocessor, procedures to enter the pond, weir and aquifer characteristics, calculate unsaturated infiltration, set up MODFLOW data files and execute the MODFLOW program, read the results, calculate and display the results, and create graphical data files to be used by the Graphics Module. The input of runoff volumes into the infiltration module can be accomplished by simply specifying the file name of the corresponding runoff hydrograph or manually entered one time increment at a time. After calculation of infiltration losses, the runoff hydrograph can be routed through infiltration and a new "routed" runoff hydrograph generated which can then be reused in other pond routing models. The MODFLOW model was specifically modified for use with the MODRET model which incorporates modeling of weir and

orifice overflow or overflow based on manually-specified elevation vs. flow relationship (rating curve).

5.1.8 TOUGH

The acronym to Transport Of Unsaturated Groundwater and Heat⁽⁴⁾, is a set of multi-dimensional numerical models for simulating the coupled transport of water, vapor, non-condensable gas, and heat in porous and fractured media. Initially developed in Lawrence Berkeley National Laboratory (LBNL) in the early 1980s (Pruess, 1987) primarily for geothermal reservoir engineering, the suite of simulators is widely used for applications to nuclear waste disposal, environmental remediation problems, energy production from geothermal, oil and gas reservoirs as well as gas hydrate deposits, geological carbon sequestration, vadose zone hydrology, and other uses that involve coupled thermal, hydrological, geochemical, and mechanical processes in permeable media.

5.2 CASE STUDIES AND APPLICATIONS IN FLOW AND TRANSPORT MODELLING

In this section a set of case studies where numerical modelling was used as a resource/tool to define methodologies, policies and operational strategies in Managed Aquifer Recharge¹ is chronologically presented.

Sunada et al. (1983) used early computed code to simulate the impact of a rectangular infiltration basin in groundwater and ultimately evaluate the benefits of artificial recharge in other areas. The study area is the San Luis Valley in Southern Colorado, USA, where at the time groundwater was the major source of irrigation water and farmers struggled at the high cost of pumping and difficulties in obtaining well permits. A microcomputer program was developed to transfer the knowledge by graphically displaying the response of the aquifer to artificial recharge. The model was designed for use by both groundwater specialists and non-technical water users and represented advancement at a time where relatively inexpensive computers started to become available common working tools. In this case the computer program designed for APPLE II + 48 K microcomputer was based in Glover's solution (1960) in a rectangular basin in a finite element grid – **Figure 7** - described the groundwater response to artificial recharge in an infinite, homogeneous aquifer at a first approach and in a stream aquifer system where stream discharge was also simulated. Glover (1960) was the first to obtain solutions for AR using the governing differential equations for groundwater flow. The developed model successfully allowed for the evaluation of the benefits of artificial recharge as well as determines the best operational policies at the site.

¹ Note: Since some of the presented studies are dated back to the 1980s and 1990s, where the concept of Managed Aquifer Recharge was not widely used. Artificial recharge concept was kept in the text.

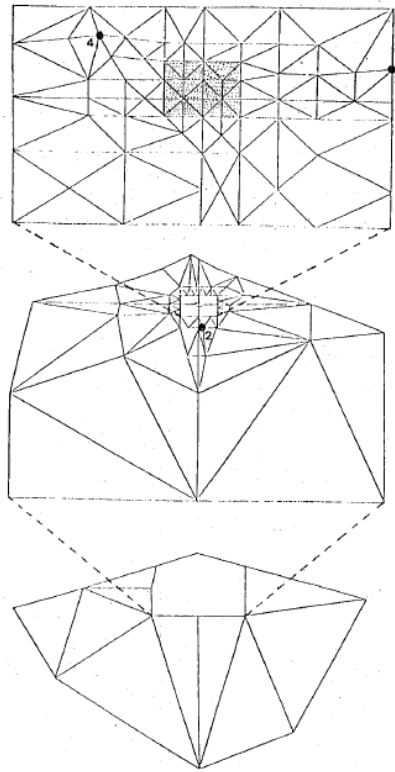


Figure 7 – Finite element grid of area of artificial recharge. Shaded Area represents basin (Adapted from Sunada et al. 1983)

Jammal & Associates Division (1993) focused in development and viability of retention systems within the Indian River Lagoon Basin in St. Johns River, Florida (USA). These systems are referred as storage areas designed to store a defined quantity of runoff following a storm event, allowing the runoff to naturally percolate through the permeable soils of the basin floor and side slopes into the shallow ground water aquifer. In this study, after a long period of testing and data collection in four instrumented ponds (two of them in a riverbank), a list of numerical models were selected for analysis (**Figure 8**). The objective was to define the best model (tool) to simulate these structures.

1. Simplified Analytical Method
2. PONDFLOW
3. Modified MODRET

Figure 8 – List of SElected models (Adapted from PSI/Jammal & Associates Division, 1993)

This list of pond recovery models was representative of the current state of the geotechnical engineering practice in Florida, except for the Simplified Analytical Method which was a product this study. In addition it was determined that the most commonly used model at the time (MODRET model) was modified to overcome numerical instability found in some situations. These models are all similar in that the receiving aquifer system is idealized as a laterally infinite, single-layered, homogenous, isotropic water table aquifer of uniform thickness, with a horizontal water table prior to hydraulic loading. The three dimensional shape of the pond is assumed to be that of an equivalent rectangular trench. A sensitivity

analysis was conducted in these models and a set of recommendations was defined concerning model capabilities and necessary input data (**Figure 9**). The three models predict remarkably close results over a wide range of aquifer thickness and recovery periods.

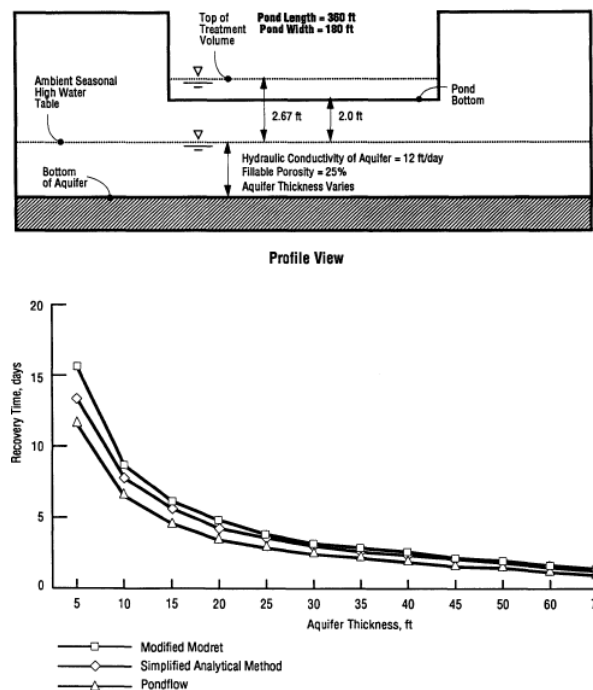


Figure 9 - Comparison of Predicted Recovery Times for a Hypothetical Pond (Adapted from PSI/Jammal & Associates Division, 1993)

All three models can take into account unsaturated vertical flow prior to saturated lateral flow. However, the PONDFLOW and Modified MODRET models can also allow input of a discretized runoff hydrograph which allows for simulation of infiltration during a storm event. It is recommended that, unless the normal seasonal high water table is over 2 feet below the pond bottom, unsaturated flow prior to saturated lateral mounding be conservatively ignored in recovery analyses. In other words, there should be no credit for soil storage immediately beneath the pond if the seasonal high water table is within 2 feet of the pond bottom. This is not an unrealistic assumption since the height of capillary fringe in fine sand is on the order of 6 inches and a partially mounded water table condition may be remnant from a previous storm event. It is also recommended that the filling of the pond with the pollution abatement (or treatment) volume be simulated as a "slug" loading (i.e., treatment volume fills the pond within an hour). Note that the same recommendation does not apply for the recovery of the design runoff volume for closed ponds (i.e., with no positive outfall) where the design storm events can be 24 to 96 hours long and infiltration during such storm events can be significant. It is also defined that, in addition to these 1-layered, uniform aquifer idealization models, more complicated fully three dimensional models with multiple layers (such as MODFLOW) may be used where the aquifer is markedly heterogeneous and non-uniform within the radius of influence of the transient hydraulic loading in the pond or the potential detrimental impacts of pond failure warrant the extra effort in obtaining a more refined estimate of infiltration.

Wright & du Toit (1996) studied AR effects in Atlantis (South Africa) where the large number of factories demanded a significant amount of potable water, which is acquired by artificially recharging and recovering a shallow sandy aquifer. A 2-D integrated finite-difference model was developed in AQUAMOD, using MT30 for solute-transport model, as a tool for water management. The result was a highly cost-effective water resource management scheme that sustained the urban growth with a cheaper cost of water without large distance transporting from a far distant surface water reservoir.

Due to quantity problems encountered during summer and long periods of intense freezing in Bucharest water supply – was highly dependent on surface water – Stefanescu & Dessargues (1998) studied the possibility of increasing the proportion of groundwater usage by increasing storage in shallow aquifer by artificial recharge methods. A regional scale 3D numerical model of 540 km² was assembled MODFLOW in steady state, limited by the two main rivers in the region (Arges and Dambovita) - **Figure 10**.

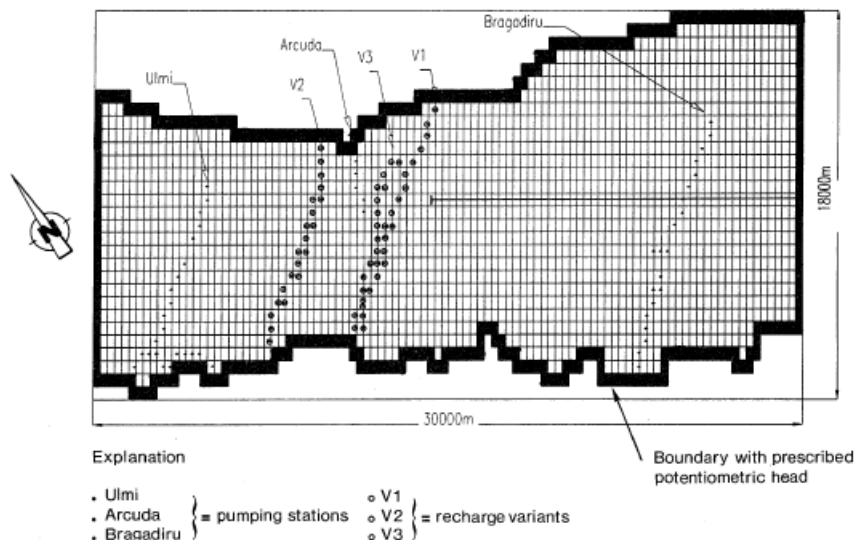


Figure 10 – Horizontal network and locations of pumping and recharge areas (Adapted from Stefanescu & Dessargues, 1998)

The simulated scenario consisted in the selection of an infiltration area near two treatment stations, which ensured standard quality of infiltration water without long distance transport and long enough distance to recovery (pumping) wells to ensure effective attenuation of contaminants. The AR procedures produced effects in potentiometric contours (1-3 m). MODPATH was used to calculate transport path and travel times. The model results showed that due to long travel time between recharge and pumping areas (over five years) good biological quality could be achieved, making the phreatic aquifer a reservoir for Bucharest water supply.

Chatdarong (2001) aimed to study the recharge behaviour in San Joaquin Valley agricultural area as well as the economic feasibility and practicality of artificial recharge facilities in the conjunctive use for irrigation purposes. HYDRUS-2D, based in Richards' equation for unsaturated water flow and Fickian-based advection dispersion equation for heat and solute

transport, was used in the simulations if a two-dimensional model based on the study area infiltration ditch. It is assumed that the modelled region is a 1 m thick box, soil and unconfined aquifer are homogeneous and isotropic, and subsurface flow occurs only perpendicular to the infiltration ditch - **Figure 11**.

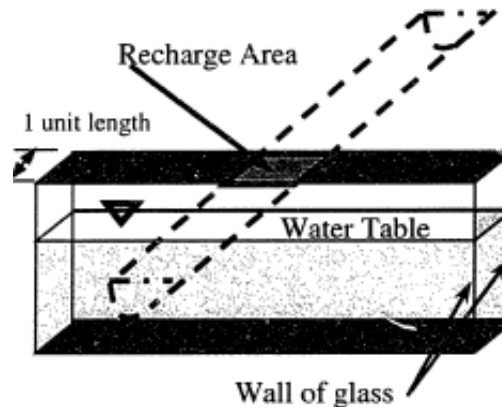
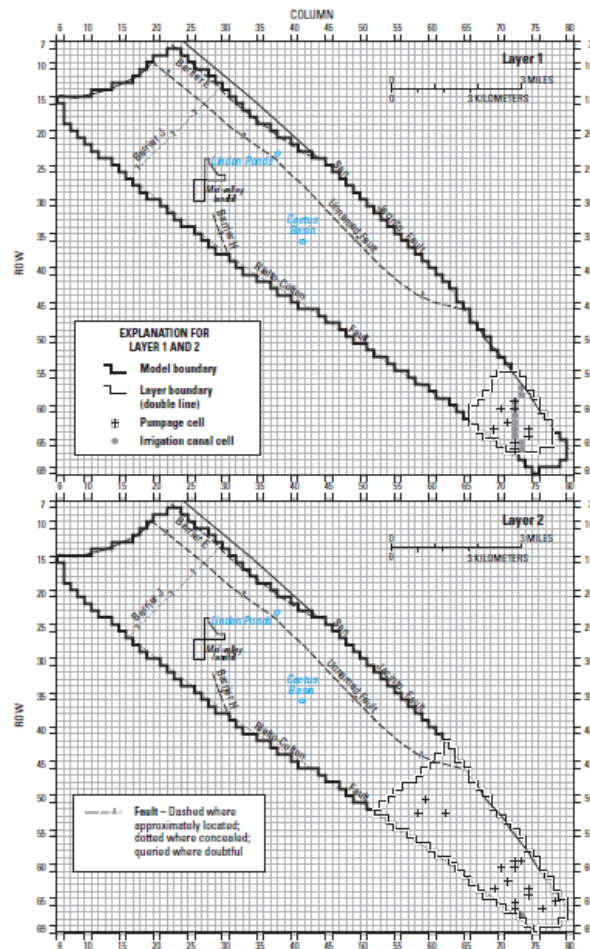


Figure 11 – Recharge Water Simulation Model in Hydrus 2-D (Adapted from Chatdarong, 2000)

Simulation allowed for the determination of effects of soil characteristics in infiltration by using different soil types encountered in the study area, effect of depth to groundwater table and spacing between adjacent recharge structures. Ultimately a GIS tool was produced from de conjunction of the simulation results which allowed for the selection of the best infiltration site in the study area.

Woolfenden & Koczot (2001) conducted a study to evaluate the hydraulic effects of artificial recharge, started in 1994, of imported water from Sierra Nevada in Rialto-Colton Basin (San Bernardino County, California). The main objectives were to, in a first phase describe geohydrology and water chemistry, and determine the movement and ultimate disposition of artificial recharged water simulating long-term effects on water levels likely to occur in two different AR scenarios: (1) continued recharge in ponds, (2) discontinued recharge in ponds. This included the development and calibration of a groundwater flow model of Rialto-Colton Basin aquifer system. A MODFLOW finite-difference model was used to simulate flow both in steady-state and transient state and post processing MODPATH through particle tracking allowed for the understanding of water movement. Model results allowed to understand the reach of infiltrated water and effectiveness of this process and served as a decision support tool.



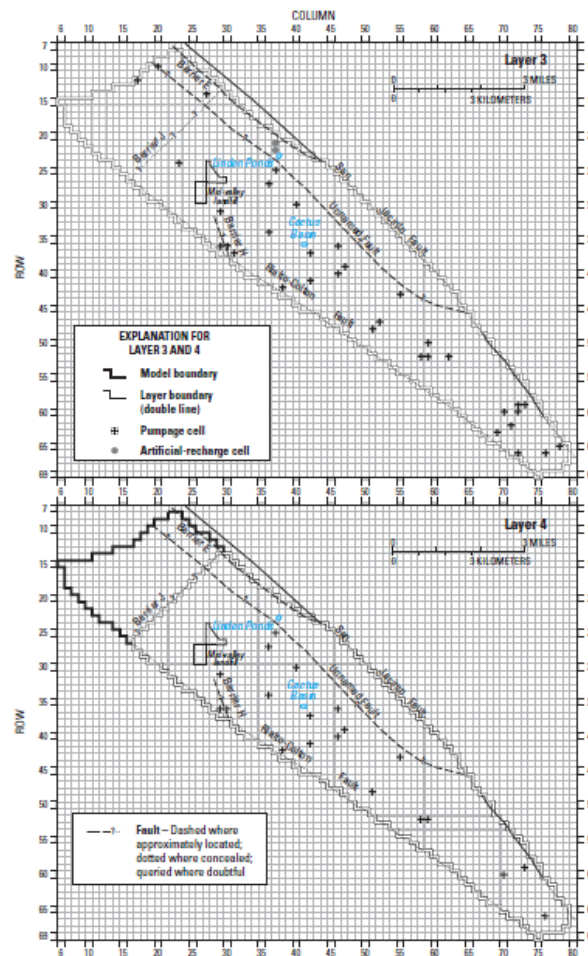


Figure 12 - Model grid and boundary conditions for layers 1–4 of the Rialto–Colton Basin groundwater flow model, San Bernardino County, California (Adapted from Woolfenden & Koczot, 2001)

Haimmerl (2002) evaluated the effectiveness of groundwater recharge dams by assembling a 2D numerical model using HYDRUS. These structures, built in Wadi Ahin in the north of Oman, were used to store the water on the surface and enable a controlled release for artificial recharge in terms of managed recharge. The water infiltration process was simulated in the numerical modelling comparing results from data collected in previously conducted field infiltration tests (Figure 13). The boundaries have been defined as no-flow boundaries except the surface where evaporation and the infiltration from the test basin have been specified. The 2D-model proved the results of the field tests that the efficiency of groundwater recharge depends on the duration of the infiltration and the water level in the test basin.

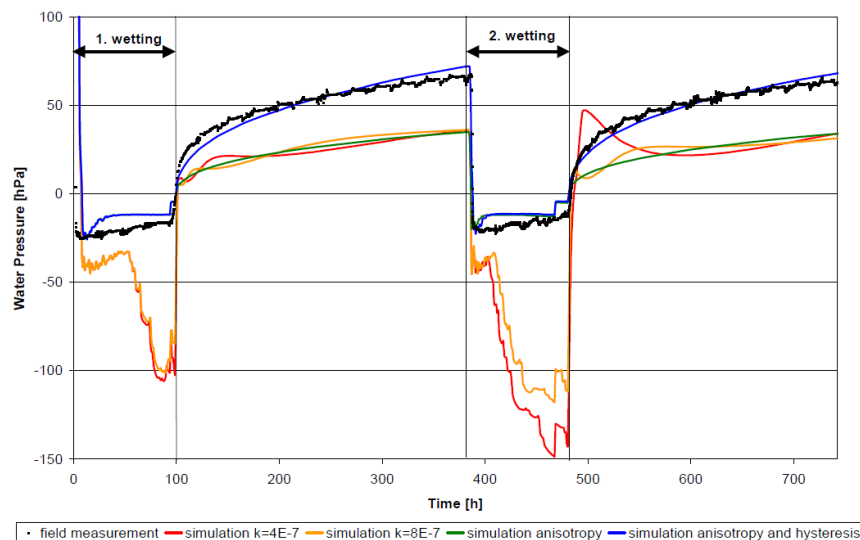


Figure 13 – Measured and Computed Water pressures within different calibration adjustments (Adapted from Haimerl, 2002)

Numerical modelling was used to simulate and understand the role of the unsaturated zone directly beneath an unused artificial recharge site in the Cherry Valley alluvial fans, located in San Gregorio Pass, California (USA) (Flint, 2003). The numerical model was developed in TOUGH2 finite-difference code (Pruess et al, 1999) and calibrated using data from 50-day artificial recharge experiment previously conducted. According to the author, the geometry of the site requires a three-dimensional approach because of deep migration of recharged water through the alluvial fan deposits, as well as lateral flow of natural recharge from the nearby stream. The modelling domain is composed of 50 000 grid elements. The bottom boundary is the water table and the upper boundary is specified flux, which was temporally and spatially variable depending on the artificial recharge scenario, and the location and amount of streamflow and natural recharge from precipitation.

The results of the model simulations were used to refine the existing conceptual model allowing for the understanding of the amount of infiltrated water that effectively reaches the deep regional aquifer and how it spreads throughout the unsaturated zone, helping to define the areas suitability for artificial recharge.

De la Orden and Murillo (2003) used numerical modelling as a tool to evaluate the effects in groundwater of artificial recharge applied for a period of 10 years in Vergel, Alicante (Spain). The Plana de Gandía-Denia coastal aquifer model was developed using MODFLOW in PMWIN software (Chiang and Kinzelbach, 1998) ran in transient state and was calibrated with data from previous studies that were conducted in the modelled area and ranged from 1990 to 1998. The model allowed concluding that only 20% of the water available for artificial recharge would remain stored in the aquifer with the remaining volume to be lost to sea. On the other hand some positive effects were to be expected from with an increase of available water in an area of water budget deficit. There was also potential decrease of saltwater intrusion advance, although a larger volume than the available at the time would be necessary to produce viable results.

The authors also developed a variable-density transport model in MODCDENSE (TECSOFT, 1998) to evaluate the impact of artificial recharge in the saltwater intrusion e vertical sections of the aquifer. The results were similar to the PMWIN model, with a push of chloride from the aquifer to the sea and a decrease of concentration to be expected.

In the development and verification of a groundwater artificial recharge system in Xanthi plain, Thrace (Greece) where the main objective is the reactivation of an old stream bed of Kosynthos River, Pliakas et al. (2005) built a finite-difference MODFLOW numerical model as a tool to estimate impact of AR (Figure 14).

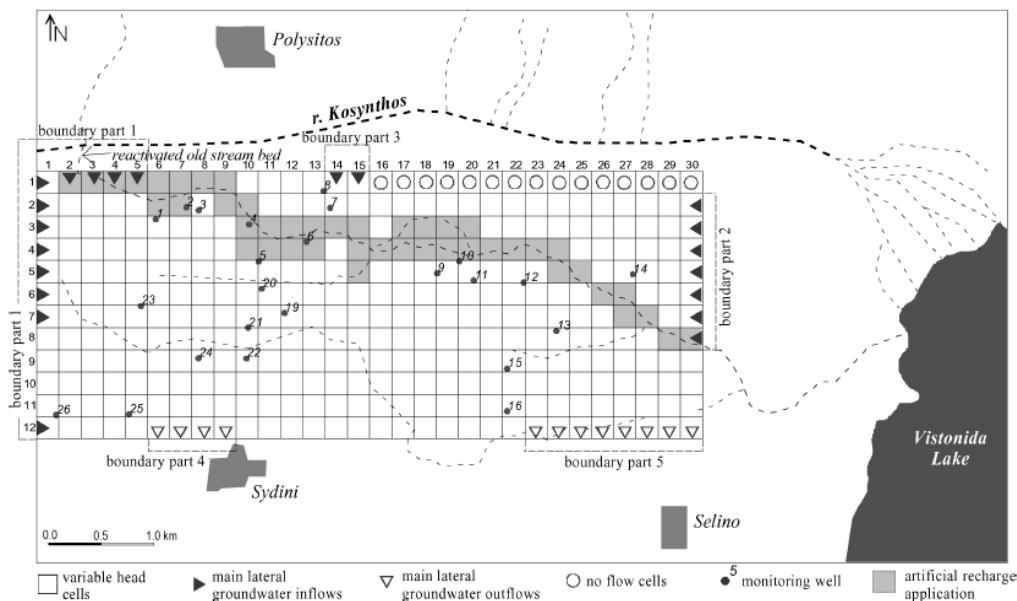


Figure 14 - The groundwater model grid of the study area, the type and the locations of characteristic cells, the boundaries of the main lateral groundwater inflows and outflows and the monitoring wells (Adapted from Pliakas et al. 2005)

A set of prediction scenarios was explored to understand the system response to artificial recharge in 9-year-period transient state. It was considered by the authors as a significant tool for rational management of groundwater resources in the study area.

GABARDINE project, which aimed to demonstrate suitability of alternative sources of water in groundwater artificial recharge by developing advanced integrated technologies and management, showed some examples of numerical modelling applied to MAR. Lobo Ferreira et al (2006) compiles the description of numerical models for three different demo-areas in the project.

One of the demo-areas was Campina de Faro aquifer system (Portugal), where a finite-difference MODFLOW model was developed using Visual MODFLOW software (Figure 15). Different scales were considered, since from a regional aquifer sized model a second more detailed local model was produced (Figure 16). One of the main objectives of this study is the optimization of groundwater rehabilitation through artificial recharge aiming the minimization

of diffuse pollution effects caused by typical Portuguese agricultural practices, by promoting artificial in a riverbed.

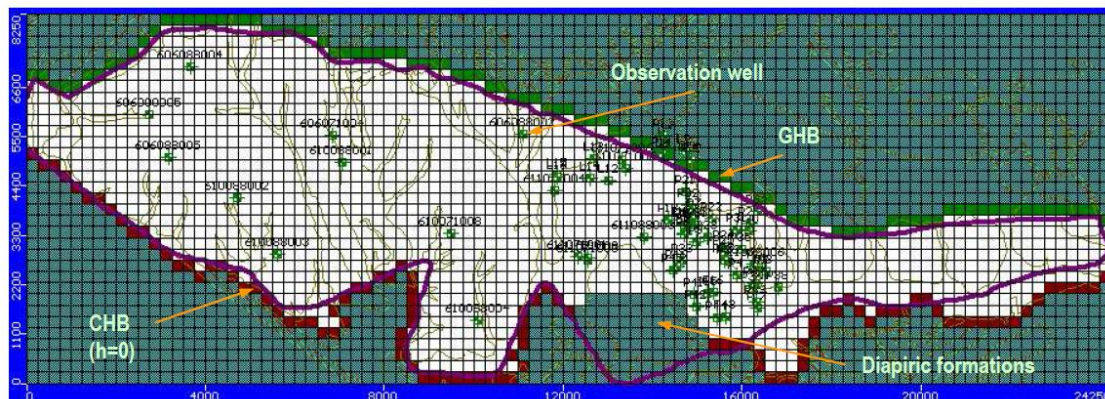


Figure 15 - Campina de Faro aquifer system regional model (model grid, active cells in white, inactive cells in green, GHB in light-green cells, CHB in red cells and observation wells in green) (Adapted from Lobo Ferreira, 2006)

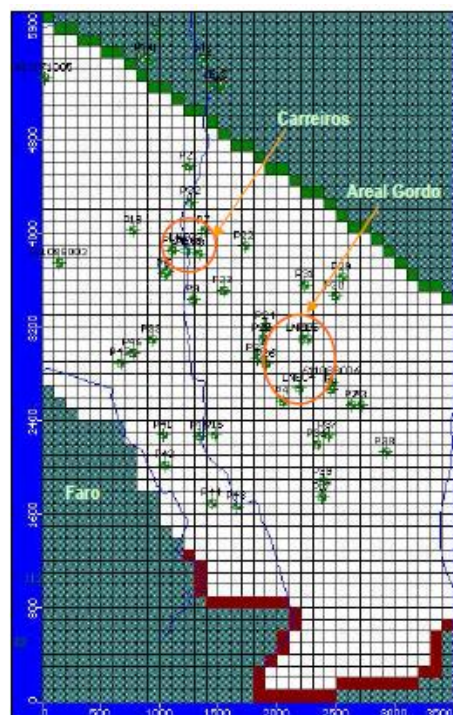


Figure 16 - Campina de Faro aquifer system local model (model grid, active cells in white, inactive cells in green, GHB in light-green cells, in the northern limit, CHB in red cells, in the southern limit, and observation wells in green) (Adapted from Lobo Ferreira, 2006)

The demo-area in Israel encompasses an area of approximately 600 km². It is bounded on the north by the city of Ashdod, on the south by the northern border of the Gaza strip, on the west by the seashore and on the east by the aquifer edges (see Figure 17). The study area covers approximately 40% of the Israel coastal aquifer, which one of the three main aquifer reservoirs in the country. The coastal aquifer, particularly in this region is intensively operated:

there are hundreds of pumping wells, tens of injection wells, infiltration ponds of freshwater and infiltration ponds of treated effluent. A three-dimensional computational model of the project area was constructed using the VASP software. The construction process was conducted in two steps: (1) a 2D mesh was built (see (2) the three dimensional structure was inserted, with the use of the DEM. A density dependent flow and salt transport was coupled in order to evaluate the impact of aquifer management and utilization on seawater intrusion processes. The calibrated groundwater flow model will be extended to simulated salt transport processes at the sea border. Ten different scenarios were simulated with the help of the computational model including both the pumping from the aquifer, injection of freshwater (through wells and infiltration ponds), artificial recharge of treated effluent, artificial recharge of desalinated water, combined use of brackish and fresh water.

Finally, a local groundwater model was developed aiming to evaluate the viability of infiltration systems in the Northern part of Gaza (Palestine) (**Figure 17**). Water shortage and contamination is a dire problem in Gaza that is in need of immediate attention. Water resources are currently facing extreme over exploitation which is leading to the sharp decline in the water tables of the aquifer systems in the area. This also results in increasing the salinity of the groundwater mainly as a result of sea water intrusion thus making it unsuitable for further domestic use sometimes not even suitable for agricultural activities. In addition to this, water loss as a result of evaporation has triggered the need of new water management options such as artificial groundwater recharge. Visual MODFLOW and its integrated modules (MODPATH and MT3D) were used and modeled the effects of (1) infiltration ponds near a wastewater treatment plant (BLWWTP) built at the outskirts of the village of Beit Lahiya and (2) NGWWTP infiltration ponds located east of Jabalia Town adjacent to the eastern border with Israel. The model was both calibrated for steady and transient state and represented an important tool to define a monitoring program for the effects of artificial recharge in the study area.

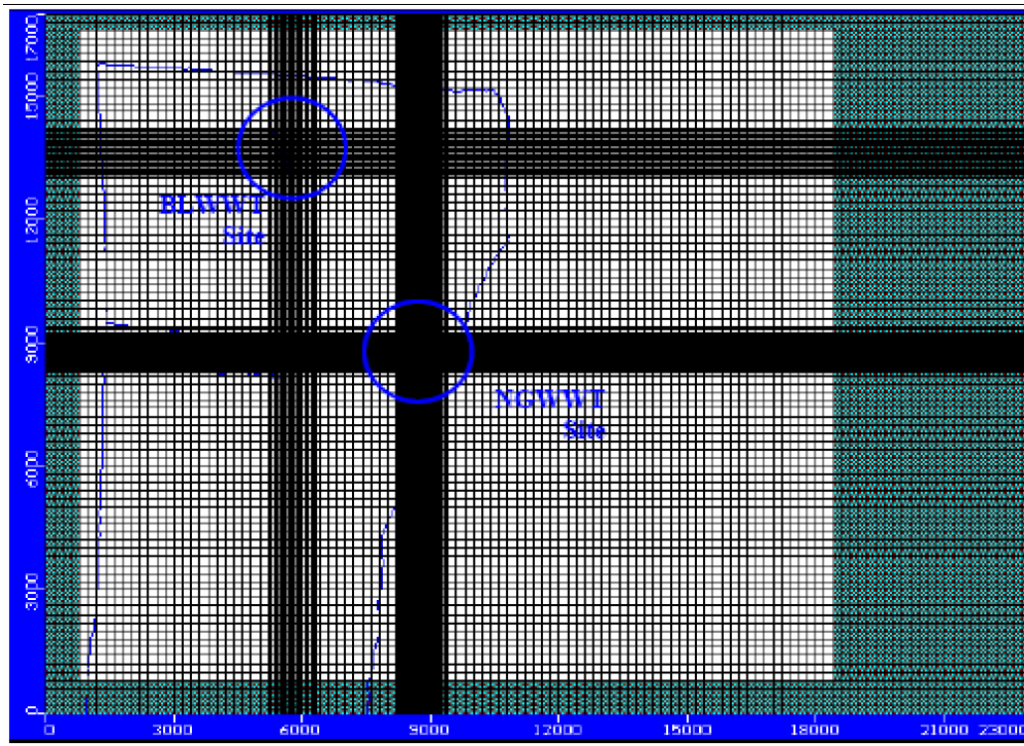


Figure 17 – Local Northern Gaza Strip model grid (adapted from Lobo Ferreira et al, 2006)

Santo Silva et al (2006) applied numerical modeling for studying the applicability of artificial recharge methods in Recife plain (Brazil) to decrease the drawdown observed in Cabo aquifer due to over-exploitation and increasing urban areas, using rainwater injection in wells. A 2D vertical grid aquifer scale model was developed using finite element CODE-BRIGHT coupled with GiD software for pre and post processing. Calibration used field data from local artificial recharge experiment, and an injection well boundary condition located in the middle of the grid (Figure 18).

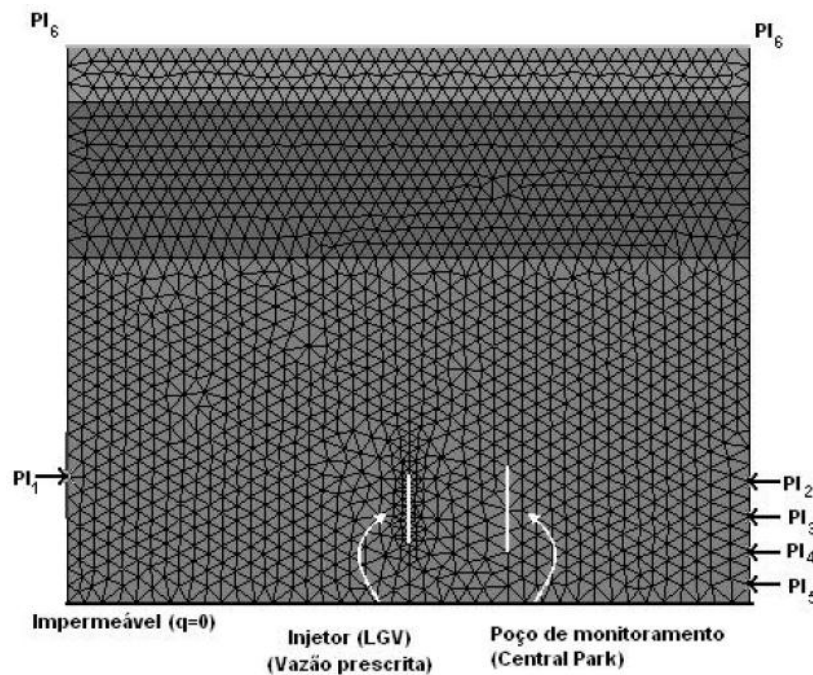


Figure 18 – 2D Finite Element vertical grid used in ASR well injection modelling

Two scenarios were simulated where (1) different well screen length and (2) continuous artificial recharge were tested. Model results showed that artificial recharge was viable in the study area, and while well screen length showed no particular positive effects, continuous artificial recharge for prolonged periods of time increased the groundwater levels.

In EPTISA (2009), numerical modelling was used to simulate alternative managed aquifer recharge methodologies and explore the effects of these methodologies while facing a possible increase of water pumping from Crestatx aquifer in Majorca (Spain). The studied area showed some problems due to prolonged overexploitation, where a continuous decrease of groundwater levels was being observed. This new model, based in one previously developed by Instituto Geológico y Minero de España in 1996, was developed in Visual MODFLOW software, using MODFLOW for groundwater flux modeling, MODPATH for particle tracking and MT3D for transport modeling and was run both in steady and transient state. The finite differences grid was composed by seven layers and divided by two main hydrogeological units divided by geological impermeable structures (**Figure 19**): (1) Crestatx aquifer and (2) Navarra aquifer.

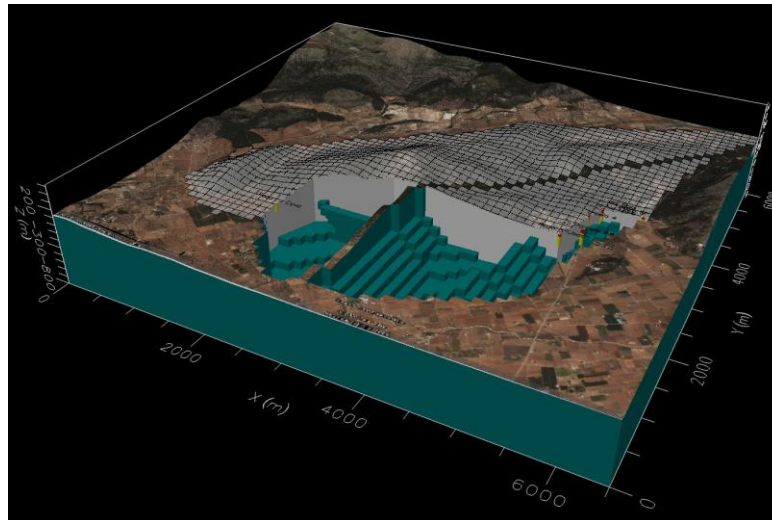


Figure 19 – Active aquifer model area (GRAY) (adapted from EPTISA, 2009)

This numerical model was the base for simulating a set of artificial recharge scenarios aiming to validate AR effects considering available injectable volumes and number of necessary injection wells to achieve a sustainable use of the aquifer. The simulated artificial recharge infrastructure is a mixed system where hydraulic superficial and underground structures are considered, with both injection wells and infiltration dams. The results allowed the understanding of necessary volumes for positive effects of AR to take place and the most effective infrastructures in the proposed artificial recharge scheme.

In Goyal et al. (2009) a finite-element groundwater flow model, using HYDRUS-2D software, was used to simulate draw-up and drawdown of piezometric pressure heads in the aquifer storage recovery cycles of varying buffer storage volumes and residence times in a highly brackish, semi-confined aquifer under shallow water-table condition in Hisan region (India). Physical flow region implemented in HYDRUS-2D involved a soil profile of 500 m width and 69 m depth, with an exocentric elliptical cavity of 1 m radius at 54 m depth. The authors concluded that the developed model offered satisfactory results for saturated field hydraulic conductivity from inverse modelling used as simulation of ASR cycles of 300 days. It was also concluded that HYDRUS showed good prediction results when compared with other models and it is a good prediction tool for this type of groundwater studies at aquifer scale.

In a joint research project with Portugal and Tunisia, Lobo Ferreira et al. (2009) used numerical modelling as a tool to understand effect of artificial recharge methodologies concerning the use of infiltration basins located in Cap Bon (Tunisia) as a way to increase groundwater quality, the effect of saltwater intrusion and increase water availability for agriculture. The numerical model was assembled in Groundwater Modelling System (GMS) software using finite element FEMWATER code. Three main scenarios were explored at a municipality scale, with different infiltration volumes considered (1500, 3000 and 6000 m³/day). The numerical model allowed defining that only the infiltration of 3000 m³/day or more produced an increase of the groundwater level with positive effects in combating saltwater intrusion advance.

Koukidou et al. (2010) aimed to characterize the regional groundwater flow system in the Tirnavos alluvial basin and to develop and apply appropriate models for assessing artificial recharge as a way to restore and manage regional groundwater resources in eastern Thessaly (Greece). The studied area is one of the most agriculturally productive Greek areas and groundwater is the main source for irrigation causing the significant level decline and quality deterioration. Simulation of the aquifer system was performed on finite element FEFLOW software in steady state and the calibrated model was used for the feasibility assessment of alternative groundwater management strategies based on Aquifer Storage Recovery, using an estimate of injection 20 wells and the surplus of an important local spring as source.

The model results showed that artificial recharge methodologies are technically feasible and financially reasonable, showing as a viable solution to restoration of the natural condition of the studied aquifer. The tested scenarios that considered application of AR suggest that viable condition may be achieved even with small volumes that are available during winter, and although complete recovery could take more than a decade, a trend of reversal is observed with the preservation of regional socio-economic structure that depends on groundwater.

Carleton (2010) presented numerical modelling tools to provide quantitative methods for estimating the height of groundwater mounds beneath infiltration basins. These methods included three-dimensional finite-difference groundwater-flow models. MODFLOW-2000 was used to simulate the height and extent of groundwater mounds beneath infiltration basins with various aquifer characteristics, recharge conditions, and basin areas, depths, and shapes. Hundreds of simulations were completed in which two to four values for each of seven variables were altered to estimate groundwater mounds in various hypothetical settings and design constraints. The seven variables that were altered are soil permeability, aquifer thickness, specific yield, infiltration basin depth, basin shape, magnitude of design storm, and percentage of impervious land cover.

The models of 10-acre (**Figure 20**) and 1-acre areas having a hypothetical stormwater infiltration basin were designed to simulate the groundwater mounding beneath and near the basin for a fully three-dimensional system with horizontal boundaries that are beyond the radius of influence of the infiltration basin – for modeling purposes assumed to be a simulated 0.01-ft increase in water level. The simulations were run in transient state, running for 36 hours during the period of recharge from the basin to the aquifer. Initial conditions for all simulations included a flat water table and an initial constant aquifer thickness. Beginning each simulation with a flat water table corresponded to a physical system that has recovered from any previous recharge events to a steady-state condition. Multiple layers were included in the models to simulate the effect of vertical anisotropy of permeability. For this study, soil permeability (vertical hydraulic conductivity) was estimated as one-tenth of horizontal hydraulic conductivity. The models included three layers to make possible the simulation of the vertical component of flow and the effects of vertical anisotropy of permeability. The top layer was modeled as unconfined, whereas the middle and bottom layers were modeled as confined. The simulations did not include any delay or attenuation associated with travel through the unsaturated zone.

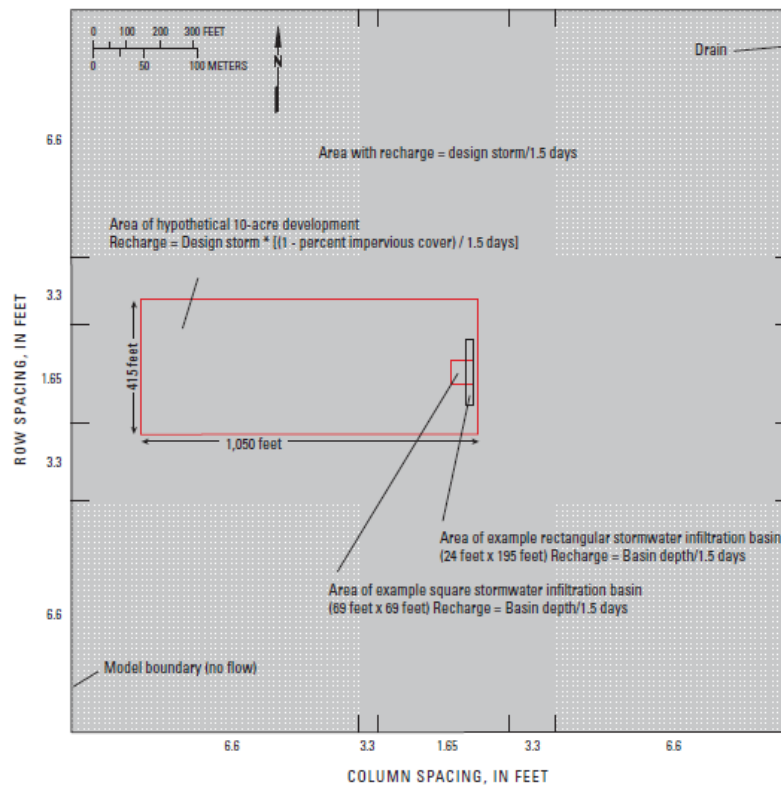


Figure 20 – Model grid and boundary conditions of a finite-difference model used to simulate groundwater mounding beneath hypothetical stormwater infiltration basins on a 10-acre development (adapted from Carlton, 2010)

The more realistic representation of the vertical component of flow and the ability to include site-specific details make finite-difference models such as MODFLOW potentially more accurate than analytical equations for predicting groundwater mounding when compared to analytical equations (such as proposed by Hantush, 1967).

Kareem (2012) used MODFLOW in Groundwater Modeling System (GMS) software to simulate the water conveyance from rainwater collecting ponds to underground reservoirs by well injection in Jolak basin, Karkuk (Iraq). In the study area, where rainfall is mostly limited to about five or six months in a year and natural aquifer recharge is very limited, rectangular ponds are suggested as a way to collect water from monsoon rains to be later diverted to deep injection replenishing falling groundwater table (**Figure 21**). The developed model was calibrated by data collected in several pumping tests conducted in the area.

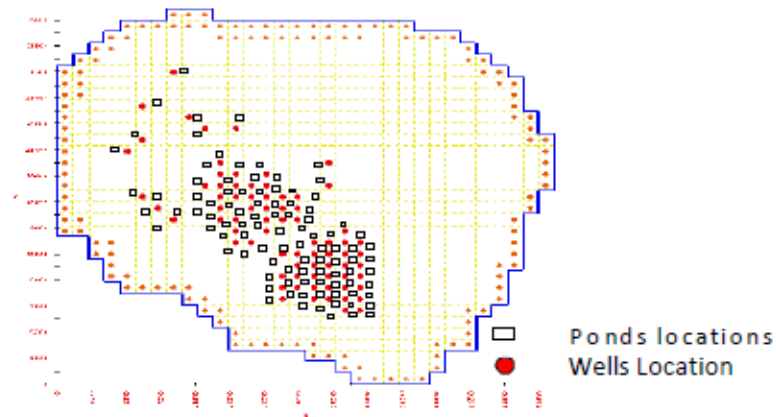


Figure 21 – Existing wells and suggested ponds locations (ADAPTED from Kareem, 2012)

Results indicated that movement of surface water into the groundwater was predominantly an effective process. It can be shown also, that collecting ponds were a key driver of surface water into the subsurface along the study area. The ground water levels in Jolak basin can be raised by means of 97 collecting ponds and 76 wells distributed over the study area. Water level at the middle of the study area can be raised to about 2 m from its present level after the steady state condition is reached within a period of 180 days.

Loizeau et al. (2012) developed a unsaturated/saturated 3D model using finite element FEFLOW code, coupled with IFMLAKE plug-in, to better understand how an infiltration basin functions in an active well field (**Figure 22**). The model takes into account the evolution of the saturated hydraulic conductivity in the natural fine sand layer under the basin and was calibrated with data collected in 6 cycles of recharge/infiltration conducted in the preexisting infiltration basins.

Simulation showed the importance of the hydraulic characteristics of the gravel with fine sand matrix located in the basins and allowed to have a broader hydrogeological vision of the area and improve existing well field management.

A three-dimensional MAR model of the Isfara Aquifer, Fergana Valley (Uzbekistan) was developed by Karimov et al. (2013) using Visual MODFLOW software. The upstream of Fergana Valley in the Syrdarya River Basin has favorable hydrogeology conditions to store extra winter flows for summer use, where semi-arid climate results in low quantity of precipitation and high summer temperatures. The main objective is to evaluate the viability of MAR activities, initiated in Isfara River Basin located in the tail end of the Big Fergana Canal (BFC) as it is easy to estimate the impact of MAR and make the necessary refinements in the Isfara Basin. The Isfara Aquifer Model covers approximately 380 km². Grid spacing in the x and y model dimension is 50 m x 100 m, and in the areas with dense irrigation canals and drainage ditches the model has 50 m x 50 m resolution (**Figure 23**). Calibration was achieved by running WINPEST, which aimed to correct parameter values by increasing the convergence with actual data obtained during several pumping tests.

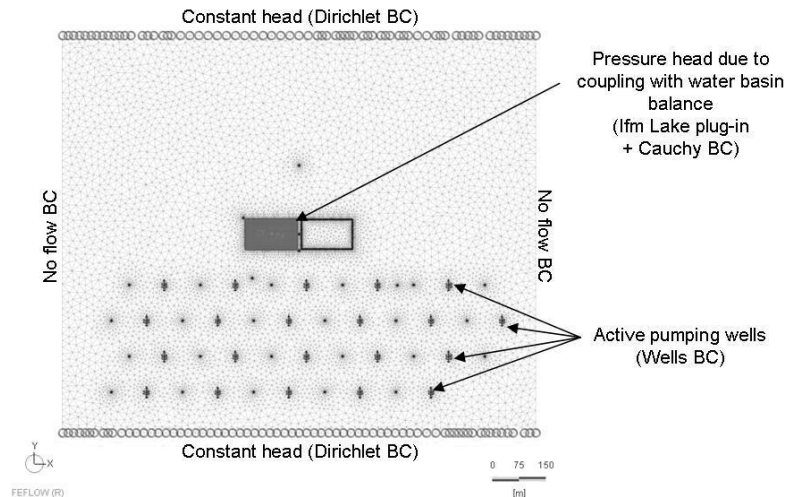


Figure 22 – View and characteristics of the 3D grid design

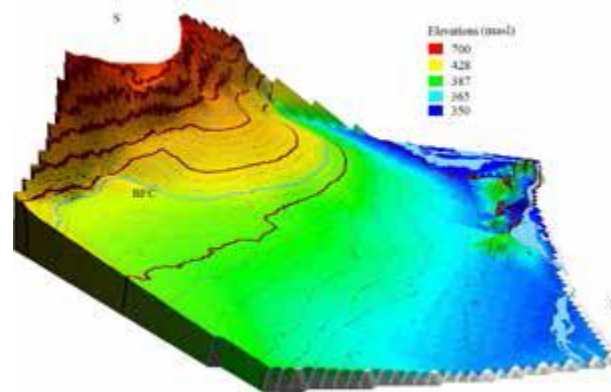


Figure 23 – Three dimensional model of the Isfara Aquifer (Adapted from Karimov et al. 2013)

Four alternative water management scenarios were considered and simulated: (1) The baseline scenario simulates actual trends in groundwater extraction for irrigation. The groundwater resources are preserved for domestic and industrial requirements as well as to cover irrigation water shortages and extractions are at minimum levels; (2) Conjunctive use of groundwater and canal water for irrigation. This scenario proposes groundwater development for irrigation in the upper part of the system and irrigation from the Big Fergana Canal in the downstream. The wells extract the annual groundwater recharge in the summer season; (3) The groundwater extraction exceeds its annual recharge by 20% and is aimed to lower the groundwater level on the periphery of the basin and arrest the salinity and waterlogging issues; (4) Managed aquifer recharge and storing of the winter flow of the Naryn River in the subsurface aquifers. The stored water in winter is projected to be withdrawn for irrigation in summer. Infiltration basins are modeled along the Big Fergana Canal. The results obtained from the conducted simulations allowed for the definitions of several strategies for water management in the study area: (1) special farmers permission and Restrictions to the amount of water that can be pumped preventing groundwater depletions (2) long-term regulation of

the groundwater storage by accumulating the excessive flow of the rivers in the subsurface horizons in winter and its recovery in summer for irrigation with regional benefits.

Sirhan & Koch (2013) modelled the effects of artificial Recharge on hydraulic heads in constant-density groundwater flow to manage the Gaza Coastal Aquifer, South Palestine. The coastal aquifers of the Gaza Strip are considered a very important source for water supply and thus very essential for the socio-economic development of the region. High rates of urbanization and increased municipal water demand, as well as extended agricultural activities, have led to an overexploitation of the aquifer, with the consequence, that the groundwater levels have dropped significantly across most of the aquifer area and induced sea water intrusion along the shoreline deteriorating quality.

The conceptual model defined in this way for the Gaza coastal aquifer has been set up in the Visual MODFLOW software consisting in one unconfined and six confined/unconfined model layers with the vertical grid size based on the hydro-geological and hydraulic properties of the geological stratigraphy (**Figure 24**).

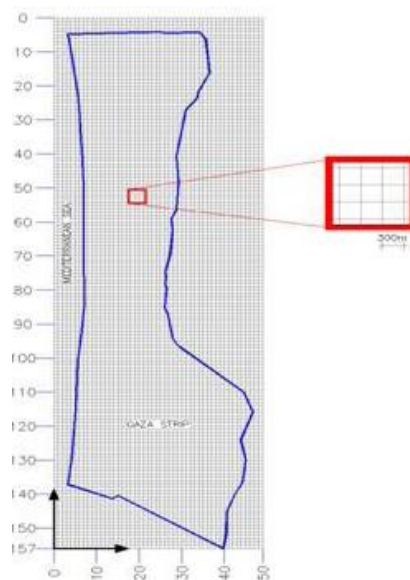


Figure 24 – Horizontal discretization of the model (Adapted from Sirhan & Koch, 2013)

The calibrated model is then the basis to explore several scenarios of management: (1) no new water resources available to recover the sustainability of the aquifer of the Gaza strip and (2) artificial recharge of reclamation wastewater is applied as a new water resource option.

The results of the first scenario are pessimistic, as they indicate a tremendous decline of the groundwater levels below the mean sea level over time, which will lead to more inland seawater intrusion. On the contrary, the results of the second scenario are more optimistic, as the simulated heads show a slight groundwater mound which rises gradually so that at end of the simulation period in year 2040 the present-day cone of depression will have completely disappeared. This shows that artificial aquifer recharge is a valid option to restore the sustainability of the Gaza coastal aquifer in the long-run.

Vicente (2013) applied numerical modelling as basis viability analysis of artificial recharge in the alluvial aquifer of the Llobregat River located in Cubeta de Sant Andreu de la Barca, Barcelona (Spain). Natural recharge has greatly decreased in this aquifer due to urban occupation, demand by industrial sector contributed to level decrease and clogging in the riverbed due to fine material deposited decrease river recharge. The main objective is to analyze the effect induced by ponds. The numerical model was developed in the Visual MODFLOW software (Figure 25).

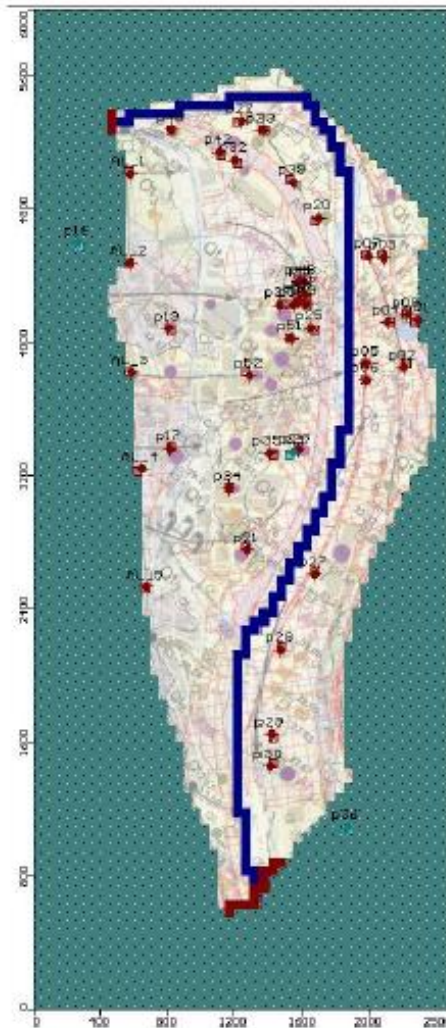


Figure 25 – Wells and River Boundary conditions (Adapted from Vicente, 2013)

The model results showed a positive effect due to basin infiltration in the aquifer storage, which is much more noticed in the start of artificial recharge procedures, decreasing throughout time.

The effect of heavy groundwater withdrawal and artificial groundwater recharge of an ex-mining pond to the aquifer system of the Langat Basin (Malaysia) was modelled by May et al. (2013) through GMS using finite difference MODFLOW (Figure 26).

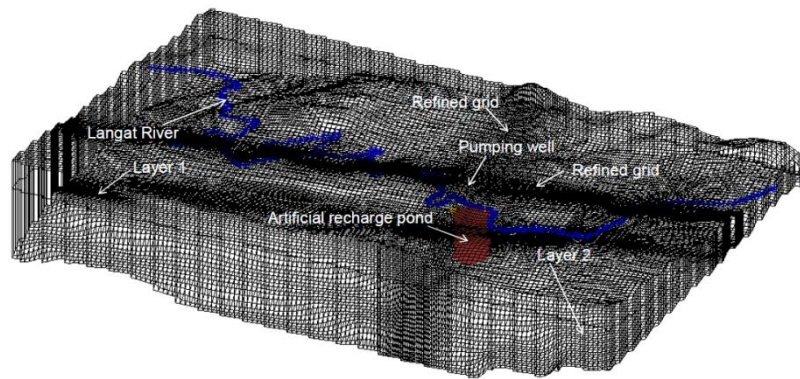


Figure 26 – Variable-spacing finite-difference grid of model area (May et al, 2013)

The model was used to predict the future water budget in the aquifer system in case of application of groundwater artificial recharge in the study area. The heavy groundwater abstraction and artificial recharge pond could alter the flow dynamics in the aquifer system. A proper methodology to handle the problem is indispensable to solving the environmental issue.

Through numerical inverse modelling Hashemi et al. (2013) quantified the recharge contribution from both an ephemeral river channel and an introduced artificial recharge system based on flood-water spreading (FWS) in Gareh-Bygone plain (Iran). The study used MODFLOW to estimate recharge for both steady and transient state conditions (Figure 27).

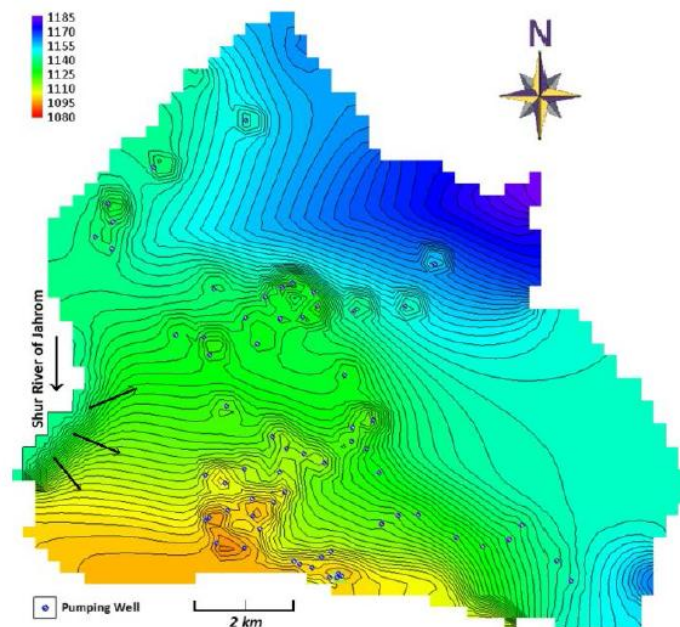


Figure 27 – Average groundwater contour map with active pumping wells and no surface recharge (Adapted from Hashemi et al, 2013)

The modeling results show that, assuming the observation wells are representative of the behavior of the studied area's aquifer, in a normal year without an extreme event the contribution of natural recharge to the groundwater storage from the river channel is about 20% and the contribution of artificial recharge from the FWS systems is about 80 %. Therefore, the FWS system is the main source of recharge in the studied area.

Most recently Händel et al. (2014) used numerical modeling is used here to assess the potential of artificial recharge under conditions commonly faced in field settings. The primary objective was to investigate if a battery of small-diameter wells could serve as a viable alternative to a surface basin under typical field conditions, while the secondary objective is to assess which subsurface parameters have the greatest control on well performance. To investigate ASR recharge processes in shallow wells and surface basins, a series of numerical simulations were performed using the finite-element software package HYDRUS 2D/3D and for result comparison simulations were ran in COMSOL Multiphysics software package. The simulated domain consists of both the vadose and saturated zones.

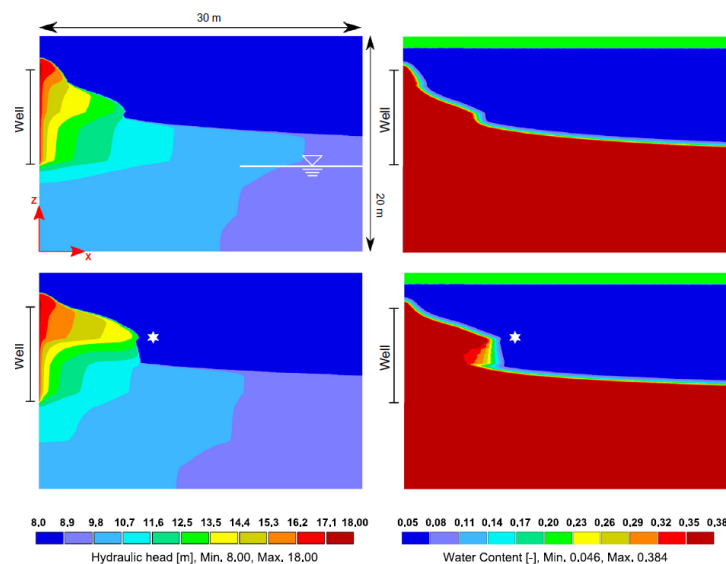


Figure 28 - Simulated hydraulic heads (left two plots) and water contents (right two plots) for the small-diameter well using layered Ks profile A (top two plots) and B (bottom two plots) at 40 days. White stars in the bottom two plots indicate the depth of 6 m where the lowest-K layer in the vadose zone is present. Other than Ks, other model settings are the same as the previous homogeneous base case simulation. Note that results are only shown for a small portion of the simulation domain (30 out of 130 m) to facilitate visualization of the near-well region (ADAPTED FROM Handel et al 2014)

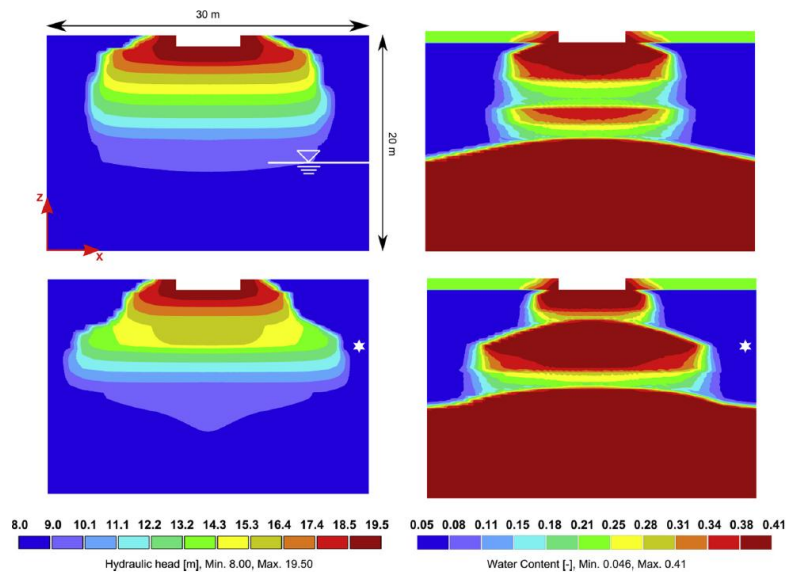


Figure 29 - Simulated hydraulic heads (left two plots) and water contents (right two plots) for the infiltration basin using layered Ks profile A (top two plots) and B (bottom two plots) at 40 days. White stars in the bottom two plots indicate the depth of 6 m where the lowest-K layer in the vadose zone is present. The plots represent a vertical cross-section through the center of the infiltration basin (adapted from Handel et al 2014)

Simulation results indicate that gravity recharge via small-diameter wells appears to have a distinct advantage over recharge via surface infiltration basins. Results also showed that contrary to an infiltration basin, the recharge rate in wells has a much stronger dependence on the horizontal component of hydraulic conductivity than on the vertical component. Moreover, near-surface layers of low hydraulic conductivity, which can significantly reduce the recharge capacity of a surface basin, have a relatively small impact on the recharge capacity of a well as long as a significant portion of the well screen is installed below those layers.

Martelli et al. (2015) studied the impact of artificial recharge in a phreatic aquifer in the Mereto Di Tomba area (Italy) by developing a numerical model that would serve as tool for managing AR activities. This area, where groundwater is one of the main sources of water for potable use, has shown a decrease of the unconfined aquifer level of about 3.5 m. The local scale model tried to understand the effects of an infiltration basin, about 5.5 m deep and 45x7 m² wide. The numerical model was developed in three-dimensional variably saturated Finite Element FLOW3D simulator (which solves Richard's equation) and calibrated with a significant amount of data collected in a set of 20 monitoring wells as well as data collected in geophysical characterization of Mereto infiltration pond. The numerical model results (**Figure 30**) showed a satisfactory match in the rise of the water levels measured in a few piezometers drilled in the pond surrounding. A negligible variation of the main water table has been observed, with the perched aquifer that rises significantly during the infiltration period and quickly reduces once the pond becomes empty.

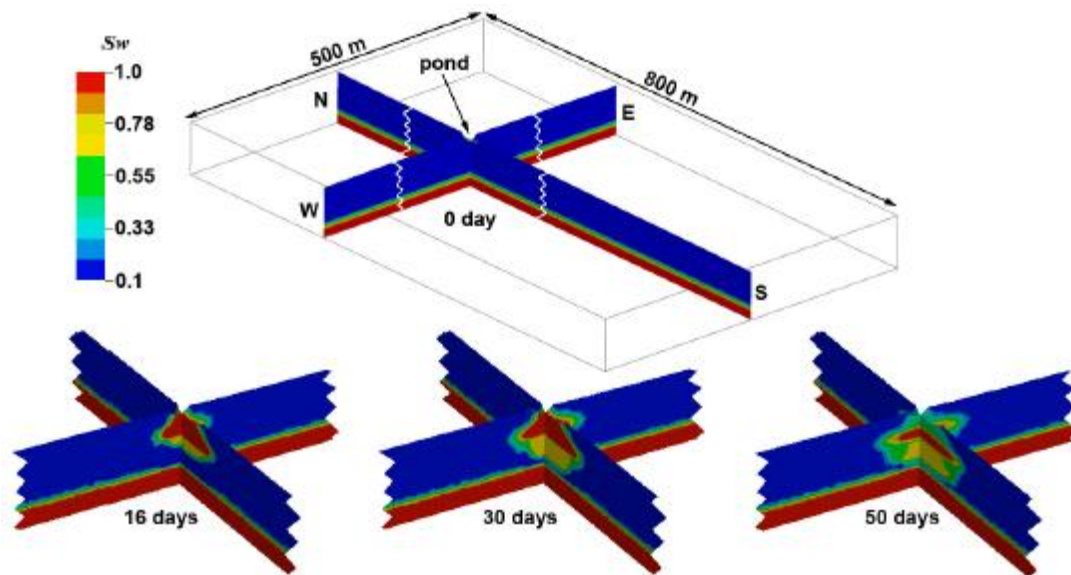


Figure 30 - Water saturation along a N-S and a W-E vertical section through the infiltration pond at the infiltration begin and after 16, 30 and 50 days of infiltration (Adapted from Martelli et al, 2015)

Chitsazan & Movehedian (2015) evaluated the impact of artificial recharge on groundwater in Gotvand Plain (Iran) using MODFLOW in GMS software (**Figure 31**). The developed model simulated the impact of a artificial recharge project, implemented by local entities in 1996 which consisted in use of floodwater spreading in an area of 440 hectares in the alluvial fan of the northern heights of Gotvand Plain. It was calibrated from September 2009 to August 2010 in an unsteady state during 12 stress periods. Hydraulic parameters were calibrated via PEST After the optimization of hydrogeological parameters, the model was validated from September 2009 to August 2010 and then it was used to assess the artificial recharge.

The results showed that the area where floodwater spreading is applied cannot make sufficient use of infiltrated water due to low hydraulic conductivity zone. Although the present artificial recharge operation makes the water budget positive, due to low specific yield and being away from consumption area, the project has a low efficiency.

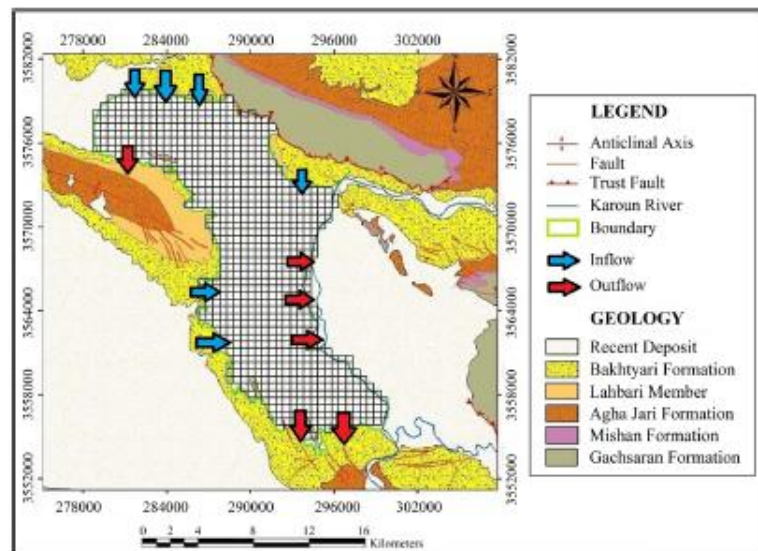


Figure 31 - Model of Gotvand-Aghili Plain groundwater along with networking and boundary condition (Adapted from Chitsazan & Movehedian, 2015)

6 HYDROGEOCHEMICAL MODELLING MAR

In the following sections a brief overview of commonly used hydrogeochemical software, followed by a set of practical applications. Accordingly to Barber (2002) field-scale reactions between mixing aqueous phases, minerals, organic carbon and ion exchange phases can be assessed relatively simply using equilibrium mixing-cells which can be used to provide a wide range of assessment of redox and pH-dependent reactions that could impact on the efficiency of an AR system. These assessments could also be used to provide quantitative evaluation of monitoring data of artificial recharge schemes. For the same author, in AR/ASR hydro geochemical modelling is relevant concerning mineral dissolution that locally can increase hydraulic conductive but have an adverse impact in aquifer structural integrity or mineral precipitation that has the opposite effect contributing to clogging.

6.1 HYDROGEOCHEMICAL MODELS OVERVIEW

In this section a set of hydrogeochemical models are presented, considering the study cases presented in the previous section.

6.1.1 INFOMI

Accordingly to Dijkhuis & Stuyfzand (1996); Stuyfzand (1998) is the acronym for 'INFiltration Of MIcropollutants'. It is a finite element 1D-model using the 'mixing cells in series' concept, incorporating: (a) a highly variable input signal for the pollutants in surface water; (b) in the infiltration basin or in a specific river segment: volatilization, photochemical and microbiological first order breakdown; (c) at the water/sediment interface: filtration of pollutants attached to suspended particles; and (d) in the saturated zone: advection, dispersion(plus diffusion), linear sorption (including DOC as a carrier), and first order breakdown (organics and radionuclides). Advection and dispersion (+diffusion) in the aquifer

system are modelled using algorithms of Appelo & Postma (1993). A flow path is essentially subdivided into at least 3 parts: (1) the infiltrating water course, (2) the water/sediment interface, and (3) the aquifer system, which may be further subdivided, for instance into bottom sludge or an upper aquiclude and the aquifer. The concentration which is calculated for the exit of each compartment forms the input for the next compartment. Standard the model generates the concentration in the aquifer along the flow path (distance travelled), and the concentration with time (the breakthrough curve) on each desired point along the flow path within the aquifer. Variables which need to be known are specified in Table 2. The most important assumptions or conditions of the model are: (1) suspended solids are filtrated at the water/sediment interface and do not play a further role, because of inert behaviour or removal by either erosion or sludge scraping; (2) steady hydrology (travel times, water depth in ponds, flow path, etc.); (3) there is no unsaturated zone; (4) each soil compartment is homogeneous and geochemically in steady state (no changes in redox environment and in leaching or accumulation of reacting components); (5) no DOC-accelerated transport of organic pollutants ; (6) trace metals are only influenced by sorption (no precipitation/dissolution); (7) each decay process is first-order (one TVz); (8) the flow velocity and longitudinal dispersivity are constant within each soil compartment; (9) linear, reversible sorption without competition; and (10) there is no temperature dependency, except for volatilization.

6.1.2 EASY-LEACHER

In Stuyfzand (1998) EASY-LEACHER is described as an analytical 2D-spread sheet model. It is based on: (a) the mass balance approach, for both reactive solutes in the water recharged and solid reactive phases in the aquifer system; (b) the cumulative frequency curve of detention times for a well or well field as derived from a separately run hydrological model; and (c) some empirical rules regarding the sequence of reactions and reaction kinetics. The model simulates for as many strata as desired: (a) displacement of the native groundwater by the water recharged; (b) the leaching of reactive soil constituents: exchangeable cations, calcite, organic matter and iron sulphides; (c) the breakthrough of reactive solutes; and (d) sorption and breakdown of organic micropollutants.

Contrary to most transport codes, the situation after each time step is directly calculated with analytical formulae, without iterations, finite elements and equilibrium calculations (calcite excluded). The composition of the recharge water is assumed constant, and the leaching of reactive solid phases is accounted for. The latter is essential for both the major constituents and organic pollutants (where the advance of redox zones determines the overall breakdown).

6.1.3 HP1

Accordingly to Jacques and Simunek (2005), HP1 was obtained by coupling the HYDRUS-1D one-dimensional variably-saturated water flow and solute transport model with the PHREEQC geochemical code. The HP1 code incorporates modules simulating (1) transient water flow in variably-saturated media, (2) transport of multiple components, and (3) mixed equilibrium/kinetic geochemical reactions. The program numerically solves the Richards equation for variably-saturated water flow and advection-dispersion type equations for heat and solute transport. The flow equation incorporates a sink term to account for water uptake

by plant roots. The heat transport equation considers transport due to conduction and convection with flowing water. The solute transport equations consider advective-dispersive transport in the liquid phase. The program can simulate a broad range of low-temperature biogeochemical reactions in water, soil and ground water systems including interactions with minerals, gases, exchangers, and sorption surfaces, based on thermodynamic equilibrium, kinetics, or mixed equilibrium-kinetic reactions. The program may be used to analyze water and solute movement in unsaturated, partially saturated, or fully saturated porous media. The flow region may be composed of non-uniform soils or sediments. Flow and transport can occur in the vertical, horizontal, or a generally inclined direction. The water flow part of the model can deal with prescribed head and flux boundaries, boundaries controlled by atmospheric conditions, as well as free drainage boundary conditions. The governing flow and transport equations were solved numerically using Galerkin-type linear finite element schemes.

6.1.4 HYDROGEOCHEM

Commercial software HYDROGEOCHEM⁽¹⁾ is a coupled model of hydrologic transport and geochemical reaction in saturated-unsaturated media. It is designed to simulate transient and/or steady-state transport of Na, aqueous components and transient and/or steady-state mass balance of Ns adsorbent components and ion-exchange sites. Along the transport path, HYDROGEOCHEM computes the species distribution of N component species, Mx complexed species, My adsorbed species, Mz ion-exchanged species and Mp potentially precipitated species. HYDROGEOCHEM computes and predicts the distribution of pressure head, moisture content, flow velocity, and total head over a three-dimensional plane in either completely saturated, completely unsaturated, partially unsaturated, or partially saturated subsurface media. It also computes and predicts the spatial-temporal distribution of multi-chemical components. The media may consist of as many types of soils and geologic units as desired with different material properties. Each soil type may be isotropic or anisotropic. The processes governing the distribution of chemical distribution include (1) geochemical equilibrium of aqueous complexation, reduction-oxidation, sorption, and precipitation and dissolution, and (2) hydrological transport by flow advection, dispersion, and effect of unsaturation.

6.1.5 PHREEQC

Parkhurst and Appelo (2013) describe PHREEQC is a computer program that is designed to perform a wide variety of aqueous geochemical calculations simulating chemical reactions and transport processes in natural or polluted water, in laboratory experiments, or in industrial processes.

The program is based on equilibrium chemistry of aqueous solutions interacting with minerals, gases, solid solutions, exchangers, and sorption surfaces, which accounts for the original acronym—pH-REdox-EQuilibrium, but the program has evolved to include the capability to model kinetic reactions and 1D (one-dimensional) transport. Rate equations are completely

user-specifiable in the form of Basic statements. Kinetic and equilibrium reactants can be interconnected, for example, by linking the number of surface sites to the amount of a kinetic reactant that is consumed (or produced) in a model period. A 1D transport algorithm simulates dispersion and diffusion; solute movement in dual porosity media; and multicomponent diffusion, where species have individual, temperature-dependent diffusion coefficients, but ion fluxes are modified to maintain charge balance during transport. A powerful inverse modeling capability allows identification of reactions that account for observed water compositions along a flowline or in the time course of an experiment. Extensible chemical databases allow application of the reaction, transport, and inverse-modeling capabilities to almost any chemical reaction that is recognized to influence rainwater, soil-water, groundwater, and surface-water quality.

It implements several types of aqueous models: two ion-association aqueous models (the Lawrence Livermore National Laboratory model and WATEQ4F), a Pitzer specific-ion-interaction aqueous model, and the SIT (Specific ion Interaction Theory) aqueous model. Using any of these aqueous models, PHREEQC has capabilities for (1) speciation and saturation-index calculations; (2) batch-reaction and one-dimensional (1D) transport calculations with reversible and irreversible reactions, which include aqueous, mineral, gas, solid-solution, surface-complexation, and ion-exchange equilibria, and specified mole transfers of reactants, kinetically controlled reactions, mixing of solutions, and pressure and temperature changes; and (3) inverse modeling, which finds sets of mineral and gas mole transfers that account for differences in composition between waters within specified compositional uncertainty limits.

6.2 CASE STUDIES AND APPLICATIONS IN HYDROGEOCHEMICAL MODELLING

In this section a brief literature review is presented for models that are related to the modelling of quality of the infiltrated/injected water. These models are particularly useful in understanding the changes that infiltration/injected water is subjected in MAR procedures, allowing optimizing procedures and/or comprehends contamination problems. Although some transport modelling is presented, the section focus predominantly in software or code specifically designed for geochemical modelling.

Whitworth (1995) modelled recharge via subsurface injection in El Paso, New Mexico (USA) with PHREEQE (Parkhurst et al. 1980), by first simulating the mixing of the injected water and the ground water to see if mineral precipitation might occur. After mineral saturation was examined, an additional simulation was made that equilibrated the solution with the minerals most likely to precipitate at equilibrium. The results of this second run gave the mass of each mineral likely to precipitate. Accordingly to the author The El Paso subsurface injection simulations serve as a reality check on the outcome of hydrogeochemical modelling of artificial recharge for the City of Albuquerque.

In Stuyfzand (1998) two models for reactive transport of pollutants and main constituents during artificial recharge and bank filtration are presented and tested: INFOMI and EASY-

LEACHER. The first is a finite element 1D-model using 'mixing cells in series and was applied in (a) the definition of the behaviour of radionuclides ^{90}Sr , ^{60}Co , ^{106}Ru and ^{137}Cs during dune sand passage after spreading basin recharge in a facility of The Hague (Netherlands) and (b) understanding of the behaviour of chloroform (CHCl_3), bromodichloromethane (CHCl_2Br), dibromochloromethane (CHBr_2Cl) and bromoform (CHBr_3) in context of basin recharge system. The second (EASY-LEACHER) is a 2D spread-sheet model, based on: the mass balance approach; travel times derived from a separate hydrological model; and empirical rules on reaction sequence and kinetics. The model was tested in deep well injection, where water quality evolution in the recovery well of deep well injection was simulated for the Pre-treated oxic water from the Zuid-Willemsvaart (a canal containing mainly river Meuse water – Netherlands) is injected into an anoxic Miocene sandy aquifer. Results showed satisfactory agreement between measured and calculated model predictions in a 100 year recharge experiment.

Parkhurst & Petkewich (2002) used PHREEQC for geochemical modelling of an ASR experiment in Charleston, South Carolina (USA). The purpose of the aquifer storage operation is to store potable drinking water in a sand and limestone aquifer underlying the city of Charleston. Application of geochemical modelling approaches were useful in understanding the induced flow in the aquifer, deducing the important chemical reactions, building hypotheses, and identifying unanswered questions related to full-scale operations. The authors also used PHAST (Parkhurst et al. 1995) for development of a three-dimensional model of the injection, storage, and recovery experiment used the hydraulic properties derived from the solute-transport analysis of chloride and the reactions deduced by speciation, inverse, and one-dimensional reactive-transport modelling.

Barber (2002) presented two main case studies where relatively simple hydrogeochemical modelling was used for prediction and interpretation of water quality trends. The first case study refers to a Soil Aquifer Treatment experiment in China where PHREEQC was used to assess possible chemical reactions on mixing of groundwater and injectant (potable water from a reservoir) while the second tried to understand reaction exchange with possible aquifer mineral matrices during a trial potable water ASR injection. Results proved to be useful for interpretation of groundwater monitoring data and the understanding of processes, their impacts in groundwater and in AR system behaviour.

Prommer & Stuyfzand (2005) carried out a reactive transport modelling study to analyze the data collected during a deep well injection experiment in an anaerobic, pyritic aquifer near Someren (Netherlands). The MODFLOW/MT3DMS-based re-active multicomponent transport model PHT3D (Prommer et al., 2003) was used for the transport simulations of the injection site. PHT3D couples the three-dimensional transport simulator MT3DMS with the geochemical model PHREEQC (v2).

Greskowiak et al (2005) carried out a modelling study to provide a process-based quantitative interpretation of the biogeochemical changes that were observed during an ASR experiment in which reclaimed water was injected into a limestone aquifer at a field-site near Bolivar (Australia). A multi-component transport model PHT3D was developed from a calibrated

three-dimensional flow and conservative transport model of the ASR trial. The model approach was able to reproduce the geochemical changes further away from the injection/extraction well. These changes were interpreted as a result of the combined effect of ion exchange, calcite dissolution and mineralisation of dissolved organic carbon.

Eckert et al. (2005) applied hydrogeochemical modelling in 1D-reaction transport model PHREEQC (v2) (Parkhurst and Appelo, 1999) to assess the purification processes that occur during riverbank filtration, in order to understand the temporal changes of the river water quality and hydraulics influence of this methodologies.

Schmidt et al. (2007) while studying the geochemical effects of induced stream-water and artificial recharge on the Equus Beds Aquifer, Kansas (USA) used PHAST to simulate flow and transport of chloride from the stream through the aquifer into a recovery well. PHREEQC (v2) was also used for major ion and trace metal chemistry modelling providing insight into environmental changes that may be occurring as a result of AR activities, as well as saturation indices. Results of the simulation indicated that calcite oversaturation was likely only for mixtures that are greater than 90 percent recharge water, calcite precipitation could reduce permeability and effectiveness of AR and amorphous ferric oxyhydroxide oversaturation is possible in the mixture of waters.

In a geochemical modelling exercise of an ASR project in Union County, Arkansas (USA), Zhu (2013) used PHREEQC to simulate the scenario of injecting partially treated surface water from Ouachita River into the Sparta aquifer at the city of El Dorado. Key reactions modelled include the initial mixing of the two waters in the proximal zone, surface exchange reactions of the major cations, iron precipitation/ dissolution reactions and the oxidizing potential of the injection water. Geochemical modelling showed that reducing the oxygen content of the injection water to enhance geochemical compatibility with the anoxic aquifer water would be beneficial and arsenic dissolution or attenuation could occur depending on the mixing ratio of injection water to groundwater.

Lu et al (2014) produced a hydrochemical assessment of the local harvested water and groundwater based on field data, lab experiments, and modelling was carried out for artificial recharge proposal in the Pinggu Basin aquifer. To model the dynamic hydrochemical changes during AR, transport process coupled with the geochemical equilibrium was resolved using PHREEQC. These were to simulate chemical reactions, soil soluble species dispersion, mineral dissolution and precipitation, and cation exchange in the recharge vadose zone. Results showed that, in the long run, recharge by the harvested water was unlikely to have a negative impact on groundwater quality.

Niinikoski et al. (2016) aimed to establish a method for monitoring the decomposition of organic matter (dissolved organic carbon – DOC) in cases where calcite dissolution adds another component to the dissolved inorganic carbon (DIC) pool, and to use this method to monitor the beginning and amount of DOC decomposition on a MAR site at Virttaankangas (Finland). To achieve this geochemical modelling using PHREEQC was conducted to estimate the amount of DOC decomposition and the mineral reactions affecting the quality of the

water, and to calculate the mean residence times of infiltrated water in the aquifer and the fractions of this water reaching observation wells. The results allowed determining that mean residence time of the infiltrated water was from 15 to 40 weeks, while decomposition of DOC commenced with a higher infiltration volume.

7 CONCLUSIONS OF THE STATE OF THE ART AND LITERATURE REVIEW IN MANAGED AQUIFER RECHARGE MODELLING

Following the literature review for MAR modelling, the main conclusion, considering that for every model there is a different set of input data required, so one of the most important factor in selecting the appropriate model to a specific area/study is to verify what data is available/obtainable in order to feed it as much as possible allowing it to produce reliable results.

Based on the Decision making methodology for the application of pollutant transport models proposed by Diamantino et al (2006) the final decision for the selection and eventually the purchasing of a new model will have to be based on local or regional available skills and know-how on groundwater modelling at the governmental environmental institution. The authors do firmly support the idea of governmental environmental institution to establish research contracts with local Universities and/or State Research Labs, and, if available, eventually also with private firms with relevant expertise on groundwater assessment and modelling. Also, for the author, this will be a case by case political decision depending on the willingness of the governmental environmental institution to overcome existing or potential groundwater pollution problems that may affect the regional environment and the public health.

Used models vary, but finite difference MODFLOW base software seems to be by far more frequently used, both due to be easily available and well documented, there are several programs adapted to specific problems. Due to its complexity finite elements are not so abundantly used, although the FEM grid is far more adjustable to complex limits of study areas. On the other hand, FEM HYDRUS was commonly selected for simulations in vadose zone. In hydrogeochemical studies related to MAR, free PHREEQC software was the most used, mostly due to its very wide set of capabilities.

Aquifer and local (small area of the aquifer) seems to be the most common scales studied. Small scale models (infiltration basin or aquifer sandbox model recreation) are scarce. MAR modelling, at a large scale, has been used as a decision support tool as basis to decide the suitability of MAR methodologies, most effective measures of environmental problem containment and to explore scarcity scenarios.

MAR modelling is being used worldwide, in particular in semi-arid to arid regions where scarcity problem is common and MAR presents as reliable solution, and in areas the use of recycled water is increasingly used in SAT-MAR as a way to increase water quality and availability.

References

- Aly, H.A. and Peralta, R.C. (1995) Efficient Use of Artificial Recharge in Groundwater Pump and Treat Remediation Systems. In Johnson, A.I. and Pyne, D.G. (eds.) (1994) Proceedings of the 2nd International Symposium on Artificial Recharge of Groundwater, Florida, USA, 679–687p.
- Appelo, C.A.J., Postma, D. (1993) Geochemistry, groundwater and pollution. Balkema Publishers, 536p.
- Barber, C. (2002) Artificial Recharge of Groundwater and aquifer storage and recovery of water and wastewater: approaches for evaluation of potential water quality impacts. In Thangarajan, M., Rai, S. N., Singh, V. S. (eds.) (2002) Proceedings of Conference on Sustainable Development and Management of Groundwater Resources in Semi-Arid Region with Special Reference to Hard Rock (IGC 2002), India, 256p.
- Bedekar, V., Morway, E.D., Langevin, C.D., and Tonkin, M. (2016) MT3D-USGS version 1: A U.S. Geological Survey release of MT3DMS updated with new and expanded transport capabilities for use with MODFLOW: U.S. Geological Survey Techniques and Methods 6-A53, 69 p.
- Carleton, G.B. (2010) Simulation of Groundwater Mounding Beneath Hypothetical Stormwater Infiltration Basins. U.S. Geological Services. Scientific Investigations Report 2010–5102, 64p.
- Chatdarong, V. (2001) Artificial Recharge for Conjunctive Use in Irrigation: The San Joaquin Valley, California. Department of Civil and Environmental Engineering, Massachusetts Institute of Technology, 60p.
- Chiang, W.H. & Kinzelbach, W. (1998) Processing Modflow. A simulation system for modelling groundwater flow and pollution. Guide for the program. 334p.
- Chitsazan, M., Movehedian, A. (2015) Evaluation of Artificial Recharge on Groundwater Using MODFLOW Model (Case Study: Gotvand Plain-Iran). Journal of Geoscience and Environment Protection, 3, 122-132p.
- Coll, A., Pasenau, M., Escolano, E., Perez, J.S. Melendo, A., Monros, A. (2016) GiD v.13 User Manual. CIMNE, 187p.
- Diamantino, C., Lobo Ferreira, J.P., Novo, M.E. (2006) Policies for the application of pollutant transport models in groundwater. Decision making methodology for the application of pollutant transport models. MANPORIVERS Project Deliverable 35. Methodologies for the assessment of groundwater quantity and quality and the management of groundwater for sustainable development, 63p.
- Diersch, H. (2014) FEFLOW: Finite Element Modeling of Flow, Mass and Heat Transport in Porous and Fractured Media. Springer Science & Business Media, 996p.
- Dijkhuis, L.G., Stuyfzand, P.J. (1996) INFOMI 3.1: a 1-D transport model for micropollutants in a water course and in the underground after infiltration. Kiwa-report SWI 96.219 (in dutch).

Eckert, P., Rohns, H.P., Irmscher, R. (2005) Dynamic processes during bank filtration and their impact on raw water quality. In. Recharge systems for protecting and enhancing groundwater resources. Proceedings of the 5th International Symposium on Management of Aquifer Recharge ISMAR5, Berlin, Germany, 17-21p.

EPTISA (2009) Actualización del Modelo Matemático de Flujo del Acuífero de Crestatx (Mallorca). Asistencia Técnica para el Desarrollo de la Actividad Cuatro del Convenio Específico entre el Instituto Geológico y Minero de España y el Gobierno Balear sobre Investigación en Aguas Subterráneas. Instituto Geológico y Minero de España, 62p.

Flint, A.L. (2003) The Role of Unsaturated Flow in Artificial Recharge Projects. TOUGH Symposium Proceedings. Lawrence Berkeley National Laboratory, Berkeley, California, 6p.

Glover, R.E. (1960) Mathematical derivations as pertain to groundwater recharge. Agricultural Research Service, USDA, Ft. Collins, Colorado. 81p.

De la Orden, J.A., Murillo, J.M. (2003) La recarga artificial en el acuífero de Vergel (Alicante) como técnica paliativa de los efectos de la intrusión marina y su evaluación mediante modelación matemática. Tecnología de la Intrusión de Agua de Mar en Acuíferos Costero: Países Mediterráneos. Madrid, 767-774p.

Goyal, V., Jhorar, B.S., Malik, R.S., Streck, T. (2009) Simulation of groundwater recharge from an aquifer storage recovery well under shallow water-table condition. Current Science, Vol. 96, No. 3, 376-385p.

Greskowiak, J., Prommer, H., Vanderzalm, J., Pavelic, P., Dillon, P. (2005). Modeling of carbon cycling and biogeochemical changes during injection and recovery of reclaimed water at Bolivar, South Australia, Water Resources Research, vol. 41 (10), 41(10), W10418, 16p.

Guo, W., and Langevin, C.D. (2002) User's Guide to SEAWAT: A Computer Program for Simulation of Three-Dimensional Variable-Density Ground-Water Flow: Techniques of Water-Resources Investigations Book 6, Chapter A7, 77p.

Haimmerl, G. (2002) Infiltration Tests and Numerical Simulations to Evaluate the Efficiency of Infiltration in Arid Countries. Third International Conference on Water Resources and Environment Research. 121-125p.

Hantush, M.S. (1967) Growth and decay of groundwater mounds in response to uniform percolation. Water Resources Research, v. 3, 227-234p.

Händel, F., Liu, G., Dietrich, P., Liedl, R., Butler Jr., J.J. (2014) Numerical assessment of ASR recharge using small-diameter wells and surface basins, Journal of Hydrology, Volume 517, 54-63p.

Harbaugh, A. W. (2005) MODFLOW-2005, The U.S. Geological Survey Modular Ground-Water Model—the Ground-Water Flow Process. U.S. Geological Survey Techniques and Methods 6-A16, variously p.

Hashemi, H., Berndtsson, R., Kompani-Zare, M., Persson, M. (2013) Natural vs. artificial groundwater recharge, quantification through inverse modeling. *Hydrology and Earth System Sciences*, 17, 637–650p.

Jacques, D., Simunek, J. (2005) User Manual of the Multicomponent Variably-Saturated Flow and Transport Model HP1, Description, Verification and Examples, Version 1.0, SCK.CEN-BLG-998, Waste and Disposal, SCK.CEN, Belgium, 79 p.

Jammal & Associates Division – Professional Service Industries, Inc. (1993) Full-Scale Hydrologic Monitoring of Stormwater Retention Ponds and Recommended Hydro-Geotechnical Design Methodologies. Indian River Lagoon Basin, St. Johns River Water Management District, Florida. Special Publication SJ93-SP10, Vol. 1. 180p.

Kareem, I.R. (2012) Artificial Groundwater Recharge in Iraq through Rainwater Harvesting (Case Study). *Engineering & Technologies Journal*, Vol. 31, Part (a), No.6, 1069-1080p.

Karimov, A., Smakhtin, V., Mavlonov, A., Borisov, V., Gracheva, I., Miryusupov, F., Djumanov, J., Khamzina, T., Ibragimov, R., Abdurahmanov, B. (2013) Managed aquifer recharge: the solution for water shortages in the Fergana Valley. Colombo, Sri Lanka: International Water Management Institute (IWMI), Research Report 151, 51p.

Koukidou, I., Panagopoulos, A., Arampatzis, G., Hatzigiannakis, E. (2010) Groundwater flow modeling as a tool for assessing aquifer restoration using artificial recharge. The case of Tirnavos alluvial basin, central Greece. *E-Proc. 10th Int. Conference Protection and Restoration of the Environment*, Corfu, 1-8p.

Langevin, C.D., Thorne, D.T., Jr., Dausman, A.M., Sukop, M.C., and Guo, Weixing (2008) SEAWAT Version 4: A Computer Program for Simulation of Multi-Species Solute and Heat Transport: U.S. Geological Survey Techniques and Methods Book 6, Chapter A22, 39p.

Li, Q., Ito, K., Wu, Z., Lowry, C. S. and Loheide II, S. P. (2009) COMSOL Multiphysics: A Novel Approach to Ground Water Modeling. *Ground Water*, 47, 480–487p.

Lin, H.J. ; Richards, D. R. ; Yeh, G. ; Cheng, J.; Cheng, H. (1997) FEMWATER: A Three-Dimensional Finite Element Computer Model for Simulating Density-Dependent Flow and Transport in Variably Saturated Media. Final Report. RMY Engineer Waterways Experiment Station Vicksburg MS Coastal Hydraulics Lab, 143p.

Lobo Ferreira, J.P., Diamantino, C., Moinante, M.J., Oliveira, M.M., Leitão, T.E., Henriques, M.J., Medeiros, A., Dimitriadis, K., Styllas, M., Soupilas, T., Maheras, P., Anagnostopoulou, C., Tolika, K., Vafiadis, M., Machairas, C., Sanchez-Vila, X., Barbieri, M., Bensabat, J., Hadad, A., Rabi, A., Tamimi, A.R. (2006) GABARDINE Groundwater artificial recharge based on alternative sources of water: advanced integrated technologies and management. Deliverable 51: Test sites and their characteristics. Laboratório Nacional de Engenharia Civil, 185p.

Lobo Ferreira, J.P., Oliveira, L., Rocha, E. J., Gaaloul, N. (2009) Índice de suporte à escolha de áreas favoráveis à recarga artificial (GABA-IFI): Análise das componentes ambientais, sociais e

económicas. 9. SILUSBA - Simpósio de Hidráulica e Recursos Hídricos dos Países de Língua Oficial Portuguesa, 13p.

Loizeau S., Rossier, Y., Gaudet, J.P. (2012) Improving the knowledge of a complex well field functioning including infiltration basins with unsaturated/saturated 3D modeling. 3rd Feflow User Conference, Berlin, 7p.

Lu, Y., Du, X., Yang, Y., Fan, W., Chi, B., Wang, Z., & Ye, X. (2013) Compatibility Assessment of Recharge Water with Native Groundwater Using Reactive Hydrogeochemical Modeling in Pinggu, Beijing. CLEAN - Soil, Air, Water, 42(6), 722–730p.

Martelli, G., Granati, C., Paiero, G., Teatini, P., Comerlati, A., Carvalho, T., Carvalho, J., Affatato, A., Baradello, L., Yabar, D. (2014) Artificial Recharge of Phreatic Aquifer in the Mereto Di Tomba Area (Upper Friuli Plain). 16th Conference on Water Distribution System Analysis, WDSA 2014. Procedia Engineering 89, 1241 – 1248p.

May, R., Jinno, K., Yusoff, I. (2013) Effects of Heavy Pumping and Artificial Groundwater Recharge Pond on the Aquifer System of Langat Basin, Malaysia. World Academy of Science, Engineering and Technology International Journal of Environmental, Ecological, Geological and Mining Engineering Vol.7 No.2, 92-100p.

McDonald, M. G. and Harbaugh, A. W. (1984) A modular three-dimensional finite-difference ground-water flow model, Open-File Report 83-875, U.S. Geological Survey, 528p.

Niinikoski, P., Saraperä, S., Hendriksson, N., & Karhu, J. A. (2016) Geochemical and flow modelling as tools in monitoring managed aquifer recharge. Applied Geochemistry, 74, 33–43p.

Olivella, S., Gens, A., Carrera, J., Alonso, E. E. (1995) Numerical formulation for a simulator (CODE_BRIGHT) for the coupled analysis of saline media. Engineering Computations, Vol. 13 No. 7, 1996, pp. 87-112p.

Parkhurst, D.L., Appelo, C.A.J. (1999): Users guide to PHREEQC (version 2). U.S. Geological Survey. Water Resour. Inv. 99-4529, 312p.

Parkhurst, D.L., Appelo, C.A.J. (2013) Description of input and examples for PHREEQC version 3—A computer program for speciation, batch-reaction, one-dimensional transport, and inverse geochemical calculations. U.S. Geological Survey Techniques and Methods, book 6, chap. A43, 497p.

Parkhurst, D. L., Engesgaard, P., Kipp, K. L. (1995) Coupling the geochemical model PHREEQC with a 3D multi-component solute-transport model. V.M. Goldschmidt Conference, State College, Pensilvania, Program and Abstracts, 77-78p.

Parkhurst, D.L., Petkewich, M.D. (2002) Geochemical Modeling of an Aquifer Storage Recovery Experiment, Charleston, South Carolina. In Aiken, G.R., Kuniandy, E. (ed), U.S. Geological Survey Artificial Recharge Workshop Proceedings, Sacramento, California, 38-41p.

Parkhurst, D.L., Thorstenson, D.C., and Plummer, L.N. (1980) PHREEQE - a computer program for geochemical calculations. U.S. Geological Survey, Water Resources Investigations, Report 80 96, 195p.

Pliakas, F., Petalas, C., Diamantis, I. and Kallioras, A., (2005), Modeling of Groundwater Artificial Recharge by Reactivating an Old Stream Bed, Water Resources Management: An International Journal, Published for the European Water Resources Association (EWRA), 19, issue 3, p. 279-294,

Pollock, D.W. (1989) Documentation of a computer program to compute and display pathlines using results from the U.S. Geological Survey modular three- dimensional finite-difference ground-water flow model. U.S. Geological Survey Open-File Report 89–381, 188p.

Pollock, D.W. (2016) User guide for MODPATH Version 7—A particle-tracking model for MODFLOW. U.S. Geological Survey Open-File Report 2016–1086, 35p.

Prommer, H., Barry, D., A., Zheng, C. (2003). MODFLOW/MT3DMS based reactive multicomponent transport modelling. Ground Water, 41(2), 247-257p.

Prommer, H., Stuyfzand, P.J. (2005) Identification of Temperature-Dependent Water Quality Changes during a Deep Well Injection Experiment in a Pyritic Aquifer. Environmental Science & Technology 2005 39 (7), 2200-2209p.

Pruess, K. (1987) TOUGH User's Guide. Lawrence Berkeley National Laboratory & Sandia National Laboratories, 77p.

Pruess, K., Oldenburg, C., and Moridis, G. (1999) TOUGH2 User's Guide, Version 2.0. Report LBNL-43134, Lawrence Berkeley National Laboratory, Berkeley, California, 198p.

Restrepo, D.R., Ruiz, M.F., Malcom, M.M., Pinyol, N., Vilarrasa, V. (2016) CODE_BRIGHT User's Guide. Departament d'Enginyeria del Terreny, Cartogràfica i Geofísica. Universitat Politècnica de Catalunya, 183p.

Sanford, W.E., and Konikow, L.F. (1985) A two-constituent solute transport model for ground water having variable density. U.S. Geological Survey Water-Resources Investigations Report 85-4279, 89p.

Sanford, W. (2002). Recharge and groundwater models: an overview. Hydrogeology Journal, 10(1), 110–120p.

Santo Silva, G.E., Montenegro, S.M., Cavalcanti, G.D. (2006) Aplicação e Modelagem da Recarga Artificial com Águas Pluviais para Recuperação Potenciométrica de Aquífero Costeiro na Planície do Recife-PE. RBRH – Revista Brasileira de Recursos Hídricos Volume 11 n.3 Jul/Set 2006, 159-170p.

Schmidt, H.C.R., Ziegler, A.C., & Parkhurst, D.L. (2007). Geochemical Effects of Induced Stream-Water and Artificial Recharge on the Equus Beds Aquifer, South-Central Kansas, 1995-2004. US Department of the Interior, US Geological Survey, 58p.

- Simunek, J., Huang, K., van Genuchten, M.Th. (1998) The HYDRUS code for simulating the one-dimensional movement of water, heat, and multiple solutes in variably-saturated media. Version 6.0. Research Report No. 144, California. U.S. Salinity Laboratory, USDA, ARS, Riverside, 164p.
- Sirhan, H., Koch, M. (2013) Numerical Modeling of the Effects of artificial Recharge on Hydraulic Heads in constant-Density Ground Water Flow to manage the Gaza Coastal Aquifer, South Palestine. 6th International Conference on Water Resources and Environment Research. Water & Environmental Dynamics, Koblenz, Germany, 115-147p.
- Stefanescu, C. and Dassargues, A. (1996) Simulation of pumping and artificial recharge in a phreatic aquifer near Bucharest, Romania, Hydrogeology Journal. 4(3), 72–83p.
- Stuyfzand, P.J. (1998) Simple Models for Reactive Transport of Pollutants and Main Constituents During Artificial Recharge and Bank Filtration', in J. H. Peters et al. (eds.), Proceedings of the 3rd International Symposium on Artificial Recharge of Groundwater, TISAR 98, Amsterdam, The Netherlands, A. A. Balkema Publishers, 427–434p.
- Sunada, D.K., Molden, D.J., Warner, J.W. (1983) Artificial groundwater recharge, San Luis Valley, Colorado. Completion Report No. 123. Colorado Water Resources Research Institute, Colorado State University, 116p.
- TECSOFT Inc. (1998) MOC DENSE EM. User manual. 10 pp.
- Trefry, M. G. and Muffels, C. (2007), FEFLOW: A Finite-Element Ground Water Flow and Transport Modeling Tool. Ground Water, 45, 525–528p.
- Vicente, D.R. (2013) Análisis de la Técnica de Recarga Artificial en la Cubeta de Sant Andreu de la Barca (Barcelona). Proyecto final de carrera. Departamento de Ingeniería Geológica, Escuela Técnica Superior de Ingenieros de Minas de Universidad Politecnica de Madrid, 138pp.
- Whitworth, T. M. (1995) Hydrogeochemical computer modeling of proposed artificial recharge of the upper Sante Fe Group aquifer, Albuquerque, New Mexico. New Mexico Geology, v. 17, no. 4, 72-78p.
- Woolfenden, L.R., Koczot, K.M. (2001) Numerical Simulation of Ground-Water Flow and Assessment of the Effects of Artificial Recharge in the Rialto–Colton Basin, San Bernardino County, California. U.S. Geological Survey, Water-Resources Investigations Report 00.4243, 148p.
- Wright, A. and du Toit, I. (1996) Artificial recharge of urban wastewater, the key component in the development of an industrial town on the arid West Coast of South Africa. Hydrogeology Journal 4(1), 118–129p.
- Yeh, G. T., and Tripathi, V. S. (1987). Strategies in modeling transport of reactive multi-chemical components. Groundwater and the environment. Proceedings, International

Groundwater Conference. Faculty of Engineering and Faculty of Physical and Applied Science, Universiti Kebangsaan Malaysia, Kuala Lumpur, Malaysia, 26-36p.

Yu, C. and Zheng, C. (2010), HYDRUS: Software for Flow and Transport Modeling in Variably Saturated Media. Ground Water, 48, 787–791p.

Zheng, C., Mary C. Hill, and Paul A. Hsieh, (2001) MODFLOW-2000, the U.S. Geological Survey modular ground-water model - user's guide to the LMT6 package, the linkage with MT3DMS for multi-species mass transport modeling. U.S. Geological Survey Open-File Report 01-82, 43p.

Zhu, N. (2013) Geochemical Modeling of an Aquifer Storage and Recovery Project in Union County, Arkansas. Department of Civil and Environmental Engineering, Massachusetts Institute of Technology, 84p.

White book on MAR modelling

Deliverable D12.7

CHAPTER 3 – WATER BUDGET AND CLIMATE CHANGE IMPACT: ASSESSMENT OF DEMO SITE 2 ALGARVE AND ALENTEJO, PORTUGAL AND DEMO SITE 7 MENASHE, ISRAEL

J.P. LOBO FERREIRA, MANUEL M. OLIVEIRA (LNEC), JOSÉ PAULO MONTEIRO, LUÍS COSTA (UALG), YORAM KATZ (MEKOROT)

8 WATER BUDGET AND CLIMATE CHANGE IMPACT: ASSESSMENT OF DEMO SITE 2 ALGARVE AND ALENTEJO, PORTUGAL AND DEMO SITE 7 MENASHE, ISRAEL

8.1 DEMO SITE 2 DEMO SITE 2: ALGARVE AND ALENTEJO, SOUTH PORTUGAL

The demo site 2: Algarve and Alentejo, South Portugal, is composed of three DEMO sites (Figure 2):

- PT1: Rio Seco and Campina de Faro aquifer system (Algarve).
- PT2: Querença-Silves limestone karstic aquifer system (Algarve).
- PT3: Melides aquifer, river and lagoon (Alentejo).

These Demo sites are thoroughly characterised in WP4.

8.1.1 Conceptual model

The conceptual model gathers all the information required to understand the situation under demo. A comprehensive analysis of the hydrology of the watershed upstream each MAR site is provided, as well as of the underlying hydrogeology.

GIS layers of information are prepared, including the DRASTIC vulnerability to pollution index, parameters related to the unsaturated zone capacity for incorporating MAR water (e.g. depth to the water table), or the GABA-IFI index to define the most appropriate areas for MAR.

8.1.2 Large diameter infiltrating wells in Campina de Faro aquifer system

The conceptual model of the Campina de Faro aquifer system is detailed on Deliverable 4.2 from where this text was withdrawn. Figure 32 (Stigter, 2005) presents a hydrogeological section of Campina de Faro area. The oldest formations belong to the Jurassic gypsiferous material that locally outcrops near Faro and is related to diapiric activity.

According to Stigter (2005), the oldest aquifer system that occurs in the Campina de Faro area is the Cretaceous, formed by limestone layers separated by marls (**Figure 32**). They dip to the south (20°-30°) and crop out in the NW part of the area. The top of the sediments is found at a depth below 200 m, near the city of Faro (Stigter, 2000). According to Manupella (1992, *in* Stigter, 2005) the thickness of Cretaceous aquifer is larger than 1000 m. A grabben-like structure was formed at the end of the Cretaceous where Miocene limestones and, later, sands and marls were deposited in discordance (Silva, 1988, *in* Stigter, 2000).

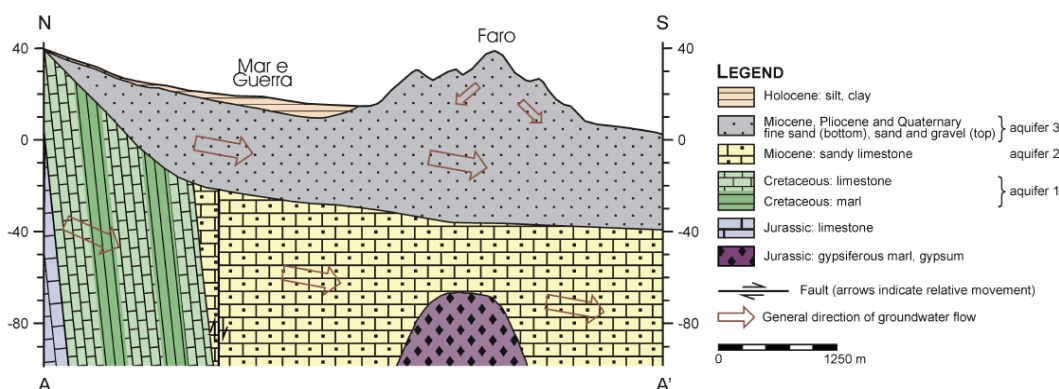


Figure 32 – Campina de Faro N-S hydrogeological section (Stigter, 2005)

Miocene fossil-rich sandy-limestone deposits constitute the second aquifer. It deepens to the East but, because of the presence of several N-S faults, a stepwise structure is present (Silva *et al.*, 1986 and Silva, 1988, *in* Stigter, 2000). There are few outcrops of Miocene limestones in Campina de Faro, also because they are covered by fine sand deposited during Miocene. The depth of the top of Miocene formations varies between 3 and 25 m below surface and the presence of marls seems to be very irregular (Silva, 1988 *in* Stigter, 2000). The topography of the top of the Miocene is irregular. Despite Miocene outcrops are very few and small, Miocene formations thickness is very large. It increases from north to south and exceeds 200 m near the coast. According to Antunes and Pais (1987, *in* INAG, 2000) a deformation might have affected the Miocene deposits and that could explain the apparent thicknesses, larger than the real

ones. The carbonated fraction varies from 60% to 95% with a decreasing trend from the base to the top (Silva, 1988).

Covering the Miocene deposits, sands, clayey sandstones, gravels and conglomerates of the Plio-Quaternary are found (“Areias e Cascalheiras de Faro-Quarteira” formation), with a thickness very variable. They crop in the NW and also near the city of Faro. Stigter (2000) refers that its thickness varies between 8 and 50 m. According to Moura and Boski (1994, in INAG, 2000) this formation has a maximum thickness of 30 m. Silva (1998, in INAG, 2000) refers that the thickness of these deposits can reach, in some places, a thickness of 60 m.

The third aquifer system is formed by the fine sand of Miocene and also the Plio-Quaternary sand and gravels. This aquifer presents an average thickness of 50 m (Stigter, 2004). Despite being partly covered by Holocenec materials, this aquifer is still considered phreatic, because their thickness is often too small to give confined characteristics to the underlying aquifer. According to Silva (1988) the average thickness of this aquifer is 25 m, but reaching maximum values of 60 m and 65 m near Galvana and in Quinta do Lago, respectively.

Some authors refer the existence of a confining layer between the second and the third aquifers. According to Silva et al. (1986), that separation is made by several silty-clayey-sandy layers (Figure 33) with variable thickness and apparently with some lateral continuity. Nevertheless, one cannot exclude the possibility of some hydraulic connection in sectors where that confining layers are absent (INAG, 2000).

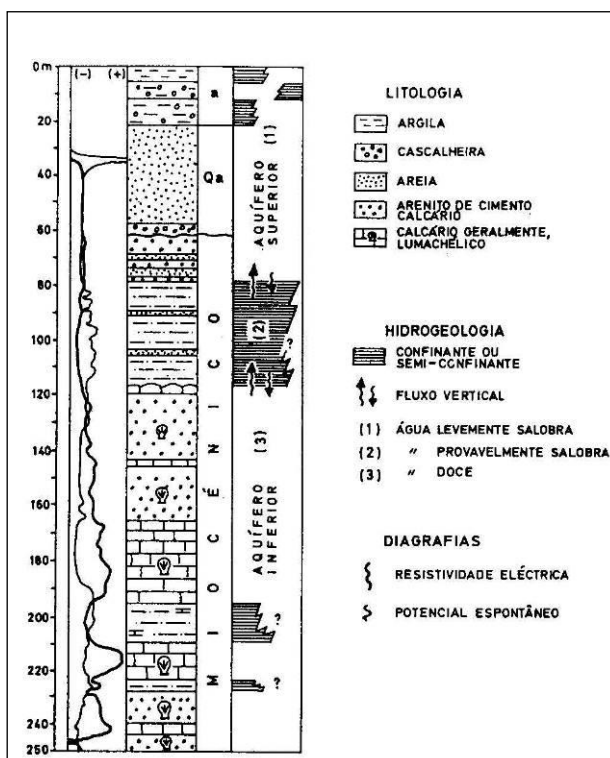


Figure 33 – Campina de Faro hydrogeological model, presented in JK15 well log (Silva et al., 1986)

Furthermore, in some situations there is a hydraulic connection artificially established due to new wells built within old large wells with the aim of extracting water from the Miocene and confined aquifer. This connection facilitates the confined aquifer contamination coming from the overlying phreatic aquifer.

According to Stigter (2005), the general direction of groundwater flow is N-S (cf. **Figure 32**). There are preferential flow paths formed by the N-S trending faults but the NW-SE trending fault acts like a barrier, which is indicated by the steeper hydraulic gradient of the water table in the north.

8.1.3 Rio Seco infiltration basins

Rio Seco MAR facilities are located in the Rio Seco water course. These facilities stand in the northern part of the Campina de Faro aquifer system and so only slightly are influenced by the hydrodynamics of this system. However MAR at this point will locally influence the hydrogeology of this system by enabling fresh water to renew polluted water existing in the system. This will mainly influence a north-south strip of the aquifer system along Rio Seco.

The general conceptual model of Campina de Faro aquifer system is provided in section 8.1.2. For the area of the hydrographic basin contributing with flow to the MAR facilities a general description is here provided. The area of the hydrograph basin of the infiltration basins shown in Figure 34 is 62.7 km². The hydrographic basin develops over five groundwater bodies identified also on Table 1.

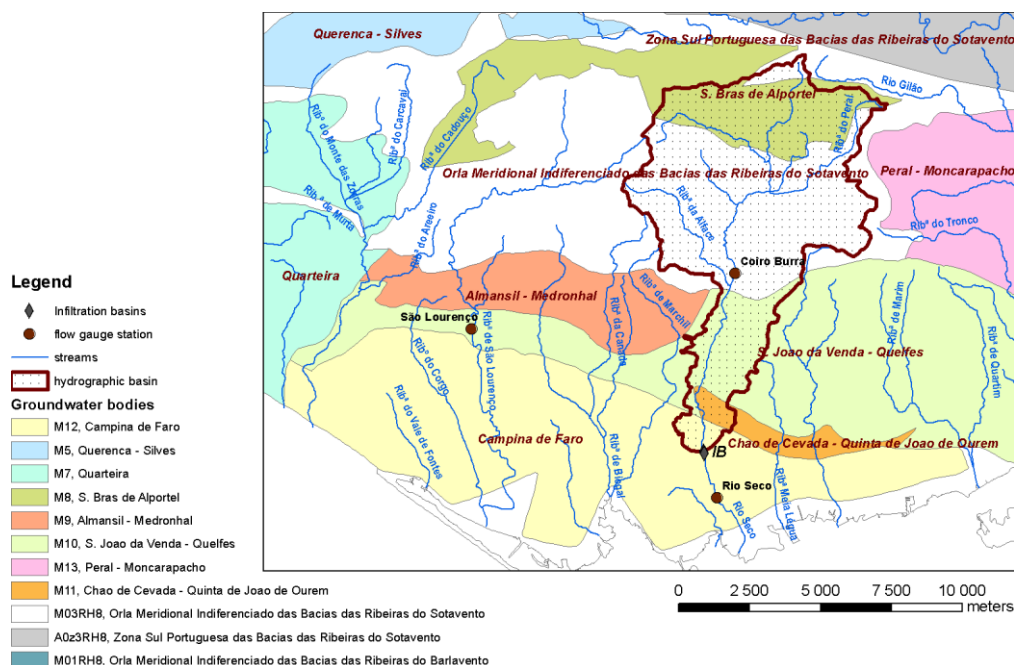


Figure 34 – Hydrograph basin above Rio Seco MAR facilities and groundwater bodies

Table 1 – Groundwater bodies intersected by the hydrographic basin above Rio Seco MAR facilities

| Groundwater body | Area (km ²) |
|--|-------------------------|
| M03RH8 - Orla Meridional Indiferenciado das Bacias das Ribeiras do Sotavento | 37.12 |
| M10 - S. Joao da Venda - Quelfes | 8.60 |
| M11 - Chao de Cevada - Quinta de Joao de Ourem | 1.28 |
| M12 - Campina de Faro | 1.59 |
| M8 - S. Bras de Alportel | 14.06 |

As a general rule it is expected that precipitation falling inside the hydrographic basin will originate surface runoff to Rio Seco or will infiltrate in the soil, recharge the aquifer systems and eventually discharge in direction to the Rio Seco water course or its tributaries. This means that in a natural dynamic equilibrium surface-ground water system, all the water that recharges the aquifer system, if not used by plants in shallow systems will eventually be part of the surface flow that passes in the MAR facilities. However two different processes may inhibit this equilibrium, first natural groundwater flow may be in a direction outward of the hydrographic basin, and this could be mainly expected in the case of the presence of karstic aquifer systems with regional flow directions different from the surface ones, and secondly anthropogenic abstraction of groundwater may lower the value of the discharge groundwater to the surface medium. It must be stated that the opposite from the first situation may also occur, i.e. water that recharges the aquifer system outside the hydrographic basin and that flows and discharges into the river network of the hydrographic basin (inward flow).

The São Brás de Alportel aquifer system is unconfined to confined, karstic, 34.4 km² area, where according with Almeida et al. (2000) natural recharge may be concentrated in sinkholes, or diffuse in epikarst structures (*lapias* fields) that occur in some areas; this aquifer system is divided into independent blocks. Almeida et al. (2000) refer to an ephemeral resurgence in Rio Seco, which is an indication of groundwater flow discharging into the hydrographic basin. It will be assumed that the groundwater flow divides coincide with the hydrographic basin meaning that all the precipitation water that falls inside the hydrographic basin and infiltrates will not flow outward and that there is no water infiltrating outside the hydrographic basin that will flow inward.

The Chão da Cevada-Quinta de João de Ourém aquifer system is also unconfined to confined, karstic, 5.3 km² area (Almeida et al., 2000), where the natural replenishment seems to equilibrate the groundwater abstractions, which is demonstrated by the groundwater level behaviour. Accordingly with Almeida et al. (2000) it is not possible to define groundwater flow

directions. The western edge of the aquifer system coincides with the Rio Seco river. To the east of the hydrographic basin, other water courses cross this aquifer system, also in a north-south direction. It is assumed that the water that infiltrates in the hydrographic basin will flow to the Rio Seco river.

The São João da Venda-Quelfes aquifer system is multilayer, with two sequences, the lower one mainly detrital and the upper one consisting of marly limestone (Almeida et al., 2000). The system extends over an area of 113 km² and its central part is crossed by the Rio Seco hydrographic basin. It is assumed that water that infiltrates in the hydrographic basin will flow to the Rio Seco river.

Finally, the “Orla Meridional Indiferenciado das Bacias das Ribeiras do Sotavento” groundwater body consists of different hydrogeological materials, with no significant hydrogeological importance that would have allowed any of them to be individualised as an aquifer system. This groundwater body extends over an area of 409 km², and is mainly composed of detrital and carbonate materials of Meso-Cenozoic age occurring in the western hydrographic basins of the Algarve. It is assumed that water that infiltrates in the hydrographic basin will flow towards the Rio Seco river.

8.1.4 Querença-Silves aquifer system

The conceptual model of Querença-Silves aquifer system is detailed on Deliverable 4.2 from where this synthesis text was withdrawn.

The Querença-Silves aquifer system (**Figure 35**) is the largest aquifer in Algarve, located in the center of the Algarve region, in south Portugal, a region characterized by a Mediterranean climate with dry and warm summers and cool wet winters. It is considered a karst aquifer formed by Jurassic (Lias-Dogger) carbonate sedimentary rocks covering an irregular area of 324 km² from the Arade River (at the west) to the village of Querença (at the East) (Monteiro *et al.*, 2006 and Monteiro *et al.*, 2007). The system is delimited south by the Alibre thrust, which is the main onshore thrust in the Algarve Basin, separating the Lower/Early and the Upper/Late Jurassic and to the north by the Triassic-Hettangian rocks (Terrinha, 1998). The Estômbar springs on the west limit of QS aquifer constitute the main discharge area of the system towards the Arade River, supporting several important groundwater dependent ecosystems.

Manuppella *et al.*, (1993) presents a cross-section of the central Algarve region (**Figure 36**). This cross-section allows a synthetized visualization of the geometric relations of the Early/Lower Jurassic lithology which support the Querença-Silves aquifer system Identified in blue, in **Figure 36**.

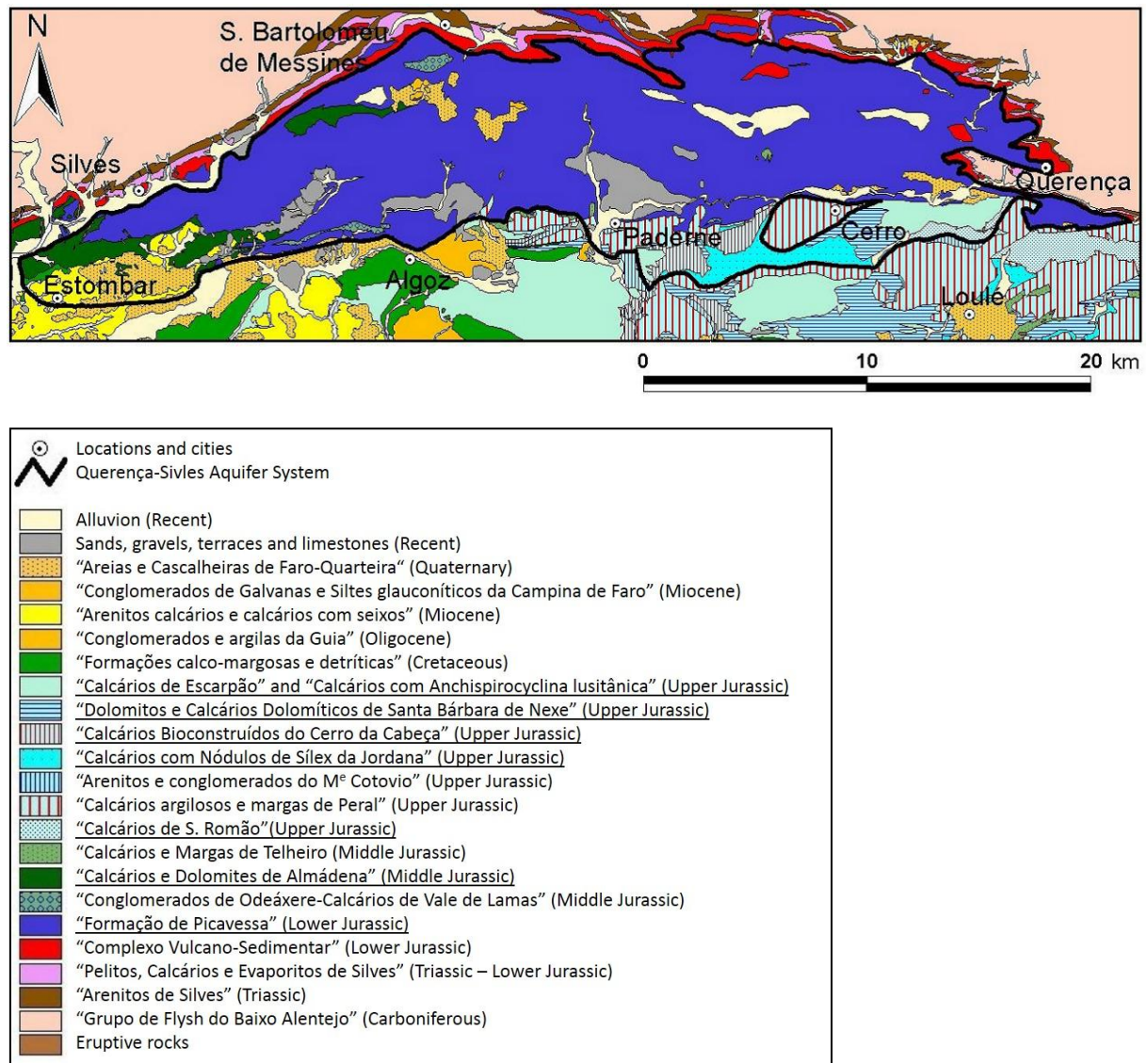


Figure 35 – Querença-Silves aquifer system's geology. Underlined features are the ones identified within the aquifer limits. Almeida *et al.* (2000)

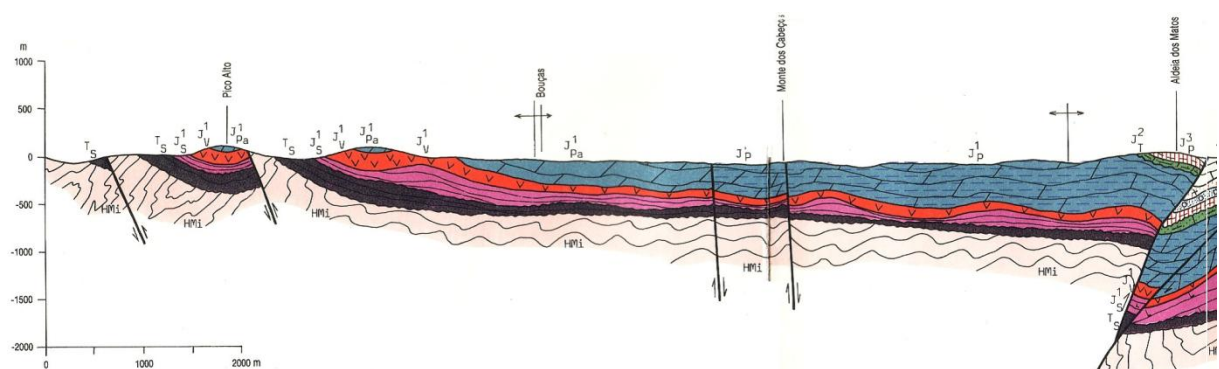


Figure 36 - Geometry of the carbonated rocks of early Jurassic which constitute the most important support of the aquifer system Querença-Silves (dark blue colour, to the left of the Algibre thrust). Adapted from Manuppella *et al.*, (1993)

Accordingly to previous studies, the hydrogeological setting of the Querença-Silves karstic aquifer, has a complex compartmented structure, with two distinct domains separated by a fault: a western domain and an eastern domain. Its western domain has a well-developed karst, westward flow direction, with the main discharge areas along the Arade river, with particular relevance to Estômbar springs (westernmost point). Its eastern domain has more random flow directions, less regular piezometric surfaces (**Figure 37**) and a lower karst development. The tectonic activity of this region results in its widespread fracturing, defining a significant number of semi-independent aquifer blocks, with more or less constrained and restricted hydraulic links between them. Such hydraulic restrictions are more expressive in the eastern domain, because in the western domain the pervasive karstic network largely obliterates such tectonic setting (Mendonça and Almeida, 2003; Monteiro *et al.*, 2006).

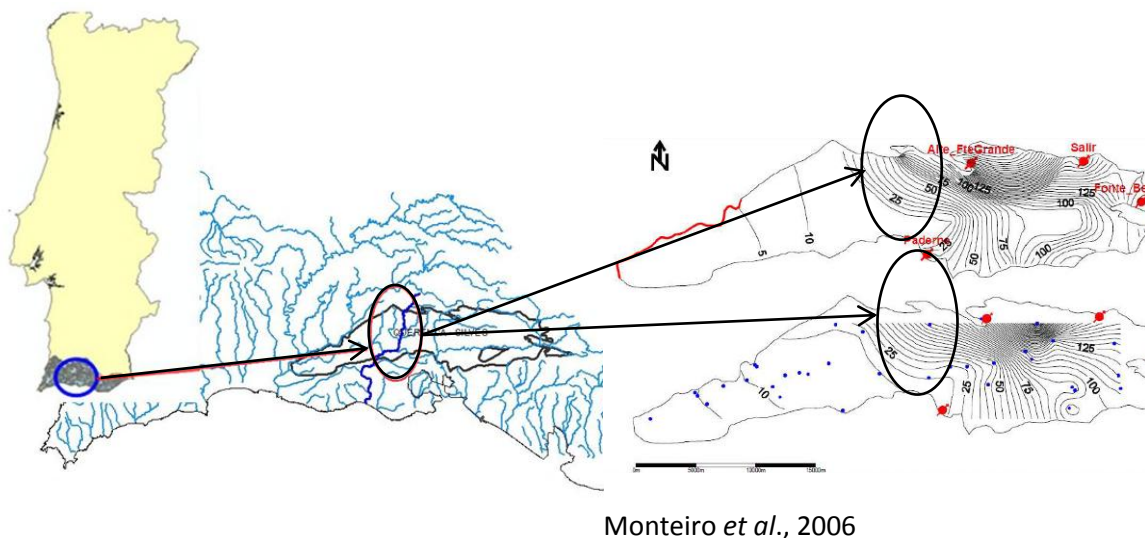


Figure 37 – Site location along Ribeiro Meirinho stream and central-western area of Querença-Silves aquifer and its piezometry (upper right: modelled; lower right: measured) (Leitão *et al.*, 2014)

The Ribeiro Meirinho stream is located in the central-western area of Querença-Silves aquifer and its upper reaches are located outside the aquifer, in Serra Algarvia. The latter are Palaeozoic terrains, composed mainly of schist and graywakes, essentially impervious lithologies, being therefore, the main source of water for this stream until it reaches the Jurassic limestones, dolomites, dolomitic limestones and other, less important, calcareous formations composing the karst aquifer of Querença-Silves.

8.1.5 Querença-Silves infiltration basins

The areas draining to the location of the three infiltration basins are represented in **Figure 38**. The river basin of the WWTP of São Bartolomeu de Messines (area = 13.6 km²) is included in the river basin of Ribeiro Meirinho (total area = 57.6 km²). The river basin of Cerro do Bardo (29.4 km²) is west of the previous one. The Cerro do Bardo river basin is almost completely installed on the Querença-Silves aquifer system (unless a small part on the north that belongs to the “Orla Meridional indiferenciado das Bacias das ribeiras do Sotavento” groundwater body (GWB)). The WWTP of São Bartolomeu de Messines river basin is almost exclusively

formed by the “Orla Meridional indiferenciado das Bacias das ribeiras do Sotavento” GWB and, in a very small area of 2.0 km², by the “Zona Sul Portuguesa das Bacias das ribeiras do Sotavento” GWB. Concerning the Ribeiro Meirinho river basin, apart the area included in the WWTP of São Bartolomeu de Messines river basin, is almost exclusively developed on the Querença-Silves aquifer system.

The conceptual model of the Querença-Silves aquifer system is described in section 8.1.4, as well as a general characterisation of the “Orla Meridional indiferenciado das Bacias das ribeiras do Sotavento” GWB is presented in section 8.1.3. Concerning the “Zona Sul Portuguesa das Bacias das ribeiras do Sotavento”, this GWB has a total area of 293 km² and is comprised of Paleozoic geological formations that compose the part of the geostructural unit of the Portuguese South Zone located in the western hydrographic basins of the Algarve. It is a low productivity area mainly composed of schist and greywackes. In this last area it is also assumed that water that infiltrates in the hydrographic basin will flow towards the correspondent water course.

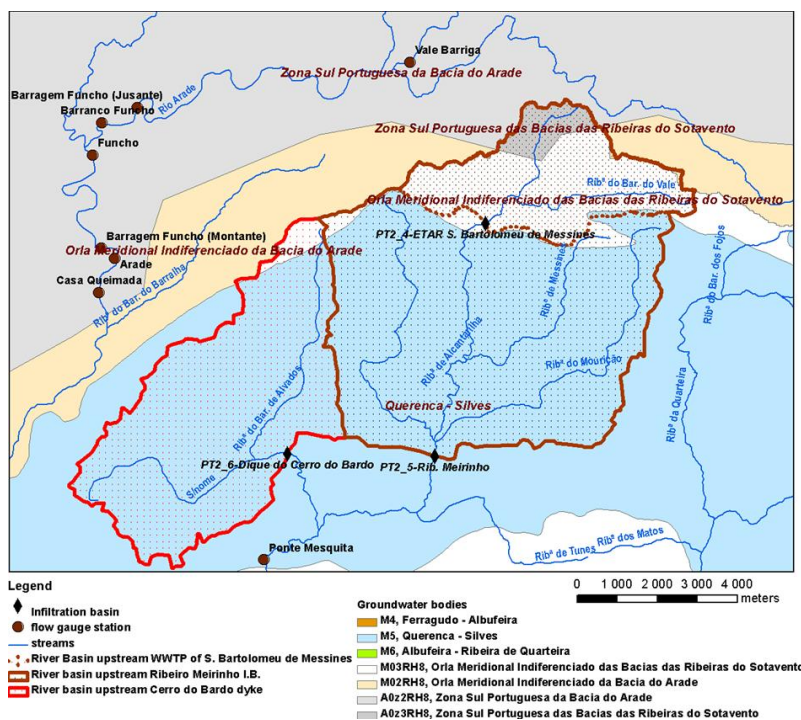


Figure 38 – Hydrograph basin above selected MAR facilities in PT2 and related groundwater bodies

8.1.6 Water budget

8.1.6.1 Natural water budget

For the demo sites a natural water budget is provided. This includes a review of ancient studies plus a new characterisation specific of the demo sites. Water budget is carried out using the daily sequential soil water balance model BALSEQ MOD.

Water budget of MARSOL demo sites where MAR techniques are to be implemented is a crucial issue for the success of the improvement of aquifer management.

8.1.6.2 Campina de Faro

Considering the aquifer area equal to 86 km², the average annual precipitation equal to 550 mm and a recharge rate (of the phreatic aquifer) between 15 and 20% of the precipitation, direct recharge has an approximate value of 10 hm³/year (INAG, 2000) or 116 mm/year. Oliveira and Lobo-Ferreira (1994) calculated the potential recharge of hydrogeological system ALG-5, that includes also Campina de Faro aquifer, and obtained a value of 36,3 hm³/year (143 mm/year).

A daily sequential water balance was developed during the GABARDINE EU project using the BALSEQ_MOD numerical model developed in LNEC. A description of this model can be found in Deliverable 12.1.

The period analysed ranged from 1981/10/01 to 1991/09/30. Daily precipitation was taken from the INAG 31K-02 – Quelfes rain gauge station (average precipitation in this period: 611 mm/year). Monthly reference evapotranspiration (ET_o) was estimated in Ribeiras do Algarve Watershed Plan for the Tavira meteorological station, using the FAO Penman-Monteith method (average ET_o 1235 mm/year). Information on soil parameters and land use was taken from the Soil Map of Portugal at the 1:50000 scale from IHERA and from 1:100000 scale 2000-Corine Land Cover.

Average aquifer recharge in The Campina de Faro aquifer system (**Figure 39**) was estimated in Lobo-Ferreira et al (2006) as 139 mm/year, 23% of the precipitation, despite, depending on the land use and the soil properties, the recharge distribution is highly variable. Lower values are in the order of 5 mm/year in the alluvium formations and larger values can go up to 380 mm/year in sandy outcrops.

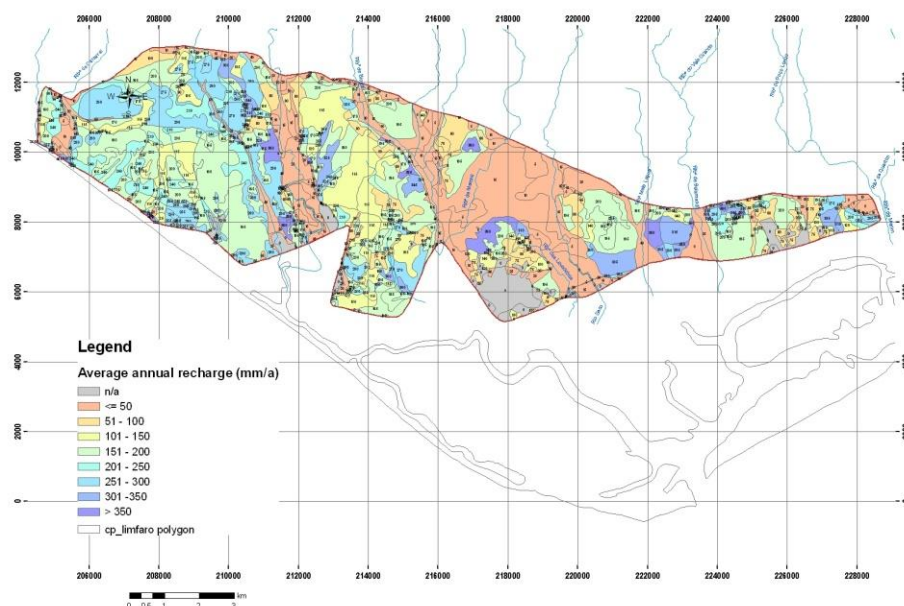


Figure 39 – Distribution of recharge in the Campina de Faro aquifer system (Lobo Ferreira et al, 2006)

For instance **Figure 40** shows the recharge distribution along the years in these types of soil/land use combinations.

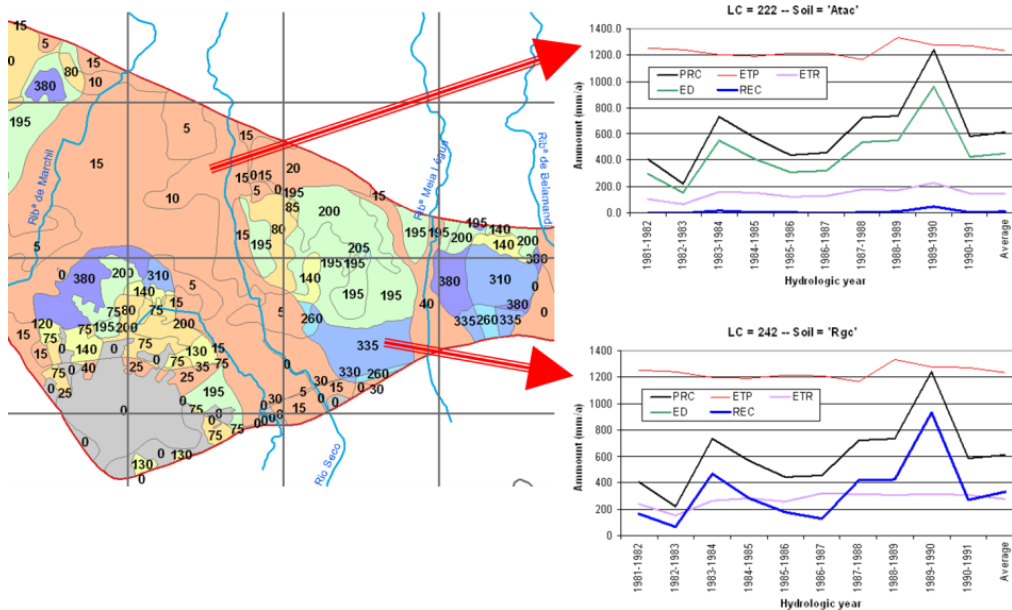


Figure 40 – Yearly variation of the modelled parameters (including aquifer recharge) in the artificial recharge area in an alluvium soil (Soil = “Atac”) and in a regosol (Soil = “Rgc”) (Lobo Ferreira et al, 2006)

8.1.6.3 *Rio Seco hydrographic basin upstream the infiltration basins*

A study for the estimation of water available for infiltration under natural conditions was developed using 10 year daily data from Rio Seco station (Figure 41).

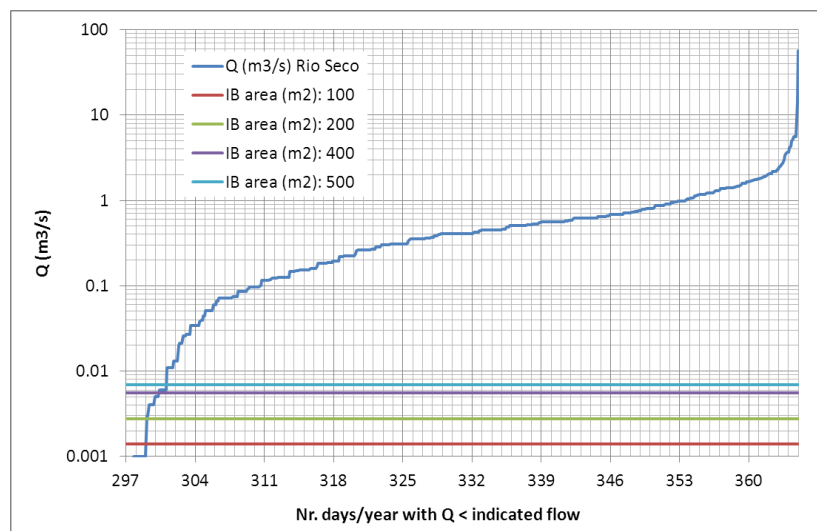


Figure 41 - River flow cumulative curve and infiltration capacity of the IB (depending on the area of the IB), considering the infiltration capacity = 1.2 m/d

Estimation of the relation between infiltration capacity of the IB and river surface flow (Figure 41) determining the average number of days per year in which river flow is higher than the infiltration capacity of the IB. The value of 200 m² corresponds to the old existing IB and the value 400 m² corresponds to the actually existing infiltration basins capacity.

The BALSEQ_MOD model was also run for the area of the hydrographic basin upstream Rio Seco river infiltration basins in order to determine the available amount of water for the infiltration basins. The period of analysis is of 13 years, from 1/10/2001 until 30/9/2014. Precipitation was taken from the meteorological gauge station 31J/01C – São Brás de Alportel belonging to the Portuguese Environment Agency (data accessible from <http://snirh.pt/index.php?idMain=2&idItem=1>) that collected reliable data until 31/05/2009. Lacking data was estimated using other rain gauge stations, namely in first place 31J/04UG – Estói, also from the Portuguese Environment Agency, and, in second place, the meteorological station of Patação, belonging to the Algarve Regional Directorate of Agriculture and Fisheries with data starting from 01-01-2006 (<http://www.drapalg.min-agricultura.pt/ema/pat.htm>). The relation of average precipitations in these stations was used to fill the gaps.

Daily reference evapotranspiration (ET_o) was estimated using the FAO Penman-Monteith method with data of daily maximum and minimum temperature, daily average relative humidity or hourly relative humidity, daily solar radiation, and daily wind speed, also measured in the meteorological gauge station 31J/01C – São Brás de Alportel. Missing data was estimated by several procedures using measurements in the 30K/02C – Picota meteorological station, also from the Portuguese Environment Agency, and, in second place, using data registered in the above mentioned meteorological station of Patação.

The procedures used to fill missing data are quite extensive and will be reported in a separate report. Average yearly precipitation and average yearly reference evapotranspiration were estimated in São Brás de Alportel meteorological station as 638 mm/year and 1023 mm/year, with the monthly and yearly distributions shown in **Figure 42** and **Figure 43**, respectively.

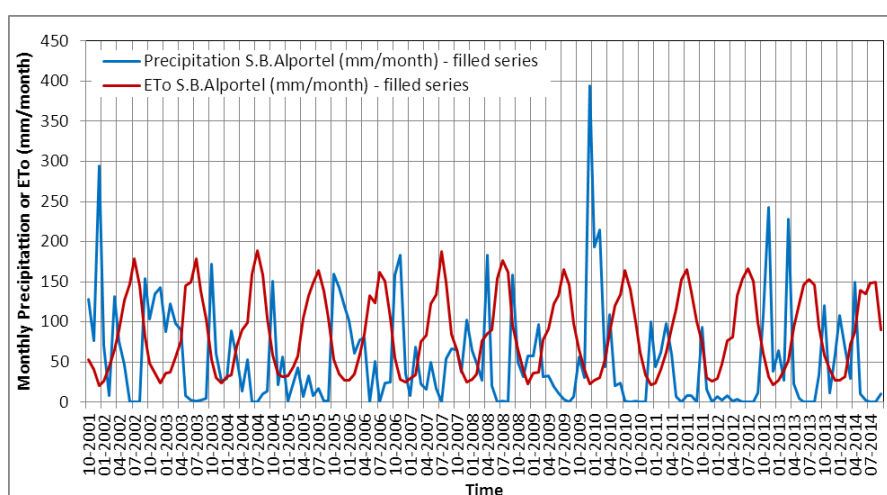


Figure 42 - Monthly rainfall and reference evapotranspiration (ET_o) fluctuation for the period 10/2001-09/2014 in São Brás de Alportel meteorological station

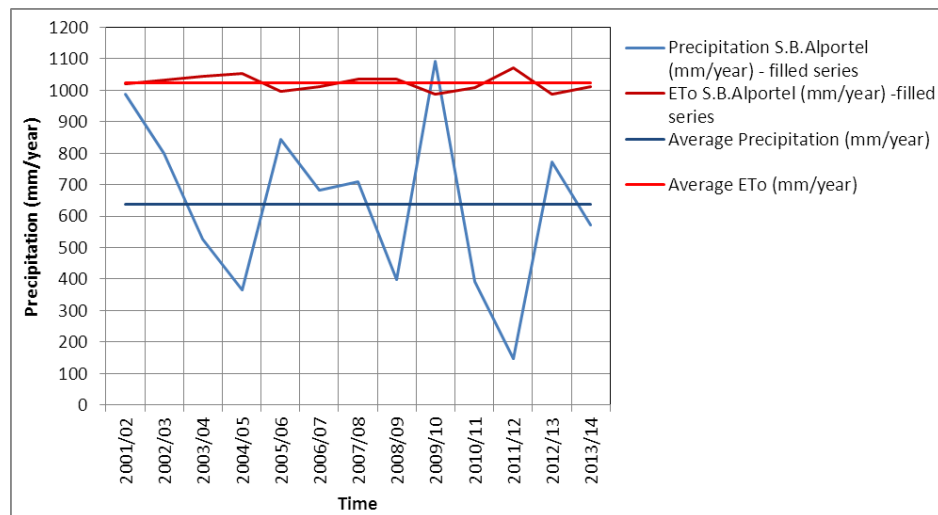


Figure 43 - Yearly rainfall and reference evapotranspiration (ETo) fluctuation for the period 10/2001-09/2014 in São Brás de Alportel meteorological station

Information on soil parameters and land use was taken from the Soil Map of Portugal at the 1:50000 scale from IHERA and from 1:100000 scale 2006-Corine Land Cover (Caetano et al, 2009).

The results obtained by the BALSEQ_MOD model may be summarised as follows: average surface runoff = 360 mm/year; average groundwater recharge = 28 mm/year; average actual evapotranspiration = 250 mm/year. The average monthly and yearly distribution of the values is represented in **Figure 44** and **Figure 45**.

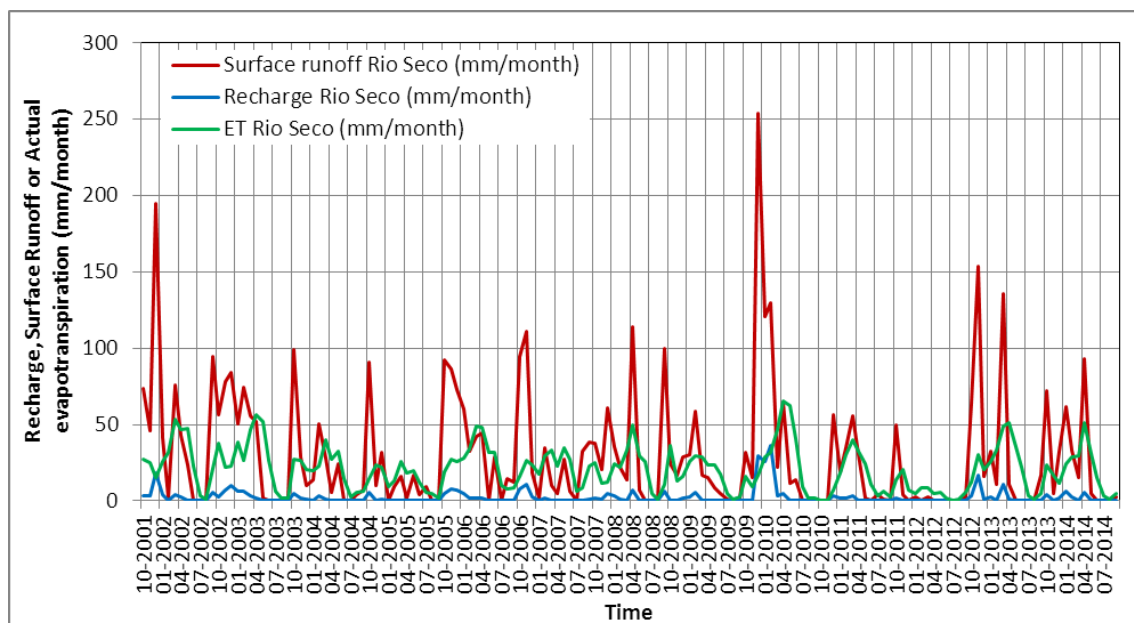


Figure 44 - Monthly surface runoff, natural recharge and actual evapotranspiration fluctuation for the period 10/2001-09/2014 in Rio Seco hydrographic basin upstream the infiltration basins

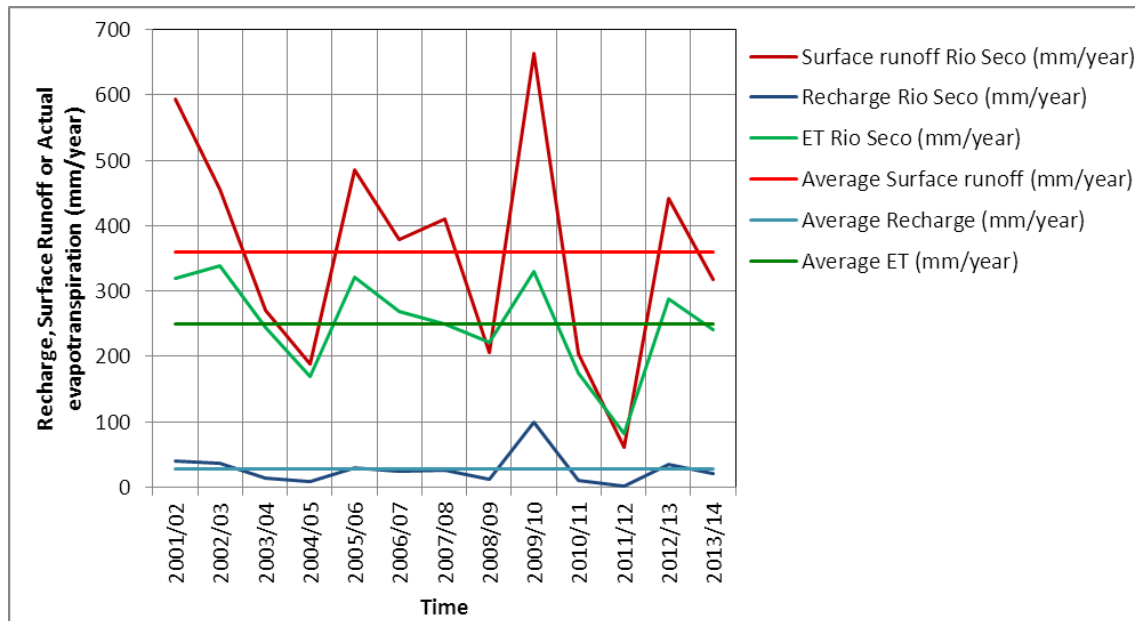


Figure 45 - Yearly surface runoff, natural recharge and actual evapotranspiration fluctuation for the period 10/2001-09/2014 in Rio Seco hydrographic basin upstream the infiltration basins

The spatial distribution of the surface runoff, recharge and actual evapotranspiration values can be observed in Figure 46, Figure 47 and Figure 48.

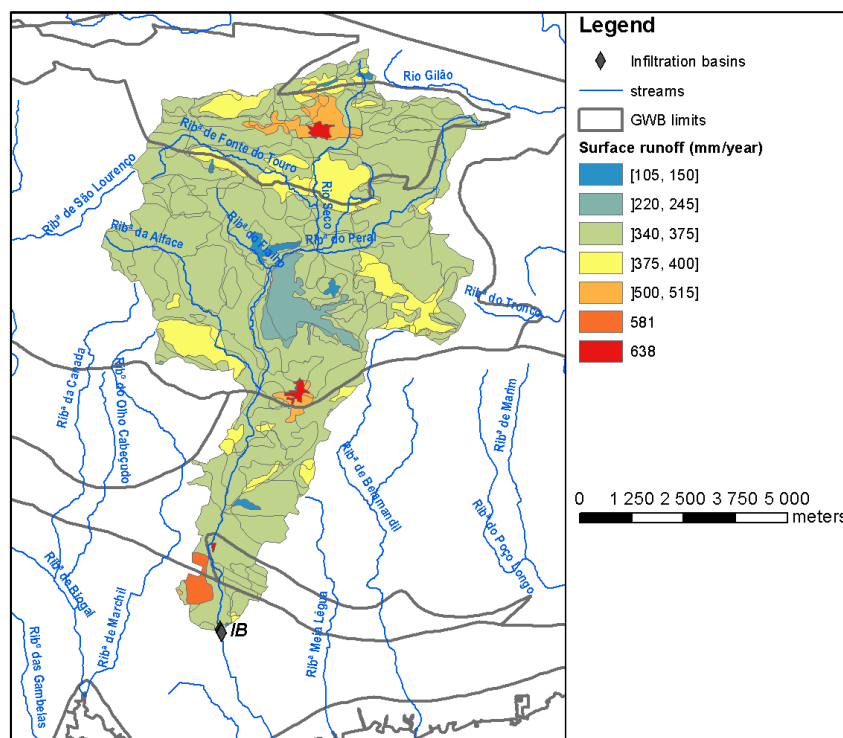


Figure 46 – Average surface runoff distribution in Rio Seco hydrographic basin upstream the infiltration basins

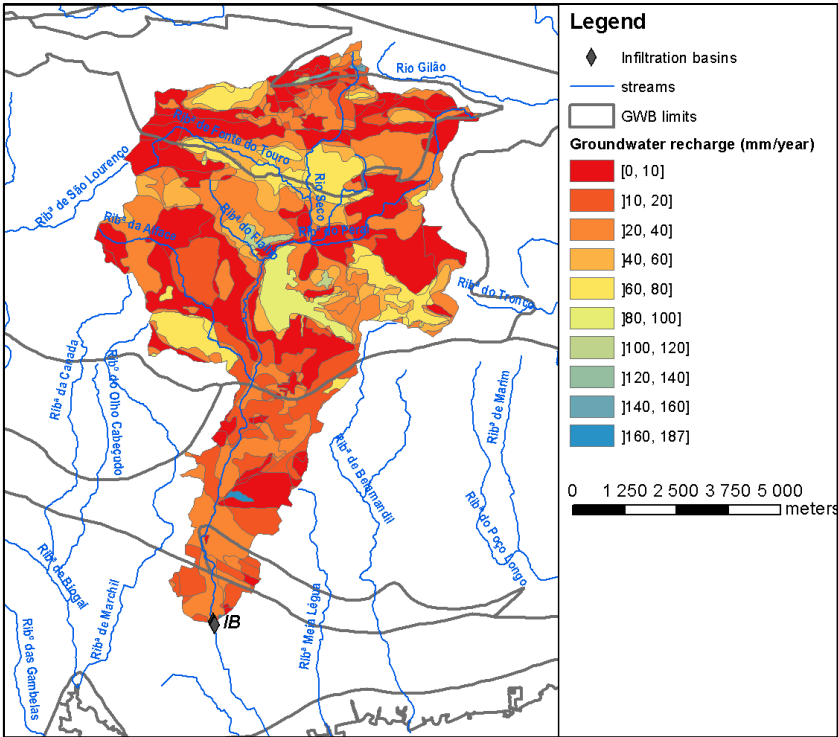


Figure 47 – Average groundwater recharge distribution in Rio Seco hydrographic basin upstream the infiltration basins

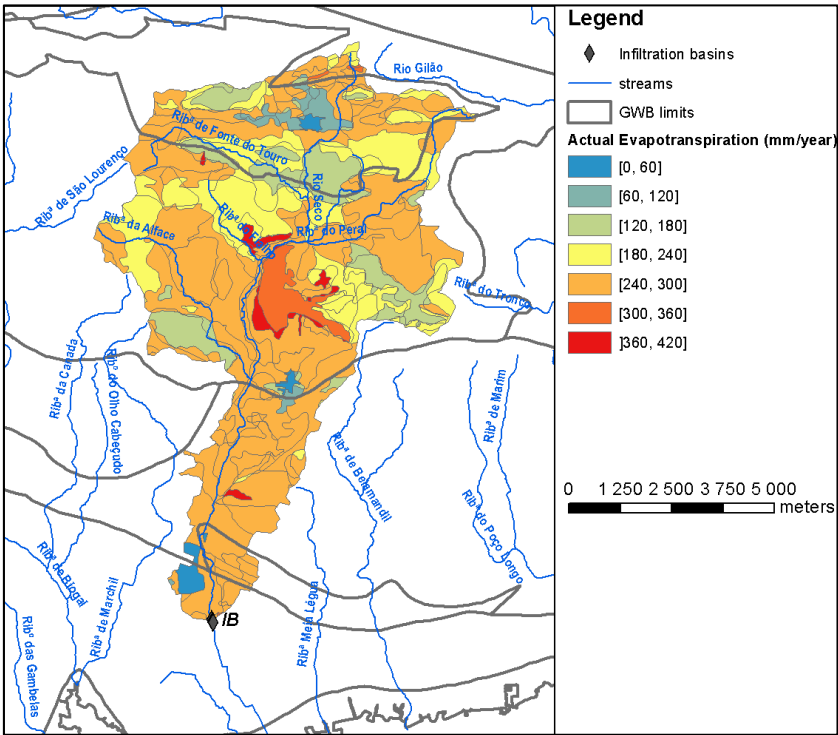
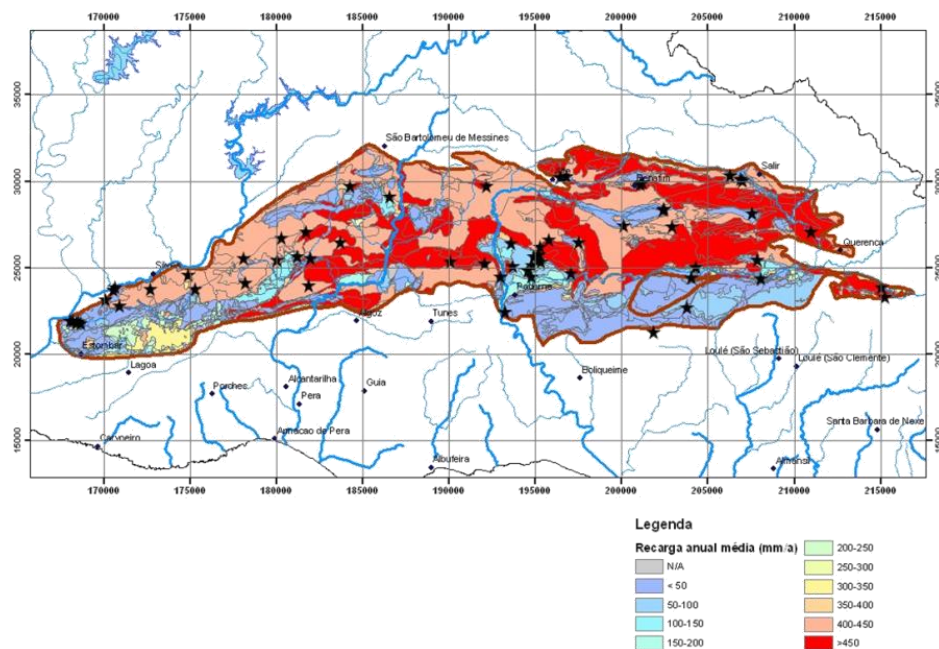


Figure 48 – Average actual evapotranspiration distribution in Rio Seco hydrographic basin upstream the infiltration basins

8.1.7 Querença-Silves

An extensive literature review allowed the identification of “three generations” for the estimation of the water balance of the Querença-Silves nowadays available as follows:

- Almeida (1985) and Almeida *et al.* (2000) estimated a total recharge of $70 \pm 17 \text{ hm}^3.\text{yr}^{-1}$, using the Kessler method (1965) in the areas where carbonated rocks outcrops are present (in which the average recharge varies between 40 and 60% of precipitation) and a sequential water balance in the soil in the areas where carbonate rocks are covered by soils or sedimentary deposits (in which recharge varies between 5 and 18% with an average of 10%).
- Vieira and Monteiro (2003) refined the previous balance with the infiltration values determined for the covered and outcropping areas of the carbonate rocks proposed by Almeida (1985) and Almeida *et al.*, (2000). However in this case it was possible to use a new generation of geological maps in which the percentage of covered and uncovered areas of the aquifer were much more reliable. The diminution of that source of uncertainty allowed to estimate a value in the range of the highest values proposed in the previously mentioned balance. In that case a total annual average recharge of $93.4 \text{ hm}^3.\text{yr}^{-1}$ was estimated.
- Oliveira *et al.* (2008) estimated a $100 \text{ hm}^3.\text{yr}^{-1}$ recharge with the sequential daily water balance model BALSEQ_MOD (**Error! Reference source not found.**), later updated by Oliveira *et al.* (2011) to $94 \text{ hm}^3.\text{yr}^{-1}$ (**Figure 49**).



Source: Oliveira et al. (2008)

Figure 49 - Average Querença-Silves aquifer recharge (period 1941-1991)

Due to its karstic properties, there is a strong relationship between the aquifer and the streams with some influent sections that can significantly contribute to its recharge (Monteiro *et al.*, 2006; Reis *et al.*, 2007, Salvador *et al.* 2012). This is the case of Ribeiro Meirinho, which undergoes a sharp reduction of the flow rate when it reaches the calcareous formations, having several sinks in its bed. It is estimated that besides direct recharge, an extra amount of $62 \times 10^6 \text{ m}^3/\text{year}$, originated from surface flow produced on the drainage area outside the aquifer, infiltrates when the rivers reach the aquifer system (Oliveira and Oliveira, 2012).

Regarding aquifer abstractions, Nunes *et al.* (2006) estimated a mean annual withdrawal for irrigation of 31 hm^3 , and Stigter *et al.* (2009) estimated a 10% of mean aquifer recharge is abstracted for urban water supply.

8.1.8 Water available for MAR and sources of water

Water available for artificial recharge uses data computed in previous section linked to each possible source of water.

In the initial phase of testing/demonstrating the MAR facilities, alternative sources of water are used such as water provided by fireman trucks tanks or groundwater pumped from different aquifers to the infiltration facilities. After these initial tests, the following available sources of water are considered:

- For the Rio Seco case study possible sources of water are river flow and greenhouse rain harvesting.
- For the large wells to be used as infiltration wells the source of water is greenhouse rain harvesting.
- For the Cerro do Bardo case study possible sources of water are river flow and rejected water from Water treatment plants or from surface storage dams.

8.1.8.1 Greenhouse rain harvesting

One possible important source of water for MAR in the Campina de Faro aquifer system (CFAS) consists in harvested rainwater from greenhouses (**Figure 50**) due to the large surface area occupied by these infrastructures. This potential source of water could in some cases be redirected to large diameter wells (**Figure 51**), which, at CFAS, present a high potential for well water recharge (as determined during large well injection tests described in Deliverable 4.2).



Figure 50 - Intensive greenhouse agricultural activity in the Campina de Faro aquifer system and traditional system of drains for collection of rainwater



Figure 51 – Traditional large diameter wells potentially suited for injection of harvested water

In order to estimate the potential rainwater that can be harvested from greenhouses the average distribution of annual and monthly value of rainwater was calculated and overlapped with the location of greenhouses at CFAS.

Average annual rainfall estimates were based on a 32 year average rainfall distribution model (from 1959/60 to 1990/91) consisting in a 1 km² resolution matrix developed by Nicolau (2002). Based on this distribution model, average annual rainfall on the CFAS was estimated as 570 mm with the spatial distribution shown in Figure 52.

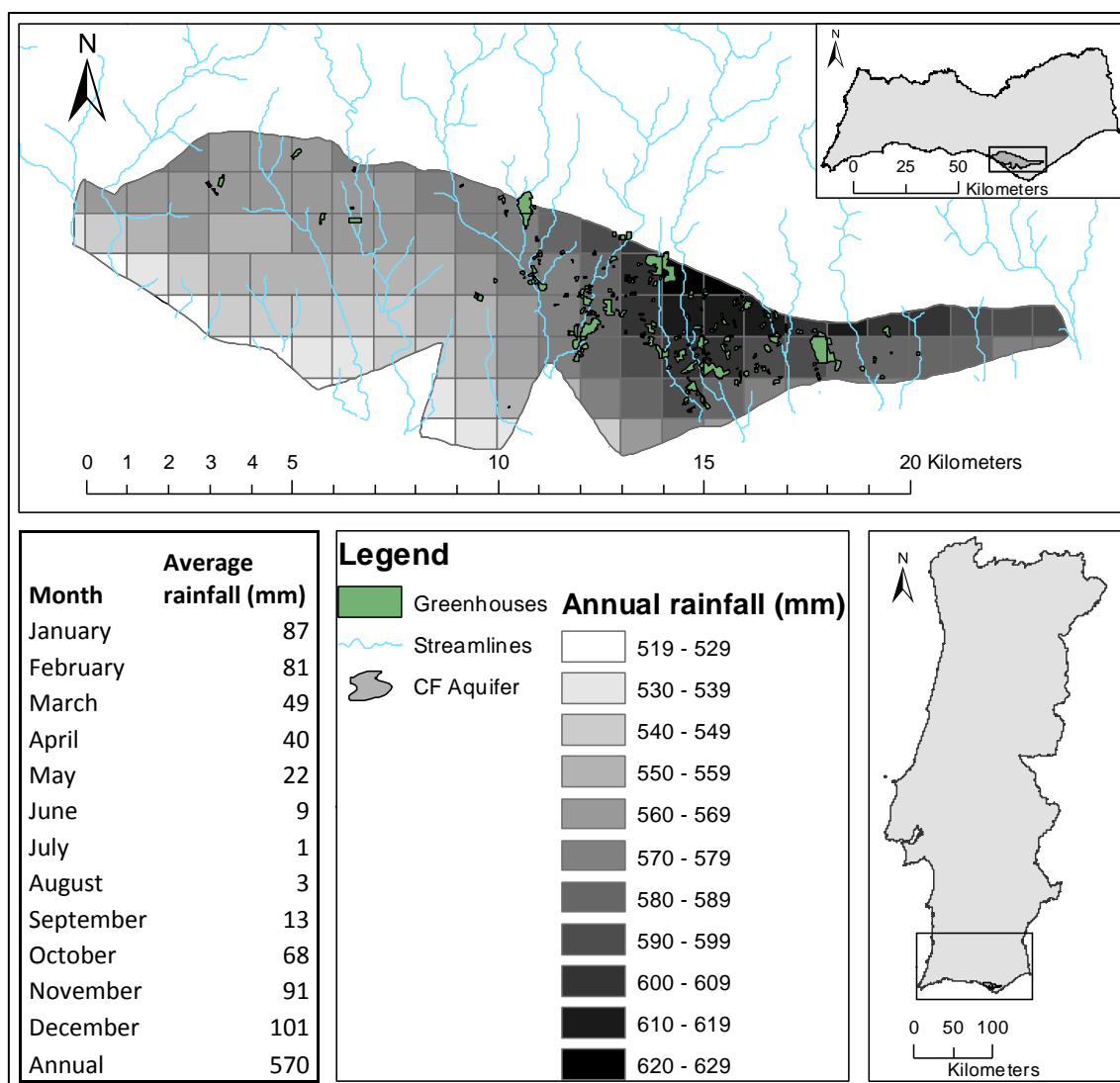


Figure 52 - Top: 32 year average annual rainfall spatial distribution on Campina de Faro aquifer system (CFAS) (based on Nicolau, 2002) and greenhouse's locations (based on APA-ARH Algarve, unpublished). Bottom left: 32 year average monthly and annual rainfall distribution values for the CFAS (based on Nicolau, 2002)

The location of greenhouses and their surface area estimation was based on the survey of the land use, using year 2007 aerial photos, developed by the Algarve Water Basin Regional Administration of the Portuguese Environment Agency (APA-ARH Algarve, unpublished). Based on this survey, the total surface area occupied by greenhouses which are totally within or intercept the CF aquifer is estimated as 2.74 km² with the spatial distribution identified in Figure 52.

Based on the estimates of the average annual and monthly rainfall distribution, the greenhouse's locations and their surface area (Figure 52), the average annual rainfall that could potentially be intercepted by greenhouses in the CFAS is calculated as 1.63 hm³/yr. The 32 year monthly and annual averages of rainfall intercepted by the greenhouses are presented in Table 2. It is unlikely that the totality of these amounts can be harvested and used for MAR

due to the lack of appropriate greenhouse infrastructures, conduits or close location to large diameter wells. Nonetheless they should be seen as the average maximum potential water available for future MAR solutions.

Table 2 - Estimated average monthly and annual potential rainfall harvested from greenhouses

| Month | Intercepted rainfall (hm ³) | Month | Intercepted rainfall (hm ³) |
|---------------|---|-------------|---|
| JAN | 0.252 | JUL | 0.00273 |
| FEB | 0.235 | AUG | 0.00823 |
| MAR | 0.139 | SEP | 0.0371 |
| APR | 0.112 | OCT | 0.191 |
| MAY | 0.0625 | NOV | 0.263 |
| JUN | 0.0275 | DEC | 0.292 |
| Annual | | 1.63 | |

8.1.9 Climate change

An analysis of the impact of climate change in the general water budget of the areas under study is performed using projections of the precipitation and temperature series.

8.1.9.1 Emission scenarios and Predicted climate change

Two different studies are presented.

For the PT2 – Querença-Silves aquifer system, Stigter et al. (2009, 2014) present a study regarding groundwater flow simulation of future scenarios using the ENSEMBLES projections (A1b scenarios) for recharge.

Oliveira *et al.* (2012) in the framework of the ProWaterMan project studied the PT3 – Melides and also the PT2 – Querença-Silves sites, considering the scenarios of the SIAM II project in Portugal (Santos and Miranda, 2006). The three scenarios used to project changes for year 2100 were the following:

- **Scenario IS92a** – “business as usual” as in 1992.
- **Scenario SRES A2** – heterogeneous world, fragmented socio-economic development, population grows.

- **Scenario SRES B2** – search of local solutions for social, economic and environmental problems, population grows but less than in scenario A2.

The average variation of precipitation and temperature projected by these scenarios are presented in **Table 3**. This Table also includes PT1 – Rio Seco demo site area projected changes for the same three scenarios. With these projected changes, recent series of precipitation and reference evapotranspiration are modified and used to run the BALSEQ_MOD model.

Table 3 – Projected precipitation and temperature variations in different climate change scenarios

| Demo site | Process | Scenario HadRM2, IS92a | SIAM: Scenario HadRM3, SRES A2 | SIAM Scenario HadRM3, SRES B2 |
|------------------------------|-----------------------------------|---------------------------|--------------------------------------|-------------------------------------|
| PT1 – Rio Seco | Monthly Precipitation | Winter: +45% | Winter: -35% | Winter: -20% |
| | | Spring: -25% | Spring: -55% | Spring: -25% |
| | | Summer: -77% | Summer: -50% | Summer: -15% |
| | | Autumn: -55% | Autumn: -45% | Autumn: -35% |
| | Monthly maximum Temperature | Winter: ? °C | Winter: ? °C | Winter: ? °C |
| | | Spring: ? °C | Spring: ? °C | Spring: ? °C |
| | | Summer: +6 °C | Summer: +3.75 °C | Summer: +3 °C |
| | | Autumn: ? °C | Autumn: ? °C | Autumn: ? °C |
| PT2 – Querença- Silves | Monthly minimum Temperature | Winter: +5.25 °C | Winter: +2.75 °C | Winter: +1.75 °C |
| | | Spring: ? °C | Spring: ? °C | Spring: ? °C |
| | | Summer: ? °C | Summer: ? °C | Summer: ? °C |
| | | Autumn: ? °C | Autumn: ? °C | Autumn: ? °C |
| | Monthly Precipitation | Winter: +40% | Winter: [-30%;-40%] | Winter: [-20%;-30%] |
| | | Spring: [-20%;-30%] | Spring: -50% | Spring: [-20%;-30%] |
| | | Summer: [-70%;-85%] | Summer: -65% | Summer: [-30%;-40%] |
| | | Autumn: [-50%;-60%] | Autumn: -40% | Autumn: [-20%;-30%] |
| | Monthly maximum | Winter: +4.25 °C; | Winter: +3 °C; | Winter: +2 °C; |

| | | | | |
|--------------------|-----------------------------|---|---|---|
| | Temperature | Spring: +4.75 °C; Summer: +5.75 °C; Autumn: +5.5 °C | Spring: +3.5 °C; Summer: +3.75 °C; Autumn: +4 °C | Spring: +2.5 °C; Summer: +3 °C; Autumn: +3 °C |
| | Monthly minimum Temperature | Winter: +4.75 °C; Spring: +4.5 °C; Summer: +5.25 °C; Autumn: +5.25 °C | Winter: +3.5 °C; Spring: +3 °C; Summer: +3 °C; Autumn: +3 °C | Winter: +2 °C; Spring: +2 °C; Summer: +2.5 °C; Autumn: +2 °C |
| PT3 – Melides site | Monthly Precipitation | Winter: [+40%;+50%] Spring: -20% Summer: [-70%;-85%] Autumn: [-50%;-60%] | Winter: [-20%;-30%] Spring: [-40%;-50%] Summer: -65% Autumn: [-30%;-40%] | Winter: [-20%;-30%] Spring: [-20%;-30%] Summer: -60% Autumn: [-10%;-20%] |
| | | Winter: +4.25 °C Spring: +5.25 °C Summer: +7 °C Autumn: +6.75 °C | Winter: +3 °C Spring: +3.5 °C Summer: +3.75 °C Autumn: +4 °C | Winter: +2 °C Spring: +2.5 °C Summer: +3.5 °C Autumn: +3 °C |
| | Monthly minimum Temperature | Winter: +5 °C Spring: +4.75 °C Summer: +6 °C Autumn: +5.75 °C | Winter: +3.25 °C Spring: +3 °C Summer: +3 °C Autumn: +3 °C | Winter: +1.75 °C Spring: +2 °C Summer: +2.5 °C Autumn: +2 °C |
| | | | | |

Adapted from Santos and Miranda (2006, PT3 and PT2 in Oliveira *et al.*, 2012)

8.1.9.2 Climate change impacts

For the study area DEMO Site 2 – PT2 Querença-Silves (QS), regarding groundwater flow simulation of future scenarios using the ENSEMBLES projections (A1b scenarios) for recharge, the summarized achieved conclusions presented in the study of Stigter *et al.* (2009, 2014) were:

- Period 2020–2050: Changes in recharge, particularly due to a reduction in autumn rainfall resulting in a longer dry period. More frequent droughts are predicted at the QS aquifer.

- Toward the end of the century (2069–2099): results indicate a significant decrease (mean 25 %) in recharge at QS aquifer, with an high decrease in absolute terms (mean 134 mm/year).
- Scenario modelling of groundwater flow shows its response to the predicted decreases in recharge and increases in pumping rates, with strongly reduced outflow into the coastal wetlands, whereas changes due to sea level rise are negligible.

For the case of the study developed by Oliveira *et al.* (2012) for PT2 – Querença-Silves and PT3 – Melides sites, and now developed for the PT1 – Rio Seco site, the future precipitation series, temperature series and reference evapotranspiration series were estimated using the methodologies presented in Deliverable 12.1.

The results obtained for the PT2 – Querença-Silves aquifer system are shown in **Figure 53** for the three emission scenarios. **Figure 54** shows the equivalent results for the PT3 – Melides hydrographic basin.

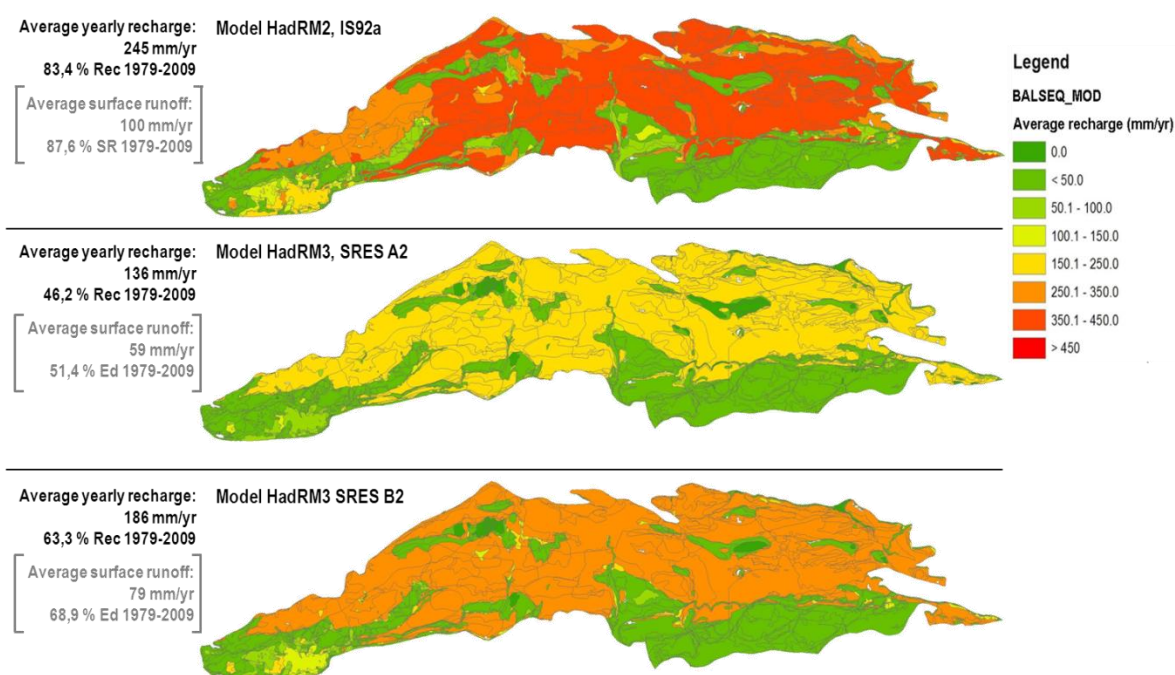


Figure 53 – Climate change impact in the water cycle in PT2 – Querença-Silves aquifer system (source: Oliveira *et al.*, 2012)

Table 4 summarises the results obtained for the three case study areas. It is possible to see that natural groundwater recharge may be as low as 40 % of the actual recharge and that surface runoff may be as low as 51 % of the actual surface runoff under scenario A2. Despite the scenario B2 is not so unfavourable it still accounts for large reductions on the water available in the water cycle. These results are a useful starting point regarding the role of MAR in this aquifer system, taking into account the future trends of climate change patterns

expected in this area.

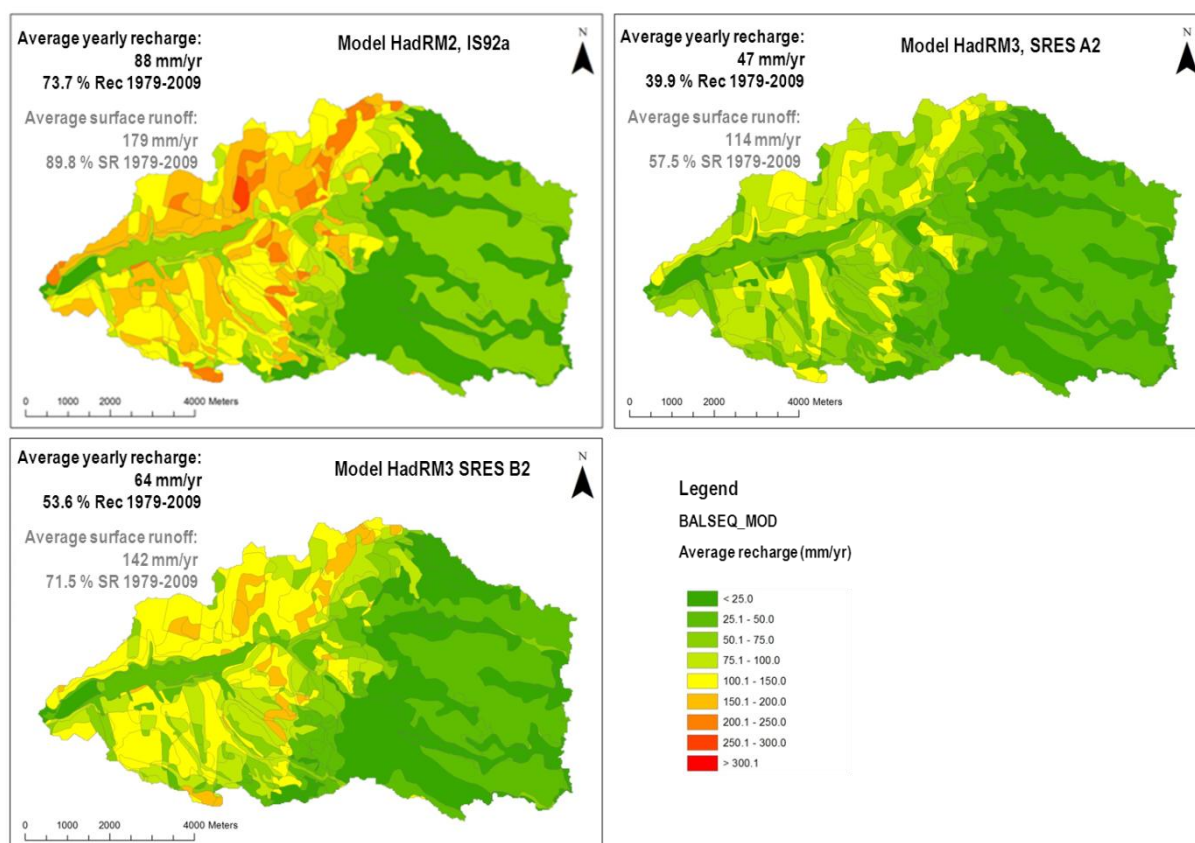


Figure 54 – Climate change impact in the water cycle in PT3 – Melide hydrographic basin (source: Oliveira *et al.*, 2012)

Table 4 – Average yearly values of natural groundwater recharge and surface runoff obtained by the actual 1979-2009 time series and estimated values under the different climate change scenarios

| Demo site | Process | 1979-2009 time series - mm/year | Scenario IS92A - mm/year (% 1979-2009 serie) | SRES A2 - mm/ year (% 1979- 2009 serie) | SRES B2 - mm/ year (% 1979- 2009 serie) |
|-----------------------|----------------|---------------------------------------|--|---|---|
| PT1 - Rio Seco | GW Recharge | | | | |
| | Surface runoff | | | | |
| PT2 - Querença-Silves | GW Recharge | 294 | 245 (84%) | 136 (46%) | 186 (63%) |
| | Surface runoff | 115 | 100 (88%) | 59 (51%) | 79 (69%) |
| PT3 - Melides | GW Recharge | 119 | 88 (74%) | 47 (40%) | 64 (54%) |
| | Surface runoff | 199 | 179 (90%) | 114 (58%) | 142 (72%) |

8.2 DEMO SITE 7: MENASHE INFILTRATION BASIN, HADERA, ISRAEL

8.2.1 Introduction

The Menashe facility is being used over 40 years for groundwater enrichment of the coastal aquifer using collected surface water. During the winter, as the major streams draining the southern Mt. Carmel slopes and the Menashe hills start to flow, part of the water is diverted by a system of dams and canals into a main conveyance canal. Driven further 16 Km west by gravitation the water is introduced into infiltration ponds for coastal aquifer enrichment, and later pumped by production wells (**Figure 5**). In addition to runoff infiltration, desalinated water originating from the nearby Hadera desalination plant is periodically introduced into the aquifer according to maintenance requirements. The physical and chemical processes involved in this type of aquifer enrichment are the essence of the demo site activity and research.

The mid-scale model deals with saturated flow within the coastal aquifer, underlying the Menashe infiltration facility area. It will correspond to both the larger watershed scale and the smaller, infiltration pond scale future models.

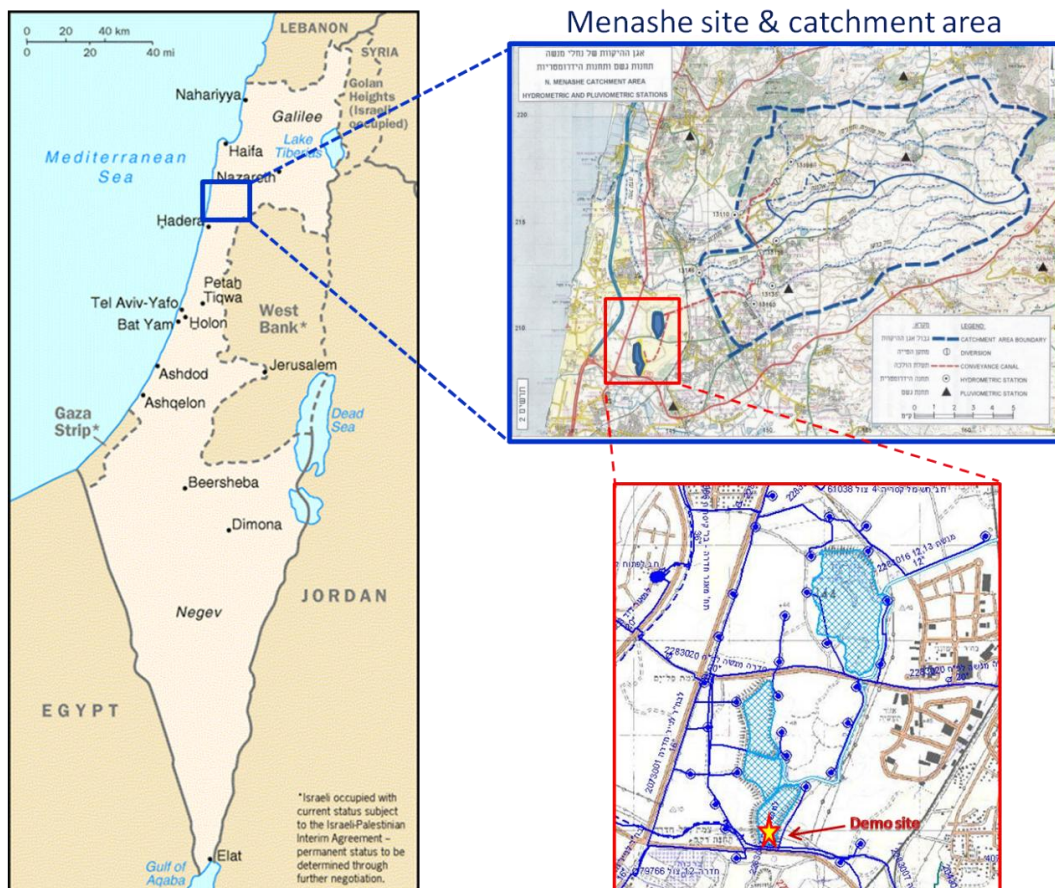


Figure 55 - Menashe infiltration site and catchment area – Location map and setting

8.2.2 Conceptual model

The Pleistocene coastal aquifer stretches along most of the coast of Israel. It reaches some 100 m depth along the coast just west of the Menashe site, and gradually wedges out towards east

till it vanishes about 12 Km from the coast. The aquifer consists of Pleistocene aged, coastal environment rocks series, dominated by calcareous sandstone and interbedded by conglomerates, silt and clay layers. At places thicker marine clay layers divide the aquifer into sub horizontal sections. This division is more dominant towards the coast and affects the western parts of the Menashe site. The entire aquifer complex is underlain in most areas by a thick, practically impermeable Neogene rock unit (Saqiye Group) and is separated from the deeper Cretaceous aquifer of the Judea Group (**Figure 56**). The aquifer is open towards west to the sea and is bounded by the fresh - seawater interface, allowing some freshwater seepage offshore.

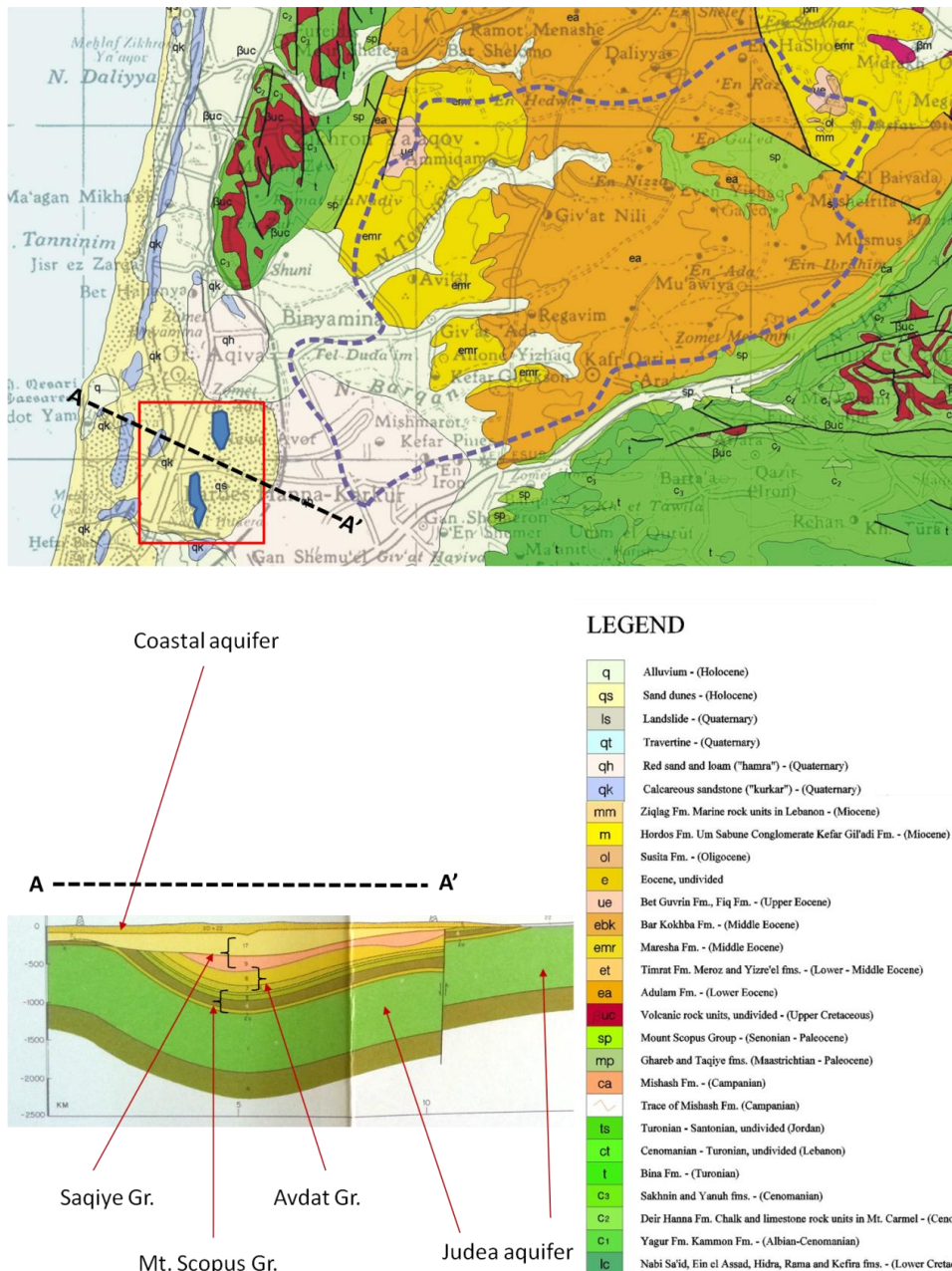


Figure 56 - Geological setting of the Menashe site and its catchment area

The geological data processed from well logs, geological and structural maps serve as the basis for the conceptual model, constructed via the GMS software package. The variety of rock types is represented by four types of materials. Following the marine clay structural maps, low permeability cells divide in places the western part of the model into sections. These layers are imbedded into the otherwise geostatistical based model computed by the T-PROGS software (**Figure 57**). The output of the T-PROGS is conditioned to the borehole data, the computed materials proportions and the material transition trends observed in the borehole data. The final horizontal model borders are still to be set according to further water level data.

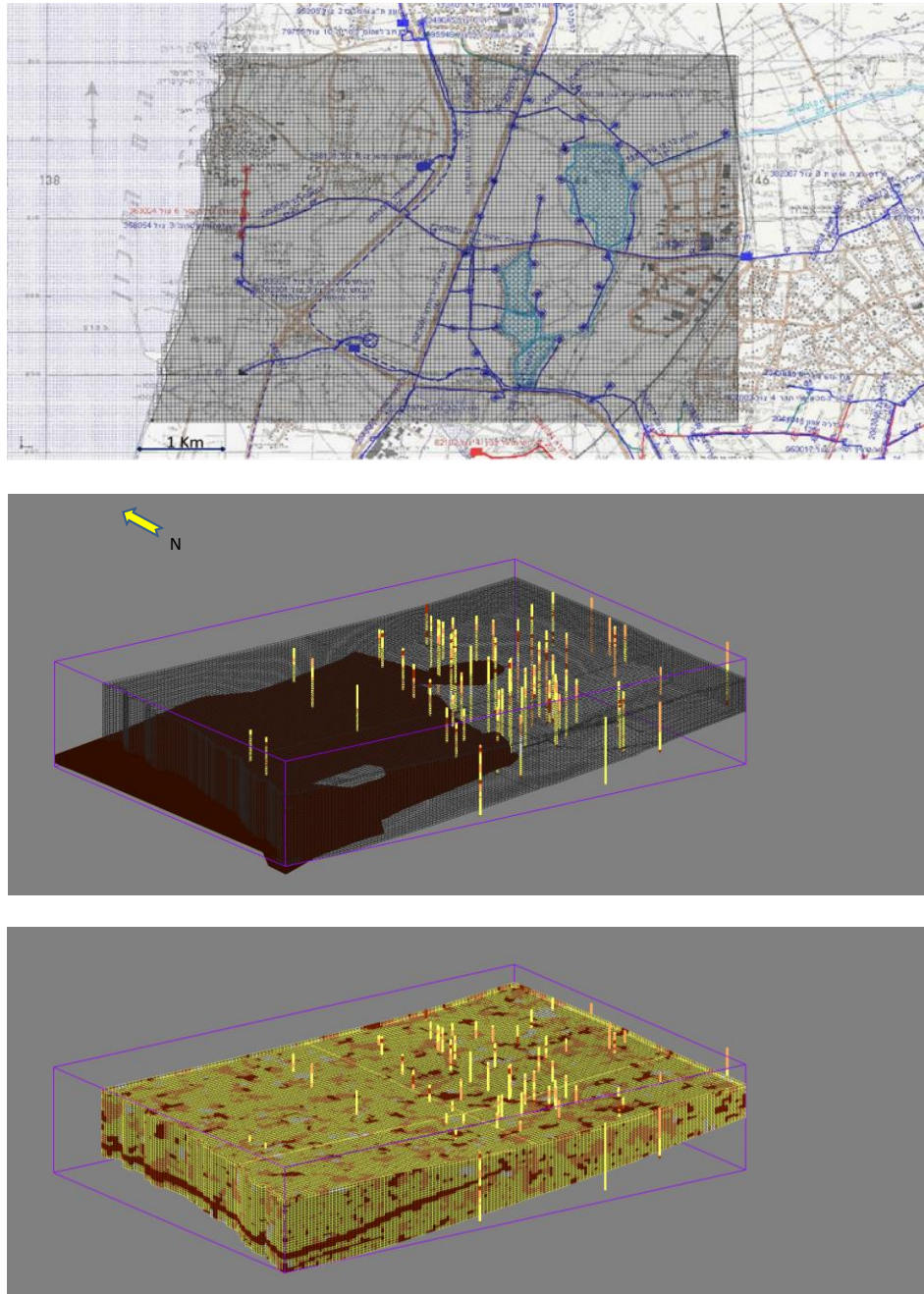


Figure 57 - Menashe site model structure

8.2.3 Water budget

The modelled area water balance is influenced by artificial enrichment, production wells activity, direct rainfall, subsurface inflow (mainly from the east) and seepage to the sea. While the average annual artificial recharge and pumping amounts are controlled (these are very roughly similar and equal ~ 12 MCM), the other parameters are yet to be computed by the model, following its final border definition and calibration.

8.2.4 Watershed Model Water Budget and Climate Change

8.2.4.1 Watershed Scale Model

For the quantification of the water budget of all the components of the hydrologic cycle, coupled surface water – groundwater model of the Menashe streams watershed is being developed. The model includes a surface water model of the four major streams of the Menashe hills, which will be iteratively coupled to an unsaturated/saturated zone model of a chalk aquitard connected to the coastal sandstone aquifer (**Figure 58**).

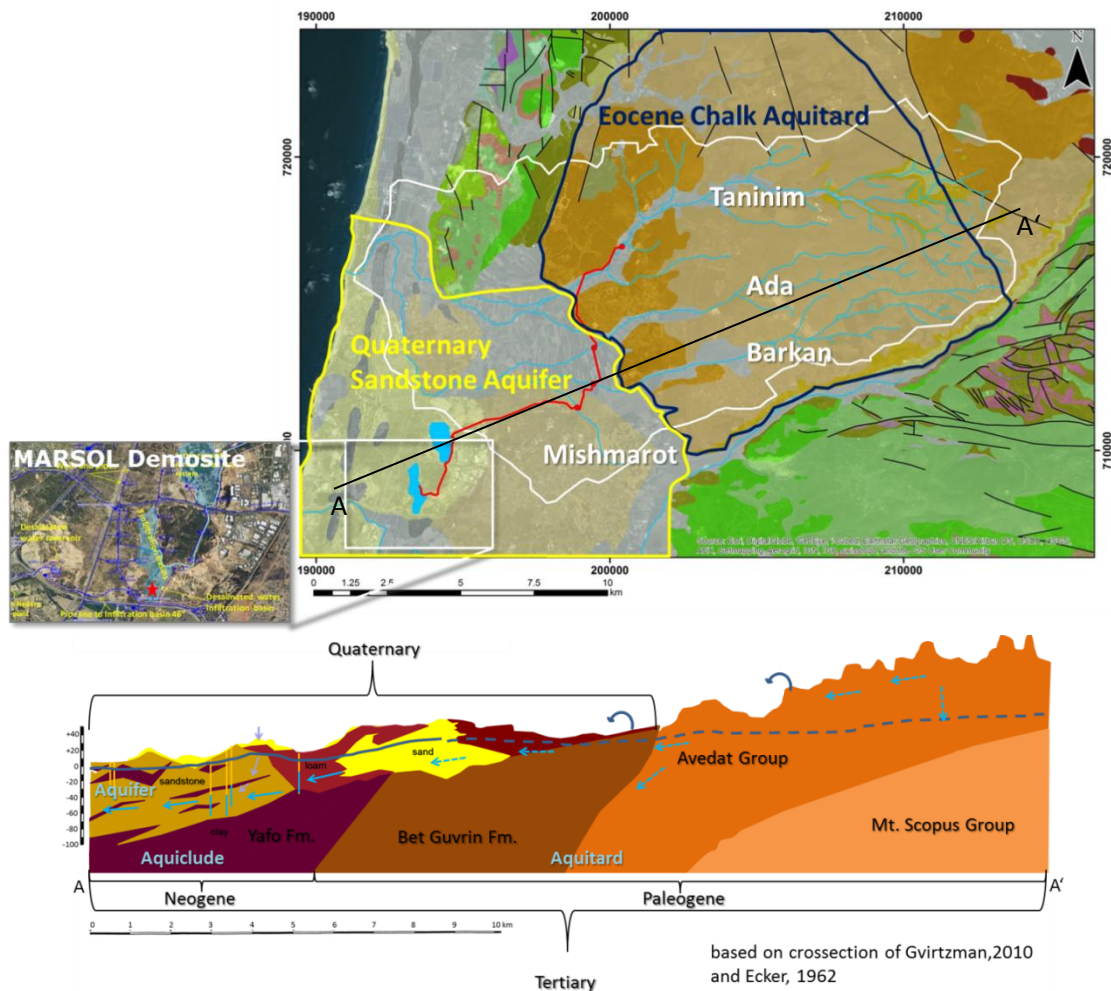


Figure 58. (a) Watershed-scale model and MARSOL demosite location on geological map; surface watershed outline (white), stream discharge diversion channel (red), approximate chalk aquitard outline (blue) and sandstone aquifer outline (yellow); (b) geological cross-section A – A', conceptual groundwater level and flow directions

Aim of the simulation is to reproduce the quantities of the hydrologic components on the basis of climate and stream discharge data of the past 50 years and then further use the developed model to simulate possible future climate scenarios and to evaluate the impact of a climatic change on the water budget.

8.2.4.2 Natural Water Budget

The current long-term water budget of the watershed is an average precipitation of about 600 mm per year, which occur between September to May, with a precipitation maximum in January and February. The potential evapotranspiration is about 1600 mm year, actual evapotranspiration is estimated to be about half of the precipitation amount and the average stream discharge is about 100 mm year which occurs from December to June. Precipitation as well as stream discharge are highly variable from year to year. The annual precipitation varies between below 400 mm and above 1000 mm, the annual discharge varies between 0 to 30 million m³ (Figure 59).

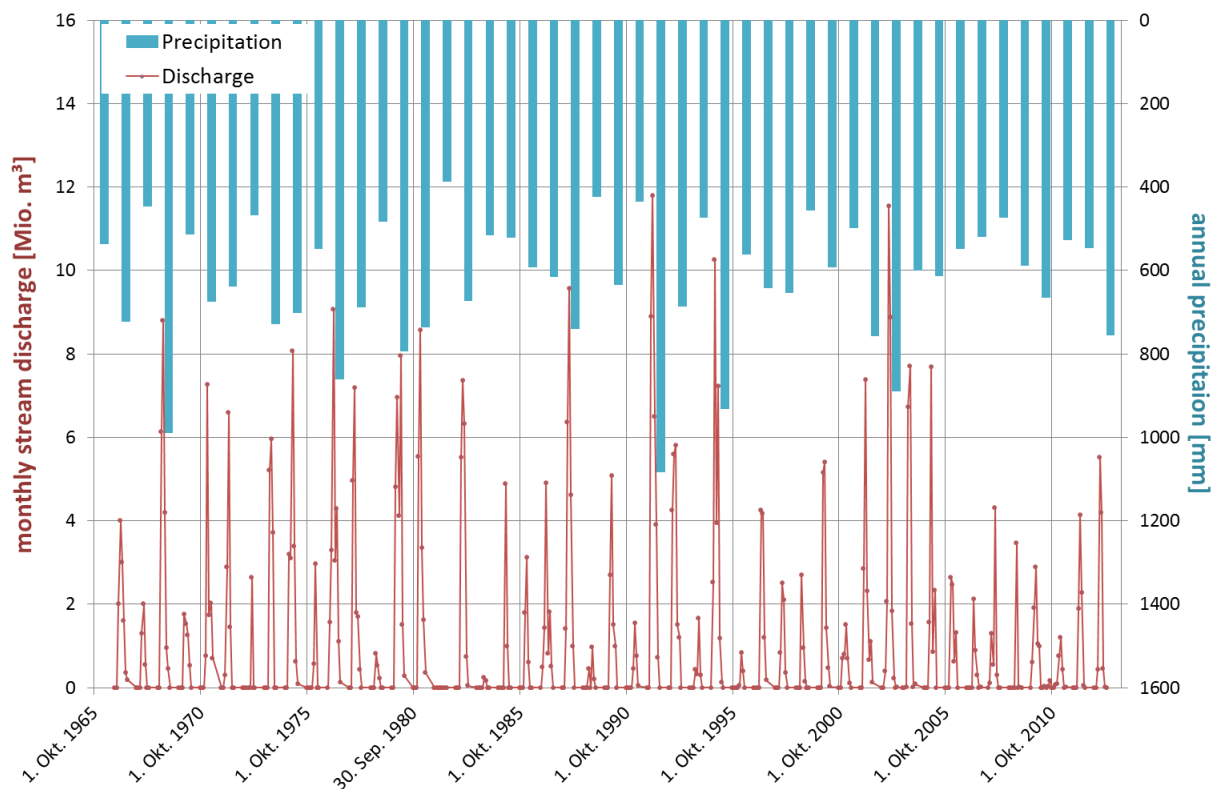


Figure 59. Annual precipitation sum in mm of the Regavim station (1965/66 - 2012/13) of the Israel Meteorological Service and monthly stream discharge at the infiltration basin inlet in Mio. m³ (1966/67 – 2012/13) from MEKOROT Company

8.2.4.3 Climate Change

Possible future climate scenarios will be based on downscaled global climate models and regional climate models based on IPCC scenarios.

For example, Alpert et al. (2008) evaluated a regional climate model of the Eastern Mediterranean, which supports the large-scale predictions for the entire Mediterranean to

have rainfall reductions up to 35% and an average temperature rise of 3–5 °C by 2071–2100. A regional study in northern Israel supports the tendency to a more extreme climate, of both wetter and drier years. The results further suggest a significant factor of increase in the number of the heavy rain days over the Jordan River basin in Israel, which in this region would lead to an average rainfall increase of about 10%.

Black (2009) calculated a reduction in winter rain in the area of Jordan and Israel by the end of the 21st century, which will be reflected in reductions of the frequency and duration of rainy events and hence the number of rainy days.

8.3 CONCLUSIONS

As mentioned in the DoW, regarding WP12, “For selected sites, strategies for selecting positions for MAR facilities will be presented and water budgets on a watershed scale elaborated to calculate water availability for MAR, and predictions on the influence of future climatic changes will be made. These sites will serve as reference for modelling strategies where the MAR installations are included into a more generalized water budget approach to allow long term predictions on MAR efficiency and economic feasibility. The main tasks of this work package are: Task 12.1: Methods evaluation (Task Leader: LNEC): Literature review on potential and currently applied modelling approaches for MAR sites and the evaluation of weaknesses and strengths (concluded) and Task 12.2: Water budget and conceptual modelling (Task Leader: LNEC): For selected sites, GIS layers of information for conceptual modelling will be prepared. Achievements for selected sites reported in this Deliverable 12.1.

As mentioned in the Introduction “Complementary information on the water budget and on modelling is being presented in the specific case-study and/or Thematic Deliverables, e.g. for Portugal in Deliverable 4.2 on “South Portugal MARSOL demonstration sites characterisation” and Deliverable 8.1 on “DSS with integrated modeling capabilities”, with modelling examples from Italy, e.g. “first application of the FREEWAT preliminary scripts on the S. Alessio site. This Deliverable will be further extended and reviewed during the progress of the project as, e.g., Task 12.3: Climate change impact (Task Leader: as in D12.1 also LNEC) is due by month 17, to include a summary of the Water budget and climate change impact assessment of Demo Site 4: Llobregat River Infiltration Basins, Sant Vicenç Dels Horts, Catalonia, Spain; Demo Site 5: River Brenta Catchment, Vicenza, Italy; And, Demo Site 6: Serchio River Well Field, Tuscany, Italy.”

The ppts of MARSOL activities related to the topics of this chapter are available in <http://www.eip-water.eu/working-groups/mar-solutions-managed-aquifer-recharge-strategies-and-actions-ag128>.

REFERENCES

- Almeida, C. (1985) - Hidrogeologia do Algarve Central. Diss. para obt. do grau de Doutor em Geologia. Departamento de Geologia da Fac. Cienc. Univ. Lisb. Lisboa, 1985, 333p.
- Almeida, C.; Mendonça, J.L.; Jesus, M.R. and Gomes, A.J. (2000) – Sistemas Aquíferos de Portugal Continental, Relatório. INAG, Instituto da Água.Lisboa.Doc. Electr. CD-ROM.
- Alpert, P., S.O. Krichak, H. Shafir, D. Haim, I. Osetinsky (2008) - Climatic trends to extremes employing regional modeling and statistical interpretation over the E. Mediterranean. *Global and Planetary Change* 63:163-170.
- APA-ARH (Unpublished) Land use assessment at the Algarve regional scale based on aerial photographs from 2007. Performed by the Algarve Water Basin Administration (Administração da Região Hídrica – ARH) from the Portuguese Environment Agency (Agência Portuguesa do Ambiente - APA).
- Black, E. (2009) - The impact of climate change on daily precipitation statistics in Jordan and Israel. *Atmospheric Science Letters* 10: 192-200.
- Caetano, M., V. Nunes e A. Nunes, 2009. CORINE Land Cover 2006 for Continental Portugal, Relatório técnico, Instituto Geográfico Português.
- Ecker, A. (1962) - Geology of the Soil-cell of the Pleistocene in the area of Pardes Hana-Cesarea. Hydro Report /8/62 - Geological Survey of Israel. (In Hebrew).
- Kessler, H. (1965) – Water balance investigations in the karstic regions of Hungary. In: AIHS-UNESCO Symposium on Hydrology of Fractured Rocks, Dubrovnik, Croatia.
- Gvirtzman, Z. (2010) - Gradual uplift and exposure of north Arabia and enhanced sedimentation in the Levant basin during Neo-Tethys closure. *GSI/26/2010*.
- Lopes, F. M. V. (2006) – A Geologia e a Génese do relevo da Rocha da Pena (Algarve, Portugal) e os seu enquadramento educativo, Dissertação de mestrado, Faculdade de Ciências do Mar e do Ambiente, Universidade do Algarve, Faro, 114 pp.
- Manuppella, G. (Coord.) (1992) – Carta Geológica da Região do Algarve, escala 1/100.000, Folha Ocidental, Serv. Geol. Portugal, Lisboa.
- Manuppella, G. (coordenação), Ramalho, M.; Rocha, R.; Marques, B.; Antunes, M.T.; PAIS, J.; Gonçalves, F. & Carvalhosa, A. (1993) - Carta geológica da região do Algarve, folha Ocidental, na escala 1:100 000. Serviços Geológicos de Portugal.
- Monteiro, J.P.; Vieira, J.; Nunes, L.; Younes, F. (2006) – Inverse Calibration of a Regional Flow Model for the Querença-Silves Aquifer System (Algarve-Portugal).Integrated Water Resources Management and Challenges of the Sustainable Development.International Association of Hydrogeologists, IAH. Marrakech. pp 44, doc. Elect. CD-ROM - 6pp.
- Monteiro, J.P.; Ribeiro, L.; Reis, E.; Martins, J.; Matos Silva, J. (2007) – Modelling Stream-Groundwater Interactions in the Querença-Silves Aquifer System. XXXV AIH Congress. Groundwater and Ecosystems. Lisbon. Portugal. pp 41-42, doc. Elect. in CD Rom. 10pp.

Nicolau R (2002) Modelação e mapeamento da distribuição espacial da precipitação – Uma aplicação a Portugal Continental (Modeling and mapping of the spatial distribution of rainfall). Universidade Nova de Lisboa.

Nunes, G., Monteiro J.P. and Martins, J. (2006) – Quantificação do Consumo de Água Subterrânea na Agricultura por Métodos Indirectos – Detecção Remota. IX Encontro de Utilizadores de Informação Geográfica (ESIG). 15 - 17 de Novembro, Tagus Park, Oeiras. Doc. Electrónico em CD-ROM. 15pp.

Oliveira, M.M., Oliveira, L.G. (2012) - “Água, ecossistemas aquáticos e atividade humana – Projeto PROWATERMAN - Referência do projeto n.º PTDC/AAC-AMB/105061/2008. Quinto relatório temático – Estimativa da recarga e do escoamento direto na área de drenagem do sistema aquífero Querença-Silves”. Relatório 180/2012 – DHA/NAS, 108 pp.

Oliveira, M.M., Novo, M.E., Lobo Ferreira, J.P. (2007) – Models to predict the impact of the climate changes on aquifer recharge. In Lobo Ferreira JP, Vieira J (eds) - Water in Celtic Countries: Quantity, Quality and Climate Variability, IAHS Red Books, London, IAHS Publication 310, ISBN 978-1-901502-88-6, 103-110.

Oliveira, M.M., L. Oliveira, and J.P. Lobo Ferreira, 2008. Estimativa da recarga natural no sistema aquífero de Querença-Silves (Algarve) pela aplicação do modelo BALSEQ_MOD. in 9.º Congresso da Água - Água: desafios de hoje, exigências de amanhã, Cascais (Portugal), 2 - 4 Abril 2008, CD.

Oliveira, L.G.S., T.E. Leitão, J.P. Lobo Ferreira, M.M. Oliveira, and M.E. Novo, (2011) - Água, Ecossistemas Aquáticos e Actividade Humana – Projecto PROWATERMAN. Terceiro Relatório Temático – Resultados Quantitativos e Qualitativos das Campanhas de 2011 e Balanços Hídricos. Referência do Projecto n.º PTDC/AACAMB/105061/2008, 2011, 99 pp.

Oliveira, L. G. S., Martins, T., Lobo Ferreira, J. P. C., Oliveira, M.M., Novo, M., Leitão, T. E. (2012) - “Contributos para o desenvolvimento de medidas para uma gestão sustentável dos recursos hídricos no Sul de Portugal”. Água, ecossistemas aquáticos e atividade humana – Projeto PROWATERMAN. Referência do projeto n.º PTDC/AAC-AMB/105061/2008. Relatório 153/2012 – DHA/NAS, 55 pp.

Salvador, N.; Monteiro, J. P.; Hugman, R.; Stigter, T. Y.; and Reis, E. (2012) – Quantifying and modelling the contribution of streams that recharge the Querença-Silves aquifer in the south of Portugal, Nat. Hazards Earth Syst. Sci., 12, 3217-3227, doi:10.5194/nhess-12-3217-2012.

Stigter, T.Y.; Monteiro, J.P. ; Nunes, L.M.; Vieira, J.; Cunha, M.C. ; Ribeiro, L.; Nascimento, J. and Lucas, H. (2009) – Screening of sustainable groundwater sources for integration into a regional drought-prone water supply system. Hydrol. Earth System Sci. 13, 1–15.

Terrinha, P. (1998) – Structural Geology and Tectonic Evolution of the Algarve Basin, South Portugal, Ph.D., University of London, London, 430 pp., 1998.

Vieira, J. and Monteiro, J. P. (2003) – Atribuição de propriedades a redes não estruturadas de elementos finitos triangulares (Aplicação ao Cálculo da Recarga de Sistemas Aquíferos do Algarve). In: Ribeiro, L. and Peixinho de Cristo, F. (eds.) As Águas Subterrâneas no Sul da Península Ibérica. Assoc. Intern. Hidrog. APRH publ., pp183-192.

White book on MAR modelling

Deliverable D12.7

CHAPTER 4 – MAR THROUGH FORESTED INFILTRATION: THE EXEMPLE OF MARSOL RIVER BRENTA CATCHMENT DEMO SITE 5, IN VICENZA, ITALY

ELISA FILIPPI (SGI), VINCENZO MARSALA (SGI), MICHELE FERRI (AAWA), ALBERTO CISOTTO (AAWA), GIOVANNI TOMEI (AAWA)

9 EXECUTIVE SUMMARY OF MAR THROUGH FORESTED INFILTRATION: THE EXEMPLE OF MARSOL RIVER BRENTA CATCHMENT DEMO SITE 5, IN VICENZA, ITALY

Southern Europe and the Mediterranean region are facing the challenge of managing its water resources under conditions of increasing scarcity and concerns about water quality. Already, the availability of fresh water in sufficient quality and quantity is one of the major factors limiting socio economic development. Innovative water management strategies such as the storage of reclaimed water or excess water from different sources in Managed Aquifer Recharge (MAR) schemes can greatly increase water availability and therefore improve water security. Main objective of the proposed project MARSOL is to demonstrate that MAR is a sound, safe and sustainable strategy that can be applied with great confidence and therefore offering a key approach for tackling water scarcity in Southern Europe.

For this, eight field sites were selected that will demonstrate the applicability of MAR using various water sources, ranging from treated wastewater to desalinated seawater, and a variety of technical solutions. Targets are the alleviation of the effect of climate change on water resources, the mitigation of droughts, to countermeasure temporal and spatial misfit of water availability, to sustain agricultural water supply and rural socio-economic development, to

combat agricultural related pollutants, to sustain future urban and industrial water supply and to limit seawater intrusion in coastal aquifers.

The two MARSOL pilot sites selected in Italy, namely **Demo Site 5 “River Brenta Catchment, Vicenza, Italy”**, are located in the upper plain of the Veneto Region. The first one site is a F.I.A. (Forested Infiltration Area) used during the LIFE+ funded TRUST project, while the other site is suitable for serving two different functions: floods retention area and managed artificial recharge.

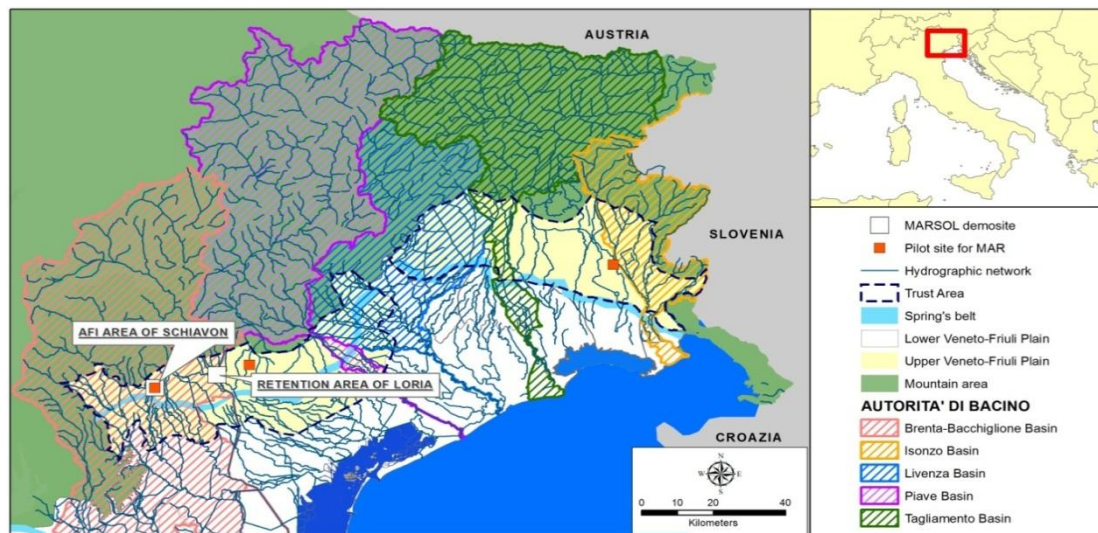


Figure 60- Location of the two test areas in the Demonstration Site 5, River Brenta Catchment, Vicenza, Italy

DEMO site activities included the implementation of monitoring and mathematical modelling in order to monitor and model infiltration rates and quality processes. The monitoring has provided insight about the enhancements that the F.I.A. and flood retention basin offer for MAR both in quantity (improving infiltration rates) and quality terms (due to the effects of the biological systems linked to the plant roots). Mathematical modelling focused on assessing the impact of the MAR in the restoration of the resurgence system. The benefits of cultivation in the MAR area to prevent clogging have been assessed as well as the potential of MAR to improve water quality aspects.

10 DEMO SITE 5 STUDY AREA

The two MARSOL pilot sites selected are shown in detail in following picture:

- Schiavon Forested Infiltration Area (F.I.A.) and
- Loria detention basin along the Lugana river

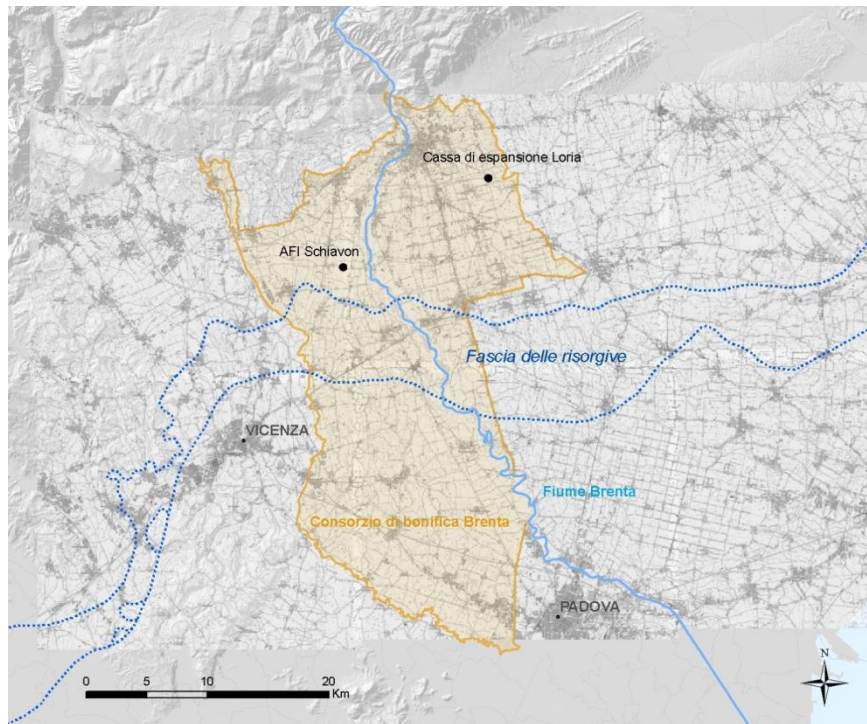


Figure 61- Map of the demonstration sites identified

The **Infiltration Area of Schiavon (F.I.A.)** is fed by the Brenta river through the existing network of irrigation channels. The F.I.A. one is located in the Vicenza upper plain aquifer, which is an undifferentiated aquifer on the foothill area of the pre-Alps, and contains one of the most significant groundwater bodies of the Eastern Alps hydrographic district, in terms of both size and water supply provided. This land is therefore strategic for all the citizens who live in the area and who use this water resource.

The natural infiltration capacity of the soil is heavily compromised, while the decrease of flows towards the groundwater represents a problem for the ecosystem balances on one hand, and a direct threat for the citizens' health on the other hand. In particular, the slow impoverishment of the water resources, caused by the depletion of the undifferentiated groundwater table of the Vicenza upper plain, causes a series of problems such as: water shortage, water conflicts, outflow of the spring belt natural system, increase in the investment costs for the water supply, etc.

During the time from 2013 to 2015, the site was studied under the Aquor project, funded by the EC in the framework of the LIFE+ programme. From the operational point of view, the site is managed by the Brenta Consortium, which has entered into a lease agreement with the land owner for a period of 5 years.

The Schiavon forested infiltration area has been chosen to represent the typical MAR settings within the River Brenta Catchment. One of the reasons for selecting the Schiavon forested infiltration area was because this site already had a set of consolidated historical data, and because it provided the possibility to reach the following objectives:

- Characterization of the heterogeneous River Brenta mega fan deposits at very shallow depth. Knowledge about sediment type composition and distribution will be required to evaluate infiltration capacity and its variability
- Hydrostratigraphical characterization of the shallow subsurface within the EU water framework directive and
- Evaluation and/or monitoring of the clogging effects.

The **Loria detention basin** is located next to the city of Treviso. In addition to the Lugana river, another water stream, the Trieste river, a flood-risk tributary to the Lugana, is intercepted. The Lugana's maximum thirty-year flow is 10 m³/sec. The basin has a stock capacity up to 40.000 m³ and it fills up four times a year.

The Loria retention basin has been chosen taking into account two possible uses for the infiltration test site, namely the infiltration capacity and the potential flood basin area.



Figure 62 – Scheme of the monitoring system in Schiavon (figure on left) and Loria Demo site (right figure)

11 DEMO SITE 5 MONITORING AND SITE CHARACTERIZATION

11.1 SITE CHARACTERIZATION

The Loria infiltration basin and the Schiavon F.I.A. were chosen to represent two typical MAR settings within the River Brenta Catchment. The following research questions were defined for the two investigation sites:

- Loria basin infiltration test site (seasonal infiltration); special relevance of this test site as EU flood directive and EU water framework directive apply:
 - How to efficiently characterize the shallow subsurface of large scale MAR infrastructures;
 - How to quantify sediment input and mobilization of fines within the upper 1-2 m depth following infiltration/recharge events;
 - How to characterize and monitor infiltration capacity (against the background of potential basin base area colmatation).
- Schiavon forested infiltration site:
 - How to characterize the heterogeneous River Brenta mega fan deposits at very shallow depth. Knowledge about sediment type composition and distribution will be needed to evaluate infiltration capacity and its variability;
 - How to conduct a hydrostratigraphical characterization of the shallow subsurface in the above mentioned framework
 - How to evaluate and/or monitor clogging effects due to colmatation in the infiltration trenches.

The MOSAIC (*Model driven site assessment information and control*) site investigation approach was employed for a problem-oriented, rapid site characterization. The MOSAIC platform comprises mobile modular data acquisition units for adaptive field investigations and contains vehicles equipped with direct push probing devices in combination with geophysical measuring techniques as well as hydrogeological and geotechnical equipment. Thereby, surface geophysics allow rapid mapping of subsurface structures while Direct Push can be used for high resolution in situ parametrization of detected layers/units. Thereby, Direct Push describes a technology that uses hollow steel rods that are hammered and/or pushed into the subsurface. Sensor probes can be attached to the end of the rod string to collect continuous vertical high resolution profiles of hydrogeological, geotechnical, geophysical or geochemical properties under in situ conditions. Alternatively, Direct Push can be used to rapidly install permanent or temporary ground water wells or to retrieve soil samples. As the Direct Push technology allows on-site decision making it is often advantageous over conventional solely sample based site characterization approaches concerning data reliability, adaptability, and efficiency.

11.1.1 Loria Infiltration Basin

Prior to the first field campaign (September 2014) the infiltration basin was flooded after a strong precipitation event. As a result, most of the basin area was covered with a fine-grained sediment layer of approximately 10 cm thickness. This limited site accessibility with the mobile MOSAIC equipment (track mounted Direct Push rigs of 4.5 t weight and mobile geophysical equipment pulled by a car) as well as applicability of geophysical measurement methods. However, it enabled us to investigate the site under unbiased site conditions after flooding. The following work was performed:

- Extensive electromagnetic profile measurements (profiles of EM38DD, EM31) and gamma-ray spectrometric measurements to characterize the heterogeneity of sediments, e.g. identification of areal zonation in composition within basin
- Hood infiltrometer tests to determine infiltration rates and to determine potential differences in infiltration capacity caused by soil cover and structure (comparison between ploughed soil, grass cover, etc.)
- Soil sampling for grain size analyses and to conduct laboratory soil column experiments on the change of infiltration capacity in response to potential colmatation.

The clay cover and sedimentary composition with a broad spectrum in grain size distribution (clay to rocks) was challenging for the application of investigation techniques. However, surface geophysics as well as Direct Push probing at shallow depths was successfully applied for site characterization. Results of the surface geophysics surveys did not indicate different aerial zonation within the basin. Following the MOSAIC site investigation approach, high resolution vertical Direct Push profiling was employed for the subsurface characterization, as ground truth for the geophysics data, and to provide in-situ measured data for enhanced site parametrization. Subsurface investigations conducted in March 2015 included the following activities:

- Cone Penetration Testing (CPT) at all marked locations 1-10 (
- Figure 63). Obtained CPT measurements revealed information about soil behaviour type that was used to infer subsurface lithology. The CPT system was deployed in combination with a frequency domain based add-on module to determine vertical profiles of volumetric water content in the subsurface. This tool allows determination of variations in soil water content on decimetre scale based on in-situ measurements and was especially useful to determine thickness of the clay rich surface cover in the northern part of the basin. Vertical profiles of the distribution of electrical conductivity were measured in addition to identify potential presence and thickness of clay containing layers that may inhibit infiltration over depth (
- Figure 63).
- Installation of 2 waveguides to a depth of 4m below ground surface to be used for continuous soil water content monitoring at location 3 (
- Figure 63) by ICCS.

- Vertical high resolution (10 cm sampling intervals) soil sampling at waveguide installation locations. Volumetric water content was determined for samples using gravimetric analyses to support in-situ measured CPT and soil water content data.
- Additional soil sampling at location 10 to a depth of 4 m below ground surface for soil description and determination of volumetric water content.
- Extensive soil column experiments to assess the impact of grain size distribution and amount of suspended sedimentary load and its mobilization during flooding events on the clogging behaviour.

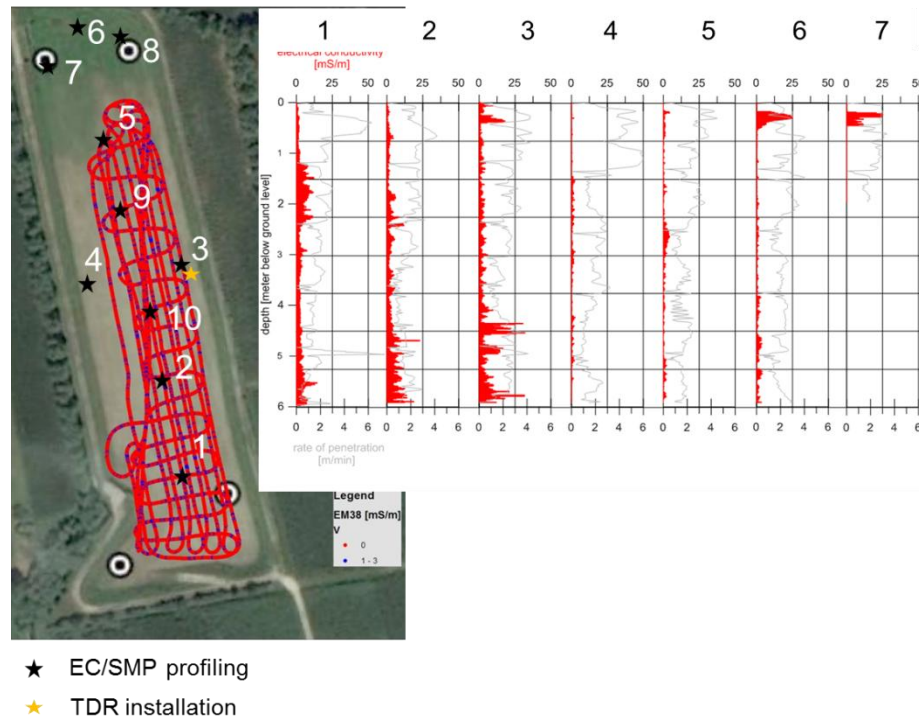


Figure 63 - Direct Push investigation locations (numbered 1-10) and selected Direct Push electrical conductivity logging results

11.1.2 Schiavon Forested Infiltration Site

Similarly, the MOSAIC approach was performed at the Schiavon forested infiltration site. Work included:

- Extensive electromagnetic measurements (profiles of EM38DD and EM31 between infiltration trenches) to characterize the unsaturated zone in terms of sedimentary areal zonation. Thereby, different zones of interest in different depths were identified.
- Geoelectric measurements (two profiles of 140 and 172 m length) for vertical characterization of sedimentary structures/layers supported the findings of the electromagnetic surveys.
- Outcrops photography and mapping for validation of the electromagnetic measurements.

Based on the geophysics results, 6 zones of interests (see Figure 64) were identified for detailed subsurface investigations during the March 2015 field campaign. Specific activities that were conducted are the following:

- Use of Direct Push vertical electrical conductivity profiling at locations 1-6 as a tool to identify potential small scale clay rich (high electrical conductivity) layers in the shallow subsurface (here up to 7m below ground surface) that may constrain water infiltration; see Figure 64 for results.
- Direct Push based installation of 2 waveguides to a depth of 3m below ground surface to be used for continuous soil water content monitoring by ICCS.
- Vertical high resolution (10cm sampling intervals) soil sampling at waveguide installation locations. Volumetric water content was determined for samples using gravimetric analyses; results can be used to calibrate initial waveguide TDR measurements performed by ICCS.
- Installation of a 2" diameter ground water monitoring well in close proximity of the waveguide installations for ground water level monitoring.
- Additional soil sampling at locations 1, 2, 5 (see Figure 64 left) for stratigraphic analysis and analysis of bulk density up to a depth of 8m below ground surface.

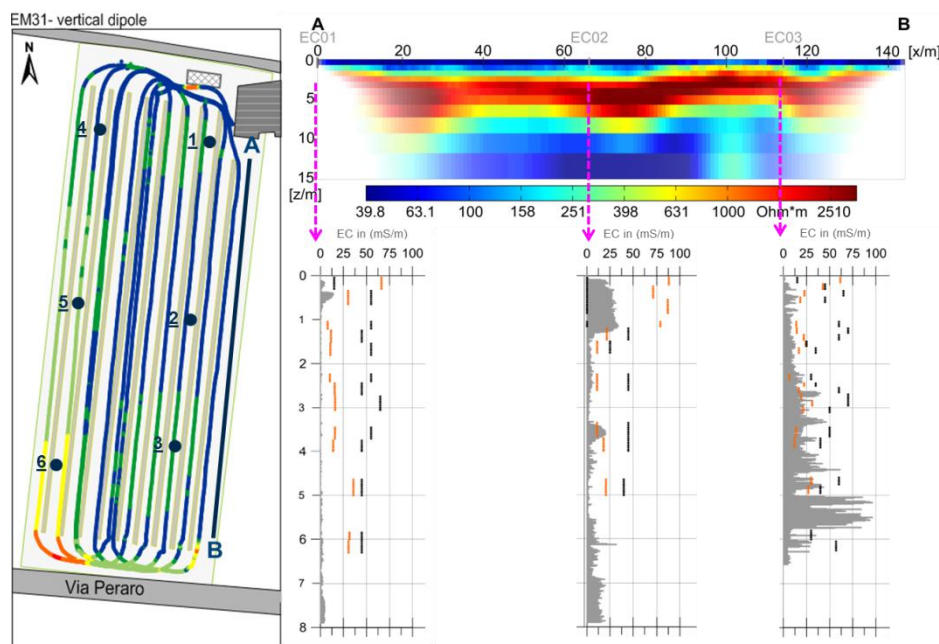


Figure 64 - Results of the site characterization. Results of the electromagnetic survey, EM32 with 6m penetration depth (left) and location of Direct Push investigation points; Electrical Resistivity Tomography (Top); selected results of vertical Direct Push electrical conductivity logging (bottom)

11.2 UNSATURATED ZONE MONITORING

The research activities involved the conceptualization and installation of prototype TDR sensors in the demo sites of WP7. The optimal location of the TDR sensors was decided based on the above type of MAR facilities, and in combination with the information from the surface

geophysics surveys conducted by MET-UFZ. The installation for the test of the TDR took place on March 2015, as shown in the following figures.

The above TDR sensors have the following characteristics:

- Schiavon Site:
 - TDR₁: Sensor length 2,80m
 - TDR₂: Sensor length 3.00m
- Loria Site:
 - TDR3: Sensor length 3.00m
 - TDR4: Sensor length 3.00m



(a)



(b)

Figure 65 - Installation of developed TDR sensors in (a) Schiavon and (b) Loria, MAR sites

During the 1st and 2nd of September 2016 the installation of the TDR monitoring and data logging system has been implemented. The monitoring system has been connected to the TDR waveguides that have already been installed at specific locations in the Loria and Schiavon sites (March 2015).

At both sites the infrastructure for the protection of the waveguides (concrete rectangular openings with concrete cover), heavy duty tubing buried underground for the protection of the signal transfer coaxial cable and a concrete sump with concrete cover for the protection of the TDR instrumentation box and the battery have already been constructed in-place.

The work consisted of the:

- Installation of low loss coaxial cables for the TDR signal;
- Connection of TDR and sealing of TDR waveguides;
- Connection and test of TDR monitoring and data logging system.

The installations were followed by various test and TDR readings.

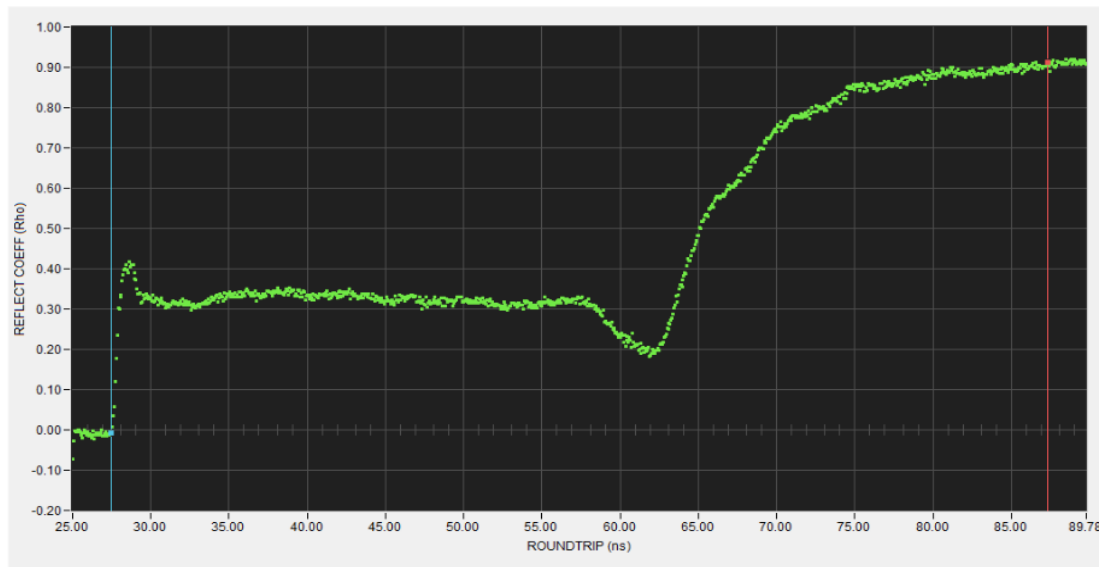


Figure 66 - Sample TDR reading at Schiavon site

11.3 MODELLING ACTIVITY OF DEMO SITE

11.3.1 Hydrodynamic model

The goal of the modelling activities was the development of a 3D physically based distributed hydrological model surface/subsurface water for the BRENTA basin (Figure 1) to be used as helpful tool in order to simulate the whole hydrological cycle and perform spatial-temporal analysis for water management and planning, using open source and free codes. In addition such a model, once calibrated on the basis of recorded historical data, can be later employed for evaluating the effects on the aquifers of some MAR techniques, such as those ones that were established inside the BRENTA basin.

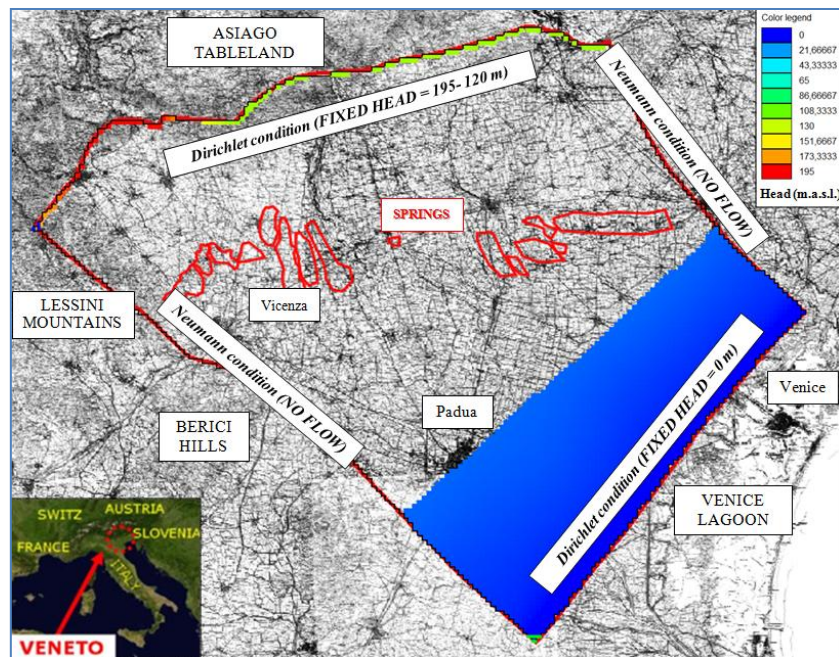


Figure 67 - Study area (Venetian Central Basin, Italy), model domain, boundary conditions

In detail the model was developed using the public domain computational code MODFLOW, presently considered an international standard for simulating and predicting groundwater conditions and groundwater/surface-water interactions. MODFLOW is developed by the U.S. Geological Survey, and solves the three-dimensional (3D) groundwater flow equation based on the discretization of a continuous aquifer system using the finite difference method, consisting on replacing the three-dimensional (3D) groundwater flow equation by a finite set of discrete points or cells in space and time where aquifer head values are calculated.

This code was selected for a series of reasons: it has a modular structure, each module representing a specific sink/source of the hydrologic system being simulated, that allows it to be easily modified to adapt the code for a particular application. It also allows to simulate steady and transitory flow conditions in an irregularly shaped flow system in which aquifer layers can be confined, unconfined, or a combination of confined and unconfined, that is exactly the geological situation characterizing the Brenta basin. In addition the various source/sink terms affecting the study area, i.e. flow to wells, areal recharge, evapotranspiration, flow to drains, and flow through river beds, can be simulated; hydraulic conductivities or transmissivities for any layer may differ spatially and be anisotropic and the storage coefficient may be heterogeneous; specified head and specified flux boundaries can also be modelled.

Therefore, first of all, the various model layers were recreated, potentially corresponding to the units defined in the conceptual geo-structural model: the definition of top/ bottom surfaces for each hydrostratigraphic unit and the distinction in active/inactive cells were performed. Later the necessary boundary conditions were established: the northern boundary of the study area was limited by the outcrop line of the basement; the southern boundary was placed at the limit of the Adriatic Sea (where hydrostatic boundary conditions were imposed for all aquifers); finally no-flow boundary conditions were assumed for both the eastern and

western limits of the calculation domain, i.e. such limits were traced orthogonally to the available piezometric contour lines (Figure 67). Then a number of geologic regions were identified for the phreatic aquifer on the basis of outcrop maps, so that different values of hydraulic conductivity could be assigned to each of them (Figure 68). This spatial distribution was then applied to all the underlying layers of the model because of the lack of accurate information for the confined aquifers.

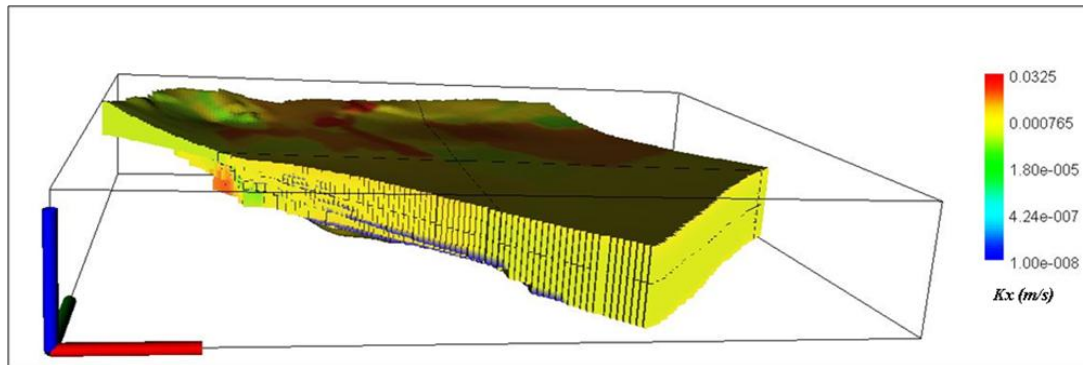


Figure 68 - Spatial distribution of hydraulic conductivity in x-direction inside the 3D model

The following various source/sink terms were estimated and later assigned to the model's cells: (1) net infiltration; (2) water discharge dispersed by rivers, irrigation channels and agricultural fields; (3) water discharge drained by rivers; (4) spring-water outflows; and (5) water flows pumped out by private and public wells.

In the case of public wells for domestic (100 units) and irrigation (50 units) use, the pumped flows were locally assigned to the 3D model cells taking into account the available information on filter locations. Instead, the private wells (industrial or domestic) couldn't be modelled in the same way due to the big number of the wells active in the resurgence zone and the very poor data obtainable. Consequently they were simulated by assuming some withdrawal areas, and assigning them outflows on the basis of literature data.

Evapotranspiration fluxes were evaluated through the Hargreaves and Samani formulation, assuming that the real evapotranspiration was a function of the water content in the soil and potential evapotranspiration. The processes, related to the separation of superficial and sub-superficial fluxes from deep infiltration, were modelled mathematically by applying the water balance to a control volume representative of the active soil. The water content $S(t)$ in the soil was updated at each calculation step dt using the following balance equation:

$$S(t+dt) = S(t) + P - R_{sur} - R_{sub} - L - ET$$

where P and ET are the components of precipitation and evapotranspiration, while R_{sur} , R_{sub} and L are the surface runoff, sub-surface runoff and deep percolation model states respectively. The surface runoff was expressed using the following equation, which is based on a threshold critical value beyond which a mechanism of dunnian flow (saturation excess mechanism) prevails:

$$R_{sur} = \begin{cases} C \left(\frac{S}{S_{max}} \right) P - P \Rightarrow P \leq f = \frac{S_{max} \theta_{max} - S}{\theta_{max} - C S} \\ P - \theta_{max} - S \Rightarrow P \leq f \end{cases}$$

where C is a coefficient of soil saturation obtained by calibration, and S_{max} is the content of water at saturation, depending on the nature of the soil and on its use. In detail the following data were considered to calculate net rainfall infiltration rates: hourly rain intensities gauged at 25 pluviometric stations, maximum and minimum daily temperatures, soil use/cover maps and pedological maps (Figure 69).

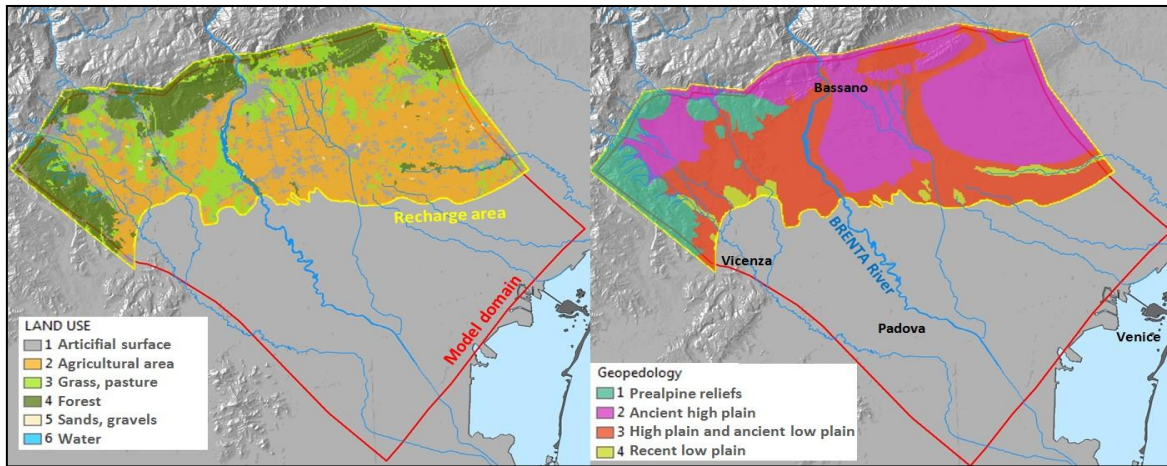


Figure 69 - Soil use/cover map and pedological map for the recharge area

As concerns the water fluxes dispersed by river beds and irrigation channels, they were estimated using empirical relations linking river (or channel) discharges to the dispersed flux per stream length unit. Such relations were derived from several field campaigns, integrated by data collected in more recent surveys. A similar procedure was also applied in order to evaluate the water fluxes drained by river beds.

Finally empirical relations between the spring discharges and the piezometric levels measured in suitable wells were assessed to obtain a continuous record of the spring discharge at various sites.

Initially steady state simulations were performed: in this case the sum of all inflows (where outflow is a negative inflow) from adjacent cells and external stresses must be zero for each cell in the model because the storage term is null. In detail the calibration of the model, was carried out by comparing:

- the simulated and observed groundwater heads collected for the study area in 2007;
- the water budget terms, previously calculated and averaged for 2007, with those ones obtained by the model.

The selection of the 2007 data set was due to the fact that it represents the historical data series approaching the most the theoretical data series obtainable by averaging all the historical data recorded in the 2000-2016 period.

The results obtained were satisfying both in terms of simulated groundwater heads (Figure 70) and water budget volumes: in particular the simulated groundwater head was characterized by an average error of about 1 meter, and 90% of the study area showed an error less than 3.50 meters.

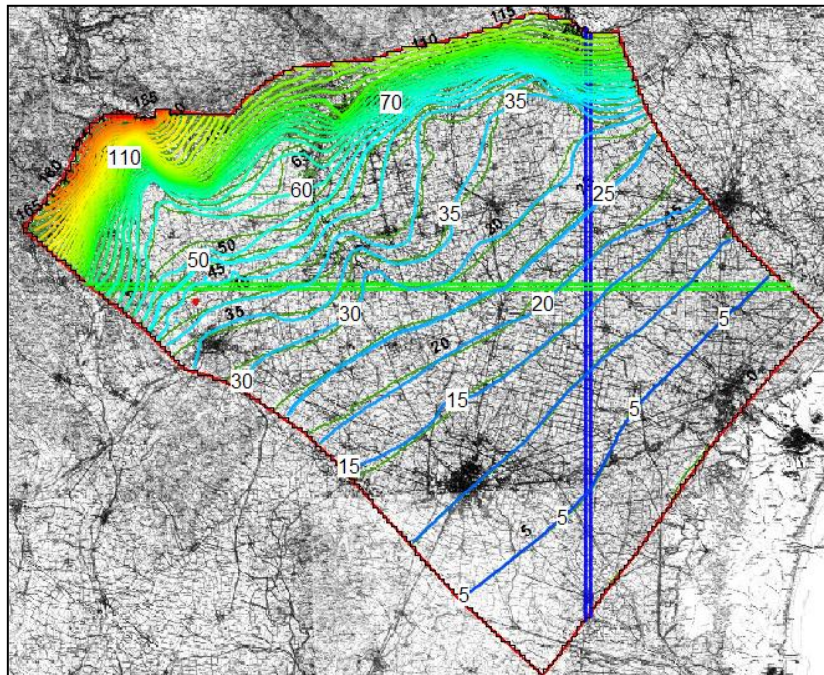


Figure 70- Comparison between the simulated isophreatic contour lines and the observed ones (green line on the background)

The steady state solution obtained was then employed as a reliable initial condition for transitory state simulations, where the storage capacity of the groundwater has also to be taken into account. In detail the specific yield and storage were assumed constant inside the various aquifers ($S_s = 3 \cdot 10^{-5}$ 1/m, $S_y = 0.2$) and aquitards ($S_s = 3 \cdot 10^{-4}$ 1/m, $S_y = 0.45$). In detail transitory state simulations were performed in order to evaluate the oscillations of the phreatic surfaces and the resurgence outflows on varying the other water budget terms. Therefore the average monthly values of net infiltration, water discharges dispersed by rivers, irrigation channels and agricultural fields, water discharges drained by rivers and water flows pumped out by private and public wells were firstly calculated and then assigned to model cells. Nevertheless the calculation was later performed on a daily basis in order to avoid any possible convergence issue.

The model was able to reproduce quite correctly the temporal trends of the various source/sink terms and observed groundwater heads (Figure 71): in particular forty-two out of fifty monitoring stations showed an average value of the absolute deviations, estimated comparing the temporal trends of simulated and observed groundwater heads, less than 5 meters.

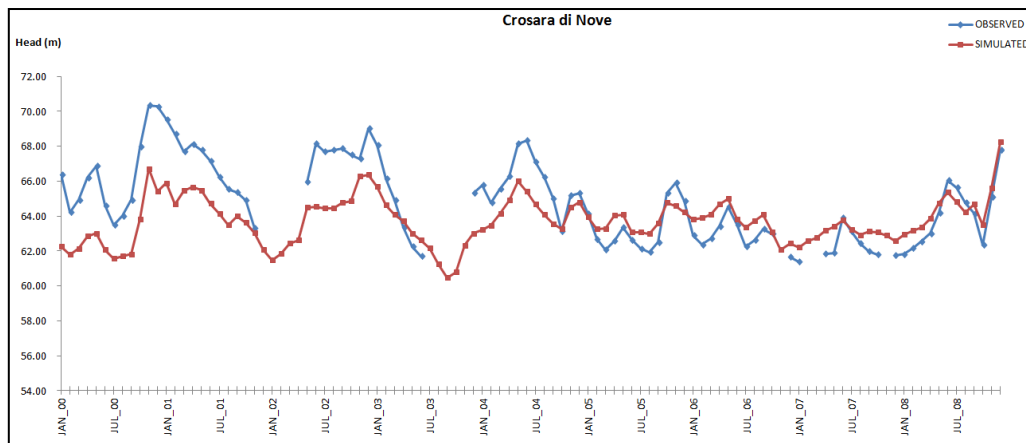


Figure 71 – Comparison between the simulated and observed groundwater heads for the monitoring station in Crosara di Nove

However the developed model did not consider any stream-aquifer interaction since the simulated river inflows/outflows were previously estimated on the basis of historical recorded data. It is evident how a similar approach has some faults because changes in the environmental system could make invalid these correlations: consequently stream-aquifer interactions were later simulated using the MODFLOW-2005 Streamflow Routing package. This package defines the characteristics of streams used in the groundwater model. Each stream is discretized into segments, which are a portion of the stream with constant or linearly varying properties. These segments are overlaid on the model grid, and the intersection of a segment with these cells is referred to as a reach. Segment boundaries are defined when there is a tributary, diversion, streamflow gage, or a non-linear change in a stream property, and their physical properties are defined at the upstream and downstream end of the segment itself.

Therefore point streambed geometry cross-section data, streambed thickness, roughness coefficients for the channel and overbank, vertical hydraulic conductivity, streambed elevation were defined into the model. In addition flow hydrographs were introduced as boundary conditions for the upstream sections of the rivers to be modelled. In detail they were calculated by a geomorphoclimatic hydrological model, previously developed and calibrated for the study area, enabling to simulate hydrologic processes in the mountain zones, delimiting the northern boundaries of the present calculation domain, where there are no aquifers. In particular the geomorphoclimatic approach relates the transfer function of rainfall-runoff characteristics of the basin to the topology of its river network, and therefore to its geomorphology and climate characteristics. Moreover it reproduces the processes of snow accumulation and melting and the processes of rainfall-runoff separation, solving the water balance in a volume of hydrological active soil (vadose zone), through a realistic description of the temporal dynamics of water content and adopting a physically based parameterization of processes that takes into account the vegetation cover, the soil texture and its slope.

Also in this phase, initially, steady state simulations were performed and the calibration of the model was carried out by comparing:

- the simulated and observed groundwater heads collected for the study area in 2007;

- the water budget terms, previously calculated and averaged for 2007, with those ones obtained by the model.

The results obtained were satisfying both in terms of simulated groundwater heads and water budget volumes: the average error in the simulated groundwater head was again about of 1 meter, and 90% of the study area was characterized by an error less than 3.50 meters. In addition the draining and dispersive river trunks were adequately simulated by the model (Figure 72). Consequently differences between the isophreatic contour lines obtained by modelling rivers with SFR package or as dispersive/draining trunks were negligible.

The steady state solution obtained was then employed as a reliable initial condition for transitory state simulations. Transitory state simulations were conducted by maintaining unchanged the water budget terms previously calculated, except the stream leakage because rivers were modelled with SFR package rather than as dispersive/draining trunks. The goal was to evaluate if there were differences in the new simulated temporal trend of stream leakage, and if this output had affected the phreatic surfaces and the resurgence outflows.

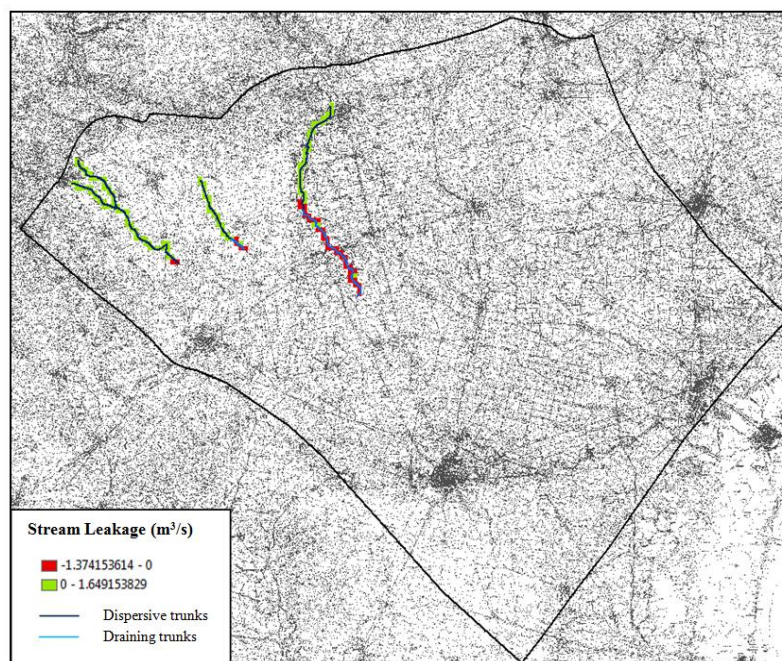


Figure 72 – Comparison between the dispersive/draining trunks of the rivers, well known in literature, and those ones obtained by the simulations carried out

Although a few information were available about the water withdrawal/restitution from/to rivers, the model was able to reproduce quite correctly the temporal trends of the various source/sink terms (Figure 73) and observed groundwater heads. In particular, also in this case, the maximum, minimum and average value of the absolute deviations, estimated comparing the temporal trends of simulated and observed groundwater heads, were calculated for each gage. Again observation sites characterized by an average value less than 5 meters were assumed well simulated. Forty-two out of fifty sites satisfied this condition.

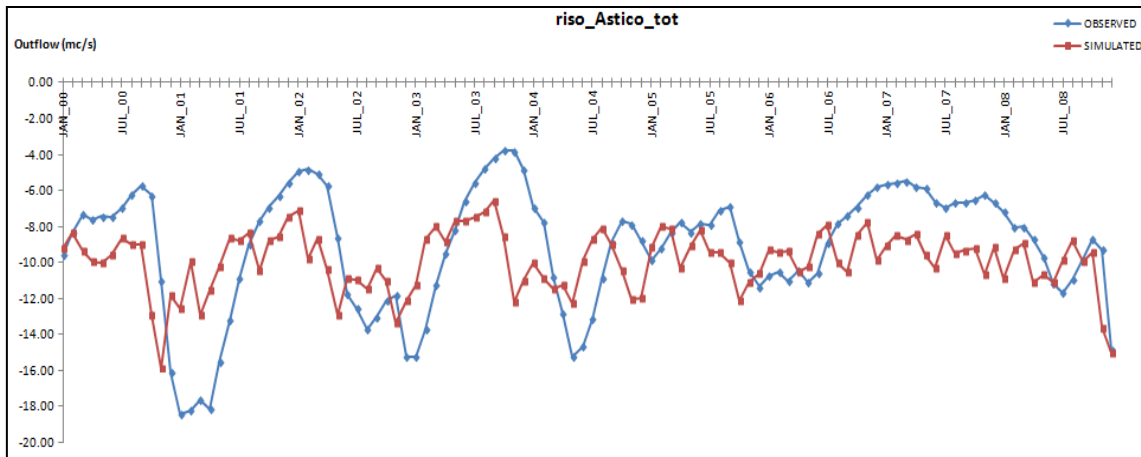


Figure 73 – Comparison between the simulated and calculated outflows for some resurgence areas

Therefore, on the basis of the results obtained, it is possible to state that the hydrogeological model developed can be effectively used as a reliable tool for simulating the whole hydrological cycle for the study area under observation, and also to evaluate the effects on the aquifers of MAR technologies, such as the Forested Infiltration Area (F.I.A.) in Schiavon, that were established inside the Brenta basin. In fact the availability of this tool permits:

- to forecast the effects of the recharge in terms of potential infiltrated water volumes;
- to quantify the portion of the territory affected by these processes;
- to manage the recharge process itself, by taking into account also parameters as the seasonality of operation of MAR strategies, etc.

In detail transitory state simulations were performed by assuming as *ante operam* scenario the results obtained by the model considering the water budget terms relative to 2007. As already reported earlier, this choice was performed since such water budget terms represent the historical data set nearest to the average conditions for the study area.

The *ante operam* scenario was then compared with two *post operam* scenarios:

- the first one considered operative only the Schiavon F.I.A., thus the average infiltrated flow, resulted from the experimental activities (18.50 l/s for hectare), was added to the other already implemented water budget terms. The F.I.A. was assumed working from October to April (212 days for year), in order to take also into account its seasonality, and during this period a constant recharge flow was set since the plant is able to guarantee a steady inflow.
- the second one considered operative the Schiavon site and other four existing F.I.A.s located inside the Brenta megafan: Tezze sul Brenta, Schiavon 2, Carmignano, Pozzoleone (Figure 74).



Figure 74 – F.I.A.s considered in the second *post operam* scenario

The average infiltrated flows for the new F.I.A.s were estimated on the basis of the average infiltrated flow, evaluated experimentally in Schiavon and equal to 18.50 l/s for a plant of one hectare, and the surface of the other plants. Again the recharge flow was retained constant inside the period comprised between October and April (212 days for a year), so that the seasonal working of the F.I.A.s was also simulated (Figure 75).

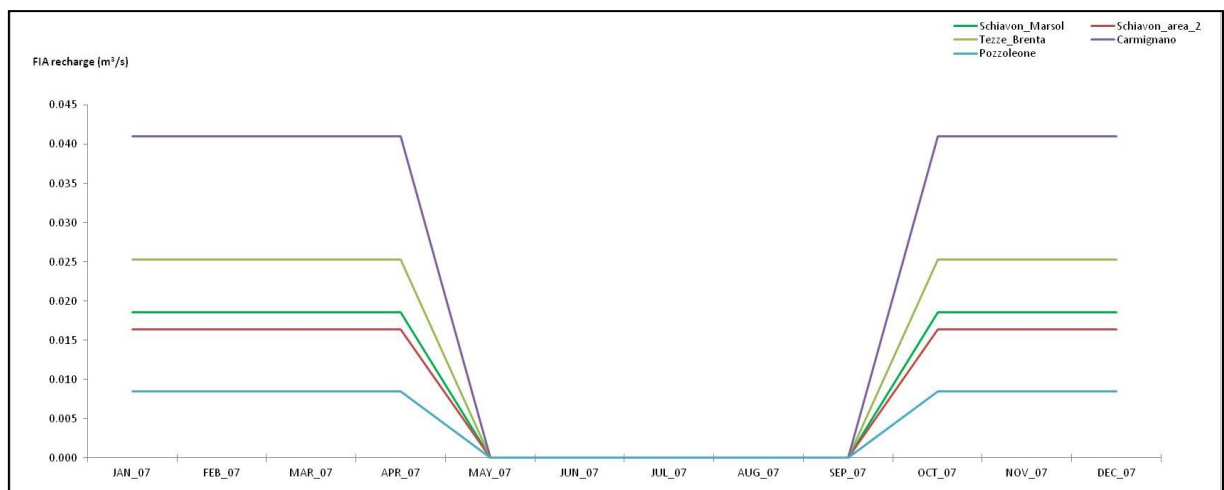


Figure 75– F.I.A. recharge flows assumed in the second *post operam* scenario

In detail the model was not calibrated by comparing the simulated and observed groundwater heads since this area is characterized by marked natural fluctuations of the water table (Figure 76), thus the mounding effect of the recharge, induced by the F.I.A. system operation, couldn't be adequately evaluable.

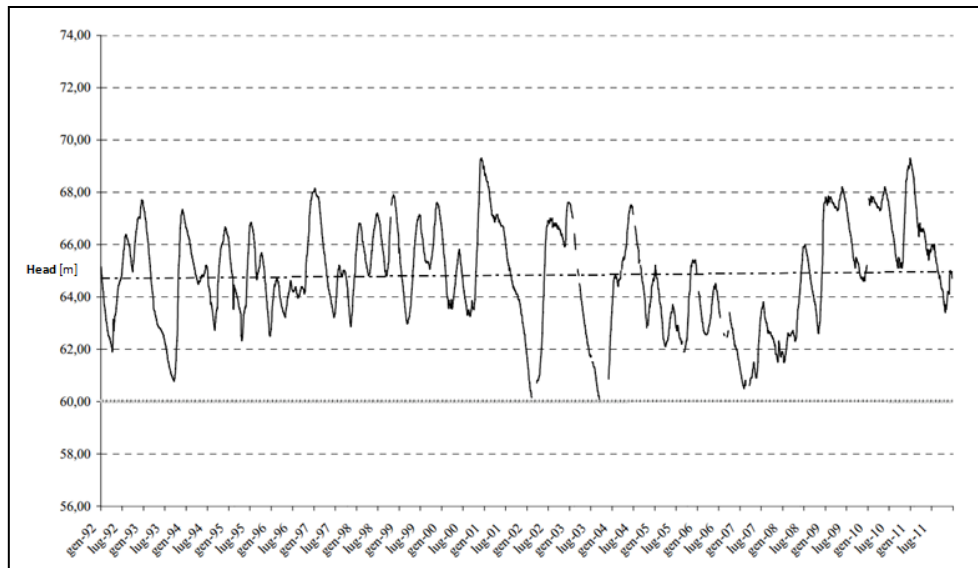


Figure 76– Water table levels recorded in the Schiavon station from January 1992 to July 2011

However a fictitious monitoring station was considered, placed inside the area that could be potentially affected by the F.I.A.s' operation (Figure 74), in order to compare the temporal trends of groundwater levels, resulted from the various simulated scenarios.

Some meaningful results were obtained from the elaborations carried out:

1. the potential infiltrated water volumes were about 348'019 m³ for a year in the first *post operam* scenario, and 1'996'531 m³ in the second *post operam* scenario.
2. the F.I.A. recharge determined an average water table mound comprised between 0 and 0.013 m for the first *post operam* scenario, and between 0 and 0.10 m for the second *post operam* scenario, as it is possible to state from the following picture, showing also the portion of the domain area affected by these processes (Figure 77).

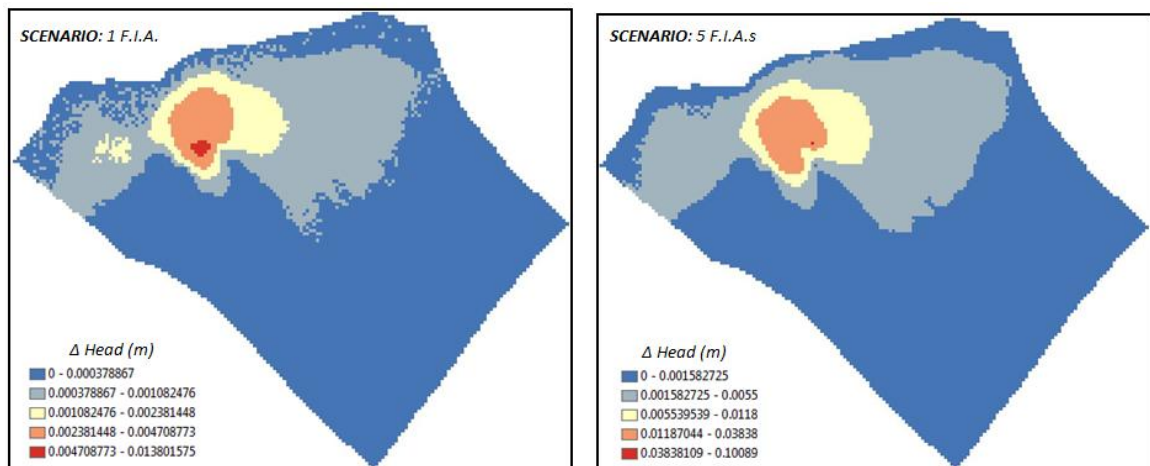


Figure 77– Average water table rise induced by the F.I.A. systems in the two simulated post operam scenarios

Therefore the assumption of ignoring the existing monitoring stations for calibration purposes was justified, since the mounding effect of the recharge induced by the F.I.A. system operation would have been certainly masked by the natural water table fluctuation of the local unconfined aquifer. The long-term record shows in fact a mean seasonal fluctuation approximately of 2 m with peaks of 5 m (Figure 76), which is by far higher than the mounding effect of the F.I.A. system operation.

In addition, by observing the temporal trend of the water table rise simulated in the fictitious monitoring station, it was evident how the F.I.A.s' seasonality influences strongly the mounding effect (Figure 78). In fact during the irrigation season the ground water levels tend to reach again the original values characterizing the *ante operam* scenario.

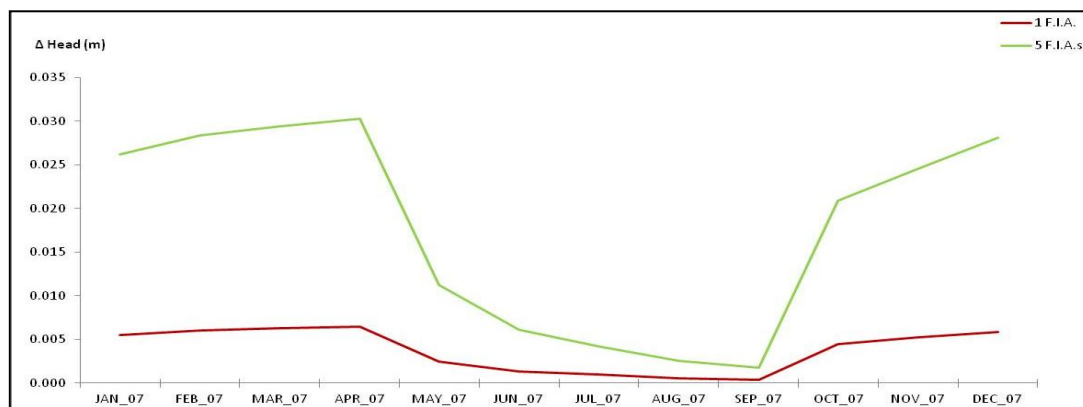


Figure 78– Simulated temporal trend of the water table rise induced by the F.I.A. systems in the fictitious monitoring station for the two post operam scenarios.

3. the increase of ground water levels determined effects on different water budget terms:

- smaller stream dispersion volumes, i.e. the water volumes supplied by rivers to the aquifers in the mountain trunks, because the difference between the river stage and the groundwater head was reduced;
- greater stream drainage volumes, i.e. the water volumes supplied by aquifers to rivers in the valley trunks, because the difference between the groundwater head and the river stage was augmented;
- greater resurgence outflows, because the difference between the groundwater head and the ground level was augmented.

Therefore, on the basis of the results achieved by the experimental and modeling activities carried out, it is possible to ascertain that similar MAR strategies could be considered valuable options to replenish the unconfined aquifer of the Brenta megafan, recently affected by a significant and generalized drop in groundwater heads due to heavy exploitation, massive land-use change and climate change. If these technologies were extended over a total area of 100 ha, the consequent potential annual recharge would be about 30 million m³ for a year, i.e. near to the total capacity of the Corlo reservoir that represents presently one of the main water resources inside this area. In addition such a recharge determines effects on different

water budget terms: smaller stream dispersion volumes, greater stream drainage volumes and above all greater resurgence outflows.

11.4 WATER QUALITY MODEL

The second *post operam* scenario was also used to evaluate the effects of recharge in term of improved groundwater quality: Nitrates concentration was considered. Nitrates indeed, are the parameter/pollutant examined, since they are the most widespread groundwater contaminants in study area due to the diffuse impact from extensive agriculture. Transport model selected is MT3DMS (USGS): a modular 3-D Multi-Species Transport Model for Simulation of Advection, Dispersion, and Chemical Reactions of Contaminants in Groundwater Systems. MT3DMS was set-up to simulate changes in concentrations of miscible contaminant in groundwater considering advection, dispersion and external sources or sinks packages.

The scenario considered operative the Schiavon demo site and other four existing F.I.A.s located inside the Brenta megafan: Tezze sul Brenta, Schiavon 2, Carmignano, Pozzoleone (second scenario *post operam*, see previous paragraph). The Nitrates concentration of average infiltrated flows for the new F.I.A.s were estimated on the basis of the average concentration of Nitrates measured on Roggia Comuna which feeds the F.I.A. Schiavon Demo site: 4 mg/l. The Nitrates concentration from dispersion of river and irrigation channel are assumed equal to 5-15 mg/l. The average Nitrates concentration of groundwater was assumed conservatively 20-25 mg/l with reference to historical groundwater quality data provided by ARPAV in study area.

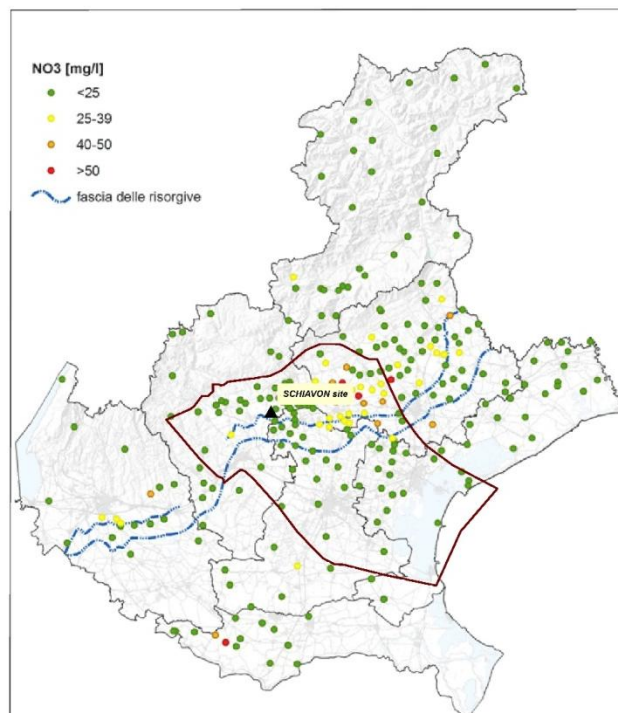


Figure 79 – Average Nitrates concentration in Veneto Region and in study area – ARPAV 2015

Figure below shows results of hydrogeological model in term of average Nitrates concentration simulated during the year 2007: orange-yellow color represents average concentration in aquifer model equal to about 20-25 mg/l, blue color shows concentration from dispersion of river equal to about 4-10 mg/l and green color the average concentration values from dispersion of irrigation channel namely ~10 mg/l.

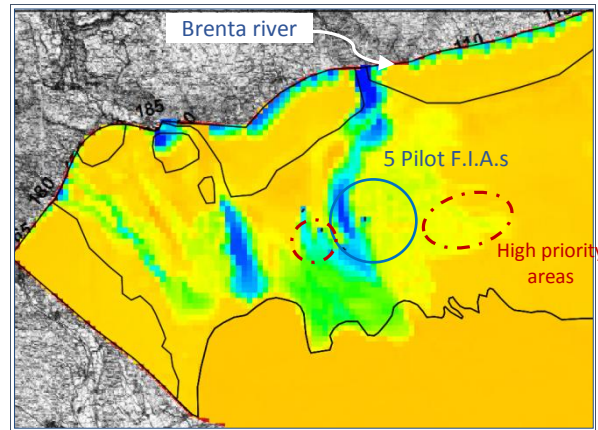


Figure 80– Average Nitrates concentration in study area resulting from modelling activity – year 2007

In Veneto Region the suitable area to realize enlarged MAR are already identified by the land reclamation Consortium within the LIFE Trust Project (EU). Figure below shows the red area in different GWB suitable to realize MAR, for instance in the GWB of Alta Pianura del Brenta the Consorzio di Bonifica of Brenta identified 100 ha of suitable area (blue circle in the figure below).

The purpose of modelling activity is therefore to support the realization of these MAR and in particular the F.I.A.s trying to identify the areas with “high priority” namely the suitable area where Nitrates concentrations seems more critical (area highlighted in red in Figure 80).

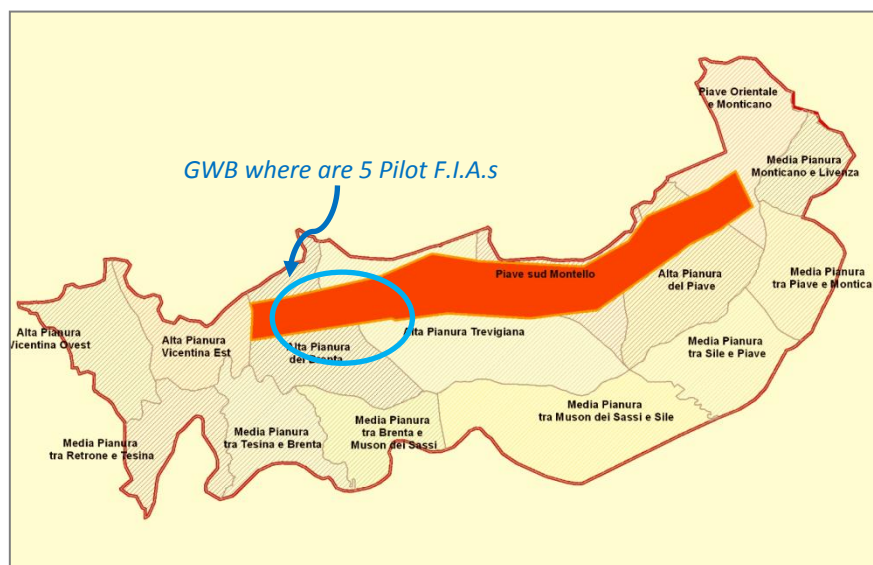


Figure 81 – GroundWater bodies in the high venetian plain (in red the potential area for MAR)

12 CONCLUSION OF MAR THROUGH FORESTED INFILTRATION IN THE RIVER BRENTA CATCHMENT, VICENZA, ITALY

The MOSAIC approach, i.e. the combination of surface geophysics and minimum invasive Direct Push technology was successfully applied for the efficient characterization of the Schiavon FIS with complex sedimentary architecture as the Loria infiltration basin as an example for large scale MAR infrastructure. The applied techniques are already available on the market today and often advantageous over traditional site investigation approaches in terms of resolution and efficiency. However, their uptake is yet beyond their capabilities.

The site characterization results clearly show that the locations of infiltration infrastructure need to be carefully chosen based on (hydro-) geological as well as hydrological aspects (e.g. sediment loads) to allow environmental and economically sound system operation. The basis therefore, is a reliable and financially feasible site characterization approach.

On the basis of the results achieved by the experimental and modeling activities carried out, it is possible to ascertain that similar MAR strategies could be considered valuable options to replenish the unconfined aquifer of the Brenta megafan, recently affected by a significant and generalized drop in groundwater heads due to heavy exploitation, massive land-use change and climate change.

Modelling activity implemented can be used as decision support to realize large scale F.I.A.s in Veneto upper Region.

The outcome of the financial analysis carried out is that the large scale MAR project shall cover an area of 75 ha and the average increase in tariffs of 1.5% applied to the municipal users will ensure the financial sustainability of the project. The size of the MAR facility in this case will comply with the minimum target of 20 MCM/y.

Finally, in addition to economic benefits for owners, F.I.A. area and consequently MAR technologies could play many positive roles for the community:

- recharging of groundwater and regeneration of springs (as demonstrated by monitoring and modelling activities);
- production of renewable energy (e.g. wood to biomass);
- reduction of greenhouse gas emissions;
- enhancement of the landscape;
- increase in biodiversity.

White book on MAR modelling

Deliverable D12.7

CHAPTER 5 – THE EFFICIENCY OF MAR IN AN IRRIGATION AREA WITH A LARGE DEVELOPMENT OF AGROINDUSTRY: THE EXEMPLE OF MARSOL DEMO SITE 3 LOS ARENALES AQUIFER, CASTILLE AND LEON, SPAIN

ENRIQUE FERNÁNDEZ ESCALANTE, RODRIGO CALERO GIL (TRAGSA), FRANCISCO DE BORJA GONZÁLEZ
HERRARTE (TRAGSA), MARÍA VILLANUEVA LAGO (TRAGSA), JON SAN SEBASTIÁN SAUTO (TRAGSATEC)

13 MODELLING OF DEMO SITE 3 LOS ARENALES AQUIFER, CASTILLE AND LEON, SPAIN

13.1 INTRODUCTION

The WP activities involve the three areas integrated into the Demo Site 4 “Los Arenales aquifer, Castilla y León, Spain”. These zones with important MAR facilities deployed are Santiuste basin, Carracillo district and Alcazarén Area, represented in the Figure 3.

Within the framework of MARSOL project, the modeling activity for this demo site has a complex background what deserves to be introduced and explained. The partner in charge, Tragsa, has conducted two models in Visual Modflow for Santiuste and Carracillo areas, by direct request of the Spanish Ministry of Agriculture. These models are active and new simulations might be performed. The biggest constraint is the property of the datasets and the

results, which are in the hands of the client. Consequently, neither the models nor the files can be shared between partners.

The third area, Alcazarén, is a new one and activities have begun in 2012, after some years of litigations in the court due to the fact that there was a transfer between two different provinces and both claimed the property of water. The model is in a very initial stage, with the conceptualization and definition of boundary conditions phases already done. Now the main activity is related to the capture of datasets, in order to advance in the development of the modeling endeavor.

Apart from the description of the areas, the geo-referenced files with all the operative facilities for three sites were provided in deliverable 12-2. They are in a compatible format to be included in any GIS program and available for potential users.

This chapter exposes, firstly, the works done by Tragsa Group regarding modeling for external clients and the advance in the knowledge of the aquifer thanks to the use of this tool.

Later, regarding the activity related to MARSOL, the models have been used to achieve some specific results and to provide guidance for very concrete actions and presentation of alternatives: in specific areas, such as zonal balances (Zbud) for defined sections in the aquifer of Santiuste (at both sides of the hydrogeological barrier); the behavior around MARSOL “piezostar” in Carracillo (see deliverable 5-1 for a detailed description of the environmental conditions and the groundwater behavior).

In the case of Alcazarén, the assignment is not enough to finish the ongoing model (currently stopped due to economical reasons) and only specific actions will be performed, driving to the future exploitation of results.

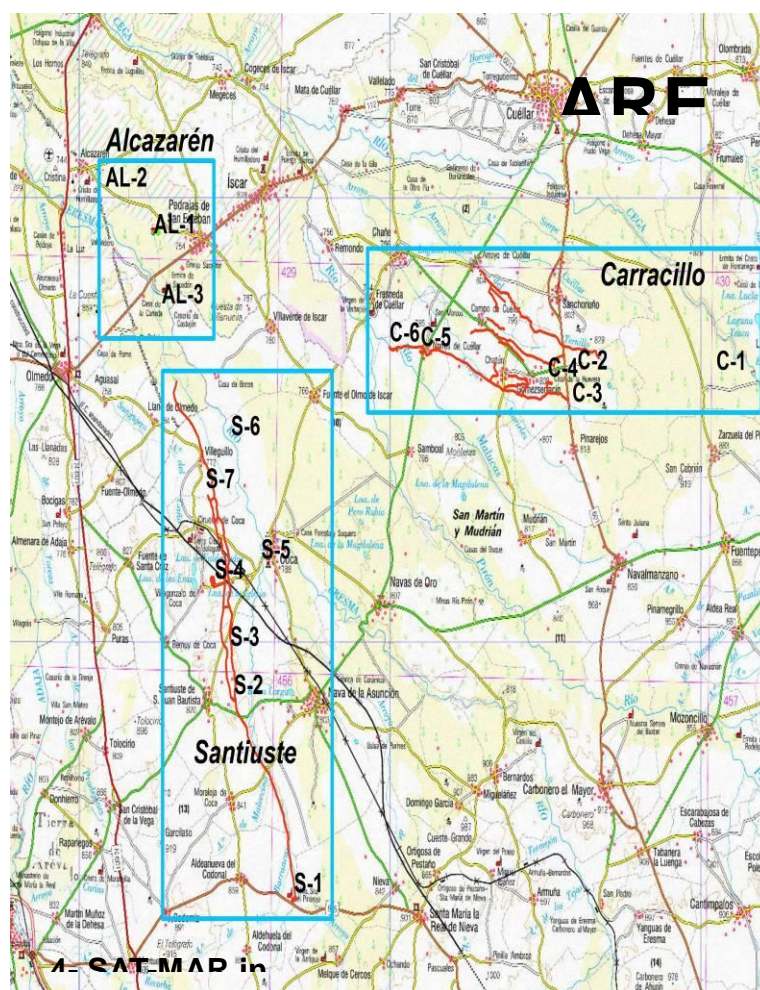


Figure 82 – Map of Arenales aquifer area and the zones with an advance deployment of MAR facilities.

13.2 MODELLING BACKGROUND IN LOS ARENALES AQUIFER

The models available nowadays for Arenales are those presented hereinafter.

13.2.1 Santiuste Basin

This area houses the pioneer facilities in Los Arenales aquifer and It has been the laboratory area for DINA-MAR project², and now the biggest demo-site for MARSOL (Lobo-Ferreira *et al.*, 2014).

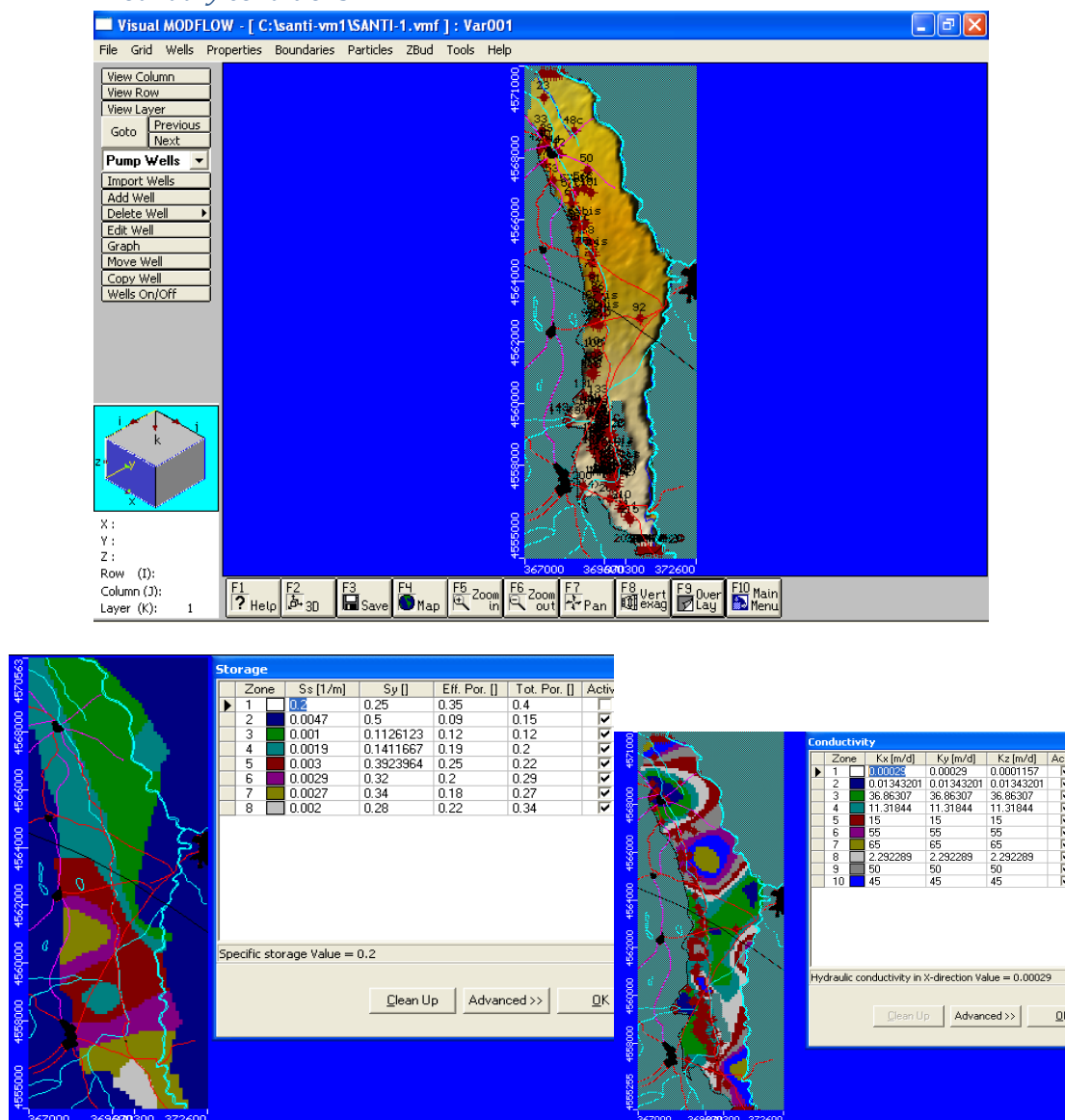
The Santiuste basin is a small aquifer of 85 km², which is limited by the Voltoya and Eresma rivers to the East, and low permeability Tertiary outcrops to the West. Despite its reduced size, it is considered an important irrigation area depending on groundwater resources. The managed recharge facility was performed making use of a small stream watercourse called Arroyo de la Ermita, that gets partially interrupted by cultivated fields and where important

² See <http://www.dina-mar.es/>

ground works have been performed during the drought periods happened in Spain during the last 30 years. These actions have almost made it completely disappear (Galán *et al.*, 2001).

The aquifer characterization rarely changes from the initial definition of the area. Due to the fact that the canal is increasing permanently with new branches and bypasses, the model requires a re-definition of the recharge cells almost every year.

13.2.1.1 Boundary conditions



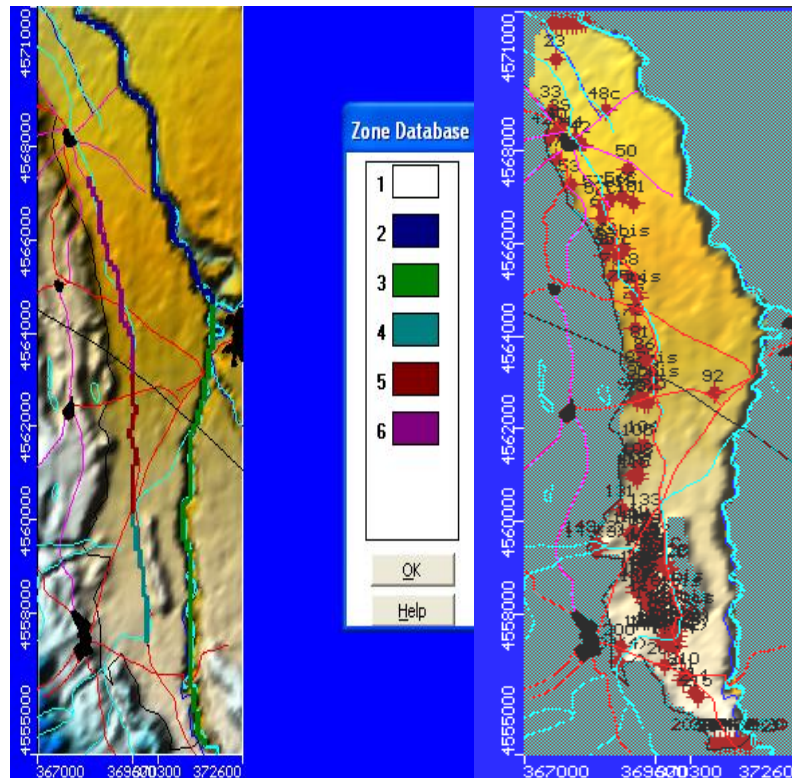
Figures 83 – Scheme for Santiuste basin charting the boundary conditions taken into account for modeling (a), the storage capacity (b) and the hydraulic conductivity distribution (c)

13.2.1.2 River-aquifer relations and extractions

Both parameters are important to be considered in MAR activities. The Voltoya and Eresma rivers, depending on the water table fluctuation, might be over or below the groundwater

level, because the oscillation surface is important most of the MAR cycles. That is why MAR activities have a direct influence in the aquifer behaviour and on its real storage.

Both parameters must be monitored in order to avoid possible floods and other potential impacts on the agriculture and on the existing facilities.



Figures 84 – Scheme for the river-aquifer relations, distinguishing five different sections (a) and the representation of the wells used for irrigation (b)

The studies for water storage evolution during MAR activities and the different scenarios to be tested are also important so as to study the sustainability of the system.

13.2.2 Carracillo District

The second set of facilities for Managed Aquifer Recharge in Los Arenales aquifer is found at Carracillo County, a relevant area where most of the recharge is accomplished by infiltration channels.

The area is placed about 40 km eastwards the aforementioned Santiuste. The MAR site covers about 150 km² at the interfluvies of Cega and Pirón Rivers. Irrigation has been extensively practised in this area with over 3,300 ha groundwater-fed cultures. Managed Aquifer Recharge by means of unlined irrigation ditches has also been practised for quite a long time, even though the largest devices started working in the winter of 2006/07, infiltrating 8 hm³ into the aquifer. Subsequently volume was increased up to 12 hm³ in the 2009/10 cycle. The MAR system is composed of 40.7 km of MAR channels, 3 infiltration ponds, an RBF system and two artificial wetlands (Lobo et al., 2014).

While Santiuste basin is a restricted basin, Carracillo presents an open surface limited by riverbeds in one side, and political boundaries in the other one.

One of the biggest decisions made by means of modeling (no exclusively) was the design of the irrigation network attending to the groundwater availability and its evolution. When the Carracillo irrigation network was deployed, there were four different designs to choose one; and the election of the best was justified, mainly, by their cost criteria, and secondly by water disposal. Finally the solution adopted and applied was the one called “4th *direct pumping from boreholes plus infiltration ponds and a double irrigation network*” (Figure 85).

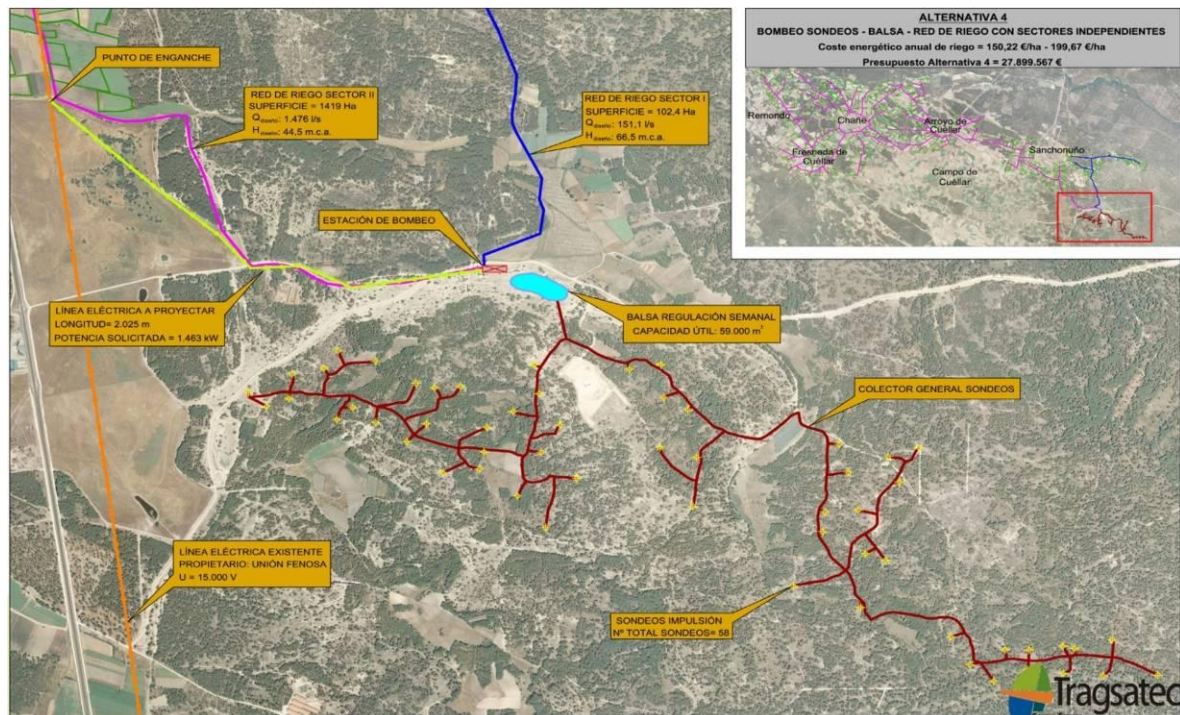


Figure 85 – 4th alternative scheme. Direct pumping from boreholes plus infiltration ponds and a double irrigation network

13.2.2.1 Aquifer characterization. Boundary and environmental conditions

Once the boundary conditions have been defined for a vast aquifer not delimited by physical barrier in some borders, it is important to pay attention on the main parameters which really experiment tangible variations along MAR activity, such as:

13.2.2.2 River-aquifer relations

In this case, the groundwater table and the flowing water in the river have, more or less; a similar height and any change modify the river-aquifer relations with alacrity. **Figure 86** displays an example for a zone where two rivers cross the permeable layer, with significant seasonal variations induced also by MAR activity.

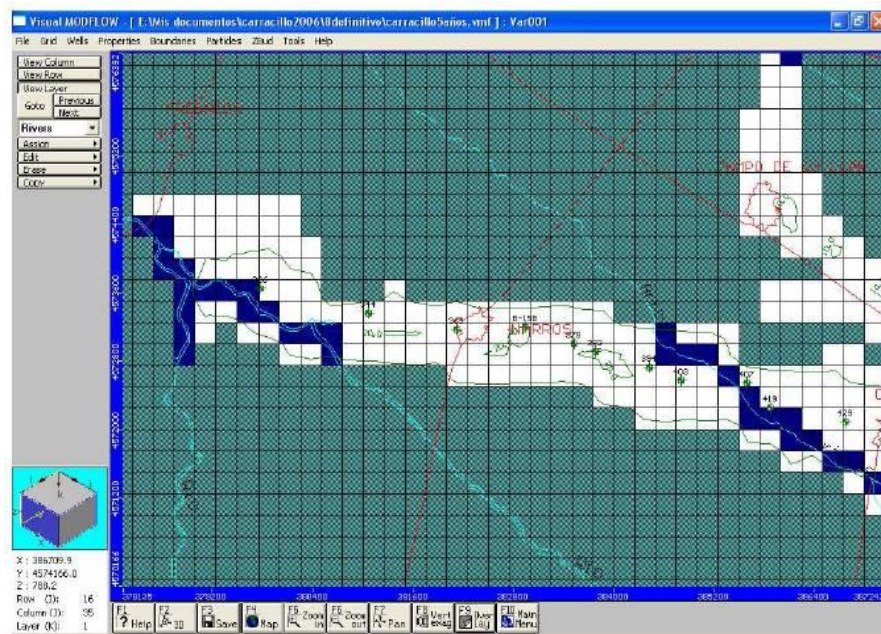


Figure 86 – Changes in river-aquifer relations due to seasonal period and MAR activities

13.2.2.3 Extractions

It is another very variable parameter what that causes important variations and huge oscillations in this sort of sandy aquifers. It is important to update the inventory of active water points regularly (Figure 87).

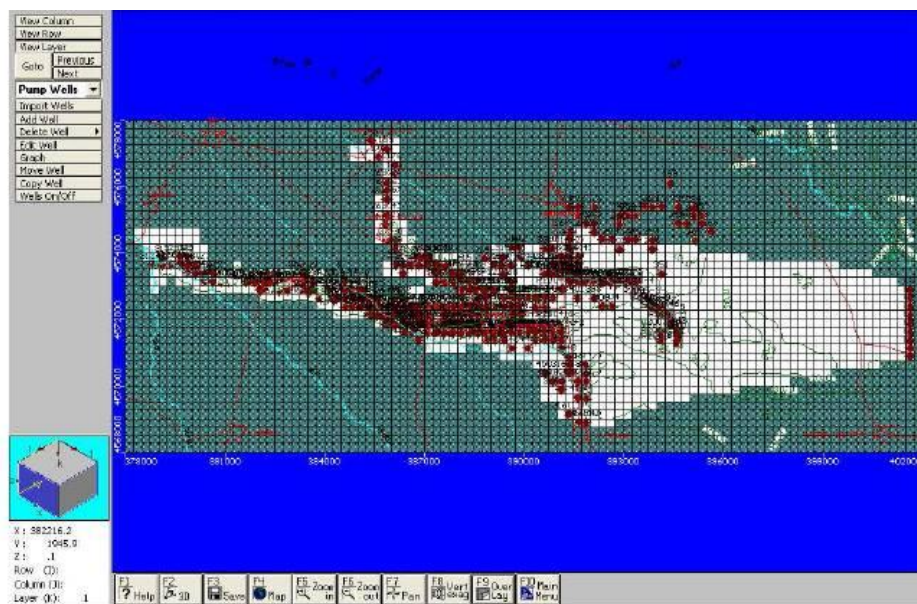


Figure 87 – Inventory of water points and extractions simulation in Carracillo Council

13.2.2.4 Natural recharge simulation

It is useful to have both components, natural and artificial recharge, combined in the water balances. Then, modeling has also been employed to dissociate both components with different scenarios and for separated zones (Figure 88).

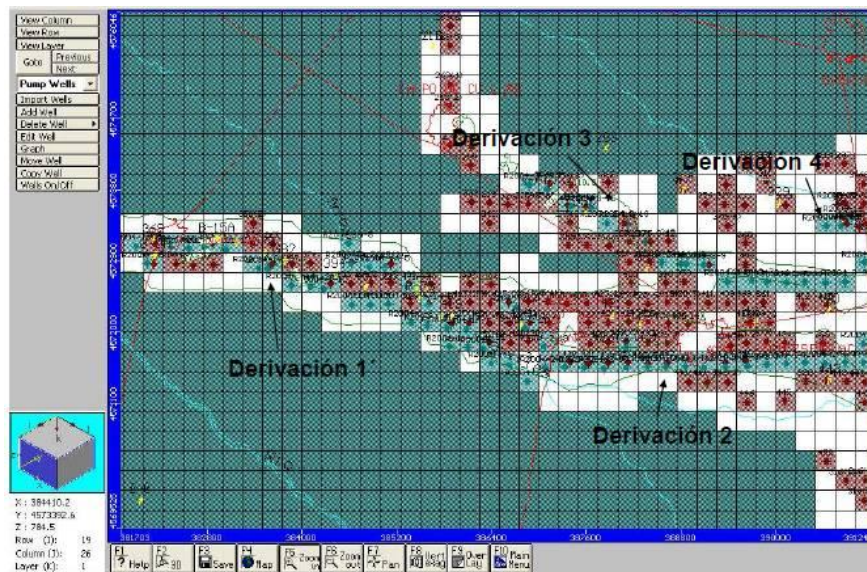
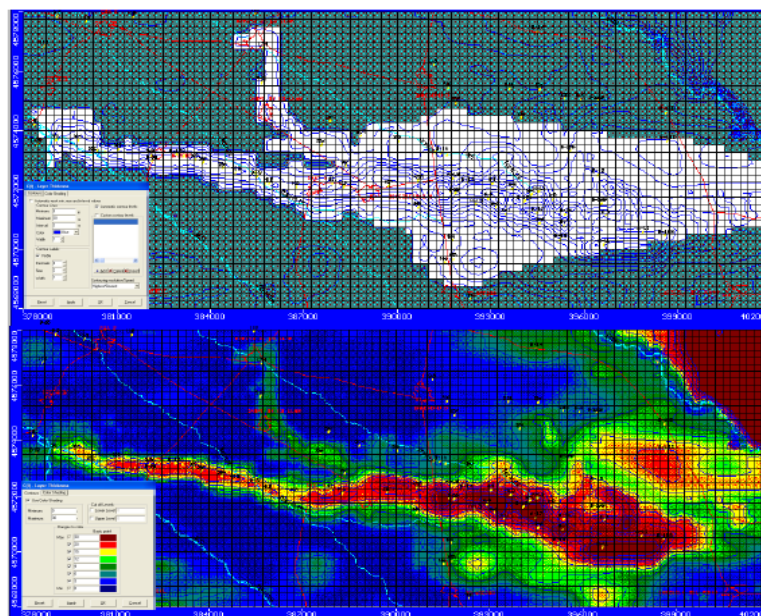


Figure 88 – Modflow screen shot used to dissociate natural and artificial recharge components

13.2.2.5 Calibration:

During the calibration process, there may attend many different components with a high variability during MAR activities. Some of the most remarkable are boundary condition changes, changes in the receiving medium geometry and even changes in some hydrogeological parameters, often motivated by the silting or clogging processes.

Some changes experimented in groundwater storage during the calibration process (**Figure 89 a & b**).



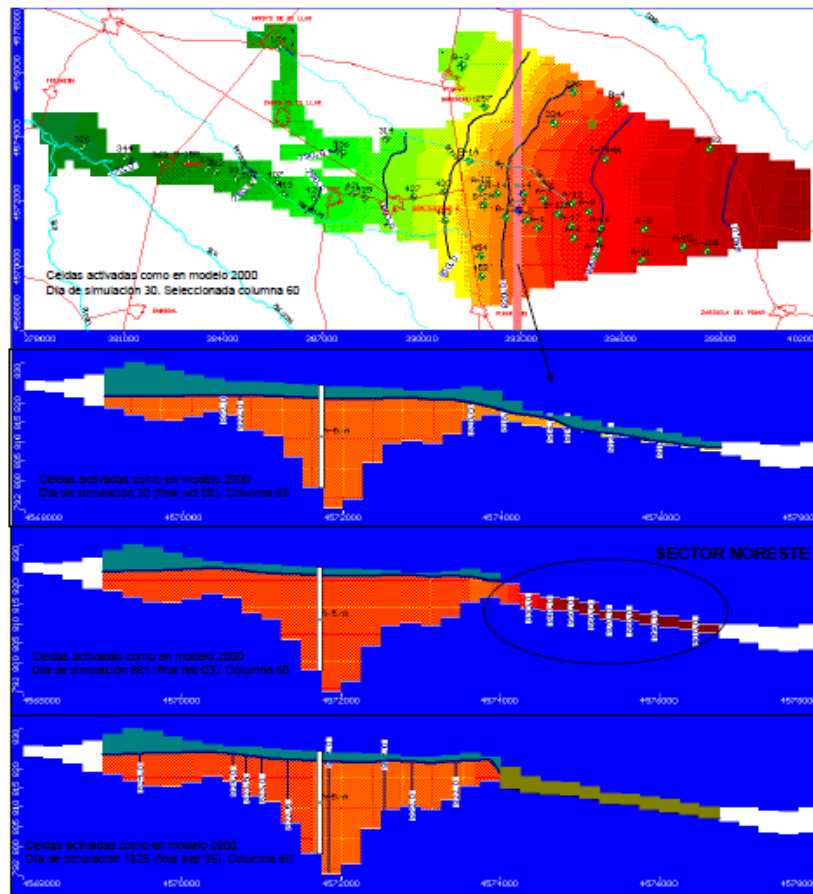


Figure 89 a) & b). Changes in water storage with different calibration premises causing divergent results

According to the different phases exposed for a model and the substantial exchanges in some parameters what happen due to MAR activity, we might conclude in a series of factors to be taken into account for alternatives design and decision making:

- Water table fluctuation control
- Variations in the infiltration rate capacity
- Determination of infiltrated volumes
- Water chemical control
- Different facilities functioning and their efficiency

13.2.3 Alcazarén Area

Alcazarén area is a SAT-MAR example recently constructed and integrated into MARSOL objectives. It is the newest demo site for irrigation purpose in Los Arenales Aquifer Area. It essentially consists in a river catchment (River Bank Filtration) with a long transport pipe and a WWTP additional supply (SAT).

Within the Duero river basin, the project is geologically located on a big tectonic basin filled with Tertiary material from Aeolian and evaporitic origin. A long mountainous range system

encircles and isolates the whole zone with combined facilities for MAR (Figure 90). Total extension of the considered aquifer is 55 km², 23 km long by approximately 2.5 km wide.

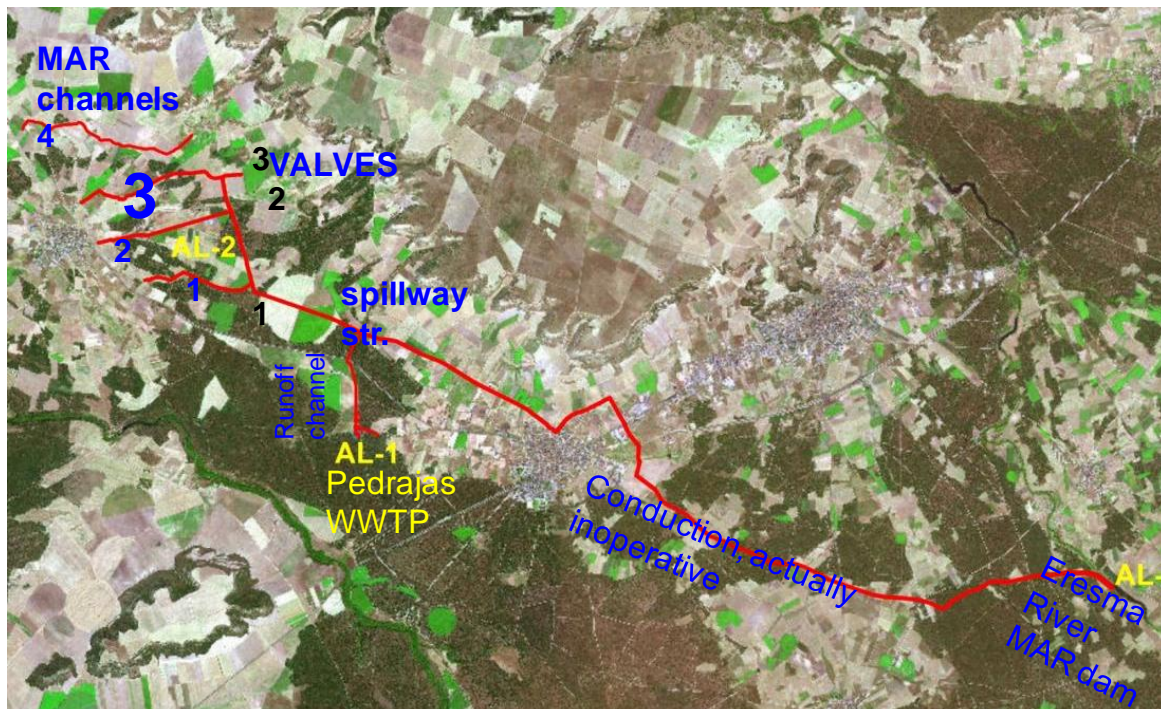


Figure 90 – Alcazarén area and the existing MAR facilities on it on orthophoto

Alcazarén has not an operative model yet, but there are two important criteria used in the design of their MAR facilities:

- 1- Canals crossing the sequence of parallel faults
- 2- The importance of specific piezometers to control water table evolution.

13.3 MODELLING ACTIVITIES

The main advantage of having some previous models is the easiness to re-define new boundary conditions to be set in local scale models, in order to improve simulation accuracy in monitored sites of interest. The targets and objectives to be solved during MARSOL development are very concrete and focussed in local necessities.

13.3.1 Santiuste Basin

13.3.1.1 New MAR channel path

In Santiuste basin, the model has been used to consult the best new branches to be dug in the canals so as to increase the infiltrated volume as much as possible (Figure 91).

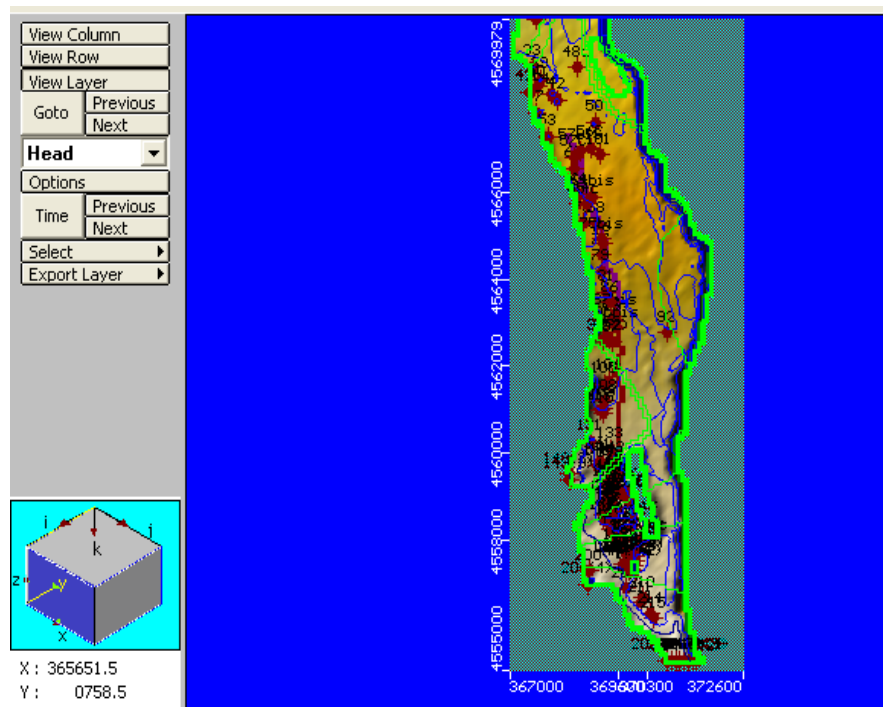


Figure 91 – Santiuste basin. Initial MAR canal path and relevant features

13.3.1.2 New monitoring Network design

The model is mainly used as a tool for DSS in the consecutive enlargements of MAR facilities, upgrades in the design for the groundwater table monitoring network (Figure 92).



Figure 92 – Santiuste basin scheme and groundwater monitoring network

13.3.1.3 Water budget in the different zones to manage MAR facilities

In the next stages, the water balance in the North and in the Southern part of the aquifer (there is a hydrogeological threshold E-W direction in the middle of the basin). The storage capacity is variable in each MAR cycle in the different areas, and, to find out what gates and stopping devices should be opened or damming water in specific paths of the canals is an important decision to be made.

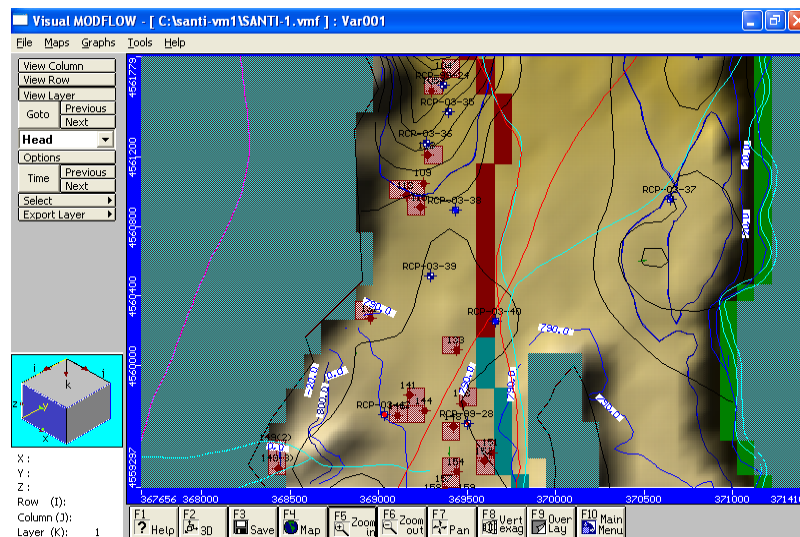


Figure 93 – Example for zonal water budgets for Santiuste basin

13.3.2 Carracillo District

The new facility designed and tested in MARSOL project to improve water quality and to remove dissolved oxygen from MAR water has been called a triplet. It is a sequence of an infiltration pond, an infiltration canal covered with natural vegetation (to improve initial water quality by simple nutrients and oxygen consumption) and finally an artificial wetland, to finish the process (Figures 94).

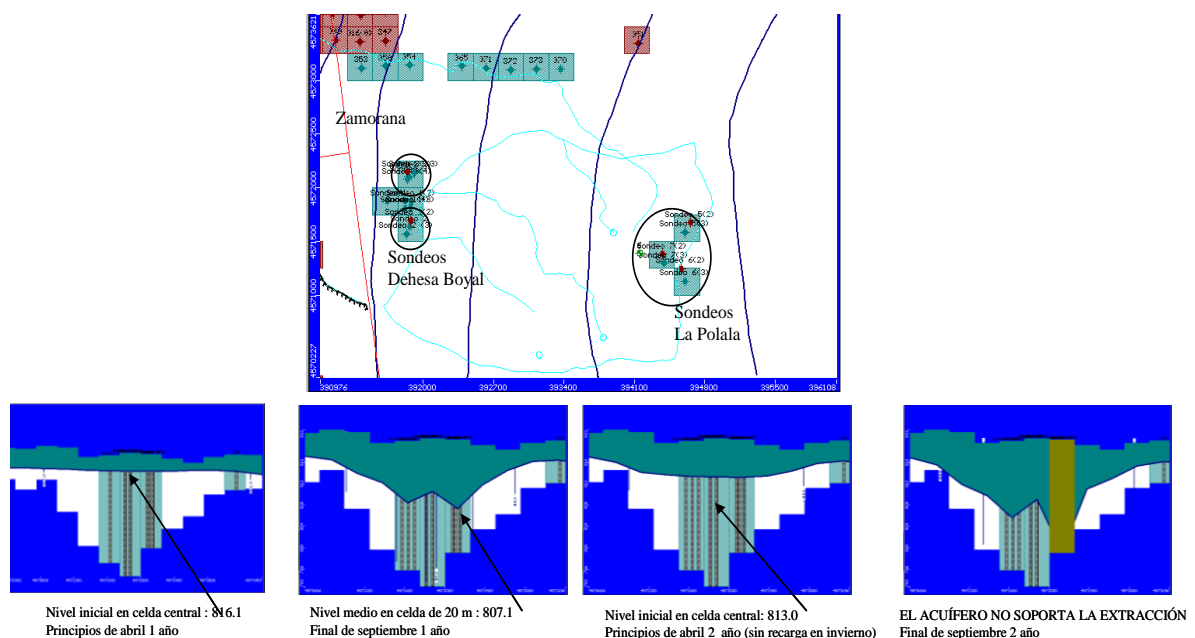
This specific test site is in a corner of the aquifer (Dehesa Boyal).



Figures 94 – Triplet scheme deployed in Carracillo council composed by an infiltration pond, a canal and an artificial wetland. Natural vegetation is preserved and used to improve the water quality prior MAR water is spread in the flat area behind the artificial wetland

13.3.2.1 Modelling the new “triplet” scheme (stagnation pond-biofilter-artificial wetland)

This system allows checking MAR water quality evolution and storage changes, opening an interesting line of action about the fitness of the technique and its use as an asset.



Figures 95 (a) (b) Initial results based on modelling in the Dehesa Boyal area (right), where the triplet scheme is being tested, to assess its convenience (a). A profile showing the expected groundwater evolution (b)

13.3.3 Alcazarén Area

In order to achieve an initial 3D model, the next steps have been accomplished:

- Generation of geographic coverages from the geophysical prospecting results and litological columns (**Figure 96**).
- Digitalization of geological profiles (*Hidrogeo Analist*)
- Geological interpolation between geophysical profiles.
- Geological surface for the basement, the water table and the surface shields (**Figures 97**).
- Initial stage for modelling (*Visual Modflow 3D builder*).

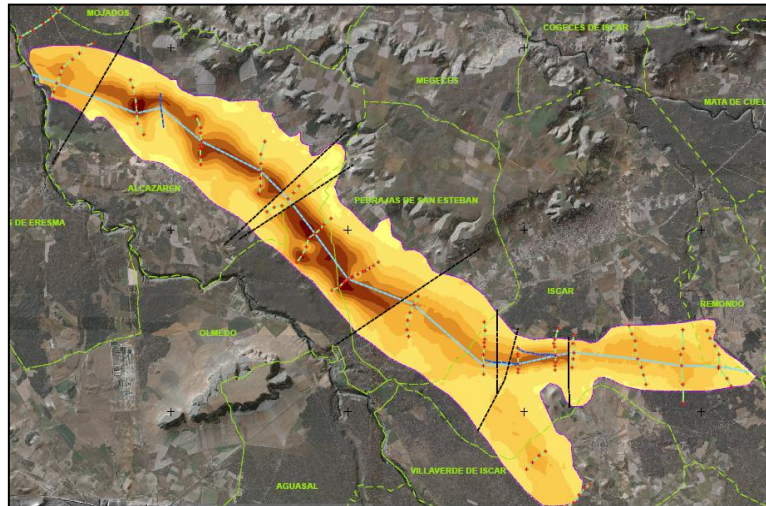
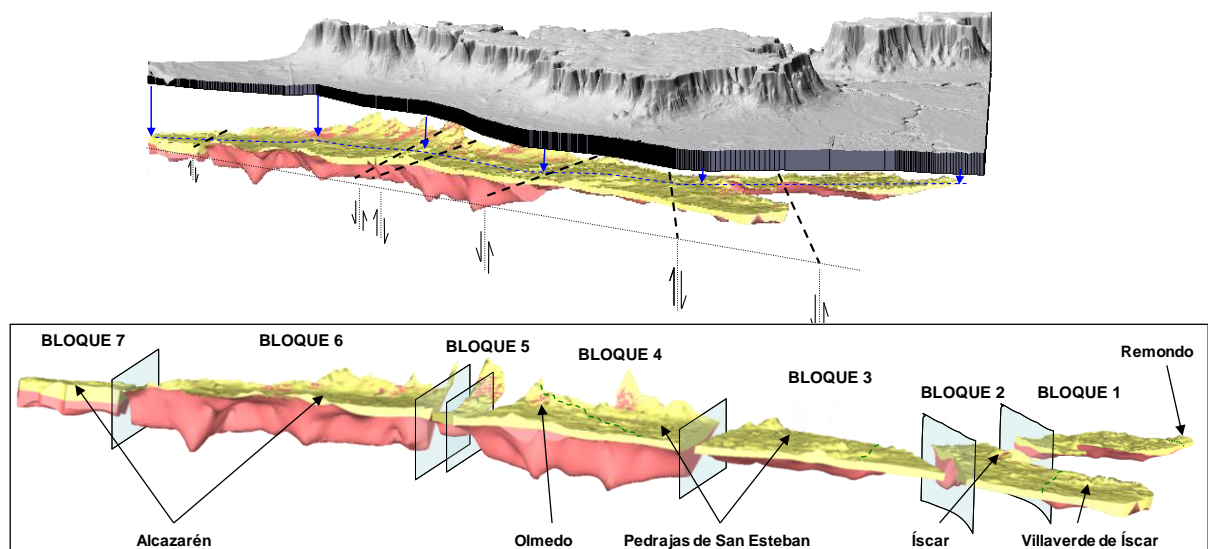


Figure 96 – Alcazarén aquifer scheme and main fault detected during geophysical prospecting phase



Figures 97. 3D Modelling for each structural subdivision in the conceptualization stage

At this initial stage, some results are being obtained, such as:

- Hydrogeological parameters
 - Aeolian sand: $K_h = 37 \text{ m/d}$ y $K_v = 3,7 \text{ m/d}$
 - *Fluvial sand*:: $K_h = 15 \text{ m/d}$ y $K_v = 1,5 \text{ m/d}$
 - *Tertiary materials*: $K_h = 0.02 \text{ m/d}$
 - *Mean storage coefficient*: (15 %)
- Mean effective porosity in the area
 - Aeolian sand: $\Phi_e = 18 - 20 \%$
 - *Fluvial sand*: $\Phi_e = 10 - 12 \%$
- Total storage capacity in the aquifer: 42 hm^3

13.4 CONCLUSIONS

At this stage, modelling is providing accurate assessment for DSS and technical solutions implementation. Some of the context where modelling is providing support are:

1. Solution based on integrated water management:
 - groundwater exploitation from boreholes/wells
 - direct pumping from ponds and streams/rivers
 - improvements in the irrigation network
2. Modelling tools to choose the best solution between several alternatives (DSS instrument)
3. Other solutions:
 - MAR facilities design, emplacement and instantiation
 - monitoring network design, selection of points to drill mar wells
4. The design and management parameters must be created “a la carte”
5. Special attention must be paid to hydrogeological thresholds in the area and clogging processes willing to modify hydrogeological characteristics.
6. Aquifer behaviour after MAR activities is not SO easily predictable due to the change of the environmental conditions caused by the activity.

REFERENCES

- FERNÁNDEZ ESCALANTE, E. (2005). Recarga artificial de acuíferos en cuencas fluviales. Aspectos cualitativos y medioambientales. Criterios técnicos derivados de la experiencia en la Cubeta de Santiuste (Segovia). Tesis Doctoral. Inscripción: septiembre de 2004. Defensa: enero de 2005. Universidad Complutense de Madrid. ISBN: 84-669-2800-6.
- GALÁN, R., LÓPEZ, F., MARTÍNEZ, J., MACÍAS, C., GALÁN, G. Y FDEZ. ESCALANTE, E. (2001a). "Recarga artificial del acuífero de los Arenales en la comarca de "El Carracillo" (Segovia). 1ª parte. Soporte físico." VII Simposio de hidrogeología, AEH, Murcia. Tomo XXIV.
- JUNTA DE CASTILLA Y LEÓN-TRAGSATEC (2011). Estudio hidrogeológico para la recarga artificial del acuífero pliocuaternario en los términos municipales de Alcazarén, Pedrajas de San Esteban, Íscar, Olmedo y Villaverde De Íscar. Unpublished internal document available to be consulted at JCyL library.
- LOBO FERREIRA, J.P., FERNÁNDEZ-ESCALANTE, E., SCHÜTH, C. and LEITÃO, T.E., 2014. Demonstrating Managed Aquifer Recharge (MAR) as a Solution for Water Scarcity and Drought in Portugal and Spain. 12º Congresso da Água /16.ºENASB/XVISILUBESA, organized by APRH, APESB e ABES, Lisbon, 5-8 de março de 2014, 15 pp.
- MACÍAS, C.; MARTÍNEZ, R & MARTÍNEZ, J. (2014). Determinación de volúmenes de agua a gestionar en las infraestructuras de la fase II del proyecto de recarga artificial del acuífero cuaternario de la comarca de El Carracillo, Segovia (sector occidental). Boletín Geológico y Minero, Vol. 125, nº 2, Apr-Jun. 2014. Pg. 173-186.
- MACÍAS, C.; MARTÍNEZ, R & MARTÍNEZ, J. (2014). Estudios preliminares para el diseño de una instalación de recarga artificial en la zona oriental del acuífero de El Carracillo, Segovia. Boletín Geológico y Minero, Vol. 125, nº 2, Apr-Jun. 2014. Pg. 187-202.
- MAPA. (2005). Asistencia técnica para el seguimiento y modelización de la recarga artificial en la cubeta de Santiuste de San Juan Bautista (Segovia). Dirección General de Desarrollo Rural-TRAGSATEC (not published).
- MIMAM. (2002). Estudio del sistema de utilización conjunta de los recursos hídricos superficiales y subterráneos de las cuencas del Cega-Pirón y del Adaja-Eresma. MIMAM-PROINTEC.

White book on MAR modelling

Deliverable D12.7

CHAPTER 6 – PHYSICAL MODEL EXPERIMENTS AT LNEC AND THEIR NUMERICAL MODELLING RESULTS

LEITÃO, T.E. (LNEC), MARTINS, T. (LNEC), HENRIQUES, M.J. (LNEC), ILIE, A.M.C. (UNIV. BOLOGNA/LNEC), LOBO FERREIRA, J. P. (LNEC)

14 INTRODUCTION TO MARSOL PHYSICAL MODELLING

In MARSOL project, Workpackage 12 deals with modelling MAR solution's implementation. To study the effectiveness of these solutions, Task 12.5 was conceived and developed using physical models - which represent the real case study sites in a small and controlled scale - to demonstrate the effectiveness of MAR, namely clogging issues and physic-chemical treatment of recharging water.

Besides, the physic-chemical treatment, the experiments were also numerically modelled with the same tools used to model the real cases, and in cooperation with Workpackage 14.

To develop Task 12.5, a new physical sandbox model was built in LNEC's modelling facilities (cf. <http://www.lnec.pt/en/research/research-infrastructures/fluvial-hydraulics-experimental-facility/>) under MARSOL project. The artificial aquifer facility (or physical sandbox model) can be used to conduct laboratory large scale infiltration and tracer tests, aiming to determine the soil infiltration rate and also the contaminants retention and/or degradation capacity, namely to simulate Soil-Aquifer Treatment (SAT) in a Managed Aquifer Recharge (MAR) basin.

The DEMO site PT3 – Melides aquifer, river and lagoon (Alentejo) was selected to model and demonstrate the use soil-aquifer-treatment (SAT-MAR) to remove rice paddy fields pollutants prior to their discharge in Melides lagoon. The results obtained in these tests have given the necessary knowledge to build, in the future, an *in situ* SAT-MAR facility.

15 PHYSICAL SANDBOX MODEL

15.1 POTENTIALITIES AND AIM

The artificial aquifer facility (or physical sandbox model) was built under MARSOL project and used to conduct laboratory large scale infiltration and tracer tests, both for saturated and non-saturated conditions. They allow determining the soil:

- infiltration rate, in full saturation conditions;
- contaminants retention and/or degradation capacity.

For MARSOL experiments, this facility was used to study Soil-Aquifer Treatment (SAT) simulating a Managed Aquifer Recharge (MAR) infiltration basin.

Additionally, this same facility can be used to simulate other situations such as:

- risk of contaminants leaching from a spill;
- reactive barriers for groundwater rehabilitation;
- contaminants release from a contaminated porous material.

15.2 SANDBOX CONSTRUCTION AND DESCRIPTION

The physical sandbox model was built during 2015/16 in LNEC hydraulics pavilion area (<http://www.lnec.pt/en/research/research-infrastructures/fluvial-hydraulics-experimental-facility/>). This facility is approx. 3.5 m long, 1 m wide and 2 m high (**Figure 98**) and can be filled with the porous medium (soil) to be studied, in this case the Melides sand.



Figure 98 – LNEC physical (sandbox) model construction

The area can be divided up to three different compartments to perform simultaneous experiments (**Figure 99**). The facility was equipped with three piezometers, Teflon cups to sample the vadose zone and monitoring devices such as multiparametric probes (water pressure, pH, temperature, electrical conductivity and redox) to monitor flow and transport, both in the saturated and vadose zones.



Figure 99 – LNEC physical (sandbox) model sections, A, B and C

15.3 EXPERIMENTAL SETUP

15.3.1 Sandbox set-up

Aiming to model and demonstrate the use soil-aquifer-treatment (SAT-MAR) basins as a tool to remove rice paddy fields pollutants, prior to their discharge in Melides lagoon, the sandbox model was used to perform three simultaneous experiments with Melides soil.

The sandbox model was divided into three sections (**Figure 100**) to test the adsorption and degradation capacity of the following different soil mixtures:

Section A – Melides soil in all the vertical profile;

Section B – 30 cm top layer of a mixture of Melides soil (60%) and organic matter (40%), followed by Melides soil in the remaining depth; and

Section C – two organic layers of about 3 cm separated by 17 cm of Melides soil, followed by Melides soil in the remaining depth.

Figure 101 presents a schematic diagram of the sandbox model dimensions and the soil profiles referred.

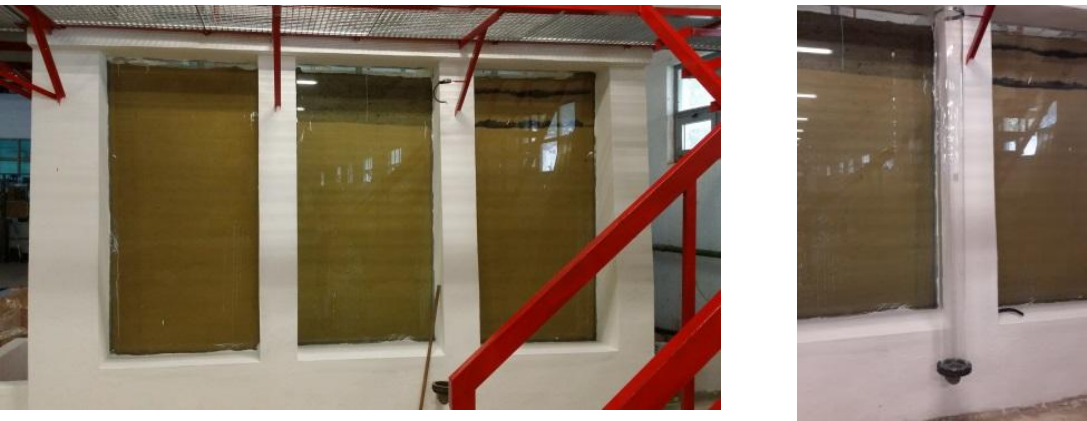


Figure 100 – Detail of three soil layers being tested simultaneously (left) and the external piezometer (right)

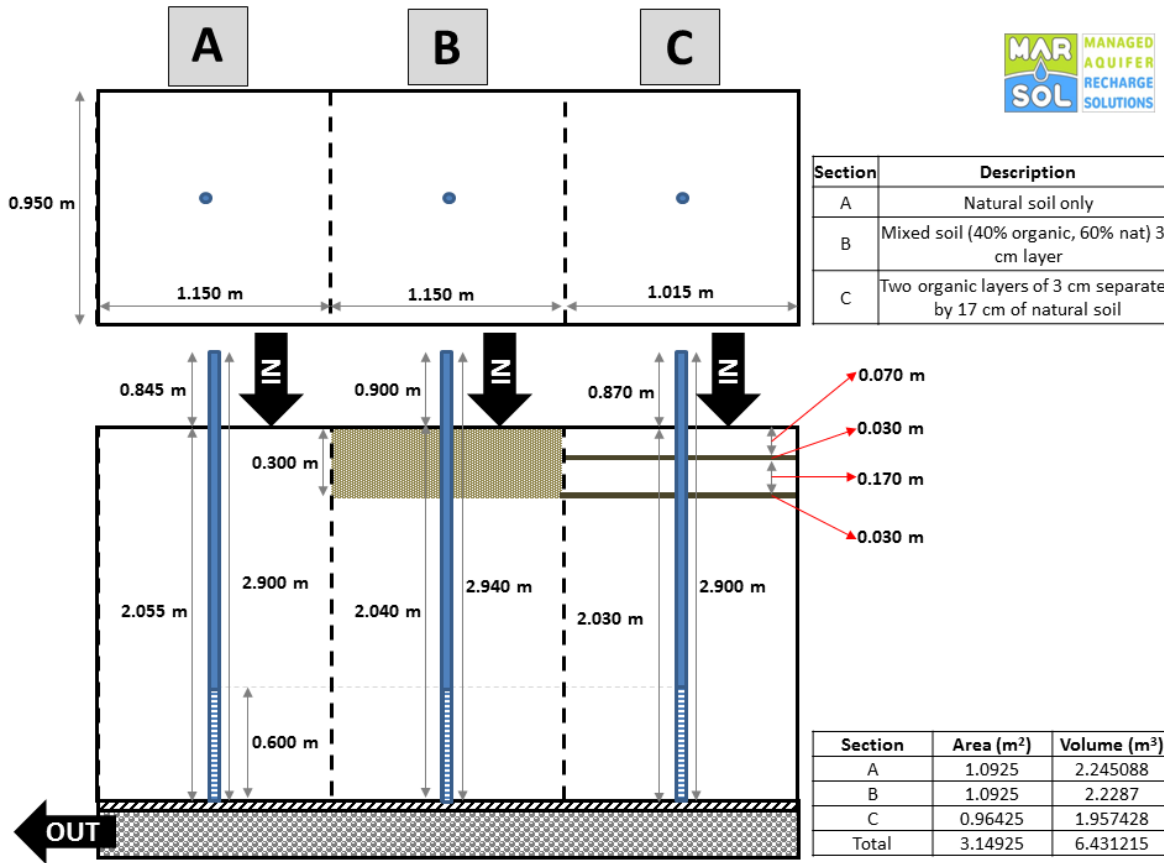


Figure 101 – Schematic diagram of the physical (sandbox) model dimensions and soil mixtures used in MARSol SAT experiments

15.3.2 Materials

To analyse the behaviour of the tracers along their infiltration path in the soil profile, and to assess the different behaviour of the three soil mixtures, the following monitoring devices were installed in each section: A, B and C (**Figure 103**):

Two Prenart capsules (**Figure 102**) in the vadose zone, at two depths, 30 cm and 60 cm.

One piezometer with continuous *in situ* reading of T, EC, water level (and discrete analysis of pH and redox).

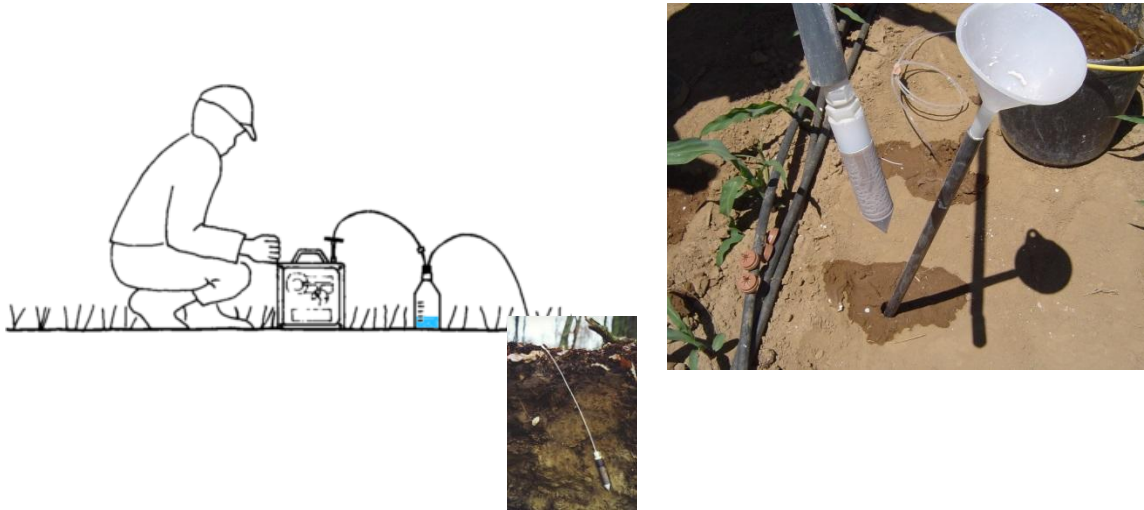


Figure 102 – Vadoses zone monitoring devices used in the physical (sandbox) model

To sample the vadose zone water, the air inside the bottle (**Figure 102**) needed to be sucked with a peristaltic pump. This process allows sampling at the desired depth.



Figure 103 – In situ monitoring devices, both for the saturated and vadose zones

15.3.3 Methodology

15.3.3.1 Tracer selection

In each section (A, B and C), two tracer experiments (Experiment 1 and 2), with spiked fertilizer and hydrocarbons, were performed in May/June 2016 to analyse the adsorption and degradation capacity of the three different soil mixtures. The fertilizer selected correspond to a common chemical fertilizer with the following concentrations: N (12%), P_2O_5 (12%), K_2O (17%), Cl (0.9%), MgO (2%), as well as very small percentages of sulphur, boron and zinc.

Furthermore, a NaCl conservative tracer was added to help identifying the increase in electrical conductivity (EC) and, with that, the more adequate sampling periods.

15.3.3.2 Experiment 1

Experiment 1 was performed from May 30th to May 31st 2016.

Experiment 1 was performed by flooding the soil surface with 0.5 m³ of water. The tracer volume was determined in order to correspond to approximately 20% of the soil basin total pore volume (2.45 m³), considering the three section's volumes (**Table 5**) and the calculated soil average porosity from data previously collected in soil column experiments.

The 500 L were spread using 20 plastic bottles with 25 L capacity (cf. **Figure 104**).

Table 5 – Physical sandbox compartment's dimensions

| Section | Lenght (m) | Width (m) | Height (m) | Area (m ²) | Volume (m ³) | Pore volume (m ³), considering 38% porosity |
|--------------|------------|-----------|------------|------------------------|--------------------------|---|
| A | 1.15 | 0.95 | 2.06 | 1.09 | 2.25 | 0.85 |
| B | 1.15 | 0.95 | 2.04 | 1.09 | 2.23 | 0.85 |
| C | 1.02 | 0.95 | 2.03 | 0.96 | 1.96 | 0.74 |
| Total | 3.32 | 2.85 | 6.13 | 3.15 | 6.43 | 2.45 |



Figure 104 – Bottles used to store the tracer for the physical (sandbox) model Experiment 1

The average flowrate (Q) measured in the outflow before the experiment was 0.063 L/s, i.e. 5.44 m³/d, corresponding to a velocity, V (Q/Area), of 1.73 m/d and permeability (V/n) of 4.55 m/d. Although this value was not obtained for full saturation conditions, it is equivalent to the values measured in laboratory for saturated conditions. Considering the 2.45 m³ sandbox pore volume, it takes about 10.8 hours for a complete PV to flow throughout the sandbox (or each 24 hours about 2.22 PV is percolated in the sandbox).

The tracer concentration in the spiked tracer water was calculated in order to correspond to 2 times the typical dose advised for most horticultural species, i.e. 2 x 500 kg/ha. The overall tracer concentration and weight were calculated for the 500 L, divided by the three sections (Table 6).

Table 6 – Fertilizer tracer concentration calculation for Experiment 1

| Section | Tracer volume m ³ (20% PV) | Number of 25 L bottles | Tracer concentration (1000 kg/ha) | Tracer concentration (mg/L) | Tracer (g) | N (mg/L) | P ₂ O ₅ (mg/L) | K (mg/L) | Cl (mg/L) | Mg (mg/L) |
|--------------|--|------------------------|-----------------------------------|-----------------------------|---------------|-------------|---|--------------------------|--------------|--------------|
| | | | | | | N, 12% | P ₂ O ₅ , 12% | K ₂ O, 17% | Cl, 0.9% | MgO, 2% |
| A | 0.17 | 7 | 0.092 | 53.62 | 9.153 | 6.43 | 6.43 | 3.78 | 4.83 | 0.65 |
| B | 0.17 | 7 | 0.092 | 54.01 | 9.153 | 6.48 | 6.48 | 3.81 | 4.86 | 0.65 |
| C | 0.15 | 6 | 0.104 | 69.67 | 10.371 | 8.36 | 8.36 | 4.92 | 6.27 | 0.84 |
| Total | 0.49 | 20 | 0.032 | 6.49 | 28.677 | 0.78 | 0.78 | 0.46 | 0.58 | 0.08 |

For the hydrocarbons, the tracer concentration was defined to be a value 15 times higher than the 0.5 mg/L detection limit used for the chemical analysis, i.e. 7 mg/L. NaCl concentration was

chosen in order to make to a clear increase in the water electrical conductivity. This corresponds to 500 mg/L. **Table 7** presents the calculations for the tracer's weight.

Table 7 – Hydrocarbon (HC) and NaCl tracer concentration calculation for Experiment 1

| Section | Tracer volume (m ³) (20% PV) | Number of 25 L bottles | HC Tracer concentration (mg/L) | HC Tracer (g) | NaCl Tracer concentration (mg/L) | NaCl Tracer (g) |
|--------------|--|------------------------|--------------------------------|---------------|----------------------------------|-----------------|
| A | 0.17 | 7 | 7 | 1.195 | 500 | 85.361 |
| B | 0.17 | 7 | 7 | 1.186 | 500 | 84.738 |
| C | 0.15 | 6 | 7 | 1.042 | 500 | 74.424 |
| Total | 0.49 | 20 | 21 | 3.423 | 1500 | 244.524 |

15.3.3.3 Experiment 2

Experiment 2 was performed after finishing Experiment 1, from June 2nd to June 3rd.

For the Experiment 2, the same amount of tracer was used, but the tracer was applied in powder on the top of the soil (**Figure 105**). In this way the tracer release was much slower. No hydrocarbons were used.



Figure 105 – Tracer grains on the top of the soil from the physical (sandbox) model, Experiment 2

15.4 MONITORING

To analyse the behaviour of the different soil mixtures simulating SAT treatment, the following sampling protocol was defined for both experiments (cf. **Table 8** and **Table 9**):

- vadose zone: six devices (two depths and three compartments) for water sampling;
- piezometers: three devices (one well and three compartments) for water quality sampling and continuous monitoring of *in situ* T, EC, pH, redox;
- soil: six areas (two depths, 30 cm and 60 cm, and three compartments), for Experiment 1.

Table 8 – Sampling protocol for the Experiment 1



|  | | Sampling protocol for the physical (sandbox) model | | | | | | | | | | | | | |
|---|--------------------|--|------------------------------|------------------------------|---------------|-------------------------------|----|------------------|----|------------------------------|------------------------------|------------------------------|-------------------------------|-------------------------------|----|
| Sample #1 2016/05/30 | # Sampling devices | Water | | | | | | | | Soil | | | | | |
| | | NO ₃ ⁻ | NO ₂ ⁻ | NH ₄ ⁺ | Ca, Na, Mg, K | SO ₄ ²⁻ | Cl | HCO ₃ | TH | NO ₃ ⁻ | NO ₂ ⁻ | NH ₄ ⁺ | PO ₄ ³⁺ | SO ₄ ²⁻ | TH |
| Vadose - basin | | | | | | | | | | | | | | | |
| Wells | 3 | x | x | x | | x | x | x | x | | | | | | |
| Infiltration water | 1 | x | x | x | x | x | x | x | x | | | | | | |
| Soil | | | | | | | | | | | | | | | |
| Sample #2 to sample #7 | # Sampling devices | Water | | | | | | | | Soil | | | | | |
| | | NO ₃ ⁻ | NO ₂ ⁻ | NH ₄ ⁺ | Ca, Na, Mg, K | SO ₄ ²⁻ | Cl | HCO ₃ | TH | NO ₃ ⁻ | NO ₂ ⁻ | NH ₄ ⁺ | PO ₄ ³⁺ | SO ₄ ²⁻ | TH |
| Vadose - basin | | | | | | | | | | | | | | | |
| Wells | 3 | x | x | x | | x | x | x | x | | | | | | |
| Infiltration water | | | | | | | | | | | | | | | |
| Soil | | | | | | | | | | | | | | | |
| Sample #8 | # Sampling devices | Water | | | | | | | | Soil | | | | | |
| | | NO ₃ ⁻ | NO ₂ ⁻ | NH ₄ ⁺ | Ca, Na, Mg, K | SO ₄ ²⁻ | Cl | HCO ₃ | TH | NO ₃ ⁻ | NO ₂ ⁻ | NH ₄ ⁺ | PO ₄ ³⁺ | SO ₄ ²⁻ | TH |
| Vadose - basin | 6 | x | x | x | | x | x | x | x | | | | | | |
| Wells | 3 | x | x | x | | x | x | x | x | | | | | | |
| Infiltration water | | | | | | | | | | | | | | | |
| Soil | | | | | | | | | | | | | | | |
| Sample #9 to 17 | # Sampling devices | Water | | | | | | | | Soil | | | | | |
| | | NO ₃ ⁻ | NO ₂ ⁻ | NH ₄ ⁺ | Ca, Na, Mg, K | SO ₄ ²⁻ | Cl | HCO ₃ | TH | NO ₃ ⁻ | NO ₂ ⁻ | NH ₄ ⁺ | PO ₄ ³⁺ | SO ₄ ²⁻ | TH |
| Vadose - basin | | | | | | | | | | | | | | | |
| Wells | 3 | x | x | x | | x | x | x | x | | | | | | |
| Infiltration water | | | | | | | | | | | | | | | |
| Soil | | | | | | | | | | | | | | | |
| Sample #18 | # Sampling devices | Water | | | | | | | | Soil | | | | | |
| | | NO ₃ ⁻ | NO ₂ ⁻ | NH ₄ ⁺ | Ca, Na, Mg, K | SO ₄ ²⁻ | Cl | HCO ₃ | TH | NO ₃ ⁻ | NO ₂ ⁻ | NH ₄ ⁺ | PO ₄ ³⁺ | SO ₄ ²⁻ | TH |
| Vadose - basin | 6 | x | x | x | x | x | x | x | x | | | | | | |
| Wells | 3 | x | x | x | x | x | x | x | x | | | | | | |
| Infiltration water | | | | | | | | | | | | | | | |
| Soil | 6 | | | | | | | | | o | o | o | o | o | x |

Table 9 – Sampling protocol for the Experiment 2

|  | | Sampling protocol for the physical (sandbox) model | | | | | | | | | | | | | |
|---|--------------------|--|------------------------------|------------------------------|---------------|-------------------------------|----|------------------|----|--|--|--|--|--|--|
| Sample #19 to 20 2016/06/02 and 03 | # Sampling devices | Water | | | | | | | | | | | | | |
| | | NO ₃ ⁻ | NO ₂ ⁻ | NH ₄ ⁺ | Ca, Na, Mg, K | SO ₄ ²⁻ | Cl | HCO ₃ | TH | | | | | | |
| Vadose - basin | 6 | x | x | x | | x | x | x | x | | | | | | |
| Wells | 3 | x | x | x | | x | x | x | x | | | | | | |
| Infiltration water | | | | | | | | | | | | | | | |
| Soil | | | | | | | | | | | | | | | |
| Legend: | | x - samples to IST | | | | | | | | | | | | | |

Furthermore, the spiked infiltration water was analysed at the beginning of the first experiment.

15.5 RESULTS AND CONCLUSIONS

15.5.1 Experiment 1

Experiment 1 was carried out during 24 hours, between 11 AM of May 31st to 11 AM of June 1st. **Table 10** presents the main characteristics of Experiment 1 regarding the inflow, piezometric level and experiment timings.

The difference of water volume on the flowmeter between 17:57 (31-05-2016) and 8:20 (01-06-2016) is equivalent to an inflow value of 0.107 L/s (5.5 m³ in 14h20 or 51600 sec) or 9.25 m³/d. Considering the calculated pore volume (2.45 m³, see Section 15.3.3), this means that water percolated during the whole experiment corresponds to approximately 3.8 times the pore volume of the physical sandbox model.

Table 10 – Main characteristics of Experiment 1

| Date/time | Inflow (L/s) | Volume reading at counter (m ³) | Depth to the water table (m) | Notes |
|------------------|--------------|---|------------------------------|---|
| 30-05-2016 11:50 | 0.096 | 10078.6 | 0 | Inflow started to achieve steady state |
| 30-05-2016 12:24 | 0.098 | - | 0 | - |
| 30-05-2016 16:38 | 0.092 | - | 0 | - |
| 30-05-2016 17:50 | - | - | 0.56 | - |
| 31-05-2016 11:00 | - | - | - | Experiment 1 starts / tracer injection |
| 31-05-2016 11:30 | - | - | - | Tracer injection stops |
| 31-05-2016 17:57 | 0.11 | 10089 | 0.87 | - |
| 01-06-2016 08:20 | 0.11 | 10094.5 | 0.8 | - |
| 01-06-2016 09:24 | 0.076 | - | 0.74 | - |
| 01-06-2016 11:00 | - | - | - | Experiment 1 finishes / injection stops |

Figure 106 presents the results obtained from the CTD diver concerning the depth to the water table and the electrical conductivity (EC). The figure shows a fast increase of the water table (decrease in the depth to the water table) after the tracer injection started which in prolonged for 1 hour after the tracer injection stopped. The water inflow during the remaining period of the experiment was tried to be kept constant, but some small oscillations in the water pressure have occurred. Nevertheless, the main reason for the water table decrease was due to the release of water in the outflow tap, done in order to balance the inflow with the outflow, while stabilizing the water table.

Concerning the electrical conductivity, **Figure 106** shows the three pic arrivals. It is possible to observe that the tracer arrived first to PzA and with higher EC values when compared to the tracer arrival in Section B and C, as a result of the higher retention capacity of Melides soil mixed with organic matter.

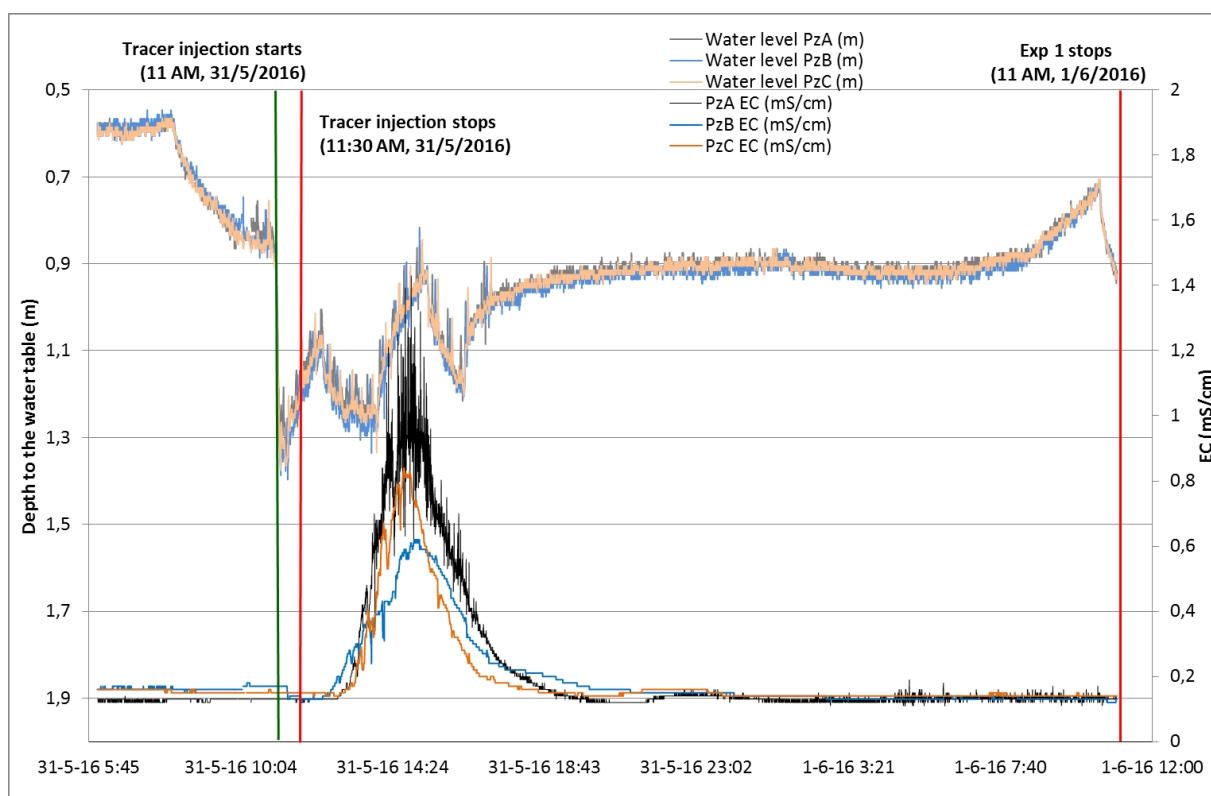


Figure 106 – Piezometric water level and electrical conductivity values in the three piezometers, Experiment 1

In addition to the continuous measurement with the CTD diver, several discrete samples were retrieved from the six vadose zone cups and the three piezometers during the whole experiment period. Table 11 presents the water quality concentrations results. In the first column, under “designation”, the first letter represents the Section of the experiment (A, B or C), the subsequent number is the soil depth (30 or 60 cm) or GW if collected in the piezometers, and the last number is the sampling number.

Table 11 – Results from the chemical analysis of water samples collected during Experiment 1

| Designation | Day Hour | NO ₃ ⁻ | NO ₂ ⁻ | NH ₄ ⁺ | Ca ²⁺ | Mg ²⁺ | Na ⁺ | K ⁺ | SO ₄ ²⁻ | Cl ⁻ | HCO ₃ ⁻ | TH |
|--------------------|-------------|------------------------------|------------------------------|------------------------------|------------------|------------------|-----------------|----------------|-------------------------------|-----------------|-------------------------------|------|
| Units | | mg/L | | | | | | | | | | µg/L |
| Tracer 1 | 31-05 11:05 | 5.9 | <0.01 | 3.7 | 18 | 3.1 | 180 | 6.9 | 27 | 275 | 53.8 | 78 |
| Vadose cups | | | | | | | | | | | | |
| A-30-1 | 31-05 13:26 | 4 | <0.01 | - | - | - | - | - | 20 | 139 | 47.9 | - |
| A-30-2 | 01-06 11:05 | 2.2 | <0.01 | 0.9 | - | - | - | - | 13 | 31 | 52.2 | - |
| A-60-1 | 31-05 13:30 | 3.2 | <0.01 | - | - | - | - | - | 17 | 80 | - | - |
| A-60-2 | 01-06 11:07 | 1.9 | <0.01 | 0.46 | - | - | - | - | 11 | 10 | 52.3 | 160 |
| Piezometers | | | | | | | | | | | | |
| A-GW-1 | 31-05 10:57 | 2 | <0.1 | <0.05 | 18 | 4.3 | 9.3 | 3.2 | 11 | 9.4 | 54.1 | <10 |
| A-GW-2 | 31-05 11:20 | 1.9 | <0.1 | <0.05 | - | - | - | - | 11 | 9.3 | 48.1 | 11 |

| Designation | Day Hour | NO ₃ ⁻ | NO ₂ ⁻ | NH ₄ ⁺ | Ca ²⁺ | Mg ²⁺ | Na ⁺ | K ⁺ | SO ₄ ²⁻ | Cl ⁻ | HCO ₃ ⁻ | TH |
|--------------------|-------------|------------------------------|------------------------------|------------------------------|------------------|------------------|-----------------|----------------|-------------------------------|-----------------|-------------------------------|-----|
| A-GW-3 | 31-05 11:40 | 1.8 | <0.1 | <0.05 | 19 | 5.8 | 9.3 | 3.6 | 11 | 9.2 | 52.8 | <10 |
| A-GW-4 | 31-05 11:59 | 1.8 | <0.1 | <0.05 | - | - | - | - | 13 | 9.2 | 55.2 | <10 |
| A-GW-5 | 31-05 12:21 | 2.1 | <0.1 | <0.05 | - | - | - | - | 11 | 10 | 55.9 | 35 |
| A-GW-6 | 31-05 12:43 | 2 | <0.1 | <0.05 | - | - | - | - | 10 | 18 | 53.5 | <10 |
| A-GW-7 | 31-05 13:00 | 2.5 | <0.01 | <0.05 | 27 | 7.9 | 12 | 4.7 | 9.9 | 45 | 47.9 | <10 |
| A-GW-8 | 31-05 13:20 | 2.6 | <0.01 | <0.05 | - | - | - | - | 10 | 54 | 47.8 | 23 |
| A-GW-9 | 31-05 13:40 | 3.5 | <0.1 | <0.05 | - | - | - | - | 11 | 93 | 44 | 20 |
| A-GW-10 | 31-05 14:00 | 3.9 | <0.01 | <0.05 | - | - | - | - | 13 | 139 | 42.3 | 35 |
| A-GW-11 | 31-05 14:21 | 4.9 | <0.01 | <0.05 | - | - | - | - | 19 | 210 | 45.8 | 56 |
| A-GW-12 | 31-05 14:41 | 5.5 | <0.01 | <0.05 | - | - | - | - | 22 | 235 | 44.5 | 110 |
| A-GW-13 | 31-05 15:02 | 5.8 | <0.01 | <0.05 | - | - | - | - | 27 | 248 | 35.9 | 130 |
| A-GW-14 | 31-05 15:30 | 5 | <0.01 | <0.05 | - | - | - | - | 29 | 202 | 72.2 | 98 |
| A-GW-15 | 31-05 15:55 | 4.2 | <0.01 | <0.05 | - | - | - | - | 28 | 145 | 84.9 | 110 |
| A-GW-16 | 31-05 16:30 | 3.6 | <0.1 | <0.05 | - | - | - | - | 27 | 107 | 122 | <10 |
| A-GW-17 | 31-05 17:00 | 2.5 | <0.1 | <0.05 | - | - | - | - | 22 | 44 | 94.9 | 27 |
| A-GW-18 | 01-06 11:00 | 1.8 | <0.1 | 0.4 | 16 | 3.7 | 9.6 | 3.4 | 11 | 9.5 | 50.6 | <10 |
| Vadose cups | | | | | | | | | | | | |
| B-30-1 | 31-05 13:31 | 3.6 | <0.01 | - | - | - | - | - | 12 | 33 | - | - |
| B-30-2 | 01-06 11:08 | 4.5 | <0.01 | <0.05 | - | - | - | - | 12 | 25 | 110 | - |
| B-60-1 | 31-05 13:35 | 3.8 | 0.04 | - | - | - | - | - | 16 | 76 | 80.2 | - |
| B-60-2 | 01-06 11:09 | 2.9 | 0.04 | 0.29 | - | - | - | - | 11 | 9.9 | 53.4 | - |
| Piezometers | | | | | | | | | | | | |
| B-GW-1 | 31-05 10:57 | 2.3 | <0.1 | <0.05 | 15 | 5.5 | 9.3 | 32 | 11 | 9.4 | 75.3 | 47 |
| B-GW-2 | 31-05 11:25 | 2.4 | <0.1 | <0.05 | - | - | - | - | 11 | 9.3 | 78.5 | 37 |
| B-GW-3 | 31-05 11:45 | 2.4 | <0.1 | <0.05 | 16 | 7.4 | 9.8 | 40 | 11 | 9.3 | 78.4 | <10 |
| B-GW-4 | 31-05 12:04 | 2.3 | <0.1 | <0.05 | - | - | - | - | 11 | 9.4 | 84.4 | <10 |
| B-GW-5 | 31-05 12:25 | 2.8 | <0.1 | <0.05 | - | - | - | - | 11 | 18 | 74.6 | <10 |
| B-GW-6 | 31-05 12:47 | 2.7 | <0.1 | <0.05 | - | - | - | - | 11 | 33 | 71.8 | 21 |
| B-GW-7 | 31-05 13:05 | 3 | <0.1 | <0.05 | 28 | 7.9 | 15 | 36 | 12 | 53 | 70.3 | <10 |
| B-GW-8 | 31-05 13:24 | 3.6 | <0.1 | <0.05 | - | - | - | - | 13 | 86 | 64.7 | 20 |
| B-GW-9 | 31-05 13:43 | 4 | 0.03 | <0.05 | - | - | - | - | 15 | 108 | 62.3 | 29 |
| B-GW-10 | 31-05 14:04 | 4.4 | 0.03 | <0.05 | - | - | - | - | 17 | 140 | 37.9 | <10 |
| B-GW-11 | 31-05 14:23 | 5.2 | 0.05 | <0.05 | - | - | - | - | 20 | 192 | 55.9 | 57 |
| B-GW-12 | 31-05 14:44 | 5.7 | 0.04 | <0.05 | - | - | - | - | 22 | 220 | 55.6 | 39 |
| B-GW-13 | 31-05 15:05 | 6.4 | 0.07 | <0.05 | - | - | - | - | 26 | 232 | 58.9 | 43 |
| B-GW-14 | 31-05 15:32 | 6.7 | 0.04 | <0.05 | - | - | - | - | 28 | 207 | 69.5 | 22 |
| B-GW-15 | 31-05 15:58 | 6.1 | 0.24 | <0.05 | - | - | - | - | 28 | 146 | 89 | 36 |
| B-GW-16 | 31-05 16:33 | 5.1 | <0.1 | <0.05 | - | - | - | - | 23 | 79 | 111 | 22 |
| B-GW-17 | 31-05 17:04 | 4.5 | <0.1 | <0.05 | - | - | - | - | 17 | 39 | 117 | 13 |
| B-GW-18 | 01-06 11:08 | 2.8 | <0.1 | 0.12 | 20 | 3.9 | 9.8 | 8.9 | 11 | 9.6 | 72.4 | <10 |
| Vadose cups | | | | | | | | | | | | |
| C-30-1 | 31-05 13:35 | 4.3 | 0.03 | - | - | - | - | - | 19 | 127 | 63.1 | - |
| C-30-2 | 01-06 11:13 | 2.4 | 0.04 | 0.65 | - | - | - | - | 11 | 13 | 39 | 63 |
| C-60-1 | 31-05 13:39 | - | - | - | - | - | - | - | - | - | - | - |
| C-60-2 | 01-06 11:15 | 4.8 | 0.08 | - | - | - | - | - | - | 48 | - | - |

| Designation | Day Hour | NO ₃ ⁻ | NO ₂ ⁻ | NH ₄ ⁺ | Ca ²⁺ | Mg ²⁺ | Na ⁺ | K ⁺ | SO ₄ ²⁻ | Cl ⁻ | HCO ₃ ⁻ | TH |
|--------------------|-------------|------------------------------|------------------------------|------------------------------|------------------|------------------|-----------------|----------------|-------------------------------|-----------------|-------------------------------|-----|
| Piezometers | | | | | | | | | | | | |
| C-GW-1 | 31-05 10:57 | 2.1 | <0.1 | <0.05 | 18 | 4.2 | 8.6 | 14 | 11 | 9.3 | 66.7 | <10 |
| C-GW-2 | 31-05 11:30 | 2.1 | <0.1 | <0.05 | - | - | - | - | 11 | 9.2 | 63.2 | <10 |
| C-GW-3 | 31-05 11:50 | 2.1 | <0.1 | <0.05 | 20 | 6.5 | 9.3 | 12 | 11 | 9.3 | 67.8 | <10 |
| C-GW-4 | 31-05 12:10 | 2 | <0.1 | <0.05 | - | - | - | - | 11 | 9.4 | 66.9 | <10 |
| C-GW-5 | 31-05 12:35 | 2 | <0.1 | <0.05 | - | - | - | - | 11 | 9.4 | 66.4 | <10 |
| C-GW-6 | 31-05 12:51 | 2.1 | <0.1 | <0.05 | - | - | - | - | 10 | 13 | 64 | <10 |
| C-GW-7 | 31-05 13:10 | 2.5 | <0.1 | <0.05 | 21 | 5.1 | 9.3 | 13 | 10 | 37 | 57.5 | <10 |
| C-GW-8 | 31-05 13:30 | 2.8 | <0.1 | <0.05 | - | - | - | - | 10 | 54 | 54.7 | <10 |
| C-GW-9 | 31-05 13:46 | 3.4 | <0.01 | <0.05 | - | - | - | - | 11 | 84 | 51.6 | 15 |
| C-GW-10 | 31-05 14:07 | 4.6 | <0.01 | <0.05 | - | - | - | - | 18 | 163 | 49.1 | 18 |
| C-GW-11 | 31-05 14:26 | 5.5 | 0.03 | <0.05 | - | - | - | - | 23 | 210 | 50.9 | 12 |
| C-GW-12 | 31-05 14:47 | 5.8 | 0.05 | <0.05 | - | - | - | - | 26 | 211 | 57.7 | 19 |
| C-GW-13 | 31-05 15:08 | 5.1 | 0.09 | <0.05 | - | - | - | - | 26 | 145 | 75 | 12 |
| C-GW-14 | 31-05 15:34 | 4.3 | <0.1 | <0.05 | - | - | - | - | 22 | 80 | 88.1 | 11 |
| C-GW-15 | 31-05 16:05 | 4 | <0.1 | <0.05 | - | - | - | - | 20 | 62 | 91.1 | 16 |
| C-GW-16 | 31-05 16:36 | 3.6 | <0.1 | <0.05 | - | - | - | - | 16 | 33 | 90.4 | <10 |
| C-GW-17 | 31-05 17:06 | 3.4 | <0.1 | <0.05 | - | - | - | - | 12 | 15 | 88.1 | <10 |
| C-GW-18 | 01-06 11:12 | 2.3 | <0.1 | 0.14 | 20 | 3.5 | 9.7 | 5.2 | 11 | 9.5 | 63.3 | <10 |

Figure 107 presents the breakthrough curves obtained in the saturated water from the piezometer installed in Section A

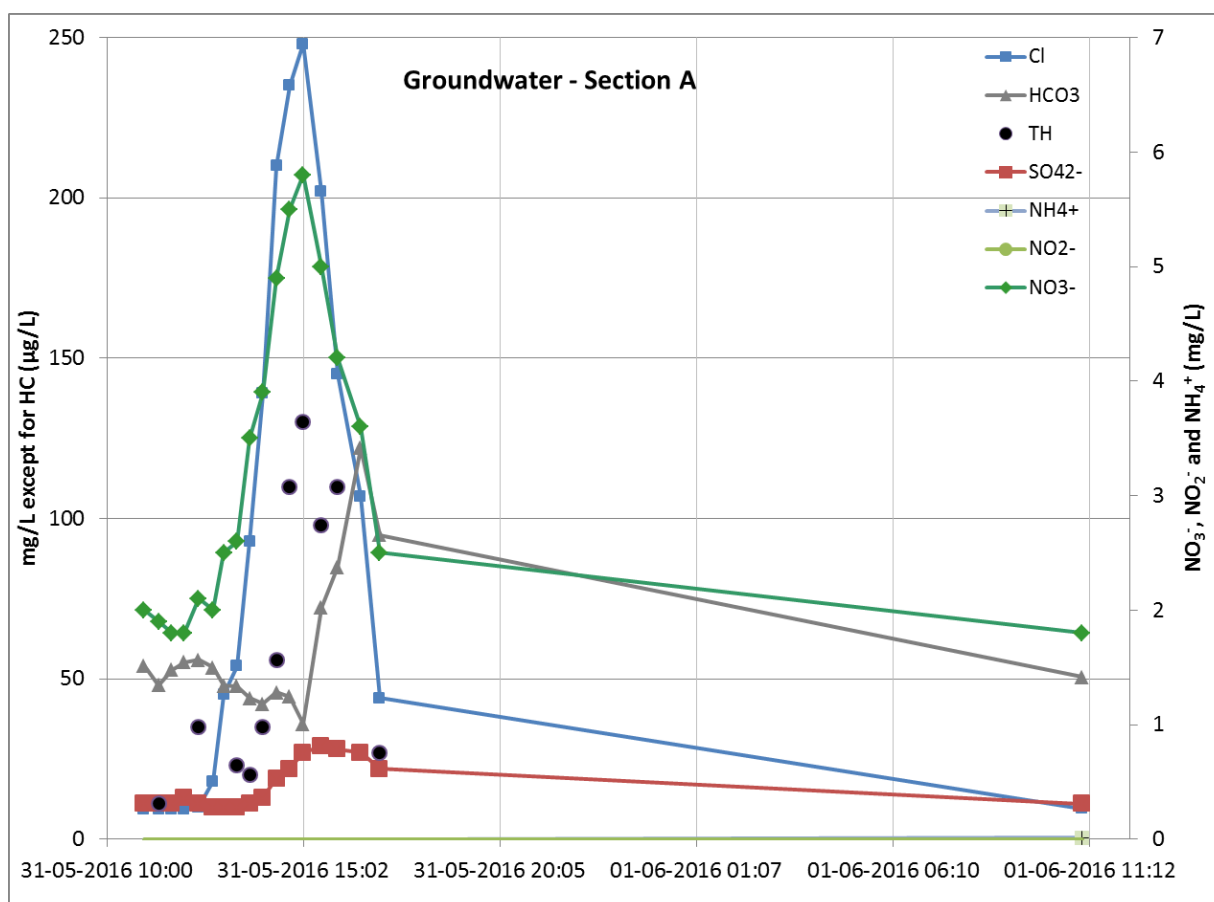
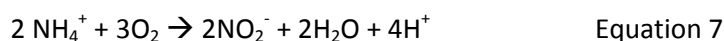


Figure 107 – Breakthrough curves obtained for the water samples from the Section A piezometer

The sharp and symmetrical curves obtained both for chloride (Cl^-) and nitrate (NO_3^-), together with the simultaneous pic arrival of both ions - in concentrations similar to the initial concentration of the tracer - confirms the inert character of Melides sand. Neither nitrite (NO_2^-) nor ammonia (NH_4^+) was found in the piezometer water samples during the experiment. Possibly the NH_4^+ existing in the tracer (3.7 mg/L) was nitrified with the presence of oxygen:



In fact, the samples collected in the vadose zone (**Figure 108**) show the presence of NH_4^+ in the samples from 30 to 60 cm in the second day (the first day there was not enough water for analysis), in minor conditions when compared to the input of 3.7 mg/L, also with very little concentration arriving to the saturated zone. In the soil samples collected at two depths after the experiment, only nitrite was found (**Table 12**).

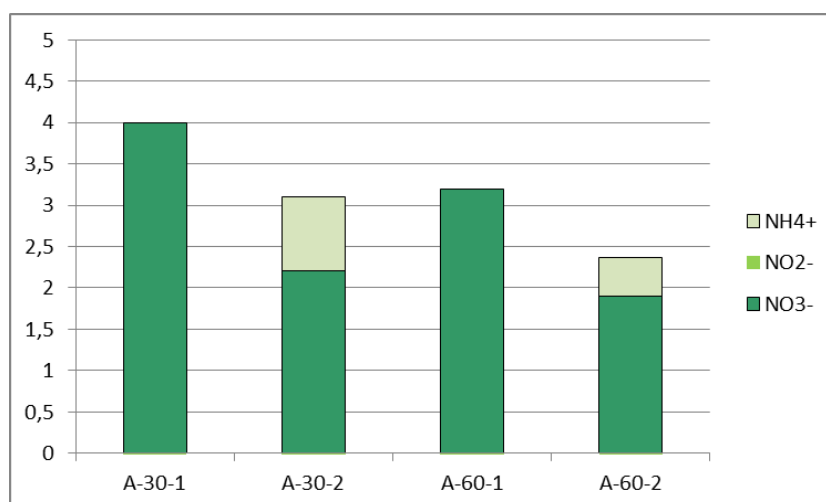


Figure 108 – Nitrogen concentrations in the vadose zone capsules (30 cm and 60 cm) from Section A

The concentration in hydrocarbons (HC) along the experiment shows values higher than the average tracer concentration, possibly due to the difficulty of making a good mixture of HC in the injected water. So, possibly the portion of the tracer injected in Section A had higher values than the mixture analysed. Nonetheless, the HC were retained in very small concentrations (10 mg/kg) in Melides soil (**Table 12**).

In the last sample, taken 24 h after the tracer injection, the concentrations of all chemical parameters were similar to the initial values.

Table 12 – Results from the chemical analysis of soil samples collected after Experiment 1 finished

| Designation | Soil (mg/kg DW) | | | | | |
|-------------|------------------------------|------------------------------|------------------------------|-------------------------------|-------------------------------|-----|
| | NO ₃ ⁻ | NO ₂ ⁻ | NH ₄ ⁺ | PO ₄ ³⁺ | SO ₄ ²⁻ | TH |
| A_30_Soil | <20 | 0.080 | <0.5 | <0.05 | <0.1 | 10 |
| A_60_Soil | <20 | 0.090 | <0.5 | <0.05 | <0.1 | <10 |
| B_30_Soil | <20 | 0.135 | <0.5 | <0.05 | <0.1 | <10 |
| B_60_Soil | <20 | 0.134 | <0.5 | <0.05 | <0.1 | 36 |
| C_30_Soil | <20 | 0.132 | <0.5 | <0.05 | <0.1 | 70 |
| C_60_Soil | <20 | 0.077 | <0.5 | <0.05 | <0.1 | <10 |

Figure 109 presents the breakthrough curves obtained in the saturated water from the piezometer installed in Section B, in which the first 60 cm of soil is a mixture of Melides soil (60%) and organic matter (40%), followed by Melides soil in the remaining depth.

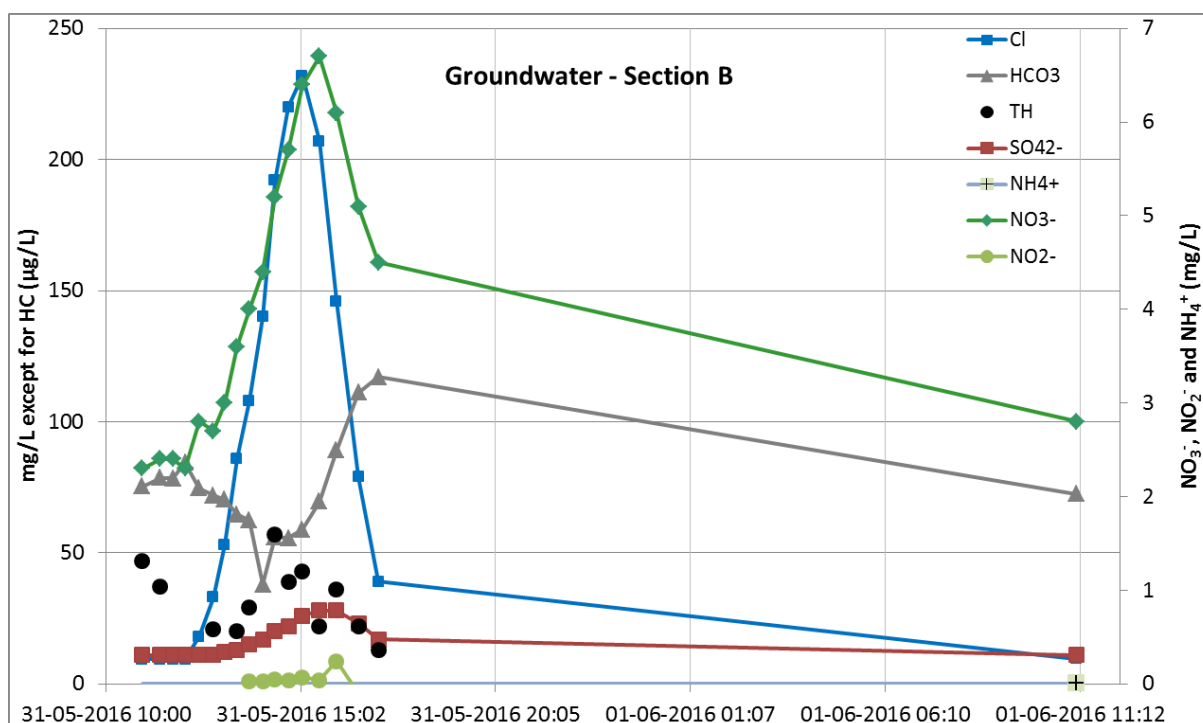
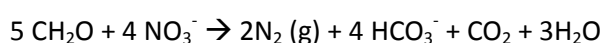


Figure 109 – Breakthrough curves obtained for the water samples from the Section B piezometer

The breakthrough curve for nitrates shows a higher dispersion when compared to Cl and to the results from Section A. Besides, the pic of nitrate arrival is 30 minutes slower (at 15:32) and has increased when compared to the initial tracer. The formation of nitrite (NO_2^-) (see also **Figure 110**), confirms the transformation of NH_4^+ into nitrite and nitrate through a nitrification process (see Equation 1 and 2 and **Table 12**). Besides, it is possible that some of the nitrate was subject to denitrification in the presence of organic matter (CH_2O), producing bicarbonate (HCO_3^-) in the process:



Equation 9

Concerning the HC, the soil from Section B shows a better ability to retain these contaminants than Melides soil alone. The HC were retained close to 60 cm, but not in the first 30 cm (**Table 12**).

In the last sample, taken 24 h after the tracer injection, the concentrations of all chemical parameters were similar to the initial values.

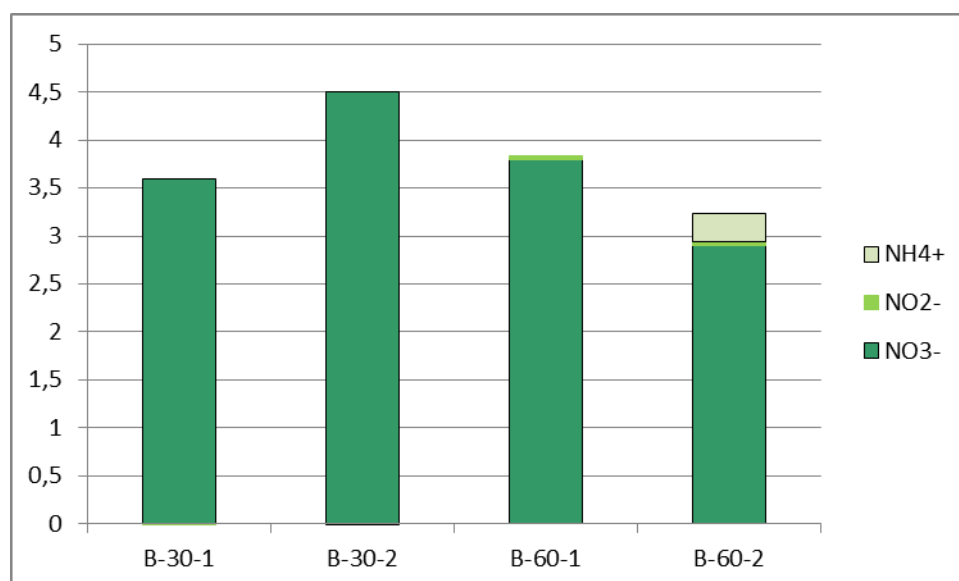


Figure 110 – Nitrogen concentrations in the vadose zone capsules (30 cm and 60 cm) from Section B

Figure 111 presents the breakthrough curves obtained in the saturated water from the piezometer installed in Section C, with two organic layers of about 3 cm separated by 17 cm of Melides soil, followed by Melides soil in the remaining depth.

The breakthrough curve for nitrates shows lower pic values when compared to Section B but also the formation of nitrite (NO_2^-) (see also Figure 112) through a nitrification process (see Equation 1 and 2). Denitrification is possible but the scape of N_2 to the atmosphere should be minor due to the lower permeability of the organic layer. The retention of HC shows the best results when comparing the three sections. The concentration retained in the first soil layers is higher (**Table 12**) and therefore the concentration on the water is the lowest (**Figure 111**).

In the last sample, taken 24 h after the tracer injection, the concentrations of all chemical parameters were similar to the initial values.

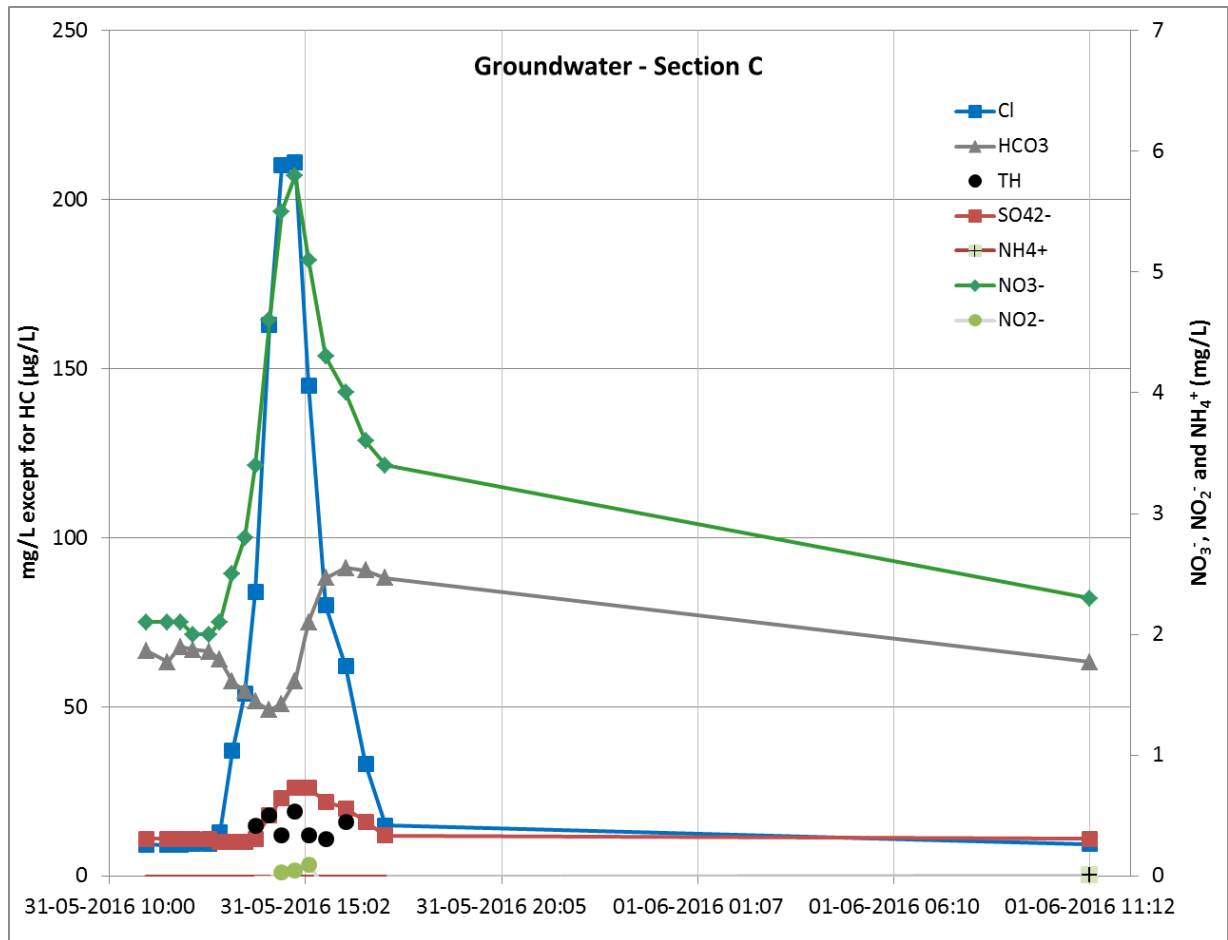


Figure 111 – Breakthrough curves obtained for the water samples from the Section C piezometer

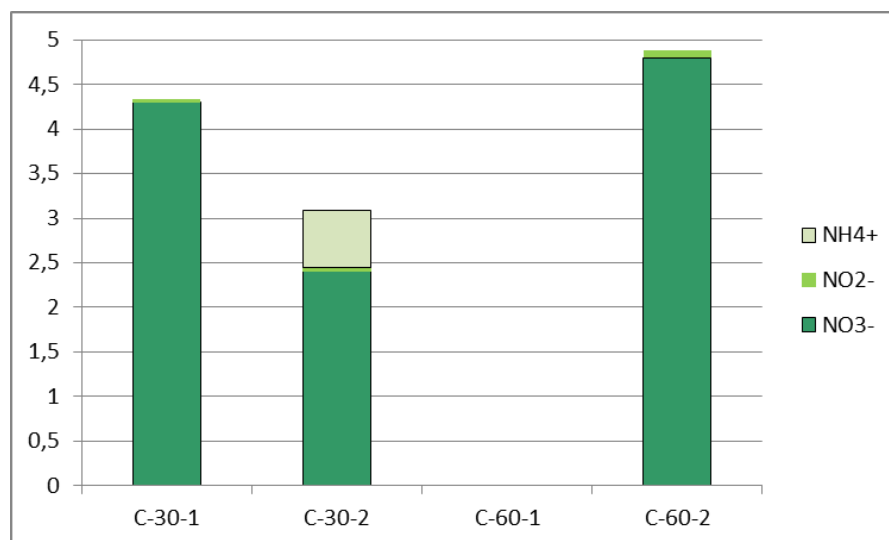


Figure 112 – Nitrogen concentrations in the vadose zone capsules (30 cm and 60 cm) from Section C

15.5.2 Experiment 2

Aiming to analyse the behaviour of same three soil mixtures (in Section A, B and C) in the case where the contaminants are slowly released, an Experiment 2 was carried out during 48 hours, between 12 AM of June 1st to 12 AM June 3rd. In this experiment the same tracer (fertilizer and NaCl) and concentrations were used, but no hydrocarbons (TH). Anyway the TH were analysed in the water sampled to see if any content still existed from the previous experiment. The tracer was placed on the soil surface in small grains (**Figure 113**) and it was slowly washed down by the irrigation process. It is expected that some soil contaminants from the previous experiment could still be attached to the soil.



Figure 113 – Detail of the soil surface with the tracer used for Experiment 2

Table 13 presents the main characteristics of Experiment 2 concerning the inflow and depth to the water table.

Figure 114 presents the results obtained from the CTD diver, for the depth to the water table and the electrical conductivity (EC). Although the inflow was kept approximately constant throughout the experiment (**Table 13**), the outflow was frequently changed while trying to adjust the depth to the water table to circa 0.8 m, the same value used for Experiment 1. This explains the water table changes observed in **Figure 114**. Concerning the EC registered in the piezometers, a much higher dispersion and a tail are observed in all sections, when compared to the corresponding section in Experiment 1. The disturbance caused by the soil sampling should be responsible for the disruption of Section C soil layers and a preferential flowpath should have been formed leading to a faster EC pic concentration and arrival in the Section C piezometer.

Comparing Experiment 1 and 2 tracer arrival, one can see that the liquid pulse tracer injection (Experiment 1) leads to a faster leaching, with an arrival to the piezometers approximately 4 hours after the experiment begins (**Figure 106**); and when the tracer is placed on the soil

surface in small grains, the leaching is slower and the pic concentration starts to arrive 5 hours after the experiment and remains for much longer (Figure 114).

Table 13 – Main characteristics of Experiment 2

| Date/time | Inflow (L/s) | Volume reading at counter (m ³) | Depth to the water table (m) | Notes |
|------------------|--------------|---|------------------------------|---------------------------------------|
| 01-06-2016 11:55 | 0.079 | - | 1.22 | Inflow restarted |
| 01-06-2016 12:00 | - | - | - | Experiment 2 starts / tracer released |
| 01-06-2016 14:30 | 0.079 | - | 1.55 | - |
| 02-06-2016 08:00 | 0.09 | - | 1.57 | - |
| 02-06-2016 09:02 | 0.082 | - | 1.12 | - |
| 02-06-2016 11:52 | 0.082 | - | 0.78 | - |
| 02-06-2016 12:54 | 0.082 | - | 0.71 | - |
| 02-06-2016 14:30 | 0.083 | - | 0.81 | - |
| 02-06-2016 16:19 | 0.083 | - | 0.85 | - |
| 03-06-2016 12:00 | - | - | - | Experiment 2 finishes |
| 03-06-2016 14:45 | 0.069 | 10110.1 | 1.3 | - |
| 03-06-2016 16:46 | 0.075 | 10110.6 | 0.86 | - |
| 03-06-2016 17:05 | 0 | - | 0.77 | Injection stopped / Divers removed |

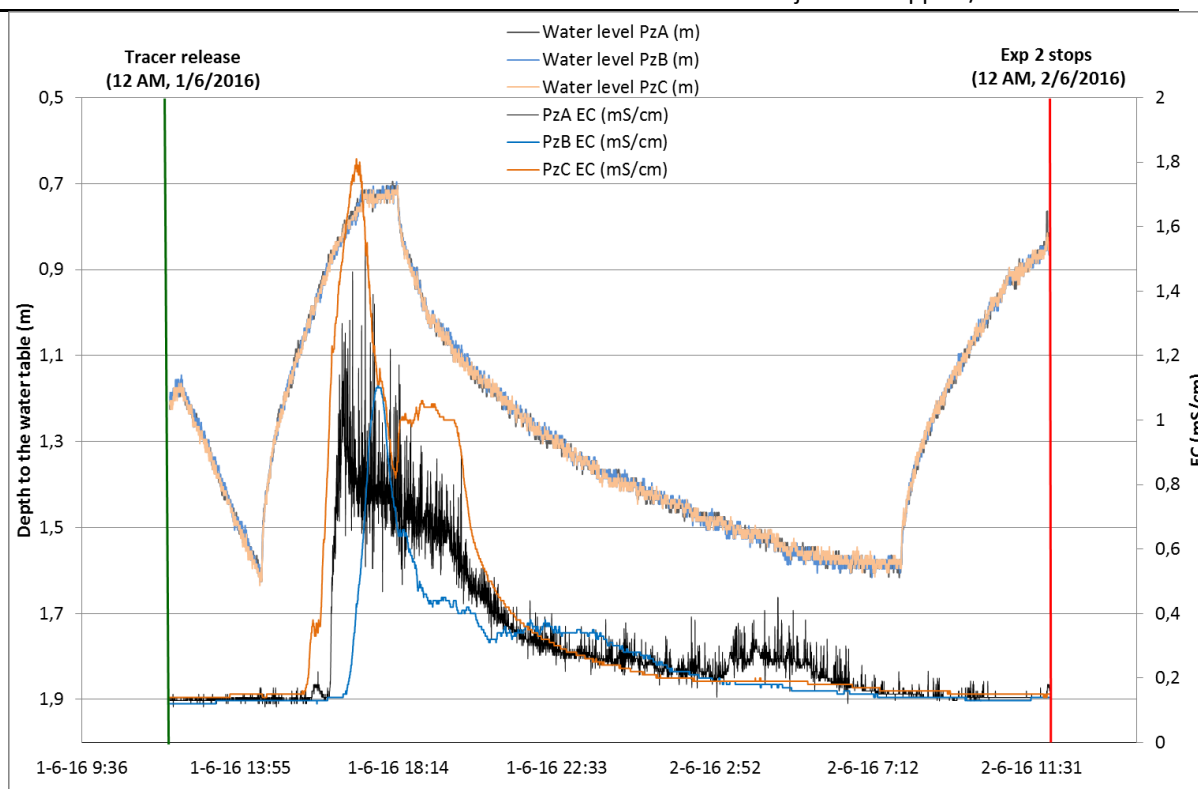


Figure 114 – Piezometric water level and electrical conductivity values in the three piezometers, Experiment 2

In addition to the continuous measurement of the EC, discrete samples were retrieved from the six vadose zone cups and the three piezometers, similarly to what was performed for Experiment 1. However, the samples were collected only at the end of each day and not hourly. **Table 14** presents the water quality concentrations. The same designation procedure was used.

Table 14 – Results from the chemical analysis of water samples collected during Experiment 2

| Designation | Day Hour | NO ₃ ⁻ | NO ₂ ⁻ | NH ₄ ⁺ | Ca ²⁺ | Mg ²⁺ | Na ⁺ | K ⁺ | SO ₄ ²⁻ | Cl ⁻ | HCO ₃ ⁻ | TH |
|-------------|----------|------------------------------|------------------------------|------------------------------|------------------|------------------|-----------------|----------------|-------------------------------|-----------------|-------------------------------|-----|
| Units | | mg/L | | | | | | | µg/L | | | |
| Vadose cups | | | | | | | | | | | | |
| A-30-3 | 02-06 | 5.6 | <0.01 | 2.1 | - | - | - | - | 21 | 251 | 45.5 | - |
| A-60-3 | 02-06 | 1.8 | <0.01 | <0.05 | - | - | - | - | 11 | 18 | 51.4 | - |
| A-30-4 | 03-06 | 1.9 | 0.01 | 0.9 | - | - | - | - | 11 | 10 | 46.2 | - |
| A-60-4 | 03-06 | 1.7 | <0.01 | <0.05 | - | - | - | - | 11 | 10 | 54.5 | - |
| Piezometers | | | | | | | | | | | | |
| A-GW-19 | 02-06 | 1.9 | <0.1 | 1.3 | 34 | 20 | 28 | 16 | 11 | 12 | 46.4 | <10 |
| A-GW-20 | 03-06 | 1.8 | <0.1 | 0.51 | 21 | 6.6 | 11 | 4.9 | 11 | 9.9 | 48.3 | <10 |
| Vadose cups | | | | | | | | | | | | |
| B-30-3 | 02-06 | 10 | 0.03 | 1 | - | - | - | - | 25 | 78 | 106 | - |
| B-60-3 | 02-06 | 2.3 | 0.01 | <0.05 | - | - | - | - | 11 | 187 | 76.1 | - |
| B-30-4 | 03-06 | 3.6 | 0.02 | 0.2 | - | - | - | - | 11 | 10 | - | - |
| B-60-4 | 03-06 | 1.9 | <0.01 | <0.05 | - | - | - | - | 11 | 11 | 67.1 | - |
| Piezometers | | | | | | | | | | | | |
| B-GW-19 | 02-06 | 3.6 | <0.1 | 0.32 | 20 | 3.9 | 23 | 6 | 12 | 13 | 83.6 | <10 |
| B-GW-20 | 03-06 | 2.9 | <0.01 | 0.25 | 24 | 3.6 | 11 | 4.2 | 11 | 9.6 | 76.3 | <10 |
| Vadose cups | | | | | | | | | | | | |
| C-30-3 | 02-06 | 6.1 | 0.03 | 1.5 | - | - | - | - | 19 | 421 | 60.2 | - |
| C-60-3 | 02-06 | 2.6 | 0.02 | - | - | - | - | - | 11 | 11 | - | - |
| C-30-4 | 03-06 | 2.3 | <0.01 | 0.18 | - | - | - | - | 11 | 14 | 55.5 | - |
| C-60-4 | 03-06 | 2 | 0.01 | - | - | - | - | - | 11 | 10 | - | - |
| Piezometers | | | | | | | | | | | | |
| C-GW-19 | 02-06 | 2.6 | <0.1 | 0.52 | 16 | 2.6 | 15 | 5 | 11 | 9.2 | 60.1 | <10 |
| C-GW-20 | 03-06 | 2.2 | <0.01 | 0.27 | 21 | 2.8 | 9.3 | 2.5 | 11 | 11 | 63.8 | <10 |

Figure 115 presents the results obtained for the nitrogen (N) cycle, namely nitrates (NO₃⁻), nitrites (NO₂⁻) and ammonia (NH₄⁺). In all Sections A, B and C the highest concentrations of NO₃⁻ and NH₄⁺ were observed in the first day (02-06-2016) and at the first vadose zone cup, 30 cm depth. In the cases where NH₄⁺ analysis was possible, the concentration in the Cup at 60 cm was below the detection limit, although it is present in the piezometers water. Values for NO₂⁻ were very low, close to the detection limit.

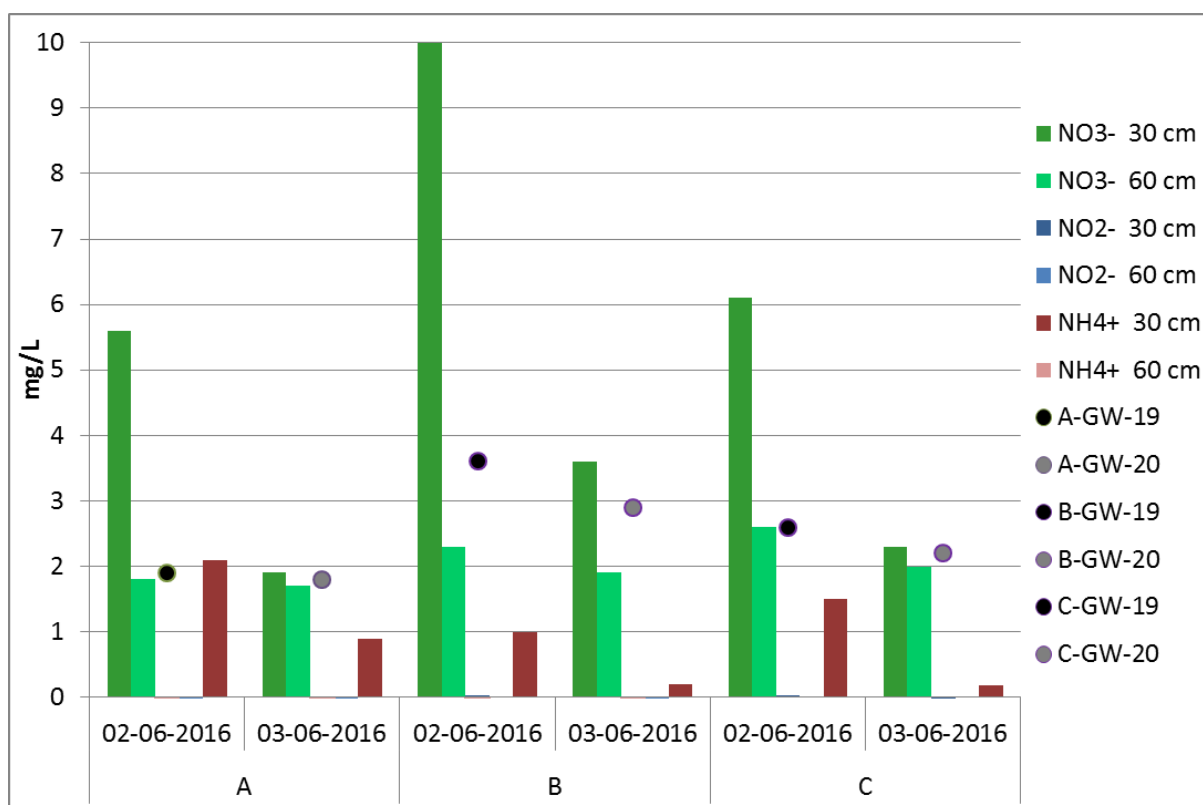


Figure 115 – Concentrations of N cycle in the water from the vadose (30 and 60 cm) and saturated (GW) zones

As could be seen in Experiment 1, also in Experiment 2 nitrification (Equations 1 and 2) occurs in the upper part of the soil (first 30 cm), with the presence of O_2 . This process seems to be stronger in Section B, where the values for NH_4^+ are lower and NO_3^- are higher. Besides, some denitrification should also occur in Section B forming HCO_3^- (Equation 3) (see **Table 14**).

No hydrocarbons were detected in the water sampled from the piezometers.

15.5.3 Conclusions

Comparing Experiment 1 and 2 results, it can be concluded that although there is a clear difference in the contaminants concentration throughout the experiment, after 48 hours the values are similar to the initial concentrations and equilibrium has been attained.

Nitrification (from ammonia to nitrate) and denitrification (from nitrate to gaseous N) seem to be the most common phenomena. Both are more likely to occur in the first soil layers due to the presence of oxygen and the possibility of N_2 gas to escape to the atmosphere. The presence of an organic layer (Section B and C) favours denitrification and seems to be more effective in Section C (although this is not so clear in Experiment 2 due to the previous soil disturbance due to sampling).

The removal of hydrocarbons is clearly more effective for Section C.

16 NUMERICAL MODELLING

A set of finite elements numerical models were designed in FEFLOW as a complementary method for understanding the behaviour of a set of selected tracers. Each section was modelled using as input the data collected before and during the conducted experiments and, as a first approach, nitrogen cycle elements (nitrates, nitrites and ammonia) were considered as tracers. Transient flow and mass transport simulations were run in vertical cross-sections considering a variably saturated media (Richards' equation). Only experiment 1 was numerically modelled taking into account that the tracer was injected in a solution and a considerable number of samples were collected with small time spacing between sampling. In experiment 2 the small number of collected samples do not allowed for comparison and analysis of tracer behaviour throughout the experiment.

Section 16.1 explains in detail input data while 16.2 and 16.3 present and discuss the obtained results for each section.

16.1 INPUT DATA

All input data considered in the modelling process is summarized in **Table 15**, referring to the set of soil physical and hydraulic properties presented in the previous sections.

Table 15 – Input data for artificial aquifer FEFLOW models

| Parameter | | Section A | Section B | Section C | Ref. |
|------------------------------------|-------------------------------------|-----------|---------------|-----------|------|
| Top section area (m ²) | | 1.0925 | 1.0925 | 0.96425 | - |
| Height of section profile (m) | | 2.055 | 2.04 | 2.03 | - |
| Total simulation time (d) | | | 3 | | - |
| Soil parameters | Natural soil | | 3.46 | | - |
| | K (m/d) | | | | |
| | Soil mixture | - | 3.27 | - | - |
| | OM layer | - | - | 1.7 | - |
| | Natural soil | | 0.38 | | - |
| | n | | | | |
| | Soil mixture | - | 0.38 | - | - |
| | OM layer | - | - | 0.4 | - |
| Boundary conditions | Upper | | Well BC | | - |
| | Input BC volume (m ³ /d) | 2.877 | | 2.538 | - |
| | Lower | | Fluid-flux BC | | - |
| | Output BC permeability(m/d) | 2.613 | | 2.305 | - |

| Parameter | | Section A | Section B | Section C | Ref. |
|---------------------------------|--|-----------------------|-----------|-----------|----------------------------|
| Solute parameters | Diffus. Coef. In Water (m^2/s) | NO_3^- | 1.7 | | bionumbers.hms.harvard.edu |
| | | NO_2^- | 1.7e-9 | | |
| | | NH_4^+ | 1.86 | | |
| | Long. Dispersivity | | 2 | | Simunek et al. (2013) |
| | Dispersivity Anis. Factor | | 0.1 | | - |
| Solute transport boundary cond. | Upper | Concentration flux BC | | | - |
| | Concentration (mg/L) | NO_3^- | 5.9 | | - |
| | | NO_2^- | 0.001 | | - |
| | | NH_4^+ | 3.7 | | - |

For each vertical cross-section a 500 element grid was generated (**Figure 116**), taking into account the dimensions as well as the distribution of the soil mixture and organic matter layers presented in **Figure 101** and described in section 15.2.

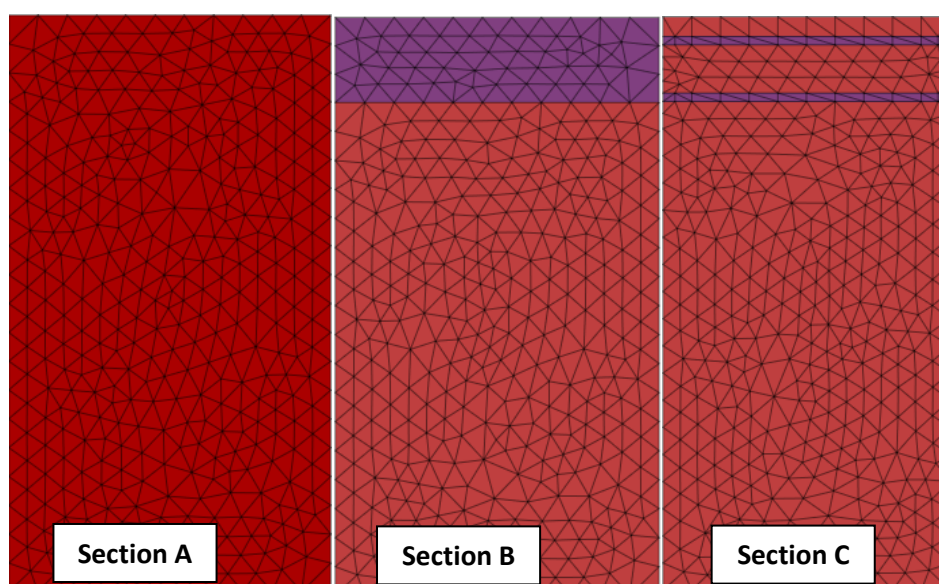


Figure 116 – Finite element grid for each modelled vertical section. Red cells represent natural soil while purple cells show the position of the soil mixture in Section B and organic matter layers in Section C

Concerning the soil permeability, a set of considerations were taken into account:

- For the natural soil in all sections the average value of permeability used refers to that obtained for first day of the soil-column experiments previously conducted.
- Soil mixture permeability refers to the value obtained for a similar mixture artificially created and also tested in soil-column experiments.
- Organic matter layer permeability value is half of the K used for the natural soil. These layers weren't previously tested in soil-column experiments due to the large organic content (mainly decomposed roots, tree barks and leaves).

Porosity is considered the same for the natural soil (and was also determined from soil-column experiments) and for the soil mixture, and is slightly higher for the organic matter layers. This last assumption results from the composition of these organic matter layers with large organic decomposing plant parts.

A set of boundary conditions (BC) were established aiming to achieve the main water flow observed in the artificial aquifer cross-sections. At the top a specific volume is injected through a Well BC. Input volume results from the proportional distribution of the injected volume to the different sections, taking into account that section C top area slightly smaller in comparison to section A and B (**Figure 101**), therefore a smaller inflow volume is considered.

At the bottom, and considering the characteristics of the artificial aquifer outflow (**Figure 101**), a Fluid-flux BC was considered with drainage values equivalent to the injected values by the top area of each section. This way the flux is continuous and it is possible to consider an equilibrium state between inflow and outflow.

Solute parameters were defined using data from previously conducted simulations (dispersivity anisotropy factor), bibliographic references (longitudinal dispersivity) and open databases (diffusion coefficient in water).

Finally, it is considered for the solute BC that a known concentration is injected at the top of each section. In this case a Concentration flux BC was used giving the concentrations values at inflow determined by analysing the tracer solution used in experiment 1 (for the exception of nitrites where a very low value was used).

The models ran, as it was referred previously, in transient state for 3 days (d), where t_0 is the time where the sprinklers at the top of the artificial aquifer were opened. Tracer injection started at $t = 0.96875$ d and stopped at $t = 0.99$ d.

To understand the tracer concentration variations throughout the experiment and along the vertical cross-sections a set of observation points (OPs) were equally positioned on the grids (**Figure 117**) – OP1 as the first and uppermost point and OP6 as lower one.

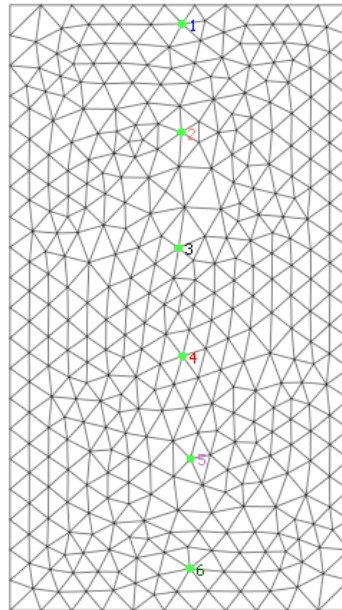


Figure 117 – Position of the observation points along each vertical section

16.2 RESULTS

Output results will be represented in Concentration [mg/L] vs Time [d] for each tracer simulated by observation point. Each concentration curve has the colour or the specific observation point showed in Figure 117. It is important to keep in mind that presented results at this point come from the non-calibrated input data. Disclosing this information is important for the sake of result interpretation.

16.2.1 Section A

Results for concentration variation through time for nitrates, nitrites and ammonia of the artificial aquifer are represented respectively in **Figure 118**, **Figure 119** e **Figure 120**.

For nitrites and ammonia it is possible to observe the increase of concentration immediately after tracer injection on the upmost observation point. This peak is followed by a fast decrease in concentration after the tracer injection stopped, assuming approximately at $t = 1$ d a concentration very close to 0 mg/L. Nitrates show, as expected from the inflow tracer solution concentration, higher concentration at the peak, compared to ammonia.

For these tracers, increase of concentration is also perceived in all other observation points, but only on OP 2 the concentration starts to decrease after $t = 1$ d.

Nitrites show very low concentration in all observation points.

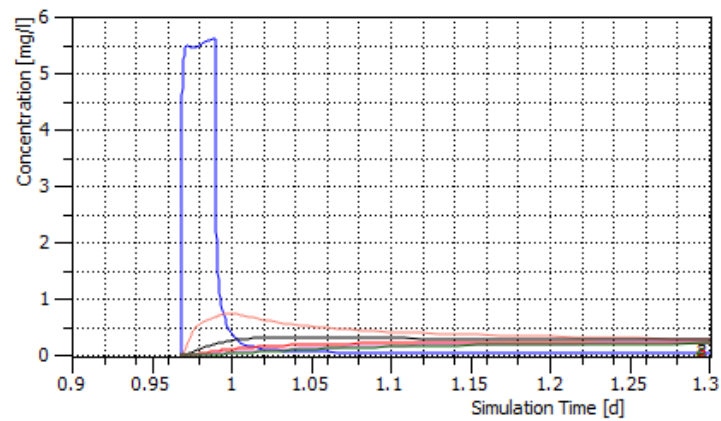


Figure 118 – Nitrates distribution throughout the experiment per observation point in section A

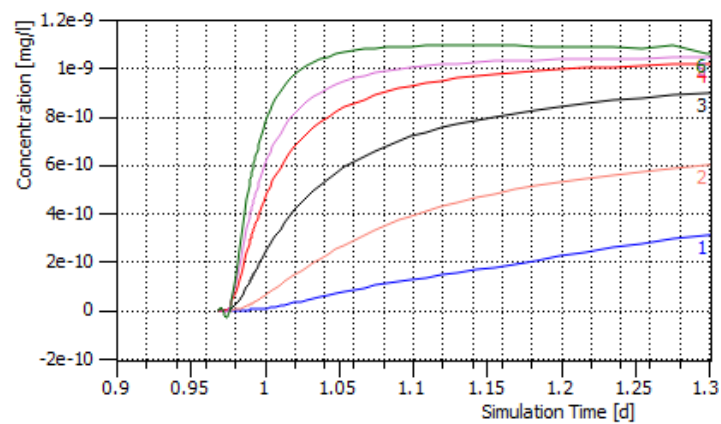


Figure 119 – Nitrites distribution throughout the experiment per observation point in section A

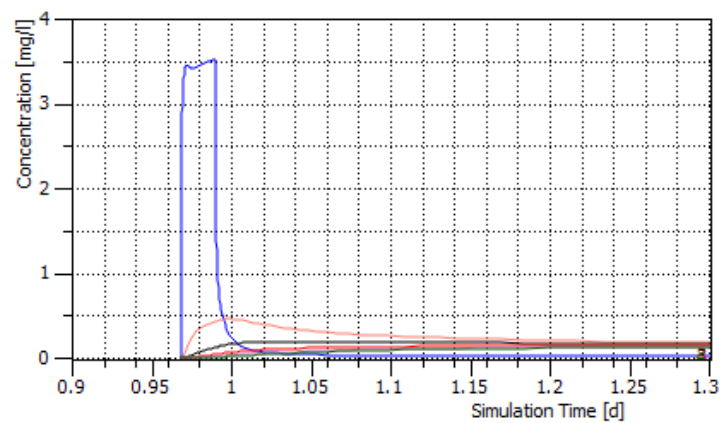


Figure 120 - Ammonia distribution throughout the experiment per observation point in section A

16.2.2 Section B

Results for concentration variation throughout time for nitrates, nitrites and ammonia of the artificial aquifer are represented respectively in **Figure 121**, **Figure 122** and **Figure 123**.

In section B, both nitrate and ammonia show a very similar behaviour to section A, with a significantly immediate increase in concentration and the abrupt decrease after tracer injection stopped. Although the maximum value observed for both traces in OP1 is equal to that observed in section A, it takes slightly more time to achieve it, possibly due to the difference in permeability between the soil mixture and the natural soil.

For all the other observation points a similar pattern to section A is registered, and nitrites show also very small concentrations.

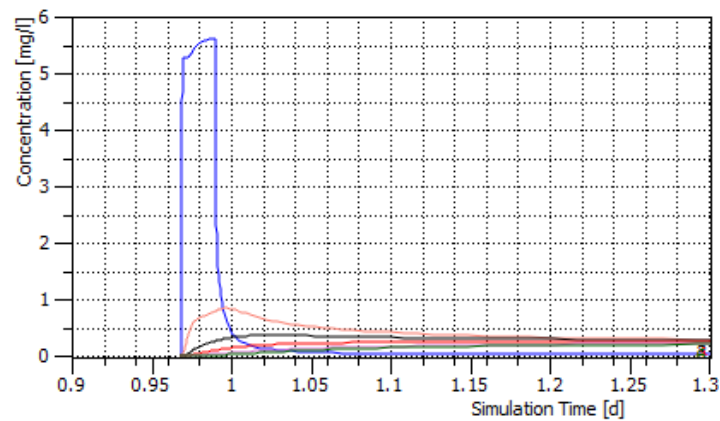


Figure 121 – Nitrates distribution throughout the experiment per observation point in section B

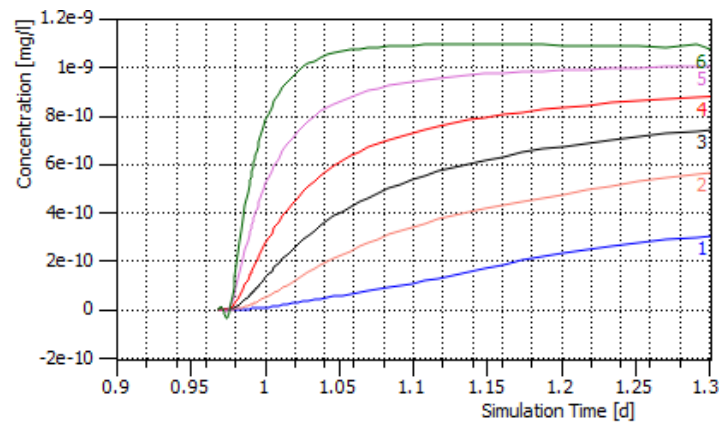


Figure 122 – Nitrites distribution throughout the experiment per observation point in section B

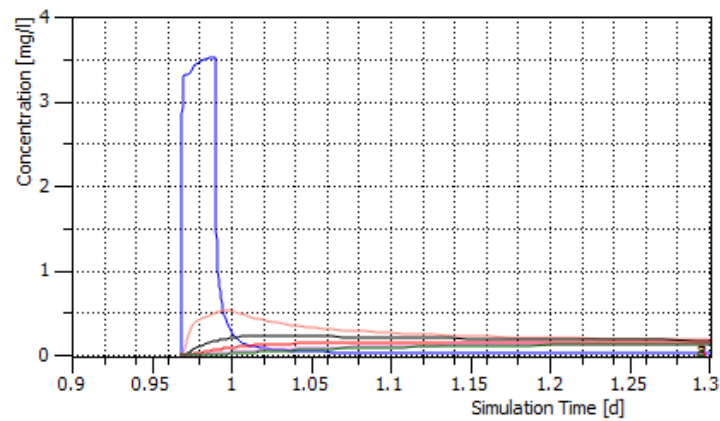


Figure 123 – Ammonia distribution throughout the experiment per observation point in section B

16.2.3 Section C

Results for concentration variation throughout time for nitrates, nitrites and ammonia in section C of the artificial aquifer are represented respectively in **Figure 124**, **Figure 125** and **Figure 126**.

Once again a fast increase in concentration in OP1 is observed for both nitrates and ammonia, although the curve is different from the other sections. The first organic matter layer (which has lower permeability) results in a very brief decrease in tracer concentration only to be followed by a second rapid increase. After the second organic matter layer the concentration of both tracers decrease again to low values (mainly in observation point 2, below the 2nd OM layer). Nitrites show once more very small concentrations as expected.

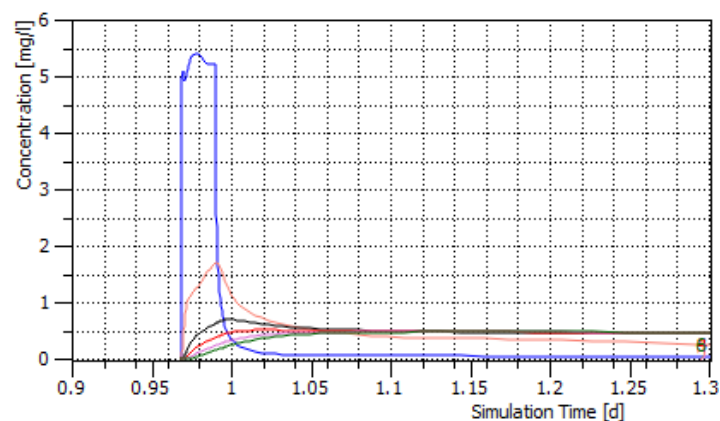


Figure 124 – Nitrates distribution throughout the experiment per observation point in section C

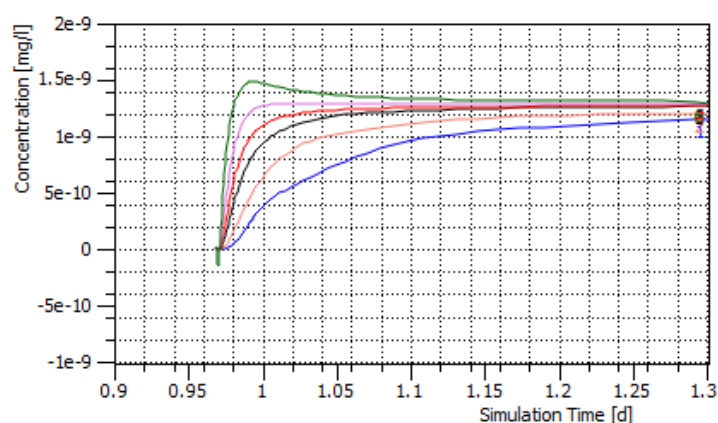


Figure 125 – Nitrites distribution throughout the experiment per observation point in section C

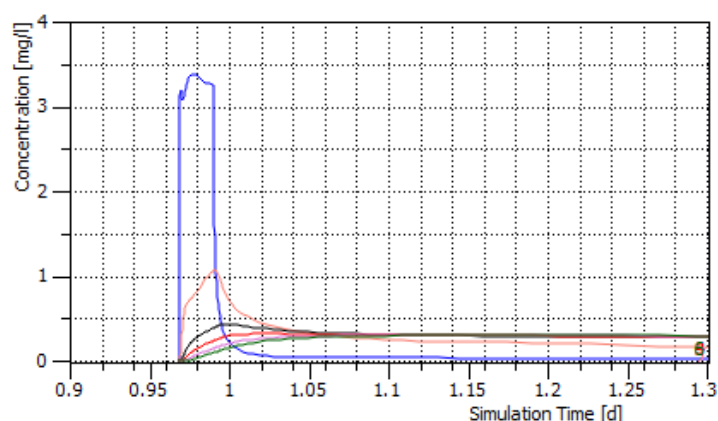


Figure 126 – Ammonia distribution throughout the experiment per observation point in section C

16.3 GENERAL RESULTS DISCUSSION

In general, the considered tracers are immediately dispersed at the uppermost part of all the vertical sections. Although smaller changes in tracer behaviour are observed due to the different hydraulic parameters of soil mixture and organic matter layers the final outcome is similar in all sections.

While there are significant differences in concentration the behaviour in the uppermost part of all section, mainly for nitrates, is similar between what was observed during experiment 1 and what was obtained by the numerical models. Significant differences were observed between model and reality in the lower part of all the vertical cross-sections where the concentrations of nitrates are several orders of magnitude higher than those calculated.

Nitrification process was not simulated, with degradation of nitrates to ammonia. If this was the case a different behaviour should have been observed in the concentration vs time graphics, where nitrates peak is observed in the uppermost OPs, a second peak in the OPs situated in the middle of the vertical section OPs related to nitrites and a final concentration peak e the lower OPs associated to ammonia.

White book on MAR modelling

Deliverable D12.7

CHAPTER 7 – NUMERICAL MODELLING OF COLUMN EXPERIMENTS

MARTINS, T. (LNEC) , LEITÃO, T.E. (LNEC), ILIE, A.M.C. (UNIV. BOLOGNA/LNEC), LOBO FERREIRA, J. P. (LNEC)

17 INTRODUCTION TO NUMERICAL MODELLING OF COLUMN EXPERIMENTS

Numerical modelling exercises were conducted using data collected in the soil-column experiments. These exercises represented a helpful tool to describe contaminants behaviour as well as some removal mechanisms and the conditions in which they occur. Solute transport was considered for the column behaviour understanding.

A set of soil-column experiments were conducted in MARSOL (please refer to Work Package 14 concerning water quality where water constituents, fate of pollutants and soil column experiments were studied) using the natural soil of the area of installation of the infiltration basins in the South of Portugal DEMO area of São Bartolomeu de Messines in the Querença – Silves aquifer system (Work Package 4).

The soil-column experiments apparatus used is briefly presented in Figure 127. In this apparatus two types of injection can be considered – continuous or by pulse. For continuous water injection, a volumetric peristaltic pump is used while for pulse injection the water was directly poured from a container to the column. Water naturally flows from the bottom outlet to the sample tubes and outflow samples were collected at defined periods and conditioned in dark glass vials or bottles for later analysis.

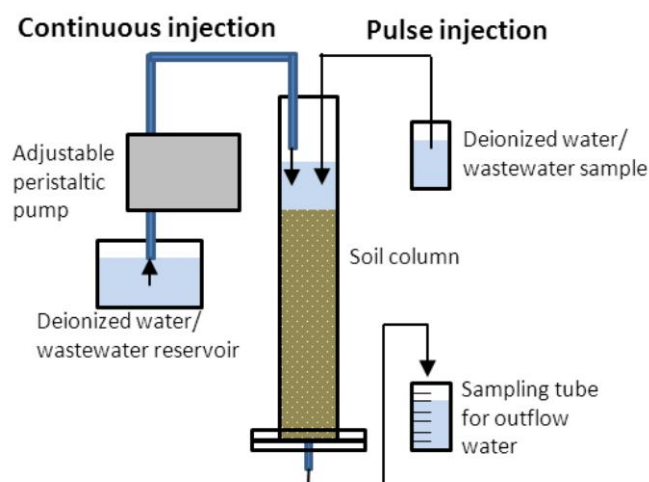


Figure 127 – Soil-column apparatus and diagram of operation

Besides the natural soil of the area of installation, water that will be used in real scale facilities was also used in the experiments - wastewater was collected in São Bartolomeu de Messines Wastewater Treatment Plant for previous injection in the columns of soil. Both soil and water were characterized concerning constitution and quality. The soil characterization and inflow wastewater quality results are presented in Martins (2016). The experiments were held in different time periods, from a few hours to several days and aimed to assess the importance of soil compaction procedures, saturation-desaturation processes and the effects of inflow water quality can have in the outflow rate. In total 5 soil-column experiments were conducted in the natural soil. Table 16 presents the main characteristics of the soil-column experiments which results were considered in the modelling process (Column 3 and Column 4).

Table 16 - Synthesis of the operating details of the soil-column experiments conducted in the natural soil

| | Column 3 | Column 4 |
|-------------------------------|---------------------------------------|--|
| Soil thickness (cm) | 20 | 30 |
| Saturation conditions | Started saturated Always saturated | Started saturated Unsaturated/ saturated cycles |
| Injection method | Continuous | Continuous/ pulse |
| Experiment time length (days) | 5 | 33 |

For the solute transport modelling Hydrus-1D (Jacques and Šimůnek, 2005) was used. This software is widely used to simulate flow and solute transport in variably saturated soils and

groundwater in both steady and transient state. One dimensional flow can be modelled at different scales from laboratory soil-columns to larger experiments. Hydrus-1D can also consider inverse problems when some parameters need to be calibrated or estimated from observed data.

18 INPUT DATA

Given that nitrogen cycle is highly dependent on redox conditions, modelling the nitrification process can be useful to understand the conditions inside the column. Also, nitrogen cycle constituents are common in the matrix of the water injected in the columns – treated wastewater.

For this modelling process only continuous saturated conditions were considered – all time length of Column 3 experiment (continuous flow) and the first saturation cycle of Column 4. Other soil-column experiments results were not considered due to the small number of outflow samples or because short sat-unsaturation cycles used where no samples were collected.

Concerning the contaminants which transport was modelled, three main compounds were considered – nitrates (NO_3), nitrites (NO_2) and ammonia (NH_4). The concentrations measured both at inflow and outflow are presented in Figure 128 (Column 3) and Figure 129 (Column 4).

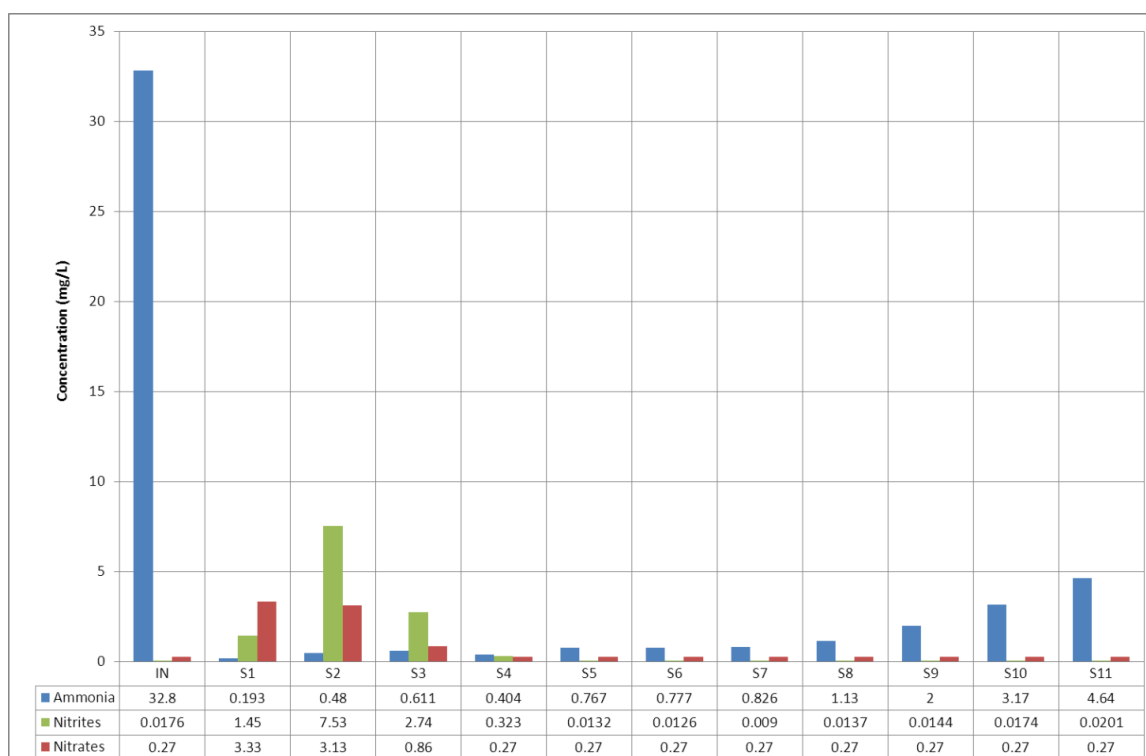


Figure 128 – Nitrogen cycle components concentration in Column 3 inflow/outflow

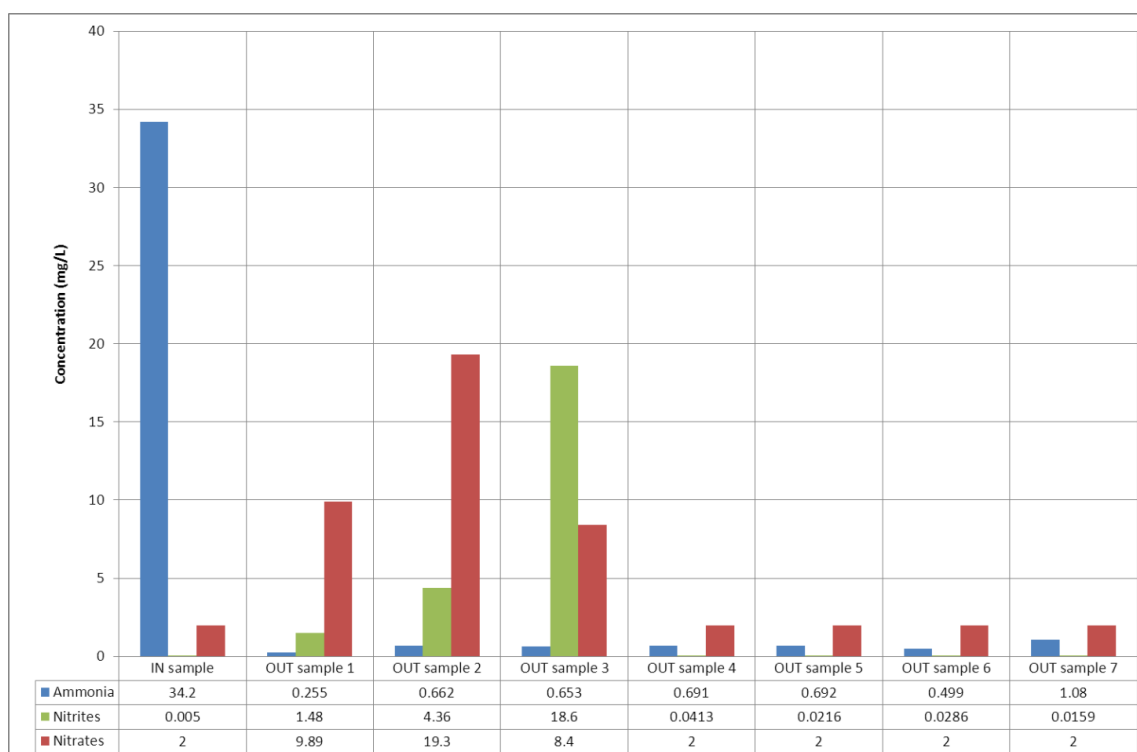


Figure 129 – Nitrogen cycle components concentration in Column 4 inflow/outflow

Simulations were run in transient state for solute transport, where the inflow and outflow concentrations were considered as solute top and bottom boundary conditions respectively. Both models were divided into five time intervals.

Input parameters for both soil-column experiments are presented in Table 17. Some of the input parameters were obtained by bibliographic research while others were inverse modelled (Ilie, 2015).

Table 17 – Input data for HYDRUS-1D C3 and C4 models

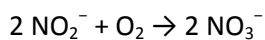
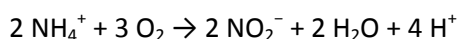
| Parameter | | Column 3 | Column 4 | Ref. | Observations |
|-----------------------------------|-----------------------------------|----------|----------|-------------|---|
| Depth of the soil profile (cm) | | 20 | 30 | - | - |
| Total time (min) | | 6131 | 3084 | - | - |
| Time-variable boundary conditions | | 12 | 8 | - | - |
| Soil parameters | Bulk density (g/cm ³) | 1.44 | 1.52 | Ilie (2015) | Determined by Rosetta Lite v1.1 from soil granulometry without considering > 2 mm fraction (clay = 78.51%; silt = 18.96%; sand = 2.53%) |
| | Qr | 0.0368 | 0.0364 | | |
| | Qs | 0.3907 | 0.3704 | | |
| | Alpha (1/cm) | 0.0446 | 0.0457 | | |
| | n | 1.7305 | 1.7596 | | |

| | | | | | |
|---------------------------------|---------------------|--------------------------------|--------------------------------|------------------------------|---|
| | Ks (cm/min) | 0.1011 | 0.0798 | | |
| Boundary condition | Upper | Constant pressure head (20 cm) | Constant pressure head (30 cm) | - | - |
| | Lower | Free drainage | | - | - |
| Solute parameters | Long. Dispersivity | 2 | 2 | Simunek <i>et al.</i> (2013) | - |
| | Diffus. Water. | 0.000833 | 0.000833 | Ramos and Carbonell (1991) | - |
| | Reaction parameters | Inverse solution modelling | | Ilie (2015) | - |
| Solute transport boundary cond. | Upper | Concentration flux BC | | - | - |
| | Lower | Zero concentration gradient | | - | - |

19 RESULTS

Simulations were successful and the model converged to a solution. Model results of contaminant concentration vs depth for both columns for the solutes are presented in Figure 130.

Both simulations show similar behaviour along the columns, with ammonia being mostly retained on the top of the column whereas nitrites show a small increase in concentration as ammonia is oxidized to nitrite, and then nitrites decrease at the column bottom as they are transformed into nitrates. This confirms that nitrification may be expected in soil-columns confirming, from the analysis of the results of the three columns, that ammonia (NH_4^+) is being nitrified while nitrites (NO_2^-) and nitrates (NO_3^-) concentration increased:



In Column 3 simulation, ammonia concentration rapidly decreases to zero at the first half of the column while in Column 4 some ammonia can be observed at the bottom section but in much lower concentration than that observed on the top. Nitrites concentrations show a small increase in the first centimetres of the column top and decreases again. In Column 4 bottom nitrites are observed at the outflow. Nitrates continuously increase in Column 4 while in Column 3 this compound increases at the first ¼ of the column thickness and slowly decreases after that.

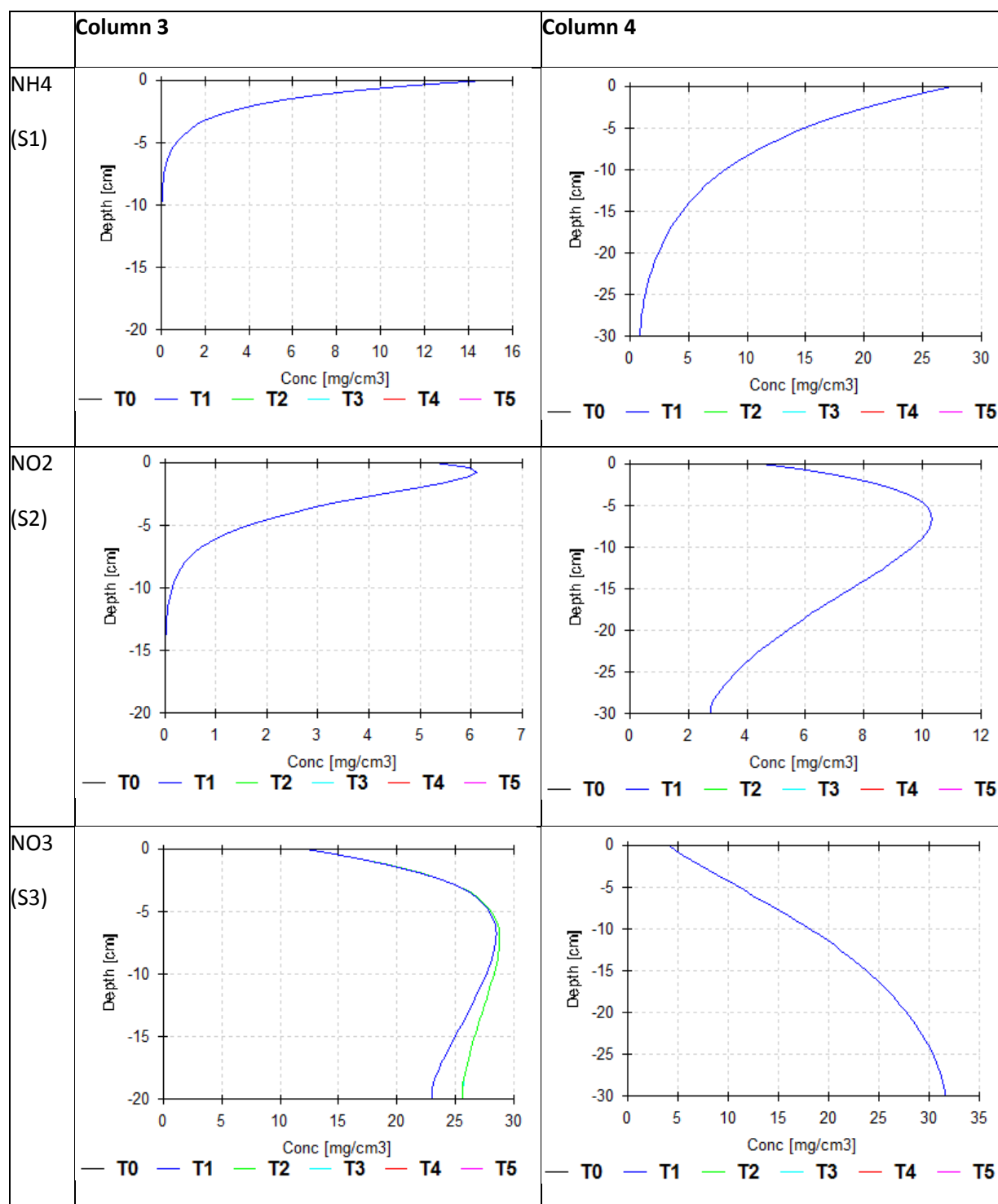


Figure 130 – Hydrus-1D results for nitrogen simulation (concentration through depth)

For the considered parameters, solute retention and possibly transformation can be observed, which can suggest that good conditions occur at the columns for nitrification, with lower oxygen content on the column top as water is injected and slight oxygenation on the bottom (where higher concentration of nitrates is observed).

Five nodes were represented along both columns, equally distributed between them. Results for variation of concentration through time taken from these nodes (from top to bottom) are presented in Figure 131 and Figure 132.

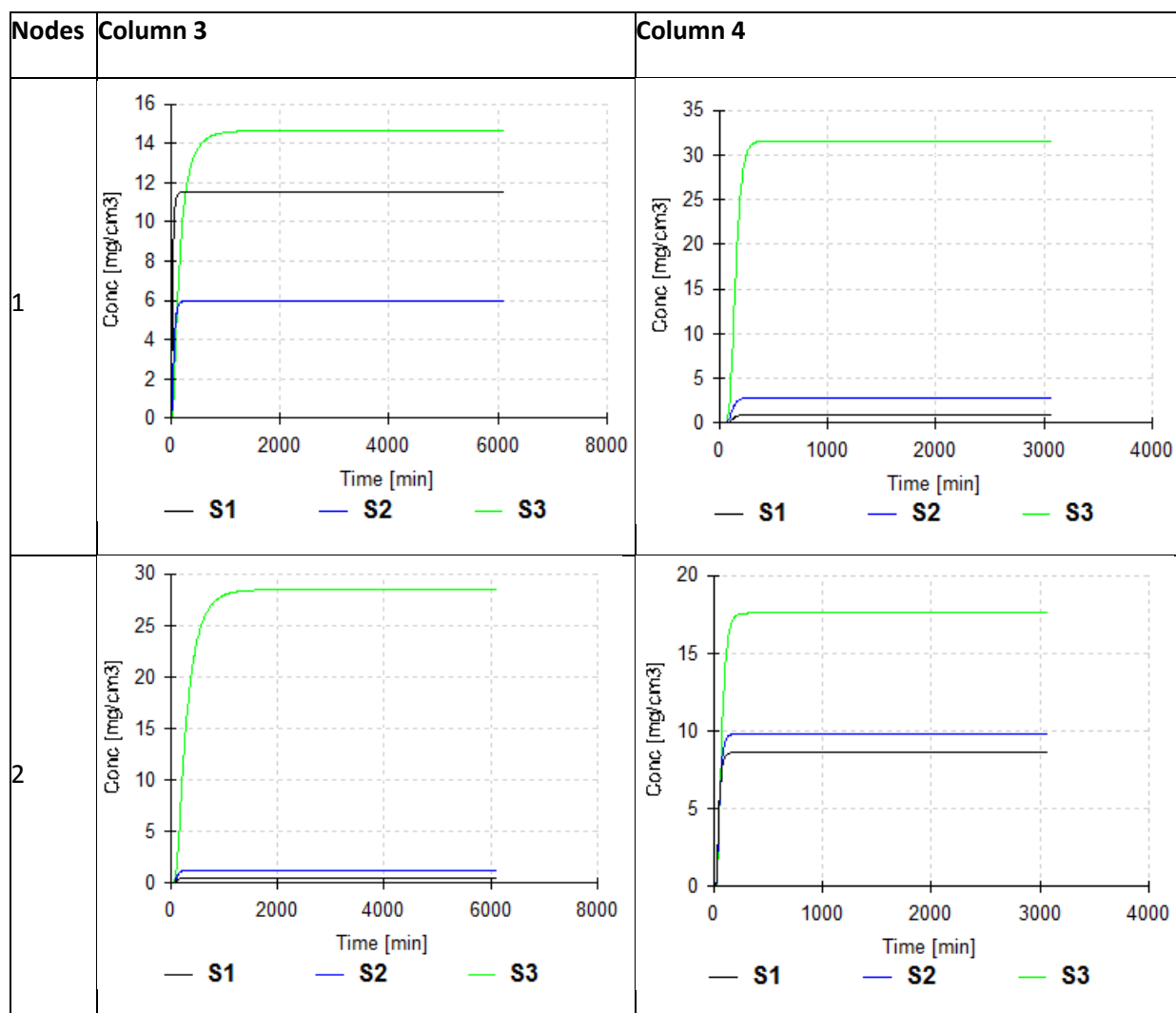


Figure 131– Hydrus-1D results for nitrogen simulation for node 1 and 2 (S1 – ammonia, S2 – nitrites, S3 – nitrates)

Solute behaviour is observed in different depths along the columns, through time (from point 1 to 5). Again ammonia (S1) concentrations are very low (or null) at the bottom in both columns.

In an overview of the model results, Column 3 achieves stabilization in these compounds concentration in the first 1000 minutes and in Column 4 at approximately 200 minutes. If pore-volumes determined in soil-column experiments are considered and that 1L of water is injected in both columns (steady state flow), these periods correspond to 5.7PV for C3 and 3.8PV for C4.

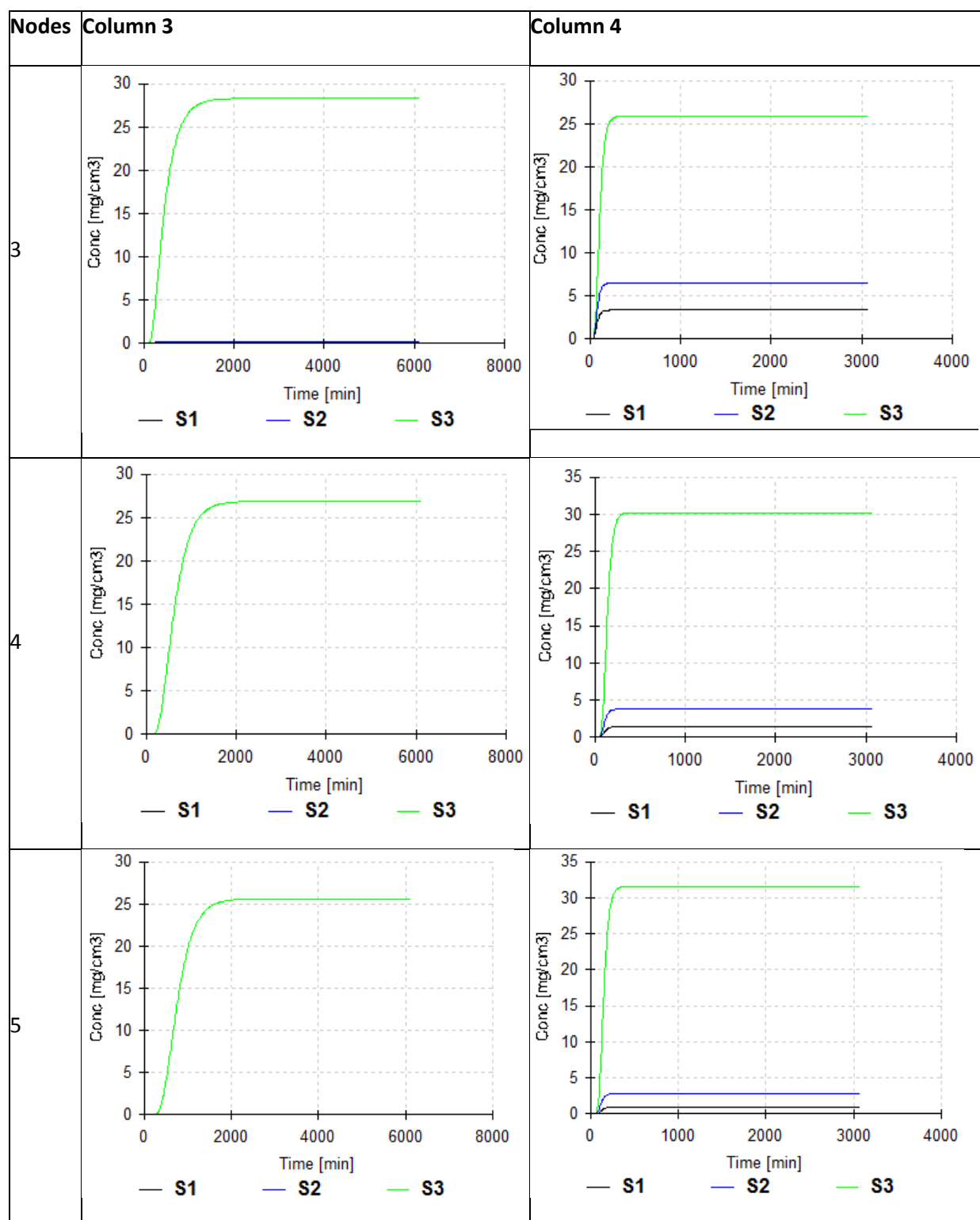


Figure 132– Hydrus-1D results for nitrogen simulation for nodes 3, 4 and 5 (S1 – ammonia, S2 – nitrites, S3 – nitrates)

20 DISCUSSION AND CONCLUSIONS TO NUMERICAL MODELLING OF COLUMN EXPERIMENTS

Although ammonia retention on the column is confirmed by inflow and outflow comparison, particularly in natural soil experiments, the observed behaviour calculated in simulations is not what is observed in the soil-column experiments results, considering nitrates concentration. In soil-columns, nitrates show low concentration at outflow, instead of high concentrations calculated in the model. This may result from the time of simulation considered, but also, in the soil columns, to a process of retention of nitrates, observed in the models, where nitrates have high concentrations at the bottom section of the column and possibly are not mobilized to the water. These models can be obviously calibrated for future experiments, but this simple approach of soil-column modelling allowed understanding and predicting the behaviour of a set of contaminants.

Given more robust data this method may be used in other contaminants, allowing for the understanding or validation of the processes that occur inside the column.

References

Ilie, A.M. (2015) Personal communication.

Martins, T. (2016) Contaminants retention in soils as a complementary water treatment method: application in soil-aquifer treatment processes. Master Thesis. Faculty of Sciences. University of Lisbon, 150p.

Ramos, C., Carbonell, E. (1991) Nitrate leaching and soil moisture prediction with the LEACHM model. *Fertilizer Research* 27, 171-180p.

Jacques, D., Šimůnek, J. (2005) User Manual of the Multicomponent Variably-Saturated Flow and Transport Model HP1, Description, Verification and Examples, Version 1.0, SCK/CEN-BLG-998, Waste and Disposal, SCK/CEN, 79 p.

Šimůnek, J., Šejna, M., Saito, H., Sakai, M., van Genuchten, M. (2013) The HYDRUS 1.D Software Package for Simulating the One-Dimensional Movement of Water, Heat, and Multiple Solutes in Variably-Saturated Media – Version 4.17. Department of Environmental Sciences, University of California, 308p.

White book on MAR modelling

Deliverable D12.7

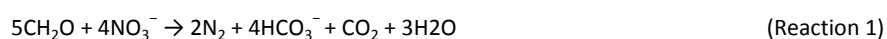
CHAPTER 8 – NATURAL ATTENUATION PROCESS MODELLING

XAVIER SANCHEZ-VILA, PAULA RODRIGUEZ-ESCALES (UPC)

21 INTRODUCTION TO NATURAL ATTENUATION PROCESS MODELLING

One of the main aims of Managed Aquifer Recharge is the improvement of the quality of the recharged water through enhancing the natural attenuation of the main pollutants. In this way, the presence of nitrate is one of the main risk because it is one of the most prevalent and common groundwater and surface water contaminant (European Environment Agency, 2007; Organisation for Economic Co-operation and Development, 2008; Rivett et al., 2008). The proportions of water bodies at high risk of nitrate pollution (showing mean nitrate concentrations greater than 25 mg/l) were reported as 80% in Spain, 50% in the UK, 36% in Germany, 34% in France and 32% in Italy (European Environment Agency, 2007). In this way, characterizing its natural attenuation process is quite important to guarantee the good operation of MAR facilities.

The main attenuation process of nitrate is biological denitrification. Biotenitrification is the reduction of nitrate to gaseous dinitrogen by anaerobic facultative bacteria that use nitrate as an electron acceptor and that are ubiquitous in surface water, soil and groundwater (Beauchamp et al., 1989). Denitrifying bacteria are generally heterotrophic and utilize organic matter as an electron donor (Reaction 1). A limited number of bacteria are also capable of carrying out autotrophic denitrification using electron donors such as reduced sulfur, dihydrogen gas, ferrous iron and uranium (IV) (Straub et al., 1996; Zumft, 1997; Beller, 2005).



Aquifers vary widely in their denitrifying capacities, but biotdenitrification appears to be possible anywhere bacteria thrive, electron donors are present and oxygen levels are low (Korom, 1992). Nevertheless, under natural aquifer conditions, a major limiting factor for biotdenitrification to occur is the lack of electron donors to provide energy to heterotrophic

microorganisms. Geochemical interactions can occur between the biodenitrification reactants and the porous geologic medium in response to biodegradation reactions. These interactions may play a critical role in EIB implementation. Because of inorganic carbon production and pH alteration, carbonate mineral dissolution/precipitation is induced by heterotrophic biodenitrification. Another important factor when monitoring EIB in the field is dilution resulting from recharge, hydrodynamic dispersion, mixing, or other processes. Because of dilution, a decrease in nitrate concentration cannot always be attributed to degradation. Monitoring the changes in the nitrogen and oxygen isotope ratios of nitrate ($\delta^{15}\text{N-NO}_3^-$ and $\delta^{18}\text{O-NO}_3^-$) allows nitrate transformation and dilution to be distinguished.

In this context, the development of biogeochemical models to reliably predict the rates of biodenitrification as well as other attenuation processes would be useful for designing MAR facilities and monitoring their performance. In this context, a field-scale reactive transport model (RTM) of denitrification integrating hydrology, microbiology, geochemistry, and isotope fractionation can provide significant benefits for the planning, characterization, monitoring and optimization of this technology in field applications. The integration of all the processes allows the evaluation of their relationships with each other and the prediction of secondary processes such as induced mineral precipitations or dissolution.

21.1 BRIEF DESCRIPTION OF SITE AND MODEL CODE

Denitrification modelling was carried out in an unconfined, carbonated, and well-connected aquifer using ethanol as a representative labile organic carbon source. The model simulated a cross section (2D) of the aquifer of 26 m of length and 4 m of depth. The denitrification test was performed for five months and then stopped. Once the background concentration of nitrate had recovered ($120 \text{ mg NO}_3^-/\text{L}$, 1.9 mM), a slug injection of ethanol was performed. The presented model was focused on this slug injection and its subsequent monitoring during two days. The model was validated using the experimental information monitored at two different depths of two observation wells (MW-2 and MW-3).

The model code used was PHAST (Parkhurst et al., 2010). This code was used both for conservative and reactive transport simulations. PHAST couples the flow simulator HST3D and the geochemical model PHREEQC-2 (Parkhurst and Appelo, 1999).

21.2 MODEL CONSTRUCTION

The conservative transport model was constructed based on the bromide tracer test. Because the field tests demonstrated that this fracture medium could be assumed to be an equivalent porous medium, we used the transport equations for porous media. PHAST solved the conservative transport model following equation 1:

$$\phi \frac{\partial c_i}{\partial t} = -q \nabla c_i + \phi \nabla (D \nabla c_i) \quad (1)$$

where D is the dispersion tensor [L^2T^{-1}], q is the Darcy's velocity [LT^{-1}] which is related to hydraulic conductivity [LT^{-1}] and groundwater gradient [-], ϕ is the porosity [-]. The model was solved under transient conditions.

Related to the reactive processes, next table (Table 18) summarizes the main equations used in the denitrification model:

Table 18. Reactive processes involved in biogeochemical modelling

| Reactive processes | | Equation |
|--|----------------------------|---|
| Biological processes (for nitrate and sulfate reduction) | Exogenous respiration rate | $r_{ED} = -k_{max} \frac{[ED]}{[ED] + K_{S,ED}} \frac{[EA]}{[EA] + K_{S,EA}} [X]$ (2) |
| | | $r_{EA} = Qr_{ED} - Sb[X]$ (3) |
| | Biomass rate | $r_X = -Y_h r_{ED} - b[X]$ (4) |
| Geochemical interaction | Calcite precipitation | $r_{min,prep} = K_{obs} \Omega - 1$ (5) |
| | | $\Omega = \frac{IAP}{K}$ (6) |
| Stable isotope geochemistry model (general rates) | Light isotopes | $r_{z,l} = r_z \frac{[Z_l]}{[Z_l] + [Z_h]}$ (7) |
| | Heavy isotopes | $r_{z,h} = r_z \frac{[Z_h]}{[Z_l] + [Z_h]} (\epsilon + 1)$ (8) |
| ED [ML ⁻³] electron donor concentration | | b [T ⁻¹] is the decay constant (0.15 d ⁻¹) |
| EA [ML ⁻³] electron acceptor concentration | | K _{obs} [ML ⁻³ T ⁻¹] is the precipitation rate constant (8.6x 10 ⁻⁶ Md ⁻¹) |
| X [ML ⁻³] biomass concentration | | Ω [-] is the saturation state of calcite |
| k _{max} [T ⁻¹] is the maximum consumption rate of the electron donor (1.1x10 ² mol C-ethanol/mol C-biomass d) | | IAP is the ion activity product |
| K _{S,ED} [M L ⁻³] and K _{S,EA} [M L ⁻³] are the half-saturation constants (1.5x10 ⁻¹ , 1.7x10 ⁻⁴ respectively) | | K is the thermodynamic equilibrium constant at 15°C (from Phreeqc database) |
| Q [-] and Y _h [-] are stoichiometric parameters (1.9 and 0.7) | | ε (‰) is the isotopic enrichment factor |
| S [-] is stoichiometric parameter for endogenous respiration (0.92, internally calculated by Phreeqc) | | |

21.3 RESULTS AND DISCUSSION

The results of the conservative transport model are shown in Figure 133. Multilevel sampling indicated an earlier arrival of bromide in the deeper part of MW-2 (Figure 15), whereas most of the bromide mass was detected at 0.14 d, a peak was observed at 0.05 d. Moreover, the concentration in the deeper part (reaching 20 mM) was twice those at shallower depths (approximately 10 mM). These differences in bromide concentration at different depths were not observed in MW-3, which indicates a homogenization of bromide transport along the flow line. Porosity was only related to the secondary porosity because groundwater flow occurs mainly through fractures. The obtained dispersivity values (1.4 m (from 0 to 14 m of the domain) and 6.5 m (from 14 to 26 m)) were consistent with the scale (26 m) of the biodenitrification application (Gelhar et al., 1992).

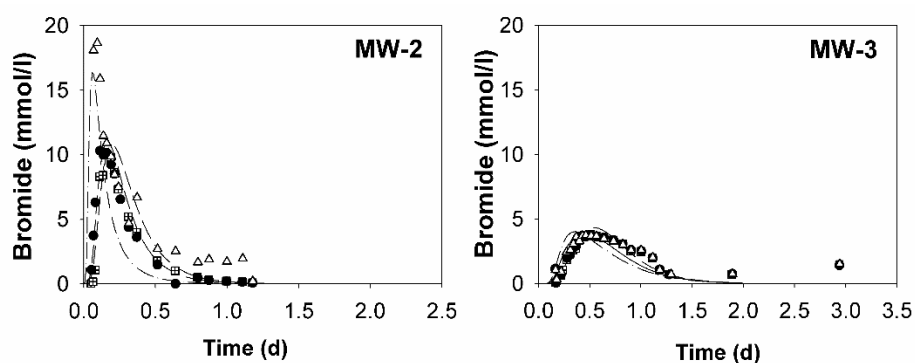


Figure 133 - Bromide BTCs at two observations points of the model.

Figure 134 shows the results of the 2D RTM for the upper and lower ends of two observation wells (MW-2 and MW-3) using the parameters from Table 1, all of them in the range of published data. In general, the model fits well the general trend observed in the field and the modeled values matched the observations. Both MW-2 and MW-3 showed decreasing nitrate concentrations until non-detectable levels were present in less than 0.2 days. This rapid reduction in concentration can be attributed to the high activity of biomass that had been stimulated by ethanol during the previous five months. Both the exhaustion of ethanol and the fast groundwater flow increased nitrate concentrations until they reached background levels in MW-2. The modeled nitrate concentration at MW-3 began to increase after less than one day, while the observed concentrations stayed at zero. The later breakthrough of nitrate observed in the field was attributed to the slower flow component described for the tracer test results that was not taken into account in the model (Figure 133).

Calcite precipitation was confirmed by the decrease of calcium in solution and the increase of the saturation index of calcite (Figure 134g and Figure 134g'). At this point, an increase in the inorganic carbon in both MW-2 (from 9.5 to 10.8 mM) and MW-3 (from 9.5 to 11.4 mM) was observed due to ethanol oxidation. The saturation index of calcite began at negative values but became positive when inorganic carbon was added to the system due to ethanol oxidation. The precipitation rate constant differed between batch scale (1×10^{-10} M/s) and field scale (5×10^{-9} M/s) (Table 1). The modeled values of pH slightly increased from 6.8 before injection to 7.1 (MW2) and 7 (MW3) following the injection (Figure 134). The timing of this increase matched that of the increase of the calcite saturation index in both piezometers. After 0.5-1 days, it recovered to the previous value of 6.8. The overlapping in the error of the measured pH values does not allow evaluating the basification of the media as shown by the modeled values (Figure 134). The observed field values may indicate that the system was buffered by the presence of carbonate minerals which masked the effect of produced inorganic carbon from the denitrification process.

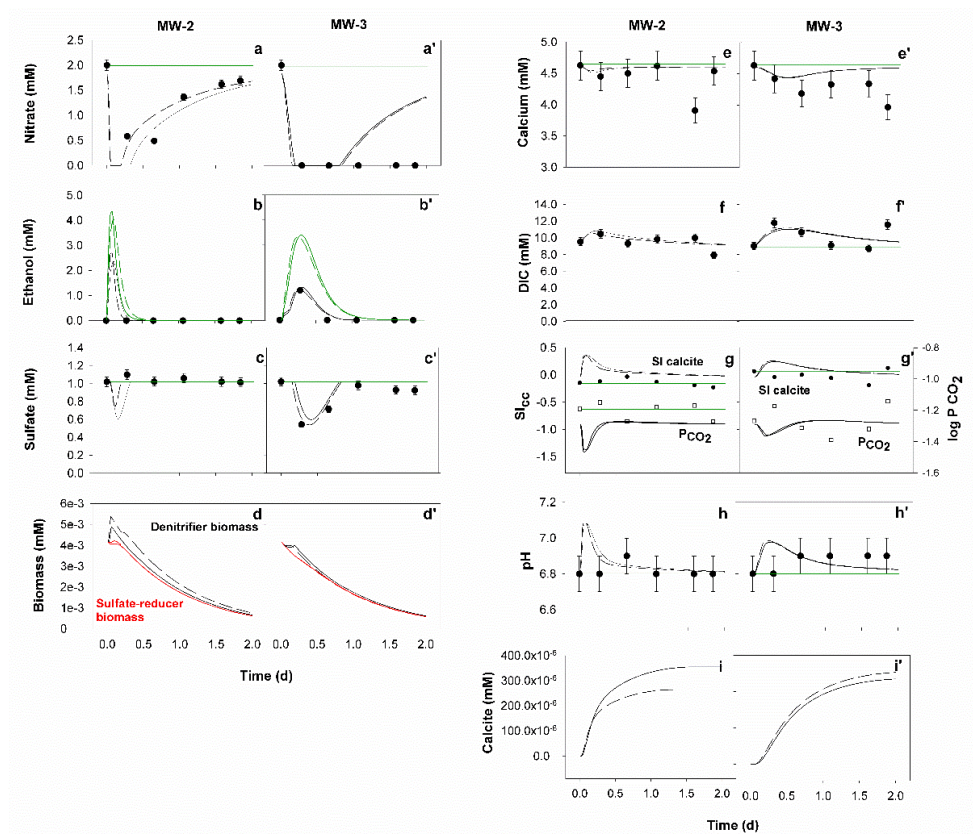


Figure 134 - Modelling results (lines) versus observations (●) for MW-2 and MW-3. Solid lines correspond to 434 m a.s.l., dashed lines correspond to 435 m a.s.l. Red lines correspond to sulfate-reducer biomass, and green lines represent the results of the conservative model without reactions

The modeled N and O isotope ratios matched the observation data reasonably well in MW-2 (Figure 135). In MW-2, the $\delta^{15}\text{N-NO}_3^-$ and $\delta^{18}\text{O-NO}_3^-$ values increased from 13.5 ‰ to 24.4 ‰ and from 5.8 to 12 between days 0.1 and 0.3 at the same time as nitrate decreased (Figure 134). On the other hand, when the nitrate concentrations increased to the background values of the aquifer, the isotopic values also decreased to their initial values.

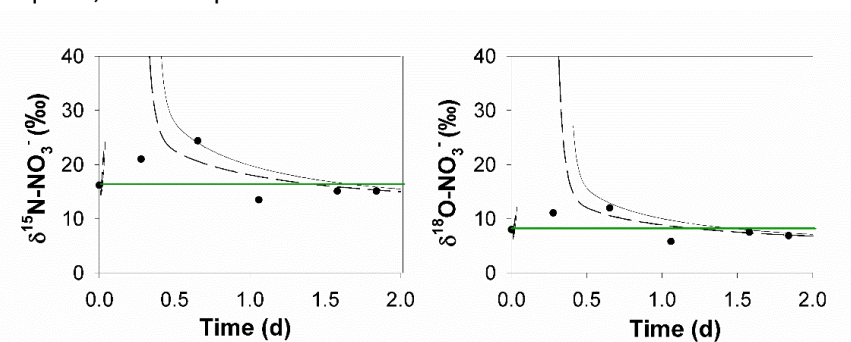


Figure 135 - Simulation of nitrate isotope data in MW-2. Solid lines correspond to 434 m a.s.l., dashed lines correspond to 435 m a.s.l. and green lines represent the results of the conservative model without reactions

Figure 136 summarizes the results of the model in the modelled cross section.

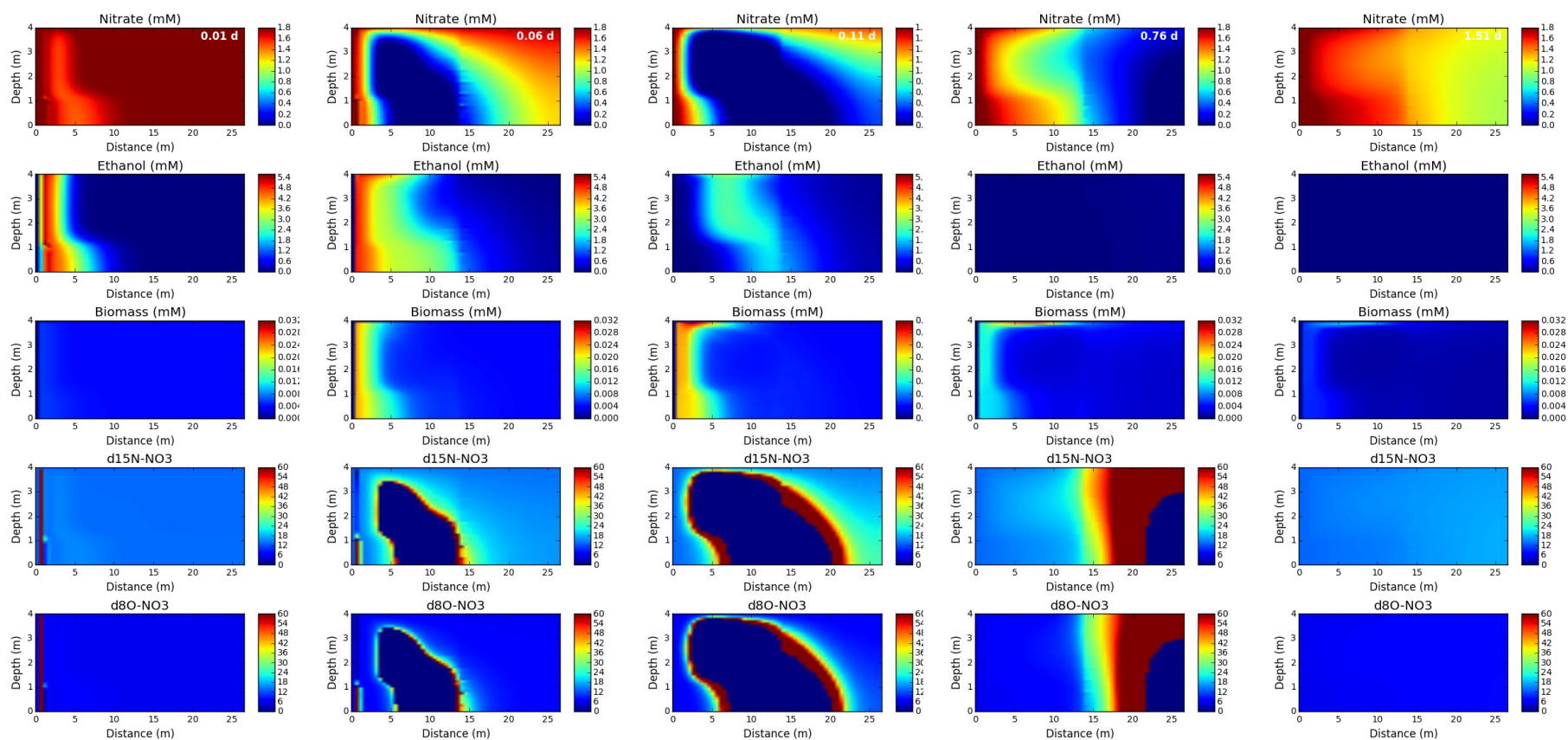


Figure 136 - Denitrification modelling cross section

21.4 CONCLUSIONS

The presented model has allowed evaluating the attenuation processes of nitrate that could occur in MAR facilities. The model considered several processes including (i) exogenous and endogenous microbial nitrate and sulfate respiration coupled to ethanol oxidation and linked to microbial growth and decay, and (ii) geochemical interactions (dissolution/precipitation of calcite), and (iii) isotopic fractionation of the reaction network (^{15}N - NO_3^- , ^{18}O - NO_3^-). This biogeochemical model could be implemented in any MAR facility in order to evaluate the natural attenuation of nitrate.

References

- European Environment Agency, E., 2007. Present concentration of nitrate in groundwater bodies in European countries, 2003.
- Gelhar, L.W., Welty, C., Rehfeldt, K.R., 1992. A critical review of data on field-scale dispersion in aquifers. *Water Resour. Res.* 28.
- Organisation for Economic Co-operation and Development, O., 2008. Environmental performance of agriculture in OECD countries since 1990., p. 576.
- Rivett, M.O., Buss, S.R., Morgan, P., Smith, J.W.N., Bemment, C.D., 2008. Nitrate attenuation in groundwater: A review of biogeochemical controlling processes. *Water Res.* 42, 4215-4232.

White book on MAR modelling

Deliverable D12.7

CHAPTER 9 – MAR DISSEMINATION AND WRAP-UP

JP LOBO-FERREIRA (LNEC), ENRIQUE F. ESCALANTE AND TERESA E. LEITÃO (TRAGSA AND LNEC)

22 MAR DISSEMINATION AND WRAP-UP

22.1 MAR DISSEMINATION

22.1.1 EIP Water AG128 MARtoMARKET

Close cooperation has been developed between European Innovation Partnership on Water Action Group 128 MARtoMARKET and FP7 MARSOL Inno-Demo project. In the EIP Water site http://www.eip-water.eu/MAR_Solutions the following is presented:

Managed Aquifer Recharge technique, or simply MAR, has become, perhaps, the best technique within the Integrated Water Resources Management (IWRM) framework, to palliate Climate Change adverse effects. As some impacts are increasing rapidly in scale and intensity, permanent “technological solutions” are required as a “water innovation in action” line. It is worth mentioning that FP7 INNO-DEMO MARSOL project, that started Dec. 1st 2013, is supporting this AG making available 8 demo sites to show the suitability of MAR techniques.

Involving the principal stakeholders and SMEs in this action group and transferring the results of this action into guidelines/policy will ensure MAR transferability to other locations. This will allow a major social advance (in Europe and worldwide) and can clearly contribute to improving living standards and job creation, as it increases the water availability to important economic sectors, improves human health and well-being, and sustains ecosystem functions and biodiversity.

Perhaps the biggest sector directly affected by MAR technique implementation will be agro-industry. In some Mediterranean countries, farmers are grouped in irrigation communities, what involves individuals, SMEs and even big industries. Their success, most of the times, is affected by water availability, and aquifers are the best way to store water as its capacity overweight traditional

damming and decreases water supply transportation costs. Successful experiences are becoming more and more popular and farmers have become a sector who claims for the implementation of new MAR facilities and opportunities.



Apart from the agro-industry, many other sector have been identified as beneficiaries, as water supply companies, waste water treatment plants and desalination agents, public bodies related to water management at care of the quality, etc. the eco-innovation label might be include in some of their processes thanks to water quality improvements by means of MAR technique.

The activities that have been addressed in this AG are:

1. Activity 1 KNOWLEDGE BASE FOR EXISTING MAR FIELD APPLICATIONS: Development of MAR knowledge-base of existing field applications for addressing different societal challenges related to water availability.
2. Activity 2 MAR to MAR-ket: Permanent demonstration activity to show industry that they can rely on hydrogeology techniques by involving nine different industrial branches as demo cases. Industry will realise the benefits and will feel more identified with the activities developed in MARSOL project and the expertise from other previous EU founded projects. Provide technical solution for their water supply guarantee and the feasibility to maintain their livelihood.

3. Activity 3 BLUE PRINT IMPACT, INDICATORS, RISK ASSESSMENT TECHNICAL SOLUTIONS FOR INDUSTRY: Development of a methodology for probabilistic risk evaluation linked to MAR activities.
4. Activity 4 TECHNICAL SOLUTIONS FOR INDUSTRY: Development of design and construction criteria, and testing protocols for different exemplary MAR schemes and their benchmarking. Developing and testing appropriate engineering solutions, e.g. underground dams and wastewater hydraulic barriers, to convert karst aquifers into large groundwater storage reservoirs. The pros and cons of each technology will be assessed systematically, and compared to alternative solutions. Economic costs and benefits of MAR options for the various.
5. Activity 5 MODELLING (incl. water balance, water availability, climate change): Mathematical models to simulate the impact of MAR on aquifer hydrology and hydro geochemistry.
6. Activity 6 TRANSFERING KNOWLEDGE INTO PRACTICE: A complex and Specific Dissemination & Technology Transfer (D&TT) Plan will be designed based in the product previous analysis, business and development plans as well as target users. The Plan will contain several programs specially dedicated to the industrial branches, beneficiaries of the technology improvements. Different activities & materials will be developed to achieve an impact on the entire industrial driven sector.



The list of the 36 partners of this AG, whose leader is Dr. JP Lobo-Ferreira (LNEC) is available in the site http://www.eip-water.eu/MAR_Solutions

Besides news on MAR activities, a large amount of pdf presentations at MARSOL/MAR workshops and conferences can also be downloaded from the site.

ANNEX 2 presents the 2nd year AG 128 MARtoMARKet report to EIP Water Secretariat.

22.1.2 IAH Working Group (WG) Mar To Market Strategies And Actions To Bring Managed Aquifer Recharge Technique To The Industry

As can be seen in the Dina-MAR site

http://www.dina-mar.es/file.axd?file=2014%2F4%2Fsubmission_MAR+to+MARKet-IAH-MAR-WG-v3.pdf

Dr. Enrique Fernández Escalante (Tragsa) and Dr. Teresa E. Leitão (LNEC) proposed, and was accepted by IAH a Working Group (WG) MAR TO MARKET strategies and actions to bring managed aquifer recharge technique to the industry, with the following concept:

Managed Aquifer Recharge technique, or simply MAR, has become, perhaps, the best technique within the Integrated Water Resources Management (IWRM) framework, to palliate Climate Change adverse effects. Due to the fact that some impacts are increasing rapidly, in scale and intensity, permanent "technological solutions" are required as a "water innovation in action" line.

R&D advances in water sector are "slow". It is required high doses of innovation, patience and a huge "hydro-imagination".

The innovative technical aspects of the planned activities include the development of novel MAR systems, or modification of existing ones, with sound technologies that can overcome the main drawbacks. MAR will increase aquifer water storage that can be used in meteorological drought periods, to supply water to human activities or to keep natural ecosystems. At the same time, will enable to solve flood problems by promoting aquifer recharge.

This strategic storage could also be used by some industrial branches and water cycle agents, for their future survival and development, as well as bringing new solutions for SMEs. "There is no business without sustainability and the opposite".

It is also worth to mention the important role developed by forest masses in major basin watersheds. According to studies in the Eastern part of Spain, the forests increase the seepage in the aquifers in comparison to close barren areas (www.dina-mar.es). It is also worth to mention the importance of vegetal masses on climate change.

The major questions to be addressed by the Working Group are based on this basis: "Industry must understand that much of their future is linked to groundwater by means of increasing **their** awareness across adapted dissemination techniques".

Some challenging lines of the action are:

- *Water efficiency linked to a bigger productivity and savings in water supply and energy costs (the demand for water is increasing currently).*
- *Guarantee for sustainability and permanence even at water scarcity situations.*
- *Water quality improvement through Soil Aquifer Treatment (SAT) technologies.*
- *MAR technique as a "Market opportunity" for market drivers and applications.*
- *Lower "Blue print" or "water foot-print" and smaller impacts in the aquifers which content is going to other places as virtual water.*
- *Huge potential to convert MAR into job opportunity creation.*
- *Demo sites to show the suitability of MAR technique. Sequential actions involving, firstly, related industrial sectors of high visibility at an international level.*
- *Hydro-economic modelling (combines factors hydro (geo) logical, structural, institutional and economic to simulate the evolution of the value of water in space and time).*

The proposal is available in the site http://www.dina-mar.es/file.axd?file=2014%2F4%2Fsubmission_MAR+to+MARKet-IAH-MAR-WG-v3.pdf

The planned activities are the following:

Managed Aquifer Recharge technique, or simply MAR, has become, perhaps, the best technique within the Integrated Water Resources Management (IWRM) framework, to palliate Climate Change adverse effects. Due to the fact that some impacts are increasing rapidly, in scale and intensity, permanent "technological solutions" are required as a "water innovation in action" line. R&D advances in water sector are "slow". It is required high doses of innovation, patience and a huge "hydro-imagination". The innovative technical aspects of the planned activities include the development of novel MAR systems, or modification of existing ones, with sound technologies that can overcome the main drawbacks. MAR will increase aquifer water storage that can be used in meteorological drought periods, to supply water to human activities or to keep natural ecosystems. At the same time, will enable to solve flood problems by promoting aquifer recharge. This strategic storage could also be used by some industrial branches and water cycle agents, for their future survival and development, as well as bringing new solutions for SMEs. "There is no business without sustainability and the opposite". It is also worth to mention the important role developed by forest masses in major basin watersheds. According to studies in the Eastern part of Spain, the forests increase the seepage in the aquifers in comparison to close barren areas (www.dina-mar.es). It is also worth to mention the importance of vegetal masses on climate change. The major questions to be addressed by the Working Group are based on this basis: "Industry must understand that much of their future is linked to groundwater by means of increasing their awareness across adapted dissemination techniques". Some challenging lines of the action are:

- (1) Water efficiency linked to a bigger productivity and savings in water supply and energy costs (the demand for water is increasing currently).
- (2) Guarantee for sustainability and permanence even at water scarcity situations.
- (3) Water quality improvement through Soil Aquifer Treatment (SAT) technologies.
- (4) MAR technique as a "Market opportunity" for market drivers and applications.

- (5) Lower “Blue print” or “water foot-print” and smaller impacts in the aquifers which content is going to other places as virtual water.
- (6) Huge potential to convert MAR into job opportunity creation.
- (7) Strengthen cooperation with international organisms, as UNESCO, World Bank, FAO, Red Cross...
- (8) Demo sites to show the suitability of MAR technique. Sequential actions involving, firstly, related industrial sectors of high visibility at an international level.
- (9) Hydro-economic modelling (combines factors hydro (geo) logical, structural, institutional and economic to simulate the evolution of the value of water in space and time).

22.2 MANAGED AQUIFER RECHARGE SITES KNOWLEDGE BASIS

Under the related DEMEAU FP7 project an analysis of European MAR sites has been performed and a corresponding report has been published. You may access this publication, prepared by the authors S. Hannappel (HYDOR), F. Scheibler (HYDOR), A. Huber (HYDOR), C. Sprenger (KWB) under this

http://www.eip-water.eu/sites/default/files/M11_1%20catalogue%20of%20european%20MAR%20applications_plus_appendix.pdf

or [link](#)  [M11_1 catalogue of european MAR applications_plus_appendix.pdf](#)

22.3 MODELLING IN WATER RESOURCE MANAGEMENT APPLICATION OVERVIEW AND REVIEW

A large amount of reasoning on Modelling in Water Resources and on MAR research need application has been developed in recent years. An unavoidable book to be referenced from the WB: <https://www.southasiawaterinitiative.org/sites/sawi/files/WRS%20SAWI%20reportjune8.pdf#page=57>.

From that book the following conclusions are highlight:

- Groundwater Model Recommendation:

All packages simulate groundwater quantity and quality using similar algorithms and offer support for users of their software packages. The difference between the evaluated software packages lies in the GUI interface and price of the software. iMOD, with the pre-processing and post-processing, strong visualization abilities, strong support, and open source availability, is the strongest candidate of the groundwater model evaluated and thus recommended for groundwater modeling. Experienced groundwater modellers, familiar with developing MODFLOW model natively or with using GMS, Visual MODFLOW, and Groundwater Vistas, will likely want to remain with the software with which they are familiar and can use efficiently. GMS provides a platform to support the modular nature of MODFLOW while Visual MODFLOW provides a GUI that guides groundwater model

development through a straightforward workflow. While MIKE SHE simulates groundwater, its fixed grid system and licensing fee limits adoption for strictly groundwater simulations. MIKE SHE shines in situations where it is important to simulate the interaction between surface and ground water.

- Conjunctive Use Recommendation:

GSSHA (WMS), MIKE SHE, and MODFLOWOWHM are suitable for integrated surface and ground water simulations required for conjunctive management. MIKE SHE and GSSHA (WMS) have better GUI interfaces and more capabilities stemming from their more complex operations of surface water control structures. However, their limitations are the cost per license, which provides a barrier to their widespread adoption, and their inability to change the mesh density near areas of concern (for example, groundwater pumping wells, tanks and check dams for groundwater recharge). That being said, GSSHA (WMS) is significantly less expensive than MIKE SHE, but is restricted in simulating groundwater movement in 2-D. For the MODFLOW-OWHM, a sub-model model can be readily developed from the larger regional model, but the two are not dynamically linked. MODFLOW-OWHM offers a full suite of MODFLOW packages to simulate integrated surface and groundwater interactions. Due to the lack of a GUI interface for MODFLOW-OWHM, developing a conjunctive use model would require more modeling expertise. MIKE SHE and GSSHA (WMS) are preferred if budgets are not limited, technical staff have limited experience with modeling, or if complicated control of surface water is required. If technical staff are familiar with creating, calibrating, and using MODFLOW packages, the MODFLOW-OWHM is good solution.

22.4 MARSOL DELIVERABLE 12.4 FINAL REPORT ON NUMERICAL MODEL WRAP-UP

MARSOL Deliverable 12.4 Final Report on Numerical Model, July 2016, concluded the following:

- Deliverable 12.4 on the Final Report on numerical model, for all MARSOL demo sites in Greece, Portugal, Spain, Italy, Israel and Malta, incorporated of the latest results obtained in WP4 Deliverable 4.4 on the Hydrogeological modelling at the South Portugal MARSOL demonstration sites, dated June 2016.
- WP 12 Modelling developments have been presented in Deliverable 12.1 (final version dated 15.05.2015), Deliverable 12.2 (draft version dated 05.06.2015) and Deliverable 12.3 (draft version dated 30.09.2015). In the next paragraphs we summarize those WP 12 Modelling deliverables.
- As mentioned in the DoW, regarding WP12, “For selected sites, strategies for selecting positions for MAR facilities will be presented and water budgets on a watershed scale elaborated to calculate water availability for MAR, and predictions on the influence of future climatic changes will be made. These sites will serve as reference for modelling strategies where the MAR installations are included into a more generalized water budget approach to allow long term predictions on MAR efficiency and economic feasibility. ... The main tasks of this work package are: Task 12.1: Methods evaluation (Task Leader: LNEC): Literature review

on potential and currently applied modelling approaches for MAR sites and the evaluation of weaknesses and strengths (concluded) and Task 12.2: Water budget and conceptual modelling (Task Leader: LNEC): For selected sites, GIS layers of information for conceptual modelling will be prepared. Achievements for selected sites reported in Deliverable 12.1.

- Further, accordingly with the Description of Work Deliverable 12.2 “GIS database of the MARSOL DEMO Sites” aims to prepare GIS layers of information for conceptual modelling for selected sites.
- This activity was developed to produce the structure of a GIS database that is able to accommodate main available information of the Demo sites, concerning background information as the conceptual groundwater flow model, water budgets under actual and climate change projected situations, vulnerability indexes, infiltration indexes, field tests, already existing data concerning geology, soil, land cover, aquifer information, river basins, streams, natural and artificial reservoirs, etc.
- Besides information for conceptual modelling the GIS database was also structured to contain the MAR facilities, infrastructures and also some related monitoring information.
- A requirements analysis was performed of several demo sites aiming to identify what kind of information was available and what kind of information could be included. The demo sites field visits and guide books were essential to perform this task. This was the case of Arenales (demo site 3, Castile and León, Spain), Sant’Alessio (demo site 6, Tuscany, Italy), and Menashe (demo site 7, Israel) MAR systems. Besides already gathered information on Lavrion (demo site 1, Greece), and knowledge by the leading authors of the Algarve demos sites (demo site 2, Portugal), allowed a comprehensive definition of the data requirements and relevant links between information.
- Deliverable 12.2 show the results of this requirements analysis and the subsequent model of the corresponding geographical data.
- Deliverable 12.3, dated September 2015, is on the Progress Report on numerical model, for selected MARSOL case-study areas (Portugal, Italy, Spain, Israel and Greece).
- A contribution from TUDa on the hydrological/hydrogeological models for the Lavrio test site (WP 3) and the Menashe test site (WP 9) is included. These contributions are related to regional and local scales.
- Complementary contributions on laboratorial scales, from LNEC and IWW, on WP 14s “Contaminants modelling at column scale”, and from UPC on “Modelling the potential impact of chaotic advection to enhance degradation of organic matter and emergent compounds” have been included.
- Background information on the water budget for modelling has been presented July 2015, in the final version of Deliverable 12.1 “Water budget and climate change impact”. Background information for Portugal and Italy is available in Deliverable 4.2 on “South Portugal MARSOL demonstration sites characterisation” and in Deliverable 8.1 on “DSS with integrated modelling capabilities”, with modelling examples from Italy.
- Regarding Demo Site 4, Llobregat Aquifer, Catalonia, Spain, UPC further contributed with a chapter on “Natural attenuation process modelling”.
- Complementary contributions on laboratorial scales, from LNEC and IWW, on WP 14s “Contaminants modelling at column scale”, and from UPC (demo site 4) on “Modelling the

potential impact of chaotic advection to enhance degradation of organic matter and emergent compounds” have been included.

- The overview presented in Deliverable 9.4 on “A combined un-saturated and aquifer flow model for the Menashe site” co-authored by Yoram Katz (Mekorot), Yonatan Ganot (ARO), Daniel Kurtzman (ARO), has also been included in this Deliverable 12.4.
- Ppts of MARSOL modelling presentations are available in eip-water.eu, e.g <http://www.eip-water.eu/working-groups/mar-solutions-managed-aquifer-recharge-strategies-and-actions-ag128> and <http://www.eip-water.eu/algarve-water-quality-workshop-great-success> .

White book on MAR modelling

Deliverable D12.7

ANNEX 1 – SELECTION OF FURTHER MODELLING RESEARCH ACTIVITIES EXTRACTED FROM INTERIM REPORTS

J.P. LOBO FERREIRA, TERESA LEITÃO, TIAGO CARVALHO AND ANA MARIA CARMEN ILIE (LNEC), JOSÉ PAULO MONTEIRO, LUÍS COSTA AND RUI HUGMAN (UALG), TIAGO CARVALHO, RUI AGOSTINHO AND RAQUEL SOUSA (TARH), LAURA FOGLIA, ANJA TOEGL AND CHRISTOS POULIARIS (TU DARMSTADT), RUDY ROSSETTO (SSSA), IACOPO BORSI (TEA), XAVIER SANCHEZ-VILA AND PAULA RODRIGUEZ-ESCALES (UPC), ENRIQUE F. ESCALANTE (TRAGSA), MANUEL M. OLIVEIRA (LNEC), ANDREAS KALLIORAS (NTUA), YORAM KATZ (MEKOROT)

23 INTERIM REPORT DECEMBER 2013 – AUGUST 2014

23.1 DEMO SITE 4 ACTIVITIES: LLOBREGAT RIVER INFILTRATION BASINS, SANT VICENÇ DELS HORTS (BARCELONA)

Hydraulic tests, including a long-term pumping test and a tracer test, have been interpreted using Standard modelling, thus providing a model available at the regional as well as the local scale.

Furthermore, a number of infiltration-related processes have also been modeled additional to assess the physical models that can explain clogging. **Figure 137** reflects the spatial distribution of bacterial growth at the micrometer scale under fixed conditions of light and temperature. The soil was taken from the surface of the site and corresponds to clean sand. A variographic analysis shows a nested isotropic structure.

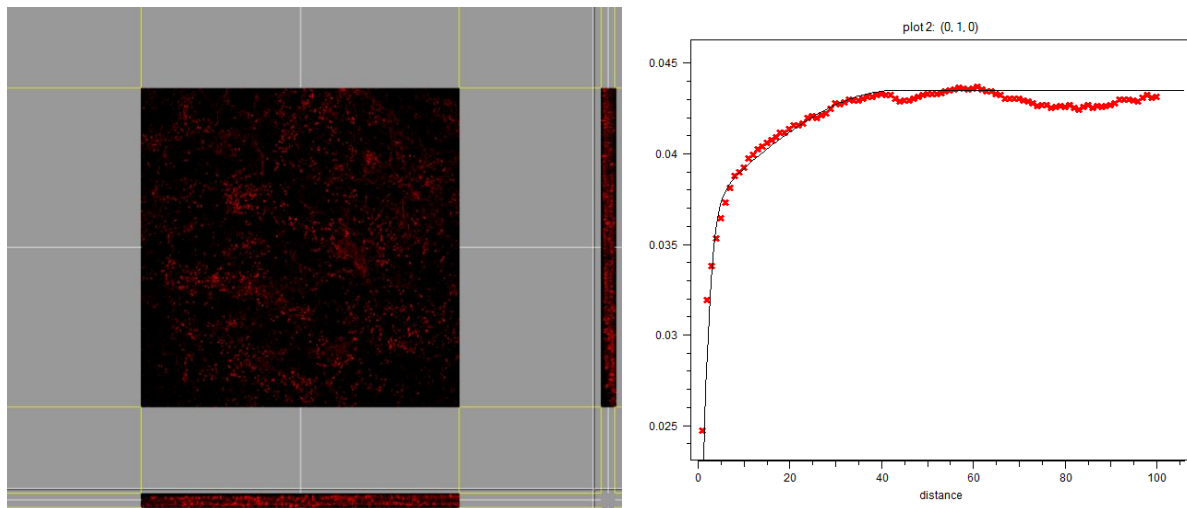


Figure 137 - Bacteria growth at the micrometer scale under fixed conditions of light and T at the topsoil (top), and corresponding isotropic variogram (bottom).

At some larger (decametric) scale, it is possible to model reactive transport problems. An example would be network reactions; that is, simultaneous degradation of solutes presenting a parent-daughter relationship. An example could be dechlorination of PCE in a 3D highly heterogeneous system representing the Llobregat River (**Figure 138**).

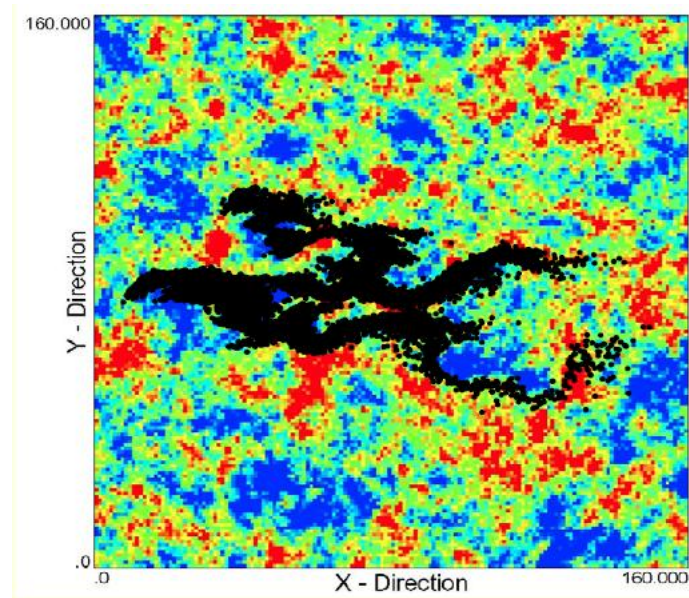


Figure 138 - 2D view of a heterogeneous 3D aquifer with a plume modelled by particle tracking

The problem is CPU consuming, and involves concepts of particle tracking with transition probabilities. The typical outcome is the expected concentrations at the outlet of the different compounds, to be directly incorporated to risk evaluations (**Figure 139**)

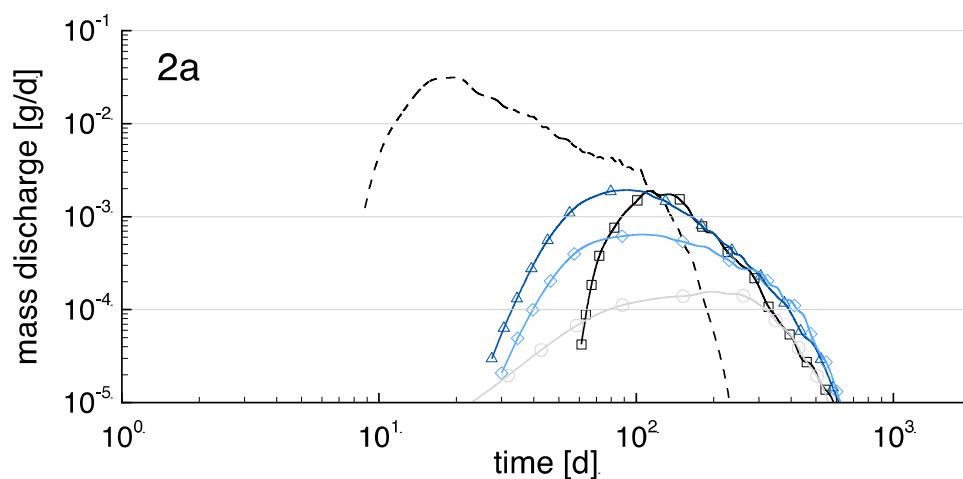


Figure 139 - Breakthrough curves of the different species in a network reaction

The intermediate scale would be metric. Using soil from the site we performed an infiltration test. The set-up is presented in **Figure 140**.

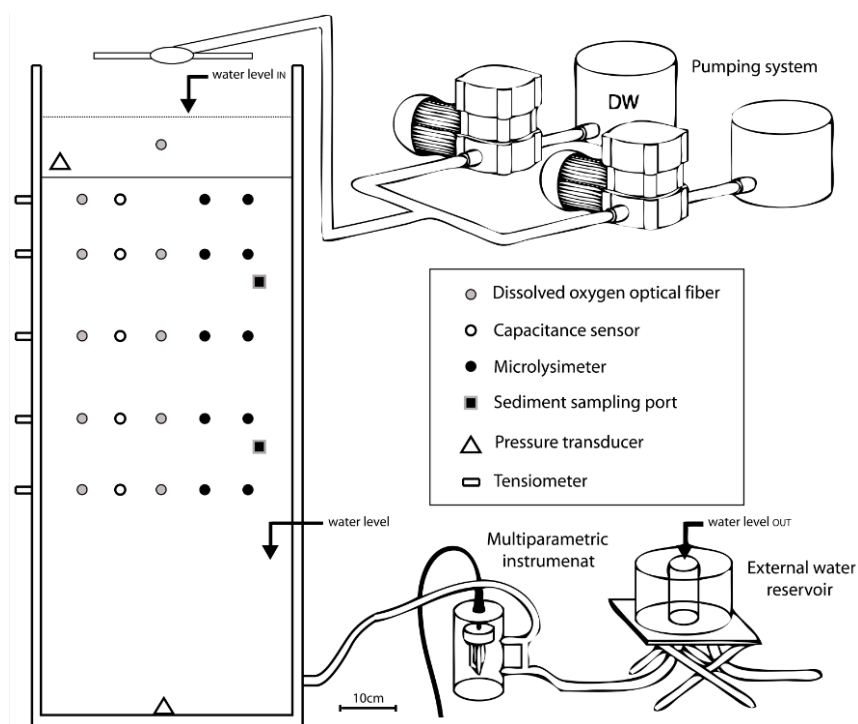


Figure 140 Set-up of the infiltration experiment. A 1 m tank was packed with soil, water infiltrated from the top. Several sensors were placed within the system to record a suite of physical, chemical and biological parameters.

A tracer test with fluoresceine was further performed. A photograph was taken at different times (**Figure 141**). The breakthrough curve was recorded at the bottom (**Figure 141**).

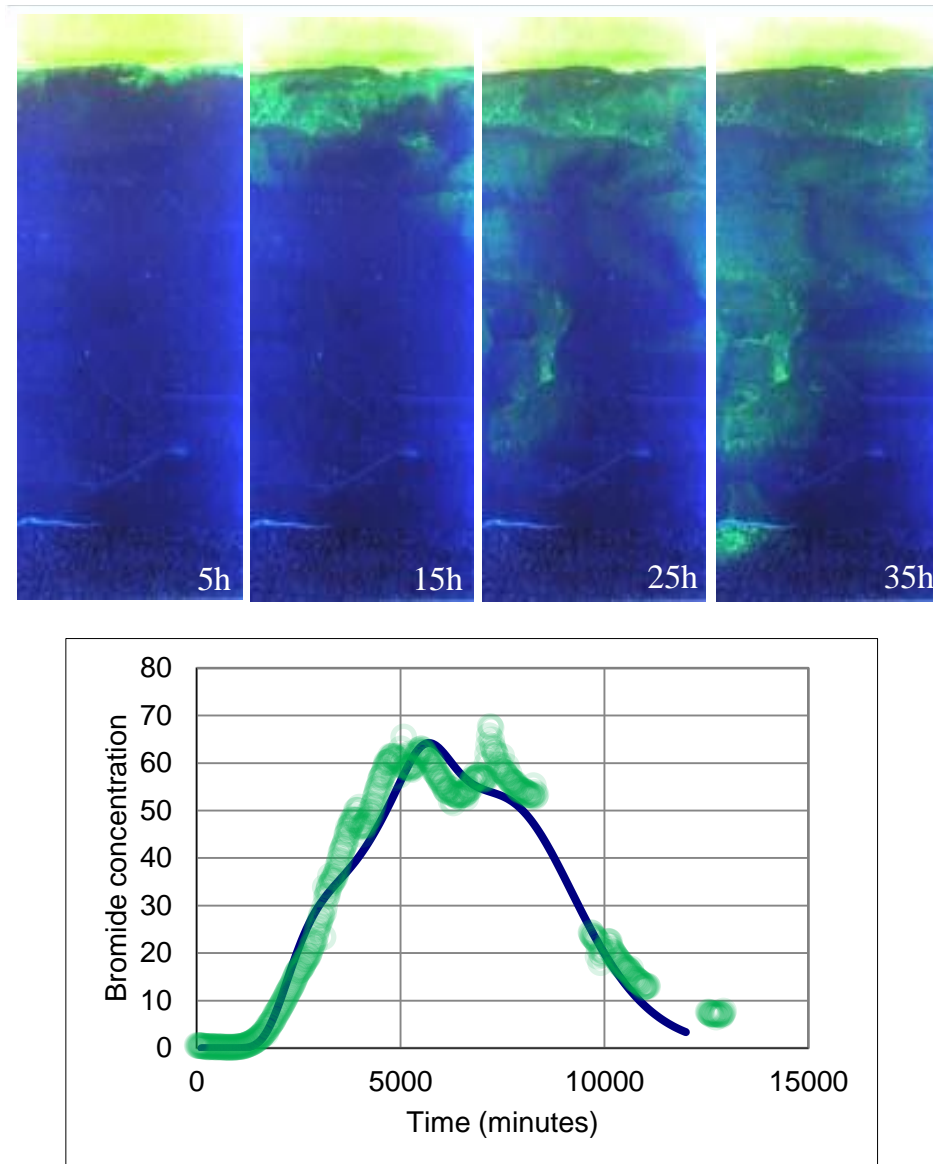
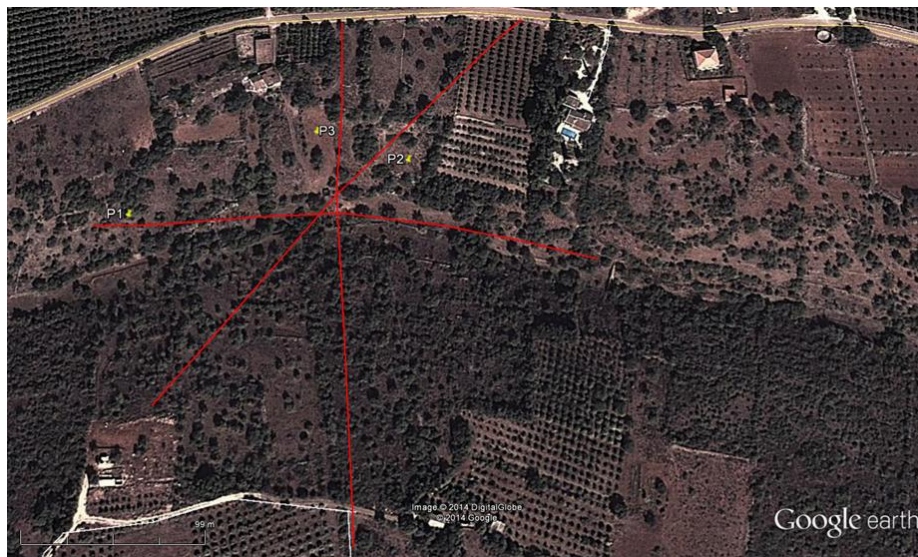


Figure 141 - Several snapshots of the tracer test performed with fluoresceine (top). Recorded breakthrough at the outlet (bottom)

24 INTERIM REPORT SEPTEMBER 2014 - MAY 2015

24.1 GEOPHYSICAL SURVEY, WITH THE RESISTIVITY METHOD, FOR PT QUERENÇA-SILVES DEMO SITE CONCEPTUAL MODEL

A geophysical survey, with the resistivity method, was performed in PT Querença-Silves Demo site (Cerro do Bardo, cf. Figure 142) with the main objective to assess the groundwater flow direction in the test site. To achieve this purpose a water recharge test was performed during one week with the injection of water mixed with salt (in the second day) in a well, and a time-lapse resistivity survey on three alignments crossing each other's near it. Salt was selected as a tracer due to his capability to reduce water resistivity and to enhance the possibility of identifying the water circulation with the geophysical electrical resistivity method. Data was collected more than once in each alignment/profile, during one week, which gives a total of 15 profiles gathered.



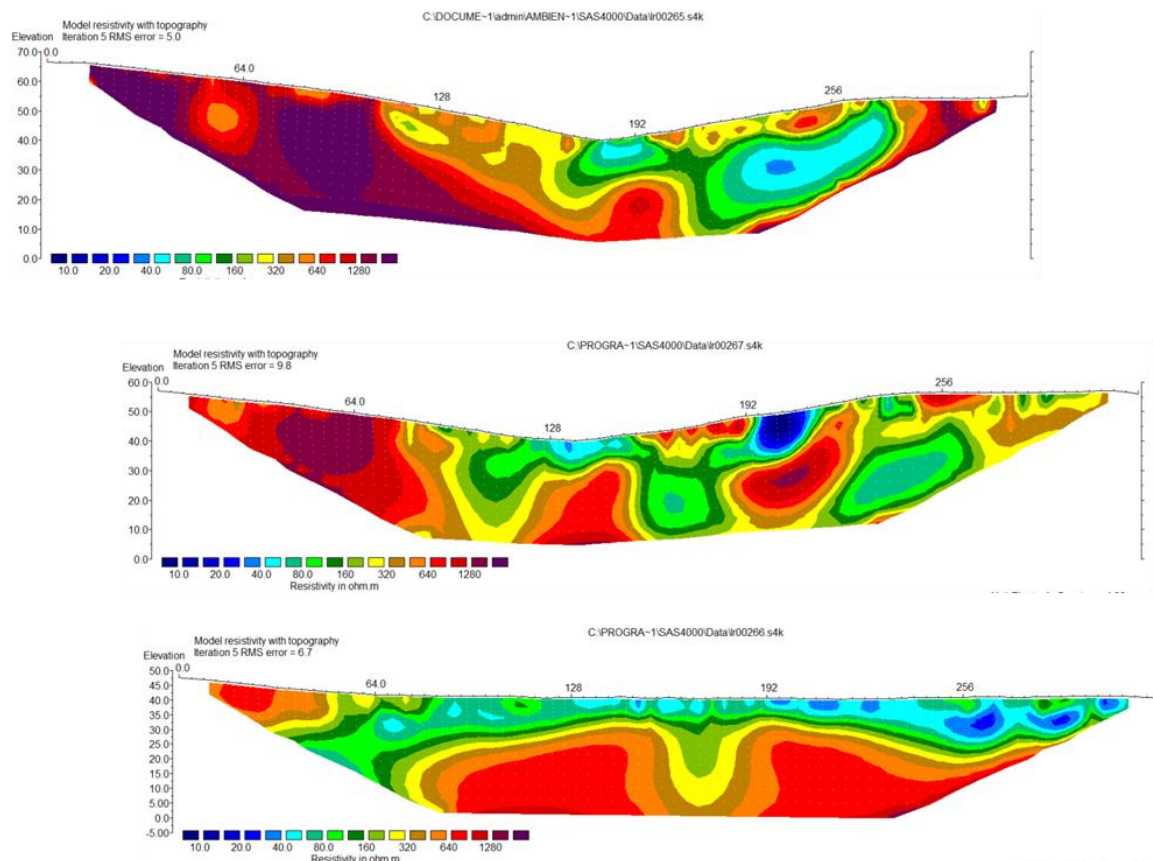


Figure 142 - Geophysical survey in Querença-Silves aquifer at Cerro do Bardo

A first survey (background or reference situation) was performed on the first day in alignment P1; and on the second day in alignments P2 and P3, with P2 readings starting just before the beginning of water injection, so the reference in this alignment could have been influenced by the injected water

Tomographic images of the subsoil in terms of the electrical resistivity and of the resistivity variation with time were obtained after data processed with Res2Dinv v3.56 software.

A set of 3 resistivity profiles were performed using the dipole-dipole array before the water injection in the well, to have the resistivity reference pattern. After the end of water injection they were repeated in the 4 subsequent days. The objective was to have more information regarding the water pathways in the area with the time-lapse evolution of the resistivity. Due to a low variation of resistivity with time, data are being reprocessed to have a more accurate input to the outflow modelling of the injected water.

In the geophysical survey the main difficulties were: in the field, the physical implantation of profile P1, due to highly dense vegetation, which delayed background data collection; in the office, the small variation of the resistivity during the survey, that made very difficult to enhance the results of the tracer.

24.2 MODELLING CONTRIBUTIONS OF THE LOCAL AND REGIONAL GROUNDWATER FLOW OF MANAGED AQUIFER RECHARGE ACTIVITIES AT QUERENÇA-SILVES AQUIFER SYSTEM (WP4)

Activities on “Modelling Contributions of the Local and Regional Groundwater Flow of Managed Aquifer Recharge Activities at Querença-Silves Aquifer System” (cf. Figure 143) have been further developed during this second reporting period.

A 3D model is being applied to assess and predict the regional effects of managed aquifer recharge (MAR) activities occurring in the QS demo site study, in particular, the injection of water surplus at a large diameter well at QS demo site study.

Local scale modelling efforts are being developed during MARSOL in order to determine the infiltration capacity of the injection well, the aquifer’s local hydraulic properties and the direction and residence time of the injected water. At a local scale event, local hydraulic parameters are determined with the support of analytical methods, such as conventional pumping test analysis techniques. To support the local scale analysis and modelling of the well injection tests, resistivity profiles using dipole-dipole array were performed before, during and up to 4 days after an injection test with salty water as a tracer with the goal of gathering more information regarding water pathways in the area with the timelapse evolution of the resistivity, though a low variation of resistivity with time was achieved. Modelling Contributions of the Local and Regional Groundwater Flow of Managed Aquifer Recharge Activities at Querença-Silves Aquifer System.

Within the scope of the project large diameter well injection tests (with and without tracers) as well as geophysical surveys have been carried out in order to determine the infiltration capacity and aquifer properties. The results of which allowed the use of analytical methods to determine local scale values of hydraulic parameters (e.g. hydraulic conductivity and storage coefficient). These values will be compared with results from pre-existing numerical flow and transport models in order to obtain complementary solutions to the problem at local and regional scales. This analysis will contribute to the selection of the most appropriate methods to interpret, reproduce and model the impacts of MAR activities planned within the scope of the MARSOL project. Subsequent to the planned injection tests and, with the support of modelling efforts, the capacity of infiltration of rejected water from water treatment plants or surface storage dams in the large diameter well will be assessed.

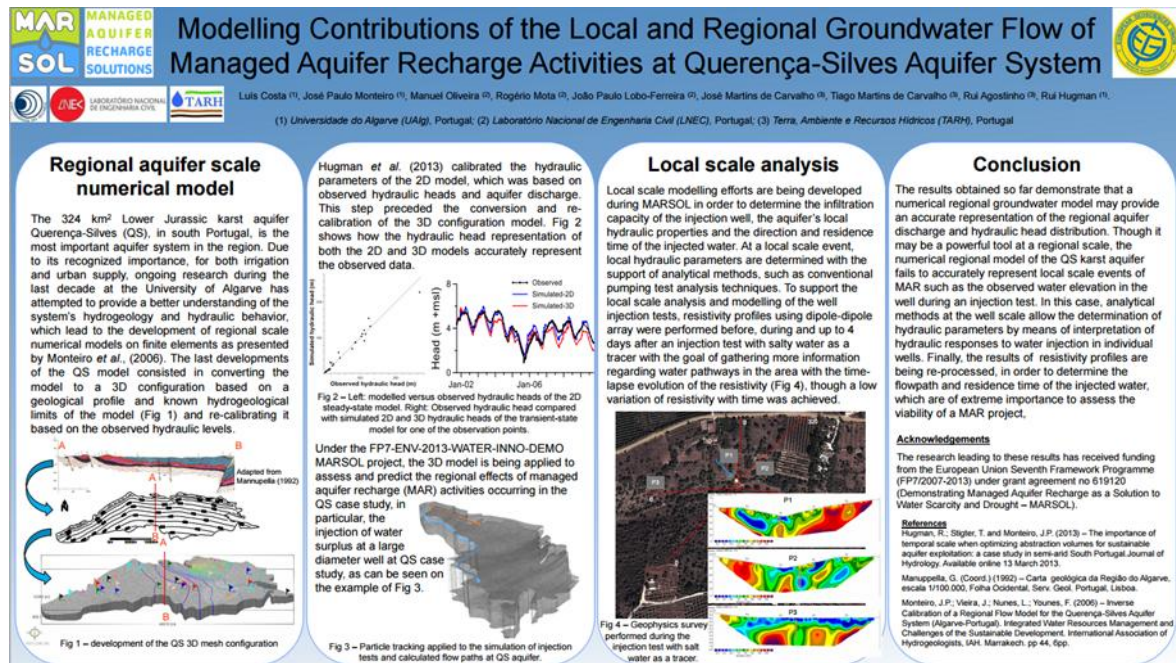


Figure 143 - Modelling Contributions of the Local and Regional Groundwater Flow of Managed Aquifer Recharge Activities at Querença-Silves Aquifer System

The results obtained so far demonstrate that a numerical regional groundwater model may provide an accurate representation of the regional aquifer discharge and hydraulic head distribution. Though it may be a powerful tool at a regional scale, the numerical regional model of the QS karst aquifer fails to accurately represent local scale events of MAR such as the observed water elevation in the well during an injection test. In this case, analytical methods at the well scale allow the determination of hydraulic parameters by means of interpretation of hydraulic responses to water injection in individual wells. Finally, the results of resistivity profiles are being re-processed, in order to determine the flowpath and residence time of the injected water, which are of extreme importance to assess the viability of a MAR project,

24.3 HYDROLOGICAL/HYDROGEOLOGICAL MODELS FOR THE LAVRIO TEST SITE (WP 3) AND THE MENASHE TEST SITE (WP 9)

24.3.1 TUDa Modelling effort

For both the Lavrio (Greece) and Menashe (Israel) case studies, TUDa is implementing a coupled surface water/groundwater model with a structure represented in **Figure 144**. The goal is to obtain a full picture of the terrestrial hydrological cycle in the watersheds in order to evaluate the regional scale impact of current and future MAR schemes considering the impact of changing climatic conditions. For example, we would like to be able to evaluate the importance of natural recharge (due to precipitation) and MAR and how they can be affected by different climatic condition.

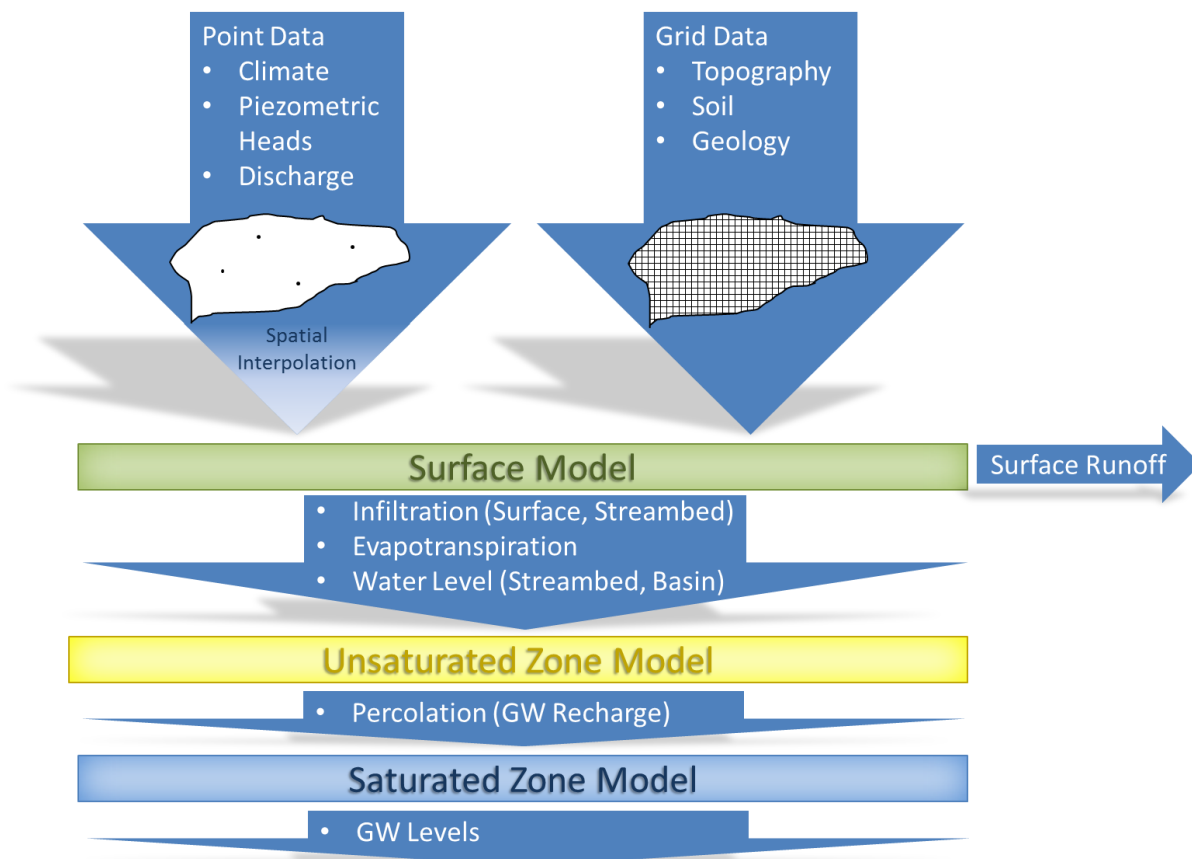


Figure 144 - Integration scheme of partial models

Different models are either already developed or under development for the simulation of the hydrological cycle. Here is the list of the models developed (or to be developed) and planned to be integrated:

1. A precipitation-runoff model at the watershed scale has been developed in both watersheds using input of temporally distributed point data (e.g. climate, stream discharge, irrigation and pumping) and spatially distributed data (e.g. topography, land use, soil type). Model outputs of this part will include actual evapotranspiration, surface runoff, direct infiltration, streambed infiltration (transmission losses) and flow accumulation in the streams.
2. A stream routing model is needed to calculate the flood progression in the stream as well as in the diversion channels.
3. The output of both surface water models is to be integrated into an unsaturated zone model, which uses direct and streambed infiltration, as well as artificial infiltration at the infiltration basin to determine soil moisture conditions and percolation to the groundwater table.
4. A saturated zone / groundwater model has been developed and it is under evaluation and computes groundwater levels using the percolation of the unsaturated zone model as input.

Regarding the data collection and the model development, the progresses are similar in the two test sites. Therefore, in the next paragraph we present:

- 1) Some details on the data collected for model development at the Menashe test site.
- 2) Preliminary model development at the Lavrion test site.

24.3.2 Status of model development at Lavrion (Greece)

The surface hydrological model, PRMS (Markstrom et al., 2008), developed by USGS was used. This model has been developed for the whole watershed of the Thoricos bay. The watershed was divided into Hydrological Response Units (HRU's) with similar properties. The main lithological units in the area are the alluvium, the karstified marble and the impermeable schist. Input data were mainly meteorological data (precipitation and average temperature) and data related to the soil properties of the HRU's. The simulation period includes 6 years (2009-2014) with daily time steps. The initial sensitivity analysis showed that the modules for the calculation of actual evapotranspiration and soil properties were the ones affecting mostly the model performance. The initial calibration aimed at lowering the simulated discharges as much as possible, since it is known that the streams get completely dry during the dry season. Discharge data collection would be critical and it is already planned, with the establishment of monitoring stations with regular measurements of discharge.

A first groundwater model for the alluvial plain has also been developed simultaneously (Schumann, 2015, Master Thesis) using MODFLOW-2005 (Harbaugh, 2005). The location and type of boundary conditions is chosen using the knowledge for the hydraulic connections between the different waterbodies. A two layer approach was used to represent the alluvial plain and the underlying karst aquifer, so that the hydraulic connections are evaluated. The simulation period used was the same as for the surface hydrological model. The data gathered during field excursions was used to perform a preliminary sensitivity analysis and calibration. The latter was satisfying but the sensitivity analysis showed that more data at locations where there is lack of information could improve the model performance.

The groundwater model for the karstified marble is under development using MODFLOW-2005 with different approximations for representing the karst (continuum approximation, Conduit Flow package, Nonlinear Flow package). For this model the aim is to test different modelling approaches found in the literature to simulate the flow in karstic regions and evaluate the most appropriate for the Lavrio site.

The full coupling of the models presented above is under development using the GSFLOW program (Markstrom et al., 2008).

24.3.3 Data collection: Menashe test site

The following data have been collected in the Menashe watershed:

- Climate Data for the aimed calibration period of the past 50 years from the Israel Meteorological Survey (17 stations for precipitation, 4 climate stations), some potential evaporation, wind speed and solar radiation data
- Geological Data from 4 geological maps (1:50,000), geological cross section of the coastal aquifer (e.g. Tolmach 1980), Information about deep geology from wells described in Gvirtzman & Zohar 2010 GSI report
- Soil Maps, soil sampling in study area according to the 5 main soil types of the area (grain size distribution, soil density, field capacity, water content, organic carbon content, lime content) & infiltration tests with Gulphpermeameter
- Land Use Data from the national database (GIS file)
- Topographic Map, location of streams and springs (1:50,000)

- Topography, ASTER GDEM in about 30 x 30 m resolution
- Discharge Data (subdaily to monthly) for the 4 diversion points, further 4 points downstream of diversion and at the inlet to the sedimentation basin (period of about last 25 to 50 years) Hydrological Survey
- Well Information, location, depth and water levels (all in all ~600 production and monitoring wells), majority filtered in the coastal aquifer, 2 wells filtered in the eocene rocks (1 of them shallow usually dry) Water Authority
- Water Quality Data:
 - major ion data of surface, spring and groundwater sampled in September 2014 (further data available through Water Authority of Israel)
 - stable water isotopes H-2 & O-18 from Surface, Spring and Groundwater from Sep 2014, Dec 2014, Apr/May 2015 and 3 month of continues measurements of two eocene springs (to be analysed)
 - H-3/He-3 groundwater age dating of the coastal aquifer, sampling May 2015 (to be analysed)

References

- Markstrom, S.L., Niswonger, R.G., Regan, R.S., Prudic, D.E., and Barlow, P.M. (2008). GSFLOW—Coupled ground-water and surface-water flow model based on the integration of the Precipitation-Runoff Modeling System (PRMS) and the Modular Ground-Water Flow Model (MODFLOW-2005): U.S. Geological Survey Techniques and Methods 6-D1, 240 p.
- Harbaugh, A. (2005). MODFLOW-2005: The U.S. Geological Survey modular ground-water model--the ground-water flow process. U.S. Geological Survey, Techniques and Methods, 6-A16.
- Schumann, P., (2015) Preliminary characterization of the hydrogeological properties of the Thorikos alluvium system (Greece), Master Thesis, TU Darmstadt.

24.3.4 Modelling the potential impact of chaotic advection to enhance degradation of organic matter and emergent compounds.

Mixing of waters with different chemical composition drive geochemical reactions (biomass mediated). Thus, the enhancement of mixing should contribute to efficient degradation of undesired substances. Unfortunately, mixing of water in the subsurface is highly inefficient. Figure 145 shows the presence of a blob of water so that reactions take place in the interphase. Degradation would be enhanced by increasing the interphase area while keeping the total volume.

Recently, a methodology called chaotic advection has been developed as a way to enhance mixing. Chaotic advection consists of efficiently combining injection and extraction of water to promote high local fluxes with high local dispersion processes.

We are studying the applicability and efficiency of chaotic advection to improve MAR by enhancing the degradation of emerging compounds that reach the aquifer by managed recharge practices.

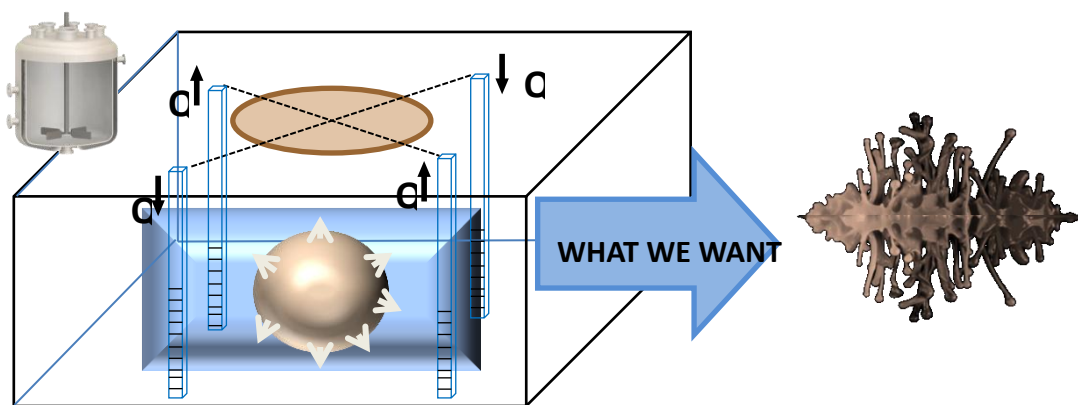


Figure 145- Shape of an injection blobs with equal volume and very different contact area

The key point is that it has been shown that emerging compound degradation is highly related to the redox state, so that each individual compounds degrades preferentially under some particular redox condition. The methodology consists of comparing the formation of pockets of redox conditions (evolving in space and time). The larger the variations in redox conditions, the higher the degradation that could be achieved.

We also compare the spreading of a tracer test in homogenous and in a heterogeneous media.

To evaluate the effect of chaotic advection we consider four wells (Figure 146, left) noted North, South, East and West. The sequence of injection and extraction is provided in the same Figure and includes sequential injection/extraction with a rotation in the wells involved as a function of time.

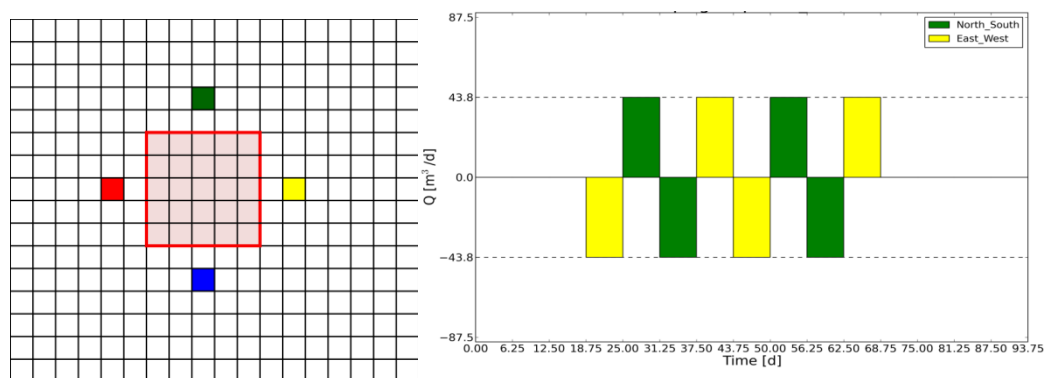


Figure 146 - Location of injection and extraction wells (left). Distribution of extraction and injection flow rates as a function of time (right) for the different wells involved

Modelling is performed by combining MODFLOW (to solve the flow problem), with PHT3D to solve reactive transport. The boundary conditions for flow involve a natural background flow from West to East. Reactive transport equations solved are shown in Table 19.

As preliminary results, it is observed (**Figure 147**) that the surface affected by anaerobic conditions is greatly enhanced by chaotic advection, while the results are basically unaffected by the presence of homogeneous or heterogeneous media.

Table 19. Reactions considered in the system, with the corresponding reactive terms

| TEAPs | REACTION | RATE |
|------------------------------|--|---|
| O ₂ | $\text{CH}_2\text{O} + \text{O}_2 \rightarrow \text{CO}_2 + \text{H}_2\text{O}$ | $r_{\text{DOC/O}_2} = k_{\text{O}_2} \cdot \frac{[\text{O}_2]}{K_{\text{O}_2} + [\text{O}_2]} \cdot [\text{Doc}]$ |
| NO ₃ ⁻ | $5\text{CH}_2\text{O} + 4\text{NO}_3^- + 4\text{H}^+ \rightarrow 5\text{CO}_2 + 2\text{N}_2 + 7\text{H}_2\text{O}$ | $r_{\text{DOC/NO}_3^-} = k_{\text{NO}_3^-} \cdot \frac{[\text{NO}_3^-]}{K_{\text{NO}_3^-} + [\text{NO}_3^-]} \cdot \frac{K_{i,\text{O}_2}}{K_{i,\text{O}_2} + [\text{O}_2]} \cdot [\text{Doc}]$ |
| Mn(IV) | $\text{CH}_2\text{O} + 2\text{MnO}_2 + 4\text{H}^+ \rightarrow \text{CO}_2 + 2\text{Mn}^{2+} + 3\text{H}_2\text{O}$ | $r_{\text{DOC/Mn}^{4+}} = k_{\text{Mn}^{4+}} \times \frac{[\text{Mn}^{4+}]}{K_{s,\text{Mn}^{4+}} + [\text{Mn}^{4+}]} \times \frac{K_{i,\text{O}_2}}{K_{i,\text{O}_2} + [\text{O}_2]} \times \frac{K_{i,\text{NO}_3^-}}{K_{i,\text{NO}_3^-} + [\text{NO}_3^-]} [\text{Doc}]$ |
| Fe(III) | $\text{CH}_2\text{O} + 4\text{Fe}(\text{OH})_3 + 8\text{H}^+ \rightarrow \text{CO}_2 + 4\text{Fe}^{2+} + 11\text{H}_2\text{O}$ | $r_{\text{DOC/Fe}^{3+}} = k_{\text{Fe}^{3+}} \times \frac{[\text{Fe}^{3+}]}{K_{s,\text{Fe}^{3+}} + [\text{Fe}^{3+}]} \times \frac{K_{i,\text{O}_2}}{K_{i,\text{O}_2} + [\text{O}_2]} \times \frac{K_{i,\text{NO}_3^-}}{K_{i,\text{NO}_3^-} + [\text{NO}_3^-]} \times \frac{K_{i,\text{Mn}^{4+}}}{K_{i,\text{Mn}^{4+}} + [\text{Mn}^{4+}]} [\text{Doc}]$ |

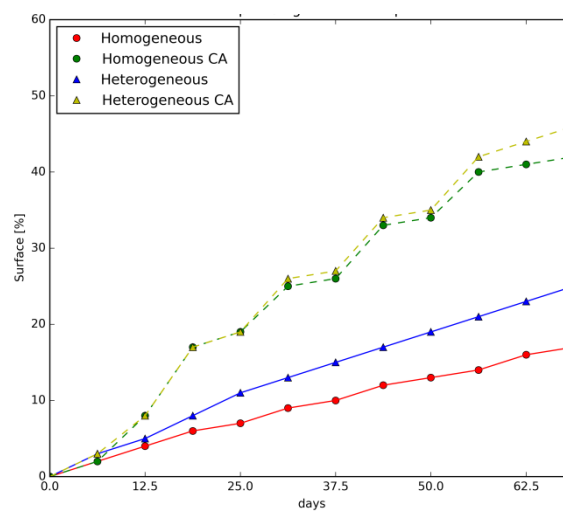


Figure 147 - Variation of anaerobic surface as a function of time under continuous pumping and chaotic advection approaches. Homogeneous and heterogeneous permeability fields are investigated

24.3.5 Saturated flow model of the Coastal aquifer – Menashe region

The geological data processed from well logs, geological and structural maps served as the basis for the conceptual model, constructed via the GMS software package. The variety of rock types was represented by four material categories, each characterised by a set of hydrological properties. Over 100 well logs were analyzed using the T-PROGS software and provided the material spatial occurrence. This stochastically generated material array, conditioned to the boreholes logs, was combined with structural map data of the major marine clay lenses present in the aquifer. The resulting model hence reflects the material proportions and transition trends as well as the division into sub aquifers by marine clay within the western part of the aquifer (**Figure 148**).

Spatial discretization and boundary conditions - The model covers an area of ~ 70 square kilometers, discretized horizontally into 70 X 70 m mesh cells. The vertical section of the aquifer, ranging roughly 50 – 100 m in thickness from east to west, was discretized into 20 layers allowing spatial resolution of ~ 5 m or less. Model base was defined by the impermeable Saquie formation underlying the aquifer. Representing a phreatic aquifer the model top was defined by the water level. Boundary conditions along the northern, eastern and southern model edges were set to be of transient head type, based on periodical water level measurements. The western edge was set to be a Constant head border dictated by the sea. Initial conditions were based on static heads measured at 37 production wells included in the model.

Calibration - During 29/12/14 – 28/1/15 ~2.6 MCM of desalinated water were introduced to the southern and central infiltration ponds. The flow regime within the saturated zone during the infiltration period and the following weeks was simulated, as field data served for the model calibration.

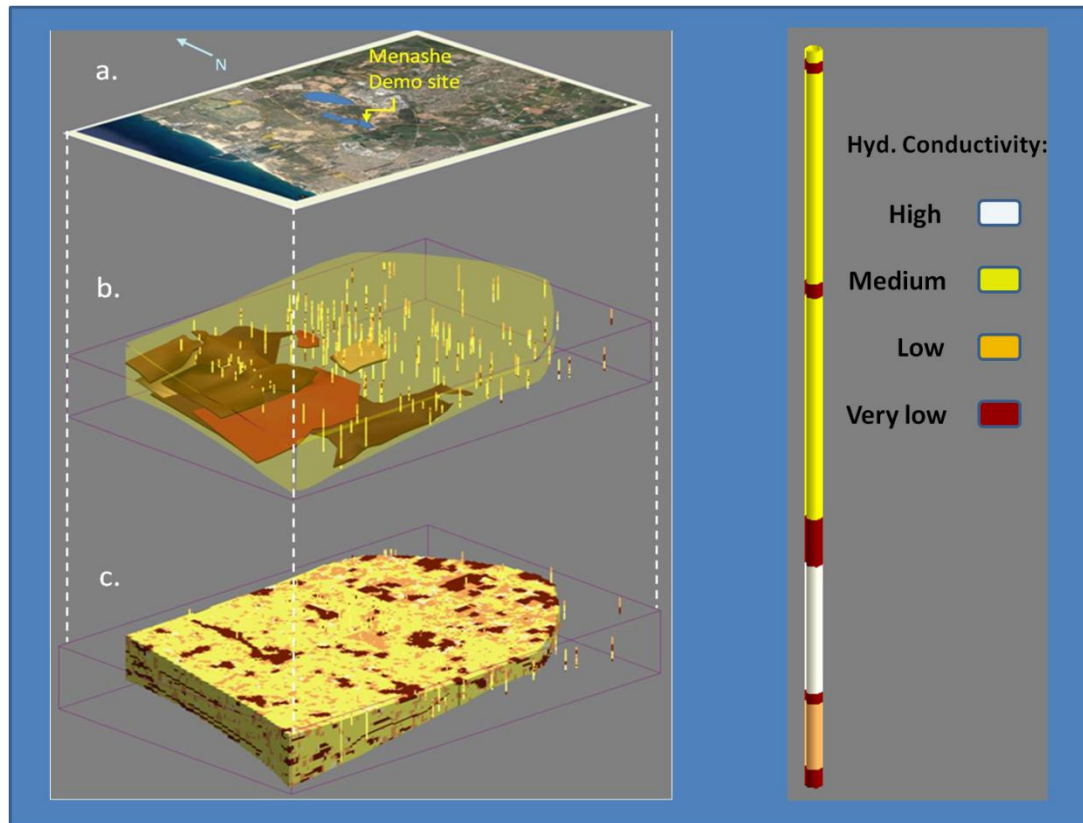


Figure 148 - Conceptual model structure. The modelled area (a), the major marine clay lenses (b) and the combined deterministic and stochastic material array representing the aquifer

The water introduced to the ponds by an average rate of $\sim 84,000$ CM/day enriched both the surface and subsurface water bodies, causing the rise of the surface water level in the southern pond by ~ 2 m and the groundwater level beneath the pond by ~ 17 m. Groundwater levels before infiltration (a) and on infiltration cease (b) are shown in **Figure 149**.

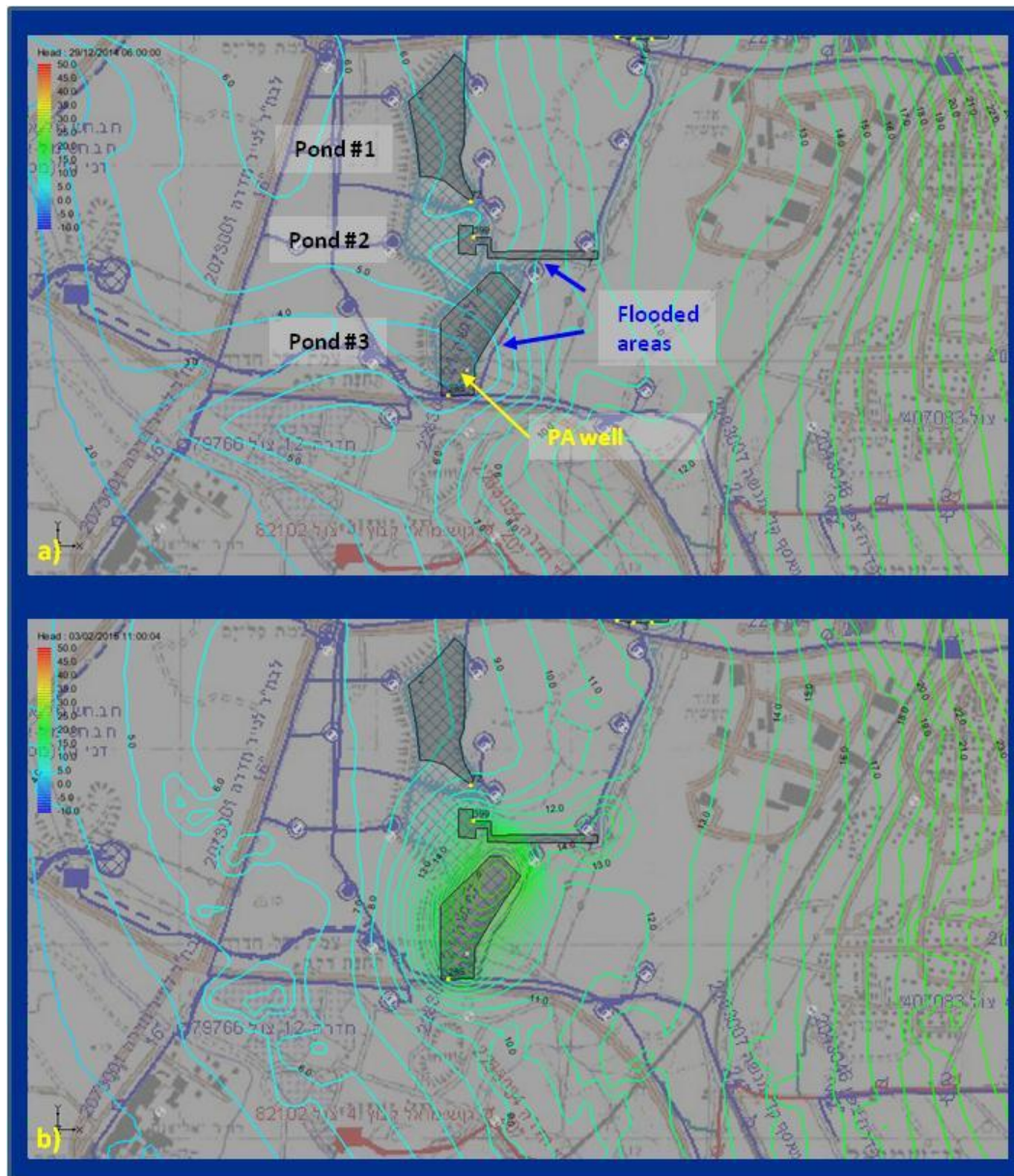


Figure 149 - Modelled water levels before (a) and after (b) infiltration

After 13 days of inflow outlets to pond # 3 were opened, directing the surface water also to flow further into the neighbouring central pond as well as up-stream distribution channel (see north-eastern water level rise in **Figure 149b**), thus avoiding the risk of flooding. According water balances were calculated for the surface, vadose zone and saturated zone water bodies of both infiltration ponds (**Figure 150**).

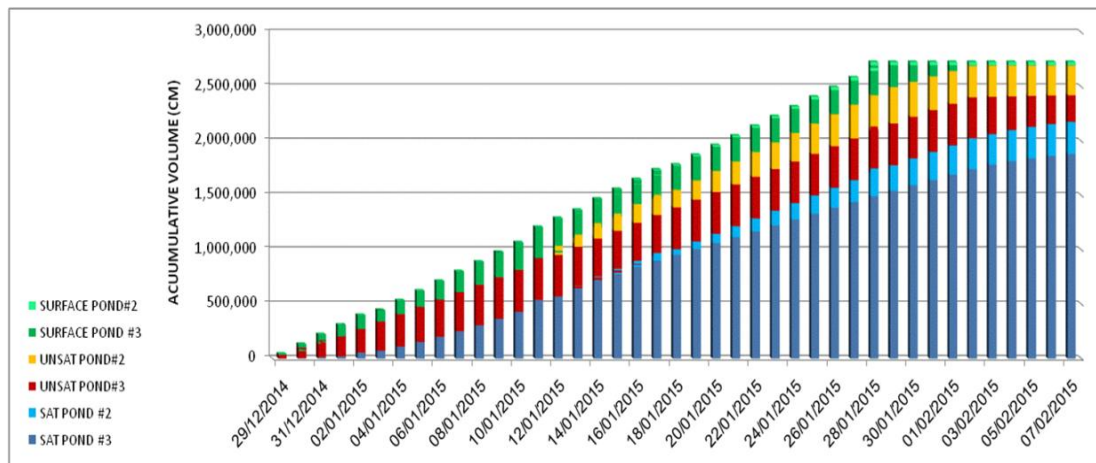


Figure 150 - Cumulative water balance for the surface and subsurface water bodies during and after MAR of 2.6×10^6 m³ (evaporation is estimated as only ~ 0.3% of the total discharge)

These water balances, conditioned to monitoring of the surface water and groundwater levels, the wetting and re-drying front advance in the unsaturated zone and further lab analysis, were used for evaluation of the groundwater enrichment and served as input for the model. The model results were calibrated vs. continuous groundwater level measurements at the southern pond and dozens of head measurements in the production wells (Figure 151).

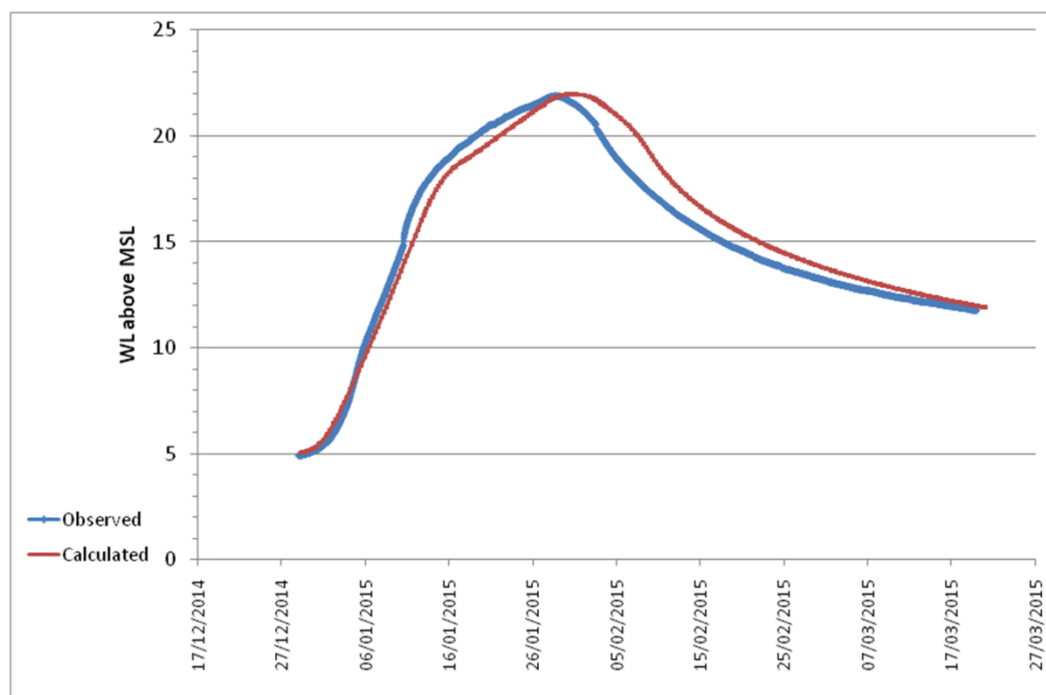


Figure 151 - Observed Vs. calculated groundwater level at the pilot site (PA well, pond #3)

24.4 MODELLING CONTRIBUTIONS IN DEMO SITE 6 SERCHIO RIVER WELL FIELD

In activities carried out for Demo Site 6 (Serchio River Well Field - WP.8), TEA is responsible to develop a Decision Support System (DSS) for the RBF plant. The core of the DSS is the Geodatabase (GeoDB), where all data concerned the RBF process are stored, and eventually queried, visualized and analyzed.

In particular, an innovative part of the DSS is composed by a set of short-cut modelling tools, acting directly on the GeoDB. They consist of formulas or analytical solutions computed directly in the GeoDB (server side) whenever a new signal from Wireless Sensors Network (WSN) is gathered into the GeoDB. The great advantage of such automated (DB-embedded) modelling is that it allows the Data Analyst to have an immediate view (from the client side) of some critical issues, such as the relationship between surface water and groundwater, in terms of temperature and level, for instance.

Such modelling tools are implemented as *stored procedure* within the PostgreSQL database using the PLPython procedural language, which allows PostgreSQL functions to be written in the Python language. They are summarized in the list below, while a detailed description is reported in Deliverable D8.1

(A) Difference between river stage and aquifer head and temperature:

Two monitoring references are identified: one concerning surface water (the average of values recorded at two surface water sensors in the river) and the groundwater sensor closest to the river bank. The difference between temperature and water level at these points is calculated. The aim is to have additional information on the groundwater/surface water interaction (GSI), in particular:

- the time series behavior of water level difference provides information on the exchange between river to aquifer, the head difference being proportional to this difference (at least in a simplified modelling approach);
- the time series behavior of temperature difference can provide information on the traveling time between riverbank and aquifer: it is well known (Sharma et al., 2012) that temperature can be used as natural tracer. Difference between river and aquifer temperature tends to stabilize for a while, and the steady state time scale can be used as a first raw estimate of the travel time. Moreover, perturbation of this equilibrium can suggest critical changes in riverbank permeability (or some other unconventional event).

(B) A simple model to detect (possible) clogging process

Even in this case two monitoring references (sw and gw) are considered. If some physical assumption are satisfied (as in the case of Serchio plant), the relationship between river and aquifer can be represented by a “filter model”, where the sw/gw interface is represented by a sort of membrane: this model can be described by a simplified 1D problem for the potentiometric head, whose

numerical solution by a finite difference scheme, explicit in time, is easy and fast. It allows to calculate the head at the gw monitoring point, and calibrate the value of riverbed conductance thanks to the large amount of data collected in the GeoDB. Once calibrated, this simple model can be used to control the difference between calculated and measured head values: if the time series of such a difference exhibits some non-stationary behavior, this could be an evidence of some change in river conductance. Thus, this procedure leads to a qualitative and fast detection of anomalous riverbank filtration behaviors. A similar approach was proposed in Mucha et al. (2004) and Nawalany (1993).

The numerical was successfully tested by a comparison with analytical solutions. The usage of this procedure within the GeoDB and in connection with the WSN data has been tested using synthetic data.

Another modelling tool concerns the calculation of a specific Water Quality Index (WQI). The definition of a normalized index to evaluate the water quality status is a widely used method adopted in water quality analysis and modelling (Kannel et al., 2007). This method consists of identifying a series of target parameters, say C_1, \dots, C_N , which are considered crucial and characteristic for the surface water under study. Each parameter, C_i , is then normalized according a reference value, say $C_{i,ref}$, and a specific weight is also defined, w_i . Thus, the WQI is calculated as the weighted sum of the normalized parameters,

$$WQI = \frac{1}{N} \sum_i w_i \frac{C_i}{C_{i,ref}} \quad (2)$$

The most used parameters in literature are temperature, pH, DO, EC, TSS. These parameters are therefore the one set in the preliminary version of the GeoDB model; such a selection will be verified during the testing phase and updated accordingly.

As for the solution of the IRBF problem, also WQI is calculated at any WSN signal update, and saved in the GeoDB.

References

Kannel P.R., Lee S., Lee Y-S., Kanel S.R., Khan S.P. (2007), Application of Water Quality Indices and Dissolved Oxygen as Indicators for River Water Classification and Urban Impact Assessment, *Environ Monit Assess* 132, 93-110.

Mucha I., Banský L., Hlavaty Z., Rodák D. (2004). Impact of riverbed clogging – colmatation – on ground water, in: *Riverbank Filtration Hydrology*, NATO Science Series IV: Earth and Environmental Sciences - Vol. 60, Hubbs S.A. Edt., Springer, Amsterdam, 2004.

Nawalany R. (1993). Mathematical modeling of river-aquifer interaction, HR Wallingford Report SR 349.

24.5 MARSOL WP 12 MODELLING WORKSHOP, PISA, ITALY, APRIL, 2015

The programmed MARSOL workshop on „Modelling“ was held in Pisa during the 21-23 April 2015. The main goal of this workshop was to showcase the use of modelling tools in the management of water resources. A number of partner speakers made presentations about recent research advancements, real case applications of modelling tools used to plan and manage water resources, especially ground water and the use of these tools in Managed Aquifer Recharge issues. A complementary one-day international workshop entitled ‘Advantages of using numerical modelling in water resources management and managed aquifer recharge schemes’, which was a joint event including members of MARSOL (FP7) and MAR Solutions AG (EIP-AG) and visit to DEMO Site 6. The events organised by the MARSOL Partner Scuola Superiore Sant’Anna targeted water authorities, water utilities, regional authorities, environmental associations, IAH members, Professionals & experts (engineers, geologists, agronomists, chemists, etc.), partners from EU FP7 MARSOL, partners from the FREEWAT H2020 project, PhD Students, MSc students and the general public. Around 120 people attended the one-day international workshop.

25 INTERIM REPORT JUNE 2015 - FEBRUARY 2016

25.1 MODELLING CONTRIBUTIONS OF THE LOCAL AND REGIONAL GROUNDWATER FLOW OF MANAGED AQUIFER RECHARGE ACTIVITIES AT WP 4 ALGARVE CAMPINA DE FARO AND QUERENÇA-SILVES AQUIFER SYSTEMS

José Paulo Monteiro, Rui Hugman and Luís Costa (UAlg), Tiago M. Carvalho, Rui Agostinho and Raquel Sousa (TARH), Manuel M. Oliveira, J.P. Lobo Ferreira, Rogério Mota, Tiago Carvalho and Teresa Leitão (LNEC).

25.1.1 Introduction

Modelling activities regarding groundwater models for case studies Campina de Faro (PT1) and Querença-Silves (PT2) concluded on schedule. Regional groundwater models for both case studies have been developed, calibrated and validated. Different MAR scenarios were performed in order to assess the effect of the foreseen MAR activities on a regional scale. Some of these results were already presented during the MARSOL meeting at the Malta workshop (*Workshop on Legal Issues, Policy and Governance of MAR Activities*, 21-23 October, Water Services Corporation Head Office, Luqa, Malta).

Results of further field experiments at PT2 scheduled for the end of March 2016 (long term injection test at Cerro do Bardo) provided enough data to refine localised groundwater flow directions.

Hereinafter is the detailed description of the activities developed in the Algarve Demo sites.

25.1.2 Campina de Faro (PT1)

In Campina de Faro (PT1), the data and results from the construction of the piezometers and the infiltration tests carried out in previous reporting periods, which included the injection of a tracer (NaCl), were analysed and the main hydraulic characteristics of the system were assessed.

The target aquifer (dated from the Upper Miocene), in the test site area, occurs from 18 to 30 meters deep, leaning towards the direction of the water flow (flowing S), and behaves as an unconfined aquifer even though locally confined by upper Holocene materials. The aquifer is composed by sedimentary formations with high heterogeneity as confirmed by the cuttings at the time of the piezometers construction.

The maximum infiltration of the basin system was estimated in 22 m³/h (1.3 m/d), by analyzing the basins' response to tests of rising, falling and constant hydraulic head. With the current water availability, the stream yearly infiltration is expected to be about 0.03 hm³. However, if to this figure is added the infiltration potential of the large diameter dug wells ("Noras") of about 35 m³/h per well, combined with the greenhouse water availability, the yearly water infiltration would reach 0.42 hm³.

The groundwater flow is therefore mostly defined by a hydraulic gradient north-south of 0.007. It is estimated that the groundwater flow per kilometric section (assuming 15 meters of saturated thickness) is around $10.5 \text{ m}^3/\text{h}$.

The hydraulic permeability was estimated between 0.7 to 2.4 m/d using two different methodologies:

- Sieve analysis, using samples collected from the top of the aquifer during the basin construction; The hydraulic permeability was estimated using Hazen Formula (0.7 m/d).
- The Thiem Formula for radial flow in a non-confined aquifer, using the data from the infiltration test (between 0.7, in Gabardine basins, and 2.4 m/d , in MARSOL basin).

In some areas of the aquifer, based on its response, hydraulic conductivity values could be a degree lower.

These are the recommended values to be used for parametrization in the numerical site modelling, in the site area; however in the rest of the study area, bibliographic mean values should be applied.

The characterization of the vadose zone was also carried out, but parameterization was not possible due to its high clay content, which hampered the use of Hazen's Formula. Yet, it is safe to conclude that few direct recharges by precipitation occur in the study area as the vadose zone has a low transmissivity character.

With the construction of the Marsol and Gabardine Basins the main recharge inputs of the study area are nowadays therefore the natural groundwater flow and the recharge flow is as presented in in Figure 152.

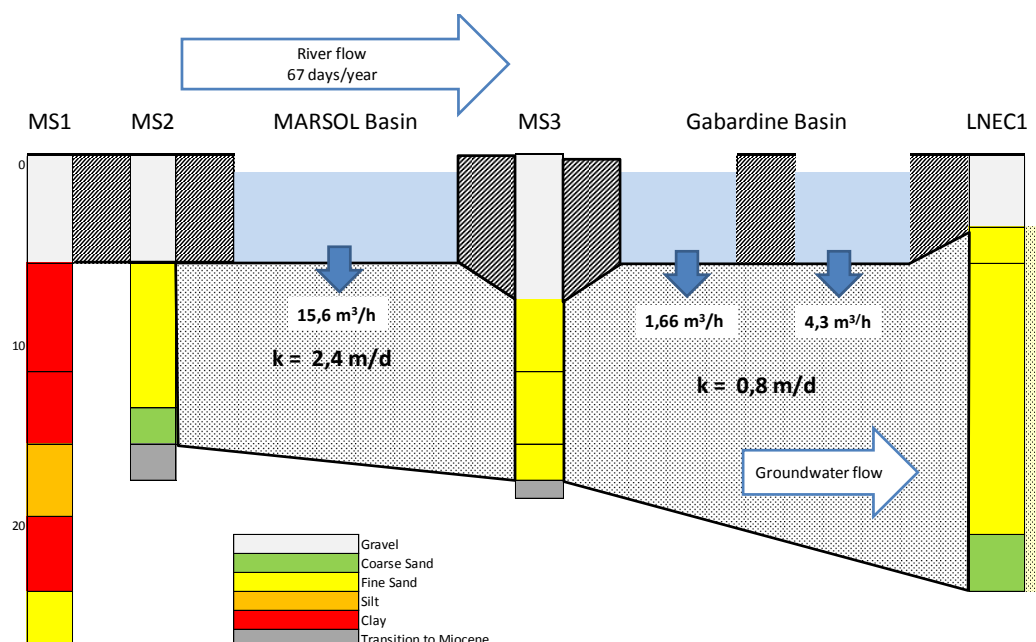


Figure 152– Campina de Faro river bed MAR facilities

25.1.3 Cerro do Bardo (PT2)

In Cerro do Bardo, the hydrogeological conceptual model was reviewed, mainly due to a great information input, provided by the construction and development of the monitoring network, which has now two new piezometers. The location of the two piezometers (CB1 and CB2) is shown in Figure 153:



Figure 153 – Location of Piezometers CB1 and CB2 in the recharge field

The preliminary results, supported by the fact that during the infiltration tests significant higher infiltrations rates were found with higher hydraulic heads, was confirmed.

The lithologic analysis of the drilled cuttings allowed the identification of a first layer, corresponding to part of the vadose zone, of about 15 to 20 meters thick, composed of limestones, clay and sand. From that depth the presence of grey limestone is dominant at least up to 70 meters depth, although with some intercalation of clay and limes. A few caves were spotted during the drilling in both piezometers.

Regarding the hydraulic characteristics accessed during a pumping test (duration of 24 hours plus 8 hours of recovery) conducted in February 2016, results clearly show the presence of two different sub-units with different hydraulic behaviour, and with much lower permeabilities of those generally found in the main Querença Silves aquifer.

The Querença-Silves aquifer at Cerro do Bardo test site can therefore be characterized by:

1. A first subunit from 15 to 20 meters depth, with permeabilities ranging between 0.15 to 0.20 m/d;
2. A second subunit/lower section with unknown depth (estimated in 100 to 150 meters) with permeabilities ranging from 0.08 to 0.15 m;

3. High yield karsified aquifer (Querença-Silves) transmissivities (Figure 154).

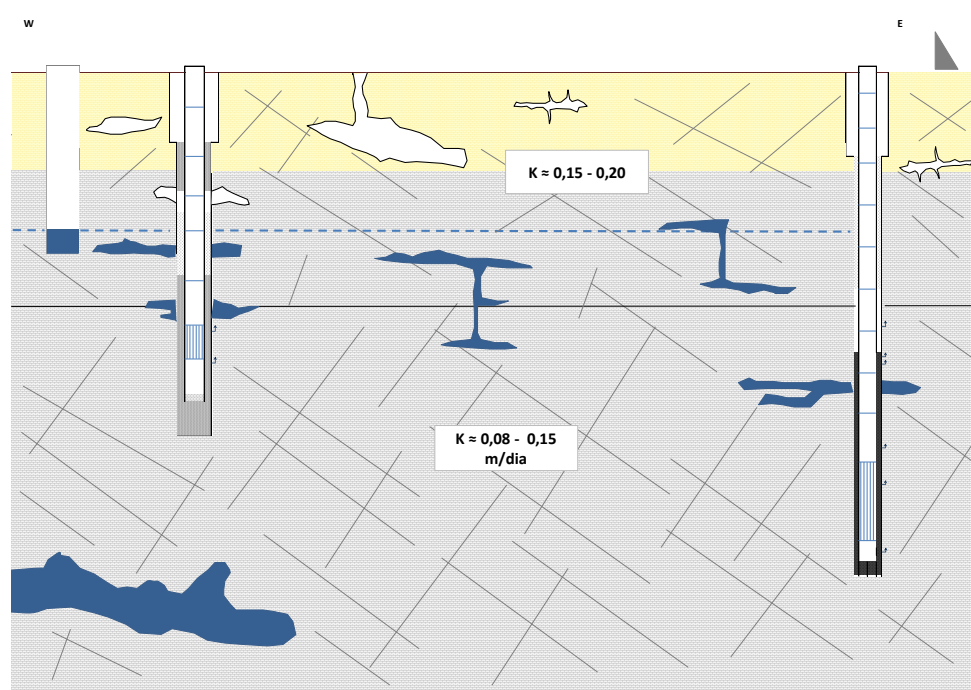


Figure 154- Hydrogeological conceptual model

Groundwater flow in the upper sector is directed by the fracturing direction and is suspected to be, in general terms, in the direction of the topographic gradient (west to east) in contrast of the regional aquifer direction (westwards).

For recharge purposes, it is also important to refer the high infiltration rates registered in the vadose zone, in Cerro do Bardo dug well, 6 m above the water level (24 meters depth), as revealed by the results analysis of the infiltration tests (Figure 155).

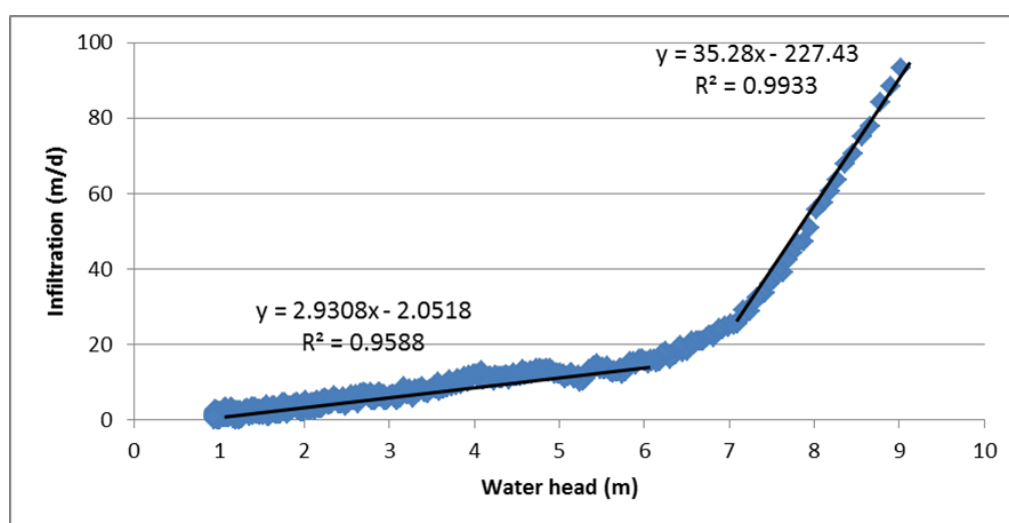


Figure 155– Results of the falling head infiltration test in Cerro do Bardo (December, 2014)

25.2 UALG NUMERICAL MODELLING OF THE MEAN SEA LEVEL AQUIFER (MSLA) OF MALTA

Personnel Involved: José Paulo Monteiro, Luís Costa and Rui Hugman (UALg)

A three-Dimensional variable density coupled flow and transport model of Malta case study is under development. The goal of this model is to determine the impact of both the small and large scale application of MAR in the case study, the Mean Sea Level Aquifer (MSLA) of Malta. In particular to assess the increase in available fresh groundwater resources and whether the injected water will reach existing public supply wells or act as a barrier to seawater intrusion. Some complications arose from the fact that the model's complexity demands for long time and high processing numerical calculations, in particular for the calibration of the model's hydraulic parameters. Despite the complications associated to this approach, it's deemed necessary due to the heterogeneous spatial distribution of abstraction and recharge of the MSLA and its nature as a freshwater lens.

The geological domain of the model (Figure 156) and the water budget of the case study have been defined as well as the modelling domain and numerical mesh. A preliminary groundwater flow model of the MSLA has been calibrated (Figure 157), results of which were submitted (Monteiro et al., (2016)) and presented at the Portuguese 13th Water Congress (Portuguese Water Resources Association APRH "13^o Congresso da Água") held in LNEC, Lisbon, Portugal (7th – 9th March).

Currently, efforts are being made in order to calibrate the coupled transport and flow model, in order to provide a more realistic approach of the groundwater lens development at the aquifer (Figure 157).

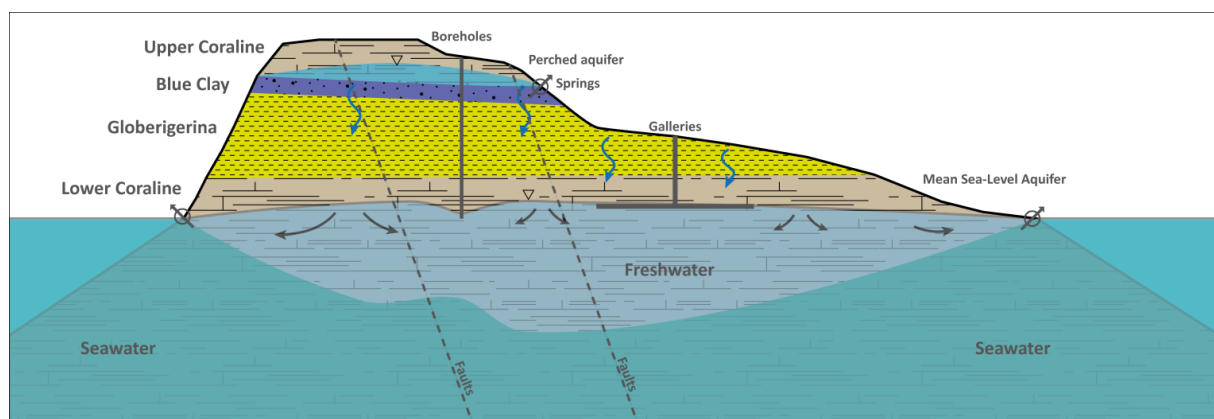


Figure 156 - Conceptual cross-section representing the lithological setting which supports the main aquifers on the Island of Malta

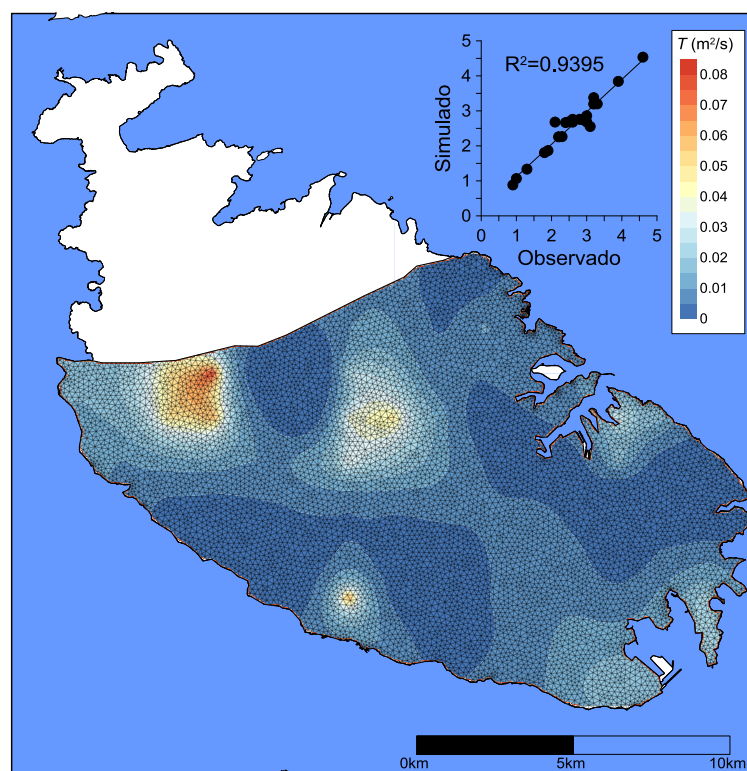


Figure 157 - Preliminary groundwater flow model presented by Monteiro et al., (2016). Finite element mesh, spatial distribution of transmissivity and scatter plot between observed and calculated hydraulic head for the year of 1944

25.3 MODELLING CONTRIBUTIONS IN DEMO SITE 6 - SERCHIO RIVER WELL FIELD

Personnel Involved: Rudy Rossetto (SSSA) and Iacopo Borsi (TEA)

To support modelling activities in Demo Site 6 (Serchio River Well Field), TEA developed modelling tools that can be applied also to other MAR scenarios. Demo Site 6 is the reference case used to test these tools, in strict collaboration with SSSA.

25.3.1 Modelling tools finalized

Beside GeoDB-based modelling tools (already described in previous versions of WP.12 Interim Report), within the period Oct. 2015 – Feb. 2016, TEA finalized the development of the solute transport capabilities included in the modelling platform SID&GRID (now named FREEWAT, in accordance to the alliance with the H2020 FREEWAT (Free and Open Source Software Tools for Water Resource Management) sister project (www.freewat.eu). In particular, in FREEWAT the hydrological model can be coupled to a solute transport model, to simulate advective and dispersive transport of several species, in saturated zone (the extension to the unsaturated zone is still under development, and the release is foreseen for May 2016). The possibility to simulate viscosity and density dependent flow is present as well. Such capabilities are particularly relevant to approach studies on seawater intrusion processes (where density variations of water due to salinity effect are crucial), or for assessing geothermal plants at low- and medium-enthalpy. Simulation of heat transport (also coupled with additional chemical species) is possible just treating heat as a *species*

and defining diffusive coefficients and other parameters in a coherent way. Solute transport is solved in FREEWAT by applying the well-known MT3DMS code (A Modular Three-Dimensional Multi-species Transport Model for Simulation of Advection, Dispersion, and Chemical Reactions of Contaminants in Groundwater Systems, <http://hydro.geo.ua.edu/mt3d>). Viscosity- and density-dependent flows are solved by applying SEAWAT (Simulation of Three-Dimensional Variable-Density Ground-Water Flow and Transport, <http://water.usgs.gov/ogw/seawat>), which is a revised version of coupling MODFLOW with MT3DMS, taking into account variations in density and viscosity during the numerical resolution of the groundwater flow equation. Figure 158 shows a screenshot of solute transport capabilities included in FREEWAT's menu.

The application of solute transport module to the modelling study of S.Alessio river-bank filtration (WP.8) is running, under the leadership of SSSA and in collaboration with Provincia di Lucca.

25.3.2 Update on modelling tools already described in previous reports

The QGIS plugin *DataExplorer*, developed during MARSOL, has been included in the official QGIS plugin. Some minor bugs have been solved, and currently (March 7th, 2016) it counts 1428 download from QGIS's Users (see screenshot of the QGIS website in Figure 159). *DataExplorer* was thought to query and visualize data stored in the GeoDB of the Demo Site 6 (developed via Postgresql/Postgis RDBMS), but actually it can be applied to any GIS vector layer loaded in QGIS (e.g. CSV, shape file, SQLite, etc.)

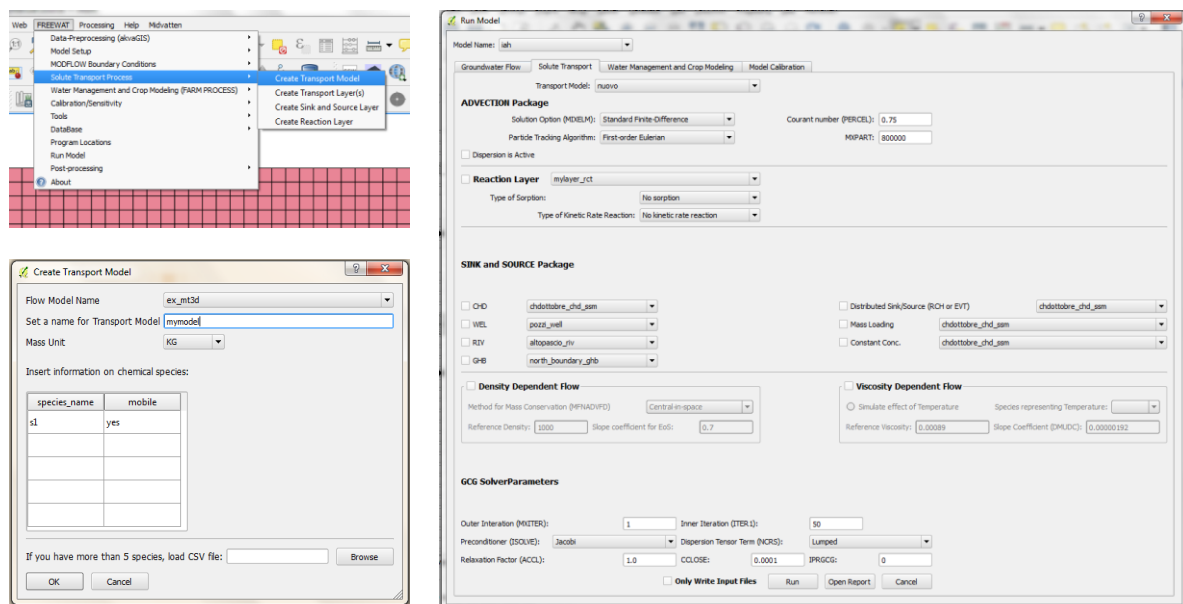


Figure 158 - Screenshots of solute transport module within FREEWAT modelling platform

For what the DB-based modelling is concerned, the 1D model for a short-cut evaluation of the riverbed conductivity variations is under calibration using field data. The numerical solution is automatically calculated directly in the GeoDB, after each new insert coming from field sensors. Therefore, once the calibration of hydrodynamic parameters will be completed (aquifer hydraulic conductivity, riverbed conductance, aquifer storage coefficient), monitoring the difference between calculated and observed values can detect (possible) variation in the riverbank conductance, eventually envisaging clogging phenomena.

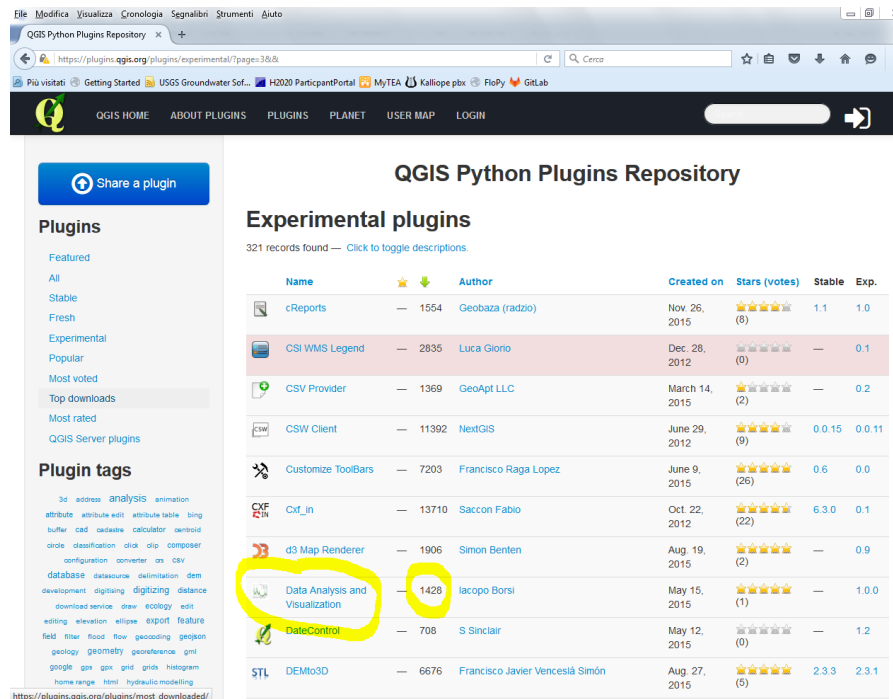


Figure 159 - QGIS Plugins web page, showing DataExplorer (last access March 7th, 2016)

25.4 TUDA MODELLING ACTIVITIES AT DEMO SITE 1 (LAVRIO, GREECE)

Personnel Involved: Christos Pouliaris, Laura Foglia (TUDa)

The modelling activities in Lavrio, Greece, involve the development of a coupled surface – groundwater model that also incorporates the unsaturated zone. The advantage of using such models is that the exchanges between the different hydrological zones are taken into account in every time step, leading to a more accurate representation of the physical processes. The software used is the Groundwater and Surface Water Flow Model (GSFLOW, Markstrom et al. 2008, version 1.2.0 released in August 2015) developed by USGS.

The surface water part of the model is simulated using the Precipitation-Runoff Modelling System (PRMS, Leavesley et al., 2005). The watershed was divided into Hydrological Response Units (HRU's) with similar properties, depending on the lithology on the different formations (alluvium, karstified marble and schist). The input data were mainly meteorological data (precipitation and average temperature) and data related to the soil properties of the HRU's. The time step used was daily and the simulation period includes 6 years (2009-2014). Main outputs of this model include the evapotranspiration and streamflow, while other parameters such as soil storage capacity are calculated.

The groundwater flow model is developed using the Modular Ground-Water Flow Model (MODFLOW-2005, Harbaugh, 2005). The model consists of 4 layers with the following properties:

- Layer 1 (Alluvium): In the first Layer an unconfined porous aquifer is developed. The thickness of the Layer is variable, with the top being the land surface, taken by a 25 X 25 m Digital Elevation Model (DEM) and the bottom being interpolated using the drilling depths taken from the Geoprobe drilling campaign (done by UFZ). The extent of the aquifer is taken by the geological maps of the area (IGME 2003, 2007).
- Layer 2 (Schist): This Layer is present in parts of the study area where it outcrops, mainly in high elevations. In the model it has a variable thickness taken combining topography and geology. There is no significant water movement in this aquifer, so in the model the hydraulic properties given are very poor and the aquifer is simulated as being confined.
- Layer 3 (Marble): In the karstified marble an unconfined aquifer with high dynamic is developed. The flow regime in this aquifer is characterized by the presence of fractures and conduits that make the system behave different than a typical porous aquifer. In these aquifers, the hydraulic conductivities are high while the small residence time reflects in the small values for storativity. The thickness of the aquifer is taken using geological cross sections.
- Layer 4 (Kaisariani Schists): This is the lower Layer of the model. These schists have a large thickness, but in the model it is set to be 40 m. The hydraulic properties are also very poor, similar to the aforementioned schists. This Layer is also considered to be confined.

The Boundary Conditions (BC's) used in the model represent the inputs and outputs of the physical system. At this occasion, the choice of BC's is restricted by the compatibility of some of the available MODFLOW packages with GSFLOW. The BC's used and their physical analogue are the following:

- Unsaturated Zone Flow package (UZF): This package is assigned to the Alluvium Layer and it is used to connect PRMS and MODFLOW in GSFLOW. It is only assigned to the Alluvium because using this BC for the karstified marble is unrealistic.
- Time Variant Specified Head package (CHD): The CHD package is used to simulate the sea level. The head is fixed throughout the whole simulation period.
- Well package (WEL): GSFLOW is not compatible with the Recharge package, so to simulate the recharge of the karstic aquifer from precipitation, the WEL package is used.
- Stream Flow Routing package (SFR): This package is used to simulate the main stream in the area and is the main package that GSFLOW is compatible with. The stream is divided in 9 segments that are connected.
- Head Observation package (HOB): This package is used in order to input the hydraulic head observation in the wells and drills, for both the aquifers, in the model.

The simulation is divided in 80 stress periods that represent the months for the period 2009 – 2014. The time step used is daily.

Sensitivity analysis was run for both parts of the model separately. This was done so that the parameters important for each part of the model are identified and then included in the calibration process. In both cases, the sensitivity was done using UCODE 2014 (Poeter et al. 2014), a software developed by USGS.

For the surface water model, the calculated composite scale sensitivities (**Figure 160**) show that the parameters affecting the model the most are those related to the evaporation process. The observations used for the sensitivity analysis are the low flows (basically 0) of the dry period. This is reasonable, since in a semi – arid region, such as Lavrio, evaporation amount is the main factor affecting how much water will be finally available for runoff and infiltration. The parameters defining the interconnection between groundwater and runoff show also high sensitivity. This leads to the conclusion that surface water – groundwater interaction is not just important in theory but it is a major component of every physical based model.

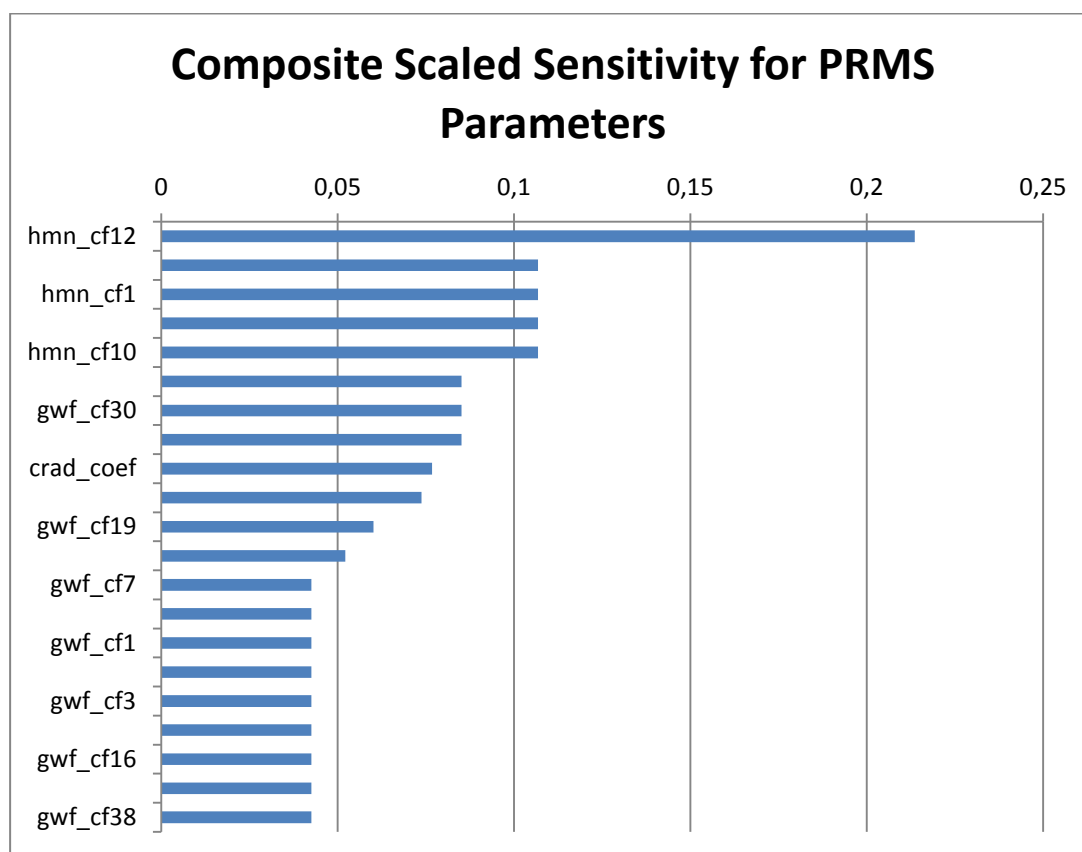


Figure 160 - Composite scaled sensitivity for the surface water model

The insensitivity of the model to the parameters related to the storage capacity of the soil zone is worth mentioning. This can be biased though and might change when the coupled model is tested. The winter and summer soil coverage with plantation was also insensitive.

In the dimensionless scaled sensitivity graph (Figure 161) it is shown that the parameters affecting the amount of calculated solar radiation for the model have high sensitivities. This is due to the fact because the calculated values will affect eventually the amount of evapotranspiration and, in the end, the amount of available water for the other processes.

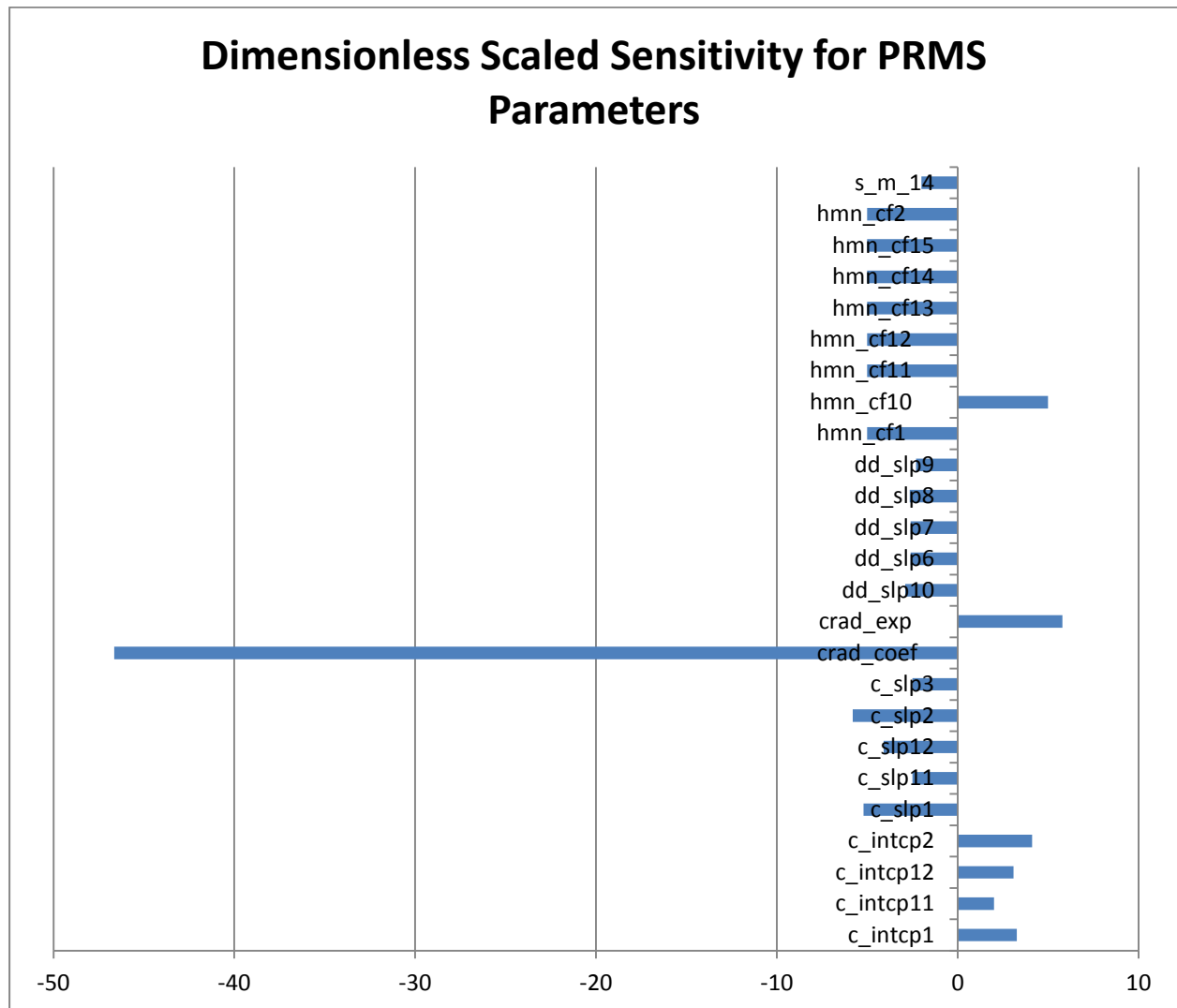


Figure 161 - Dimensionless scaled sensitivity for the surface water model parameters

For the groundwater model the sensitivity analysis showed that the model is very sensitive to the specific yield of the two aquifers. This is reasonable since, along with the chosen hydraulic conductivities, these two parameters affect the simulated heads. What also came out from the sensitivity analysis is that the highest dimensionless scaled sensitivity values are for the low flows in the summer period, which in reality is no flow period because the main stream gets dry (Figure 162). This is an important output because it highlights once again the importance of surface water – groundwater interactions in such areas and how they are represented in a model.

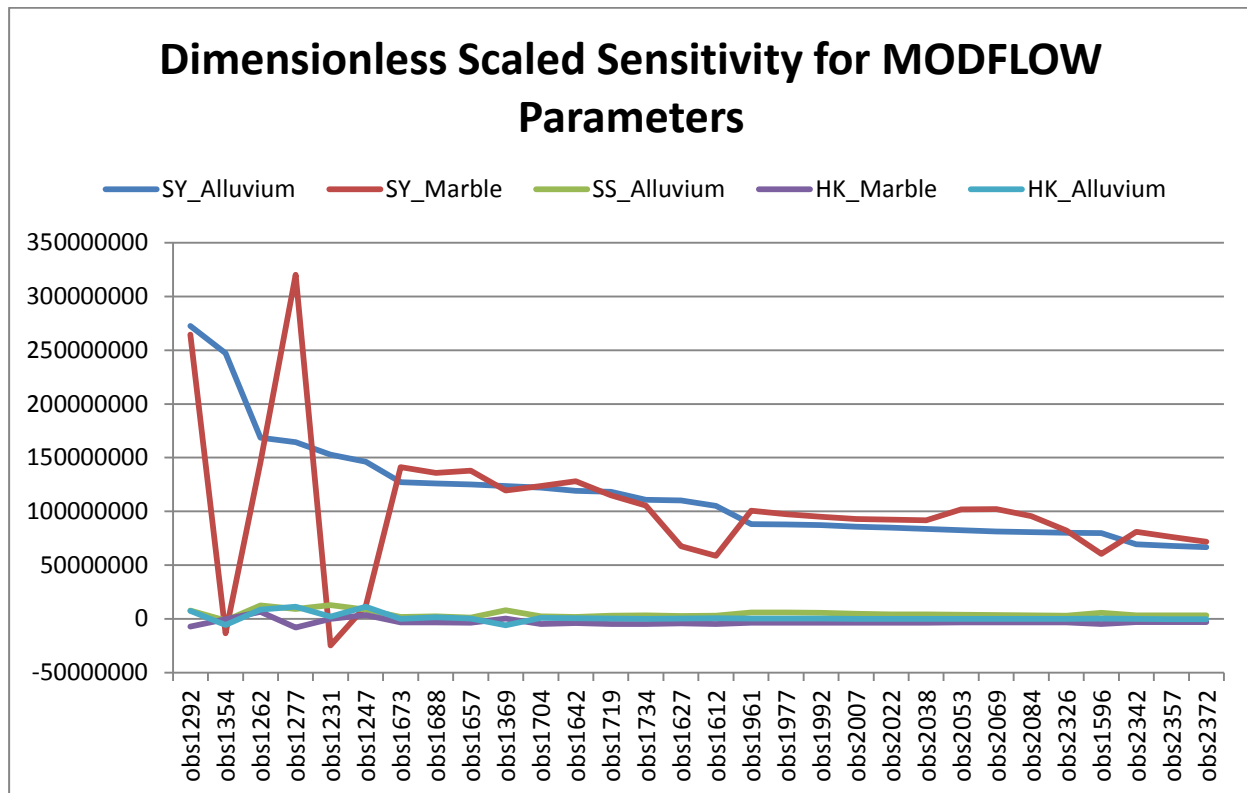


Figure 162 - Dimensionless scaled sensitivity for the groundwater model

In the composite scaled sensitivity graph (Figure 163) the importance of the specific yield parameters for the two aquifers is depicted. This is an indicator about the direction at which the calibration effort should be directed to.

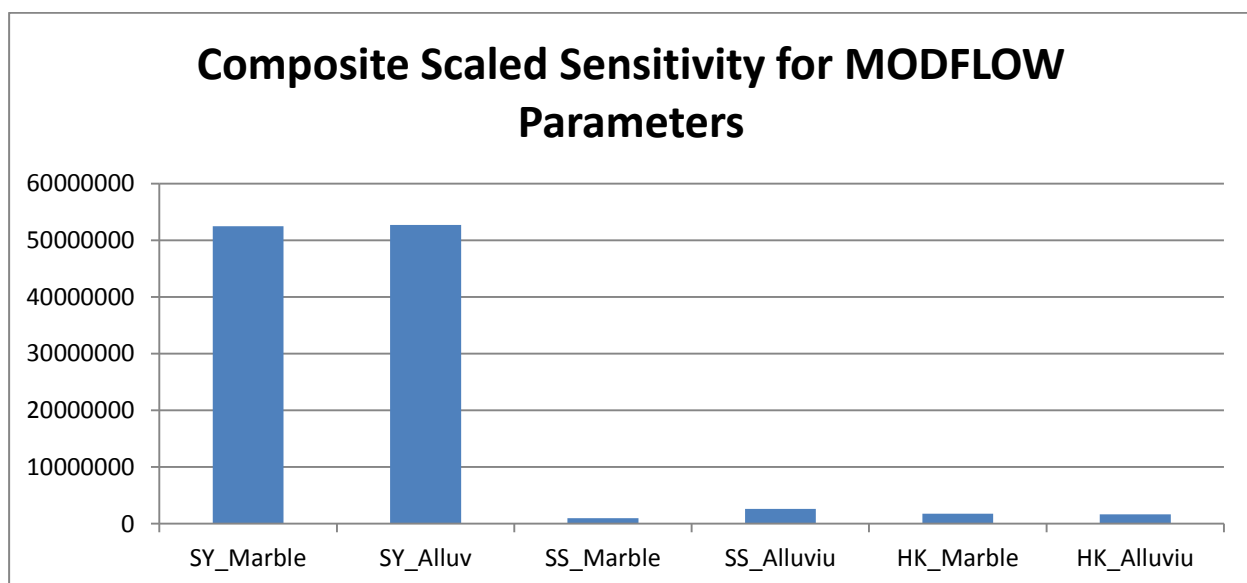


Figure 163 - Composite scaled sensitivity graph for the groundwater flow model

The following developments include calibration and sensitivity analysis of the GSFLOW coupled model. The focus of the calibration, in order to be effective, will be at selected parameters that affect the model most. This will lead to a final model that will be able to simulate the different Managed Aquifer Recharge scenarios proposed for the Lavrio MARSOL Demo Site. These are mostly infiltration basins in the alluvial aquifer, targeting at reducing the deterioration of the groundwater quality and quantity in both aquifers.

References

- Harbaugh, A.W., 2005, MODFLOW-2005, The U.S. Geological Survey modular ground-water model—the Ground-Water Flow Process: U.S. Geological Survey Techniques and Methods 6-A16, variously p.
- IGME, 2003. Koropi-Plaka sheet, Geological map of Greece, 1:50.000, Athens.
- IGME, 2007. Lavrio sheet, Geological map of Greece, 1:50.000, Athens.
- Leavesley, G.H., Markstrom, S.L., Viger, R.J., and Hay, L.E., 2005, USGS Modular Modeling System (MMS)—Precipitation-Runoff Modeling System (PRMS) MMS-PRMS, in Singh, V., and Frevert, D., eds., *Watershed Models*: Boca Raton, Fla., CRC Press, p. 159-177.
- Markstrom, S.L., Niswonger, R.G., Regan, R.S., Prudic, D.E., and Barlow, P.M., 2008, GSFLOW—Coupled ground-water and surface-water flow model based on the integration of the Precipitation-Runoff Modeling System (PRMS) and the Modular Ground-Water Flow Model (MODFLOW-2005): U.S. Geological Survey Techniques and Methods 6-D1, 240 p.
- Poeter, Eileen P., Mary C. Hill, Dan Lu, Claire R. Tiedeman, and Steffen Mehl, 2014, UCODE_2014, with new capabilities to define parameters unique to predictions, calculate weights using simulated values, estimate parameters with SVD, evaluate uncertainty with MCMC, and more: Integrated Groundwater Modeling Center Report Number GWMI 2014-02.

25.5 TUDA MODELLING CONTRIBUTIONS IN DEMO SITE 7: MENASHE INFILTRATION BASIN, HADERA, ISRAEL

Personnel Involved: Anja Tögl, Laura Foglia (TUDa)

25.5.1 Progress of Work on Model

Next to the already developed surface water model with using the Precipitation-Runoff Modelling System (PRMS) code, a groundwater flow (MODFLOW-NWT), unsaturated zone (UZFI Package) and streamflow routing (SFR2 Package) model has been developed, using MODFLOW codes. The models are coupled applying the GSFLOW code which simulates the processes in daily time steps and couples PRMS and MODFLOW iteratively in every time step.

The coupled GSFLOW model is currently being evaluated in a sensitivity analysis and prepared for parameter estimation with UCODE_2014, using head observations of 39 monitoring wells in the sandstone aquifer and daily averaged streamflow observation data at gauges of the four Menashe streams, located before the diversion of the streams to the infiltration basins.

25.5.2 Model Setup

The temporal input and observation data for the model are available since 1960s the time of the implementation of the MAR system of diverting streamflow for seasonal aquifer storage.

The PRMS surface water model (Figure 164a) is comprised of hydraulic response units (HRUs) representing the sub-watersheds of the four Menashe streams (43 HRUs), the two infiltration pond bodies (2 HRUs) and external HRUs (10 HRUs) covering the areas out of the watershed but still in the groundwater domain.

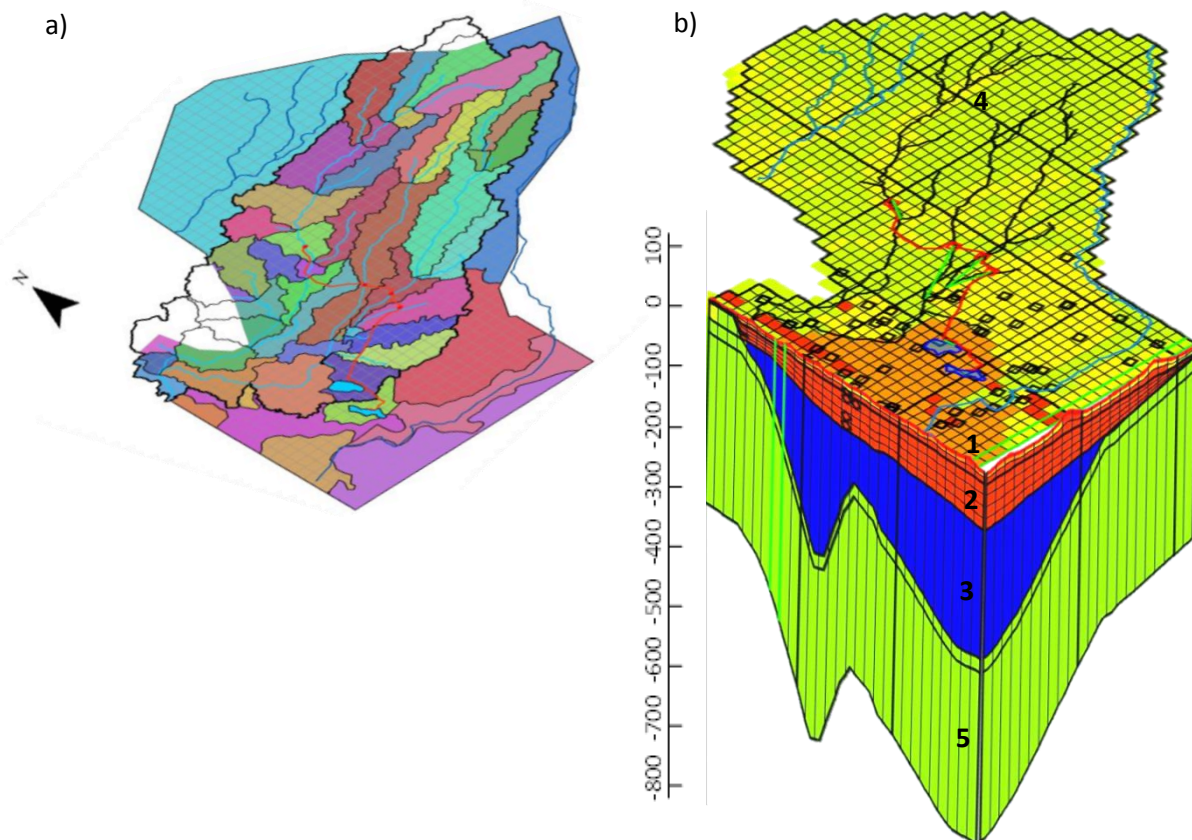


Figure 164 - a) PRMS domain, Menashe streams (light blue lines), diversion channel (red lines), watershed location (black line), HRUs (colored polygons), and the MODFLOW grids (grey lines); b) MODFLOW model domain, layer depth in meter (vertical exaggeration of 10), colors representing hydraulic conductivity (red - high, green - low, blue - very low)

The selected groundwater model domain represents the natural outline of groundwater divide of the aquitard in the eastern part. The northern and southern boundaries of the coastal aquifer are dominated by flow parallel to the domain boundary therefore these were defined as no-flow boundaries, while the coastal boundary in the west is a constant head boundary.

In the GSFLOW model natural streams and diversion channels are represented with the MODFLOW-streamflow routing (SFR2) Package and the infiltration ponds with the lake (LAK) Package.

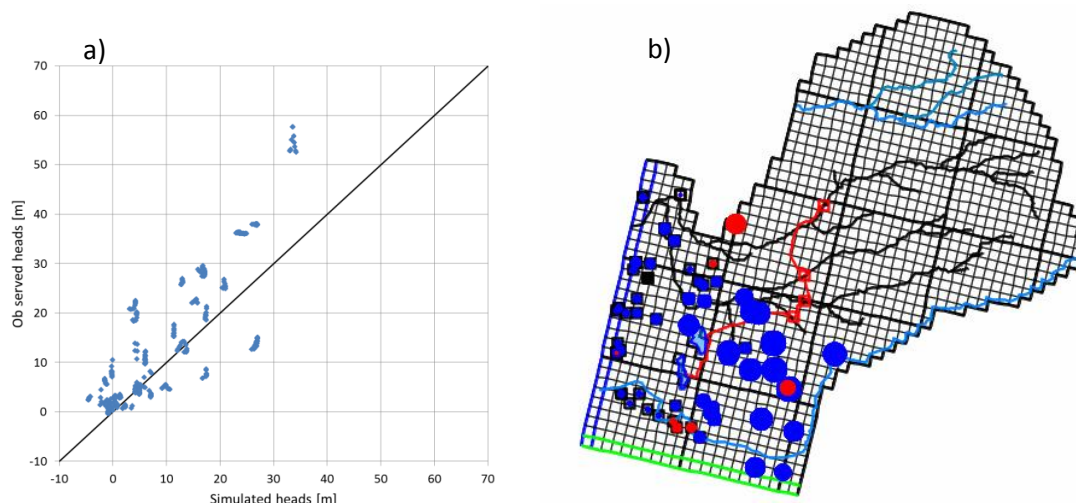
The groundwater model comprises 5 layers (Figure 164b):

- **1 - Upper Aquifer:** young quaternary sediments (sands, loams and alluvial clays) and a few sandstone outcrops
- **2 - Lower Aquifer:** main Plio-Pleistocene calcareous sandstone aquifer (partially containing clay and silt lenses, which were not separately simulated, but are within an average hydraulic conductivity of the sandstone)
- **3 - Yafo Aquiclude:** clay stone aquiclude up to 500m thick separating the sandstone aquifer from the deeper Eocene chalk and marl units
- **4 - Upper Aquitard:** weathered portion of the outcropping Eocene chalk aquitard estimated to be about 20m thick, which due to fractures is expected to have a higher conductivity and enhances close to surface runoff/interflow
- **5 - Lower Aquitard:** the main low conductivity chalk and marl aquitard

25.5.3 Model Evaluation

For the sensitivity analysis the average hydrological year 2003/04 was selected, detailed are results not presented here, but only the model fit comparing head and flow observations (Fig. 2). The 673 head observations have coefficient of determination (r^2) of 0.73 and the root-mean-square-error is 3.74. Part of the head observations have a quite good fit, while another part is simulated lower than observed in the field. Only at 3 field observation wells, located at the northern and north-eastern sandstone aquifer border, have heads simulated significantly higher.

Regarding the streamflow observations a general fit is visible, having r^2 between 0.61 and 0.84 and Nash-Sutcliffe coefficients for the Taninim and Barkan gauge are 0.60 and 0.49, while for the Ada and Mishmarot gauge it is negative. The observed peak flow is underestimated, but a high uncertainty in the observed value is expected. The major problem for the three main streams are the low flows, which are simulated too high. While the only-surface water model is able to simulate the zero baseflow in the summer month, the coupled model does simulate a baseflow. This is expected to be corrected in the parameter estimation, of the streambed conductances.



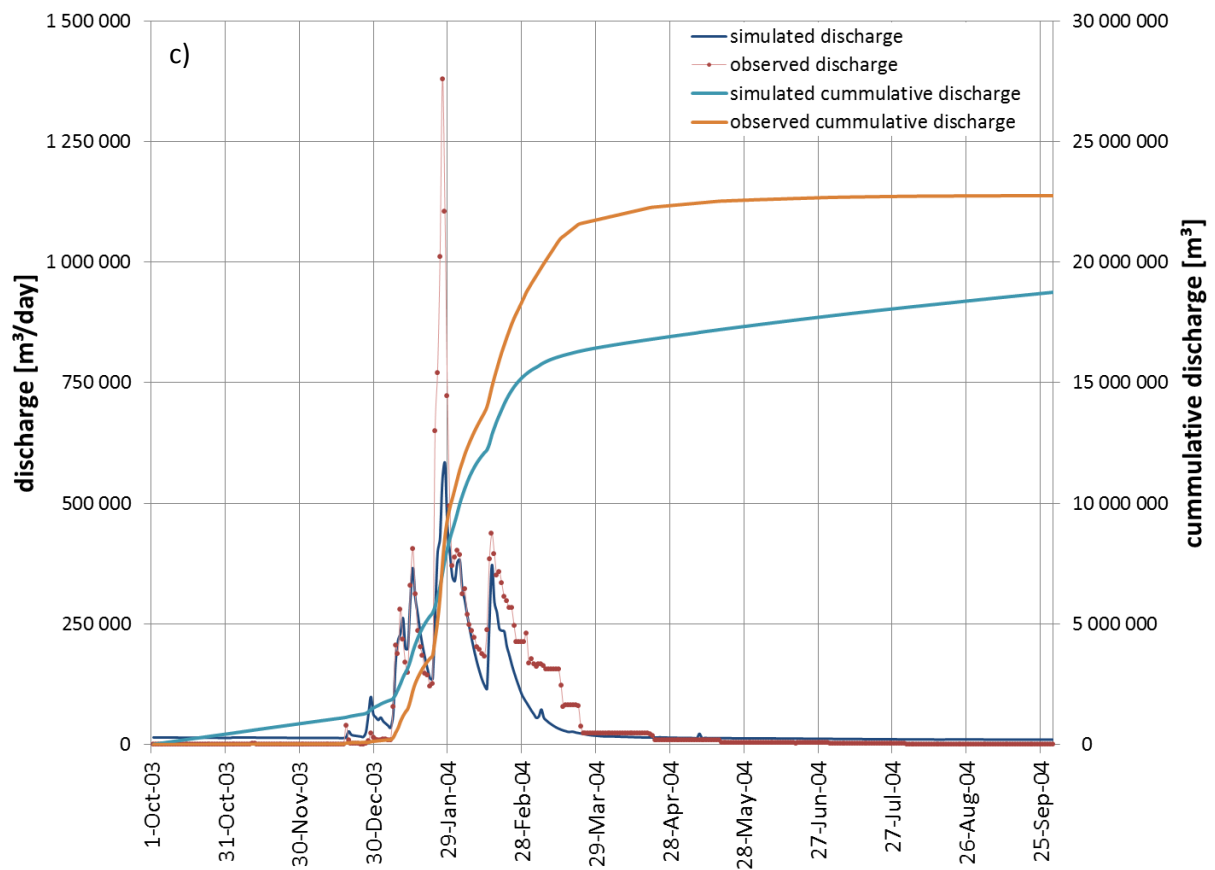


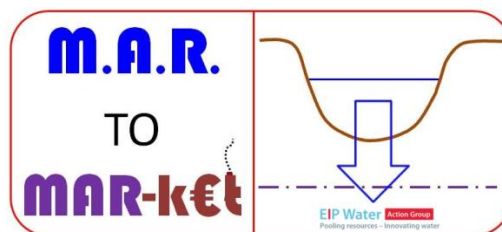
Figure 165 - Model fit for the sensitivity and calibration period of the hydrological year 2003/04, comparing simulated and field observed a) groundwater heads, b) distribution of residuals and c) sum of discharge of the four gauging stations

White book on MAR modelling

Deliverable D12.7

ANNEX 2 – EIP WATER AG 128

MARtoMARKET REPORT



EIP Water Action Group
Pooling resources – Innovating water

EIP AG 128 MARtoMARKet

Strategies and actions to bring Managed Aquifer Recharge scientific based solutions and techniques to the industry

Leader of AG 128 MARtoMARKet:

<http://www.eip-water.eu/users/jo%C3%A3o-paulo-lobo-ferreira>

Dr.-Ing. Habil. João-Paulo Lobo-Ferreira (LNEC, Portugal)

Laboratório Nacional de Engenharia Civil

Av Do Brasil 101, 1700-066 Lisboa, Portugal

phone: +351 218 443 609, e-mail: lferreira@lnec.pt

1. INTRODUCTION

This Progress Report describes the 2nd Year activities of EIP AG 128 MARtoMARKet. In summary the activity developed can be summarized as follows:

Site:

- Updating MAR information available and dissemination of pdf of Reports and presentation files on MAR in AG128 MARtoMARKet EIP site (<http://www.eip-water.eu/working-groups/mar-solutions-managed-aquifer-recharge-strategies-and-actions-ag128>)

Conferences and workshops:

- MAREnales training workshop: Between 2015 March 9th and 11th has been celebrated the training Workshop “MAREnales” in Arenales aquifer, Castille and Leon, Spain, within the framework of MARSOL project (FP-7 Water inno-demo call) and organized by Tragsa. <http://www.marsol.eu/70-0-Past-Events.html#marenales> and <http://goo.gl/XTM32b>
- A full week on MAR: the MARSOL midterm meeting:
 - The MARSOL internal mid-term meeting took place in Lisbon, Portugal, on June, 22th and 23th, 2015, on the premises of LNEC. The presentations at the meeting represented the status of the project at mid-term (months 1-18).
 - MAR Water Quality Workshop, June 24th-26th, 2015 (<http://www.eip-water.eu/algarve-water-quality-workshop-great-success>). The workshop on strategies and actions to bring science based solutions and techniques of Managed Aquifer Recharge (MAR) to the industry - MAR(solutions) to MAR-ket – brought together 50 participants in the Algarve, Portugal. The workshop was organised in four sessions introducing the background, a specific Portuguese Demo Site session, another one addressed to all 8 MARSOL demo sites, as well as a scientific session on Water Quality. Several Managed Aquifer Recharge (MAR) techniques, such as SoilAquifer Treatment (SAT) were addressed, as they are expected to be applied to the e.g. Algarve aquifers.
- MAR IN PERU. Conference In A Context Of High MAR Culture: Last August 21th 2015 a conference took place in Lima, Peru, titled: “Técnicas de Recarga Gestionada (=artificial) de Acuíferos: Experiencias en España y soluciones tecnológicas aprendidas”. The presentation exposed the Spanish expertise on MAR or artificial recharge with the aim of info exchange, experiences and error learnt from management, to be shared with Peruvian technicians. MAR is speeding up in this Andes country, pioneer on Mar in the American continent thanks to incas “amunas”. The conference, organized by ANA with the collaboration of the World Bank, presented also IAH MAR Commission and MAR to MAR-ket in this country.

- Presentation of MARSOL and the MAR to MAR-K&E Action Group at a conference in Brazil: João-Paulo Lobo-Ferreira from MARSOL partner LNEC presented both projects at the XXI Brazilian Symposium on Water Resources in Brasilia, November 2015.
- Workshop "A Gestão da Recarga de Aquíferos no Nordeste Brasileiro e na Europa", Federal University of Pernambuco, Recife, Brazil, Nov. 2015, organized by partners LNEC (PT) and UFPE (Brazil).
- 'Modelling', Pisa, Italy International Conference and Workshop: A joint international Workshop was held in Pisa on 21 April 2015 on Advantages of using Numerical Modeling in Water Resources Management and Managed Aquifer Recharge schemes. Presentations from the event can be downloaded from: <http://www.freewat.eu/node/573#presentations>
- Legal Issues, Policy & Governance Workshop, 21-23 October 2015, Malta The overall objective of the Workshop was to analyse the normative framework which governs the creation and functioning of MAR schemes in Europe and in the extra-EU countries, to assess if it would be desirable/practicable/useful/feasible to have a specific EU legislation on the issues, to discuss first proposals for such a MAR regulatory framework, and to address policy and governance issues related to the implementation of MAR schemes.
- Preparation of an open side meeting by EIP Water AG 128 MARtoMARKet on "Boosting Managed Aquifer Recharge in Europe", scheduled to take place in Leeuwarden (NL) back-to-back with the EIP Water Conference 2016 on Tue. February 9, 2016.

MAR DEMO Sites:

During 2015, six out of eight demonstration sites were either newly developed or upgraded:

- Operations of the field sites were accompanied by an extensive investigation and monitoring program using geoprobe campaigns, geophysical methods, and tracer techniques. Specifically, sensors for unsaturated zone water content monitoring and wireless data transmission systems have been developed in the first year of the project and are already implemented and tested in a field site in Italy.
- The field sites generated during 2015 high quality data on infiltrated water volumes as well as on water quality changes during infiltration. MARSOL is therefore generating comprehensive data sets on water quality aspects at MAR in general and of operating MAR sites. These data are the basis for optimizing operational regimes e.g. in accompanying laboratory column experiments for the sites in Israel and Greece, or by incorporating reactive layers at selected infiltration basins, e.g. at the Llobregat river in Spain.
- For all field sites, experimental work is accompanied by modelling efforts to understand the hydraulic characteristics and the geochemical conditions at the site, as well as the impact of the MAR systems within the selected catchments. Models are being constantly updated with data that will be generated in the course of the project. MARSOL's dissemination and training activities are coupled to the project's demonstration sites.
- In total five workshops were organized in Spain, Israel, Portugal, and Italy, partly in cooperation with other EU projects such as DEMOWARE, DEMEAU, and FREEWAT, respectively, to identify synergies and establish contacts between the project partners.

- The EIP Water Action Group AG128 “MAR Solutions - Managed Aquifer Recharge Strategies and Actions” is used as a forum to promote the MARSOL approaches on an international level.

Selected Book and Report:

- SUDS book presented at Korea WWF: “La Gestión Integral del Agua de Lluvia en Entornos Edificados” or “The comprehensive management of rainwater in built-up areas”. During Korea World Water Forum, 2015 April, a new book on urban hydrogeology was presented focusing water harvesting in cities and MAR systems to increase infiltration in urban areas by means of enhanced architectural designs. It has been written by 21 authors (most of them architects and hydrogeologists) from Tragsa Group, a MAR to MAR-€ first row member. The publication (in Spanish and in English) will be published soon on the Internet.
- LNEC report on “GROUNDWATER PROTECTION AND PRESERVATION: Results from a survey to Portuguese farmers” presents a descriptive analysis of the responses to a survey about protection and preservation of groundwater conducted with a sample of Portuguese farmers of the Algarve region. This survey was developed in the context of the project MARSOL – Managed Aquifer Recharge Solutions (European Union Seventh Framework Programme For Research, Technological Development and Demonstration – Grant Agreement nr. 619120). The report can be downloaded from <http://www.eip-water.eu/close-cooperation-between-eip-marsolutions-and-fp7-marsol-inno-demo-project>

Selected Papers:

- Fernández Escalante, E., González Herrarte, F.B. & San Sebastián Sauto, J. (2015). Recarga Gestionada de Acuíferos: Multifuncionalidad en la Zona Regable de Santiuste. - XXXIII Congreso Nacional de Riegos, Valencia, 16.-18. June 2015, 10 p.
- Lobo Ferreira, J.P., Estratégias e Ações para Fomentar o Uso da Gestão da Recarga de Acuíferos: o Exemplo do Grupo de Ação "EIP AG 128 MARTOMARKET" . Brasília, Brasil, Nov 2015, XXI SBRH e 12º SilusbaPAP020135 <http://abrh.org.br/xxisbrh/>.

2. ACTIVITY 1: KNOWLEDGE-BASE OF EXISTING MAR FIELD APPLICATIONS

2.1 OBJECTIVES OF THE ACTIVITY

Knowledge-base of existing field applications for addressing different societal challenges related to water availability. The first Deliverable is expected to be ready by Month 12 containing Technical docs on the current state-of-the-art.

2.2 ACTIVITY DEVELOPED

This Knowledge Basis was considered concluded in the 1st Year Report, although being further updated in MARToMARKet activity 1, e.g. in the report *Tragsa (2015). MARSOL 13-1 Deliverable. MAR Technical Solutions: Review and Data Base*.

3. ACTIVITY 2: MAR TO MAR-KET

3.1 OBJECTIVES OF THE ACTIVITY

Water and energy efficiency. General improvements by means of MAR.

3.2 ACTIVITY DEVELOPED

Activity was developed during 2015 on the financial analysis of the MARSOL Sites (developed by MARSOL partner SGI, Italy) to assess their financial performance expressed by indicators considering the relevant financial costs and returns. The analysis was carried out from the managing authority standpoint and was aimed to show whether and how the benefits generated by the project's implementation (mainly a better quality or an increased availability of water) are able to recover the relevant operation and maintenance costs and capital investment.

The Financial Model will be updated and refined in pace with the progress of the other MARSOL tasks, and particularly with the improvements regarding the aquifers modelling and of the infiltration rates investigations, in order to give a progressively more detailed picture of the financial performance of the site as the Study moves from preliminary/conceptual to final. Eventually, the Financial Analysis provides most of project data on costs and benefits used for the Cost-Benefit Analysis.

4. ACTIVITY 3: BLUEPRINT IMPACT, INDICATORS, RISK ASSESSMENT

4.1 OBJECTIVES OF THE ACTIVITY

- Methodology for probabilistic risk evaluation linked to MAR activities.
- Novel MAR design concepts to enhance the efficiency of microbial degradation of organic micro pollutants and to minimize adverse soil-water interactions during infiltration and storage.

4.2 ACTIVITY DEVELOPED TO RISK ASSESSMENT

This activity has been a follow-up of background MANPORIVERS project, led by partner LNEC (PT). The background activity developed by LNEC was on:

- Review on methods for assessing surface water vulnerability to pollution and geographical surface water protection zoning to pollution, such as a USGS method and WRATIC index.
- Development of two decision flow charts for better groundwater and surface water risk assessment and management.

During 2015, partner UPC (Spain) led and concluded MARSOL WP Technology Assessment and Risk (WP16) dealing with proper methodologies to assess the potential risk associated to MAR facilities. Deliverable 16.2 deals with the methodologies existing to select the best location to place infiltration basins for MAR activities. Optimal location of potential candidate areas to place such facilities within a given water basin must be based on a multidisciplinary

approach involving a number of aspects, including: natural characteristics of the aquifer system, availability of water for recharge, quality of recharge water, social impact, as well as legal, and economic issues. Such different issues should be combined in an integrated framework, and this can only be done by a combination of simplified indices integrated in a GIS framework.

5. ACTIVITY 4: TECHNICAL SOLUTIONS FOR INDUSTRY

5.1 OBJECTIVES OF THE ACTIVITY

- Development of design and construction criteria, and testing protocols for different exemplary MAR schemes and their benchmarking.
- Developing and testing appropriate engineering solutions, e.g. underground dams and wastewater hydraulic barriers, to convert karst aquifers into large groundwater storage reservoirs.
- The pros and cons of each technology will be assessed systematically, and compared to alternative solutions.
- Economic costs and benefits of MAR options for the various economic sectors will be quantified.

5.2 ACTIVITY DEVELOPED

This activity is based in MARSOL work package activities led by Tragsa (Spain). The training Workshop “MARenales”, was held in Coca and Gomezserracín (Segovia) from 2015 March 9th to 11th. It is worth including direct surveys to irrigation communities’ secretaries.

Sessions, organized by Tragsa, were especially aimed to farmers and the general population in these rural areas, so, technical language was eluded in presentations. The irrigation communities collaborated actively in its organization and dissemination.

The main problems and impacts reported by local stakeholders were:

- Excessive dependence of the climatic conditions to have the MAR facilities working.
- The groundwater table decline has motivated the closure of low depth wells.
- The “green water” is becoming more and more important in the Spanish economic activity.
- Potential affection of water table oscillations on the edifications and buildings foundations.
- A technical report justifying where the regular undisturbed water level must stand for each specific area in the aquifer is missed.
- Invisible recharge: “Do not close a well, reuse it”.
- MAR is applied in the area, increasing a general MAR culture, but only in the irrigation plots. These types of techniques should also be employed in urbanism to increase the natural infiltration rate below cities and villages, to reduce floods and surface run-off.
- MAR is essential to ensure a good irrigation water quality (less nitrates and arsenic).
- Good MAR water quality for irrigation brings an added value for farmers (better crops quality).

6. ACTIVITY 5: MODELLING

6.1 OBJECTIVES OF THE ACTIVITY

Mathematical models to simulate the impact of MAR on aquifer hydrology and hydro geochemistry, incl. water balance, water availability, climate change.

6.2 ACTIVITY DEVELOPED

- Modelling developments have been presented in MARSOL Deliverable 12.1 (final version dated 15.05.2015), Deliverable 12.2 (draft version dated 05.06.2015) and Deliverable 12.3 on the **Progress Report on numerical model**, September 2015, for selected MARSOL case-study areas (Portugal, Italy, Spain, Israel and Greece). A contribution from TUDa on to the hydrological/hydrogeological models for the Lavrio test site (WP 3) and the Menashe test site (WP 9) was included. These contributions are related to regional and local scales.
- Besides information for conceptual modelling a GIS database was structured to contain the MAR facilities, infrastructures and also some related monitoring information.
- A requirements analysis was performed of several demo sites aiming to identify what kind of information was available and what kind of information could be included. The demo sites field visits and guide books were essential to perform this task. This was the case of Arenales (demo site 3, Castile and León, Spain), Sant'Alessio (demo site 6, Tuscany, Italy), and Menashe (demo site 7, Israel) MAR systems. Besides already gathered information on Lavrion (demo site 1, Greece), and knowledge by the leading authors of the Algarve demos sites (demo site 2, Portugal), allowed a comprehensive definition of the data requirements and relevant links between information.
- From the MARSOL Consortium to the H2020 FREEWAT project: The FREEWAT project, led by the MARSOL partner Rudy Rossetto representing the Scuola Superiore Sant' Anna (Italy), commenced on the 01 April 2015 and brings together a consortium of 19 partners, six of who are also partners of the MARSOL consortium. The partners who are once again working together are TUDa, TEA, IDAEA- CSIC, NTUA-AMDC and Paragon Europe. The main objective of FREEWAT is to develop an open source public domain and GIS integrated modeling platform for water resource management. The platform will then be applied to 14 case studies through EU and beyond in order to test the simplification in adopting the WFD and other water related regulations. The FREEWAT platform will also benefit from the results obtained in MARSOL, as it will include the solute transport modeling capabilities in aquifers developed in MARSOL by TEA and SSSA. A joint international Workshop was held in Pisa on 21 April 2015 on Advantages of using Numerical Modeling in Water Resources Management and Managed Aquifer Recharge schemes. Presentations from the event can be downloaded from: <http://www.freewat.eu/node/573#presentations> For more information about the FREEWAT project visit <http://www.freewat.eu/>.

7. ACTIVITY 6: TRANSFERRING KNOWLEDGE INTO PRACTICE

7.1 OBJECTIVES OF THE ACTIVITY

A complex and Specific Dissemination & Technology Transfer (D&TT) Plan is being designed based in the product previous analysis, business and development plans as well as target users.

The Plan will contain several programs specially dedicated to the industrial branches, beneficiaries of the technology improvements. Different activities & materials will be developed to achieve an impact on the entire industrial driven sector.

7.2 ACTIVITY DEVELOPED

Conferences and workshops:

- MAREnales training workshop: Between 2015 March 9 and 11th has been celebrated the training Workshop “MAREnales” in Arenales aquifer, Castille and Leon, Spain, within the framework of MARSOL project (FP-7 Water inno-demo call) and organized by Tragsa. <http://www.marsol.eu/70-0-Past-Events.html#marenales> and <http://goo.gl/XTM32b>
- The MARSOL internal mid-term meeting took place in Lisbon, Portugal, on 22. and 23. of June, 2015, on the premises of LNEC.
- Water Quality Workshop, June 24th-26th, 2015 (<http://www.eip-water.eu/algarve-water-quality-workshop-great-success>). The workshop on strategies and actions to bring science based solutions and techniques of Managed Aquifer Recharge (MAR) to the industry - MAR(solutions) to MAR-ket – brought together 50 participants in the Algarve, Portugal.
- MAR IN PERU. Conference In A Context Of High MAR Culture: 21/08/2015: Last August 21th took place a conference in Lima, Peru, titled: “Técnicas de Recarga Gestionada (=artificial) de Acuíferos: Experiencias en España y soluciones tecnológicas aprendidas”. The conference, organized by ANA with the collaboration of the World Bank, presented also IAH MAR Commission and MAR to MAR-ket in this country.
- Presentation of MARSOL and the MAR to MAR-Ket Action Group at a conference in Brazil: João-Paulo Lobo-Ferreira from MARSOL partner LNEC presented both projects at the XXI Brazilian Symposium on Water Resources in Brasilia, November 2015.
- ‘Modelling’, Pisa, Italy: A joint international Workshop was held in Pisa on 21 April 2015 on Advantages of using Numerical Modeling in Water Resources Management and Managed Aquifer Recharge schemes. Presentations from the event can be downloaded from: <http://www.freewat.eu/node/573#presentations> / <http://www.eip-water.eu/presentations-international-joint-workshop-advantages-using-numerical-modeling-water-resources-0>
- MARsolutions participates in workshop on cooperation between Innovation partnerships: On May 28 a workshop entitled 'European Innovation Partnerships stairways towards Horizon 2020 opportunities' was held at the Museu das Comunicações in the Rua do Instituto Industrial 16, 1200-225 Lisboa. The MARsolutions Action Group was present and contribute to this workshop, cf. <http://www.eip-water.eu/marsolutions-participates-workshop-cooperation-between-innovation-partnerships>

- Legal Issues, Policy & Governance Workshop, 21-23 October 2015, Malta The overall objective of the Workshop was to analyse the normative framework which governs the creation and functioning of MAR schemes in Europe and in the extra-EU countries, to assess if it would be desirable/practicable/useful/feasible to have a specific EU legislation on the issues, to discuss first proposals for such a MAR regulatory framework, and to address policy and governance issues related to the implementation of MAR schemes.

MARenales movie:

- DINA-MAR: http://www.dina-mar.es/videos/MARenales-Film_v7.6.mp4
- Youtube: <https://youtu.be/Dw22rcEQdiw>
- MARenales training workshop: <http://www.dina-mar.es/post/2015/03/16/PONENCIAS-e2809cMARenalese2809d-CELEBRADO-EL-e2809cTRAINING-WORKSHOPe2809d-DEL-PROYECTO-MARSOL-EN-EL-ACUIFERO-DE-LOS-ARENALES-MARenales-PRESENTATIONS.aspx>

Managed Aquifer Recharge Solutions in images

- Following the workshop on "Managed Aquifer Recharge" MAR in Malta, a series of videos was produced illustrating its challenges. One general video is available [here](https://vimeo.com/148860336) (cf. <https://vimeo.com/148860336>) while a series including detailed description by partners from/in various countries also exists:
 - Germany (cf. <https://vimeo.com/148861517>)
 - Portugal (cf. <https://vimeo.com/148876691>)
 - Spain (cf. <https://vimeo.com/148876693>)
 - Italy (cf. <https://vimeo.com/149142094>)
 - Israel (cf. <https://vimeo.com/148876689>)
 - Malta (cf. <https://vimeo.com/149142291>)

8. ACTIVITY 7: FURTHER ACTIVITIES

8.1 OBJECTIVES OF THE ACTIVITY

Open task according to AG evolution & new necessities

8.2 ACTIVITY DEVELOPED

Creation of a pan-European network of EU funded projects working on MAR

Whether ISMAR 10 application in Madrid succeeds or not, a new platform has been created within this framework, involving all coordinators and partners working on **13 EU founded projects related to MAR**, either directly or collaterally, plus Mar to MAR-kät AG. The new platform starts sharing information and activities since 2015 July:

MAR PAN-EUROPEAN NETWORK



9. ANALYSES OF ENCOUNTERED BARRIERS, APPLIED SOLUTIONS AND POLICY RECOMMENDATIONS WHERE APPROPRIATE

(NB: DESCRIBE BARRIERS, SOLUTIONS AND RECOMMENDATIONS)

Engagement of partners in the Action Group 128 has been difficult, mainly due to the lack of financial support. Financing from partner institutions and/or from AG 128 related EU financed projects partially contributed to overcome this major problem. This was the case with partners from FP7 MARSOL project (cf. <http://www.eip-water.eu/close-cooperation-between-eip-marsolutions-and-fp7-marsol-inno-demo-project>) and from FP 7 DEMEAU project (cf. <http://www.eip-water.eu/managed-aquifer-recharge-sites-knowledge-basis-i>).

10. OUTLOOK FOR 2016 ACTIVITIES AND DELIVERABLES WITH MILESTONES

Besides fulfilling the Dow of AG 128 for the AG 128 3rt year (2016), extra programmed activities are related to the cooperation with the recently constituted International Working Group called "MAR to MARKET" of the IAH MAR Commission, lead by Dr. Teresa Leitão (LNEC, PT) and Dr. Enrique Escalante (Tragsa, ES).

Programmed MAR events for 2016:

ISMAR 9 Mexico City, (2016 spring): a specific session for MAR to Market is being organised by Water Inno-Demo projects partners . This AG can integrate this concept in their events.

MAR Open Meeting in the EIP Water Conference: TUE February 9, 2016, 10:00-12:30. Boosting Managed Aquifer Recharge in Europe (<http://www.eip-water.eu/side-meetings-eipwater2016>):

The MAR side event is aiming to presented and discuss the best way for "Training researchers, industry/SMEs, and end users on Water Quality regarding Managed Aquifer Recharge (MAR) and new developments in this field, to foster knowledge among all project

partners and to ensure that the project's RTD and DEMO results effectively reaches the end-users". Therefore, we intend to incorporate the achievements gathered in previous EU and national sponsored projects developed, e.g. in MARSOL case-study areas, addressing Water Quality techniques such as Soil Water Aquifer Treatment (SAT), as part of global solutions, so that aquifers, e.g. the Campina de Faro aquifer in the Algarve (PT) , that has been declared as a vulnerable area, can regain in a near future the good water quality status envisaged by the Water Framework Directive and the Portuguese Water Law. If you are interested in joining our meeting, please contact JP Lobo Ferreira lferreira@lnec.pt

MARSOL Workshop "Investigation and Monitoring of MAR Sites" Athens, Greece, March 2016.

MARSOL Workshop "Water to Market - Financial and Economic Analysis of MAR Solutions", Venice, Italy, June 2016.

Examples of programmed MAR activities at MARSOL Demo sites for 2016:

- DEMO ALGARVE AND ALENTEJO, SOUTH PORTUGAL:
 - Large diameter wells in the Campina de Faro area will be used to conduct artificial recharge experiments, where recharge rate will be controlled and piezometric levels will be monitored.
 - Ribeiro Meirinho River will be controlled along the time. In Cerro do Bardo site, piezometric levels in infiltrating well and nearby wells as well as the amount of water recharging the Querença-Silves aquifer system will be controlled taking advantage of LNEC's PROWATERMAN project available geophysical knowledge.

11.IMPACT MARKET POTENTIAL

- It is difficult to assess at the moment in the EU and in Mediterranean countries. In USA e.g. the turnover of Managed Aquifer Recharge projects per year is more than 300 million US\$.
- In Israel it is a mature business.
- A Legislative Framework Review and Analysis has been developed by partner SSSA (Italy) in MARSOL Deliverable 17.1.
- SGI (Italy) partner developed MARSOL WP 15 Deliverable 15.1 on Cost-Benefit Analysis of the MARSOL DEMO Sites. The overall estimated cost of investment in MARSOL Demo sites could be as high as 88 M€.

Lisbon, 15.01.2016,

Dr. JP Lobo Ferreira

(EIP Water AG 128 MARtoMARKet leader, LNEC, PT)